VYSOKÉ UČENÍ TECHNICKÉ V BRNĚ
BRNO UNIVERSITY OF TECHNOLOGY

FAKULTA CHEMICKÁ
CENTRUM MATERIÁLOVÉHO VÝZKUMU

FACULTY OF CHEMISTRY
MATERIALS RESEARCH CENTRE

CHARAKTERIZACE HYALURONANU A JEHO INTERAKCÍ S TENZIDY ULTRAZVUKOVOU SPEKTROSKOPIÍ A DENSITOMETRIÍ

DIZERTAČNÍ PRÁCE
DOCTORAL THESIS

AUTOR PRÁCE
AUTHOR

Ing. ANDREA KARGEROVÁ

BRNO 2014

Vysoké učení technické v Brně
Fakulta chemická
Purkyňova 464/118, 61200 Brno 12

Zadání dizertační práce

Číslo dizertační práce:	**FCH-DIZ0087/2013**	Akademický rok: **2013/2014**
Ústav:	Centrum materiálového výzkumu	
Student(ka):	**Ing. Andrea Kargerová**	
Studijní program:	Fyzikální chemie (P1404)	
Studijní obor:	Fyzikální chemie (1404V001)	
Vedoucí práce	**prof. Ing. Miloslav Pekař, CSc.**	
Konzultanti:		

Název dizertační práce:

Charakterizace hyaluronanu a jeho interakcí s tenzidy ultrazvukovou spektroskopií a densitometrií

Zadání dizertační práce:

Charakterizovat hustotu roztoků hyaluronanu. Prostudovat interakce opačne nabitých povrchově aktivních látek s hyaluronanem pomocí ultrazvukové spektroskopie s ohledem na možné využití vzniklého systému v cílené distribuci léčiv.

Termín odevzdání dizertační práce: 31.3.2014

Dizertační práce se odevzdává v děkanem stanoveném počtu exemplářů na sekretariát ústavu a v elektronické formě vedoucímu dizertační práce. Toto zadání je přílohou dizertační práce.

Ing. Andrea Kargerová Student(ka)	prof. Ing. Miloslav Pekař, CSc. Vedoucí práce	prof. Ing. Miloslav Pekař, CSc. Ředitel ústavu

V Brně, dne 3.7.2009

prof. Ing. Martin Weiter, Ph.D.
Děkan fakulty

ABSTRACT

This disertation thesis is focused on the study of physico-chemical interactions of hyaluronan (with molecular weights from 10 to 1750 kDa) with cationic surfactants measured using uncommon technique named high resolution ultrasonic spectroscopy. Densitometer was also used for the study of these interactions, in measuring of density and ultrasonic velocity of hyaluronan with different molecular weight in dependence on elevated temperature (25-50 °C). The aim is the determination of critical micelle concentration (CMC) and critical aggregation concentration (CAC) of the suractants in the absence and in the presence of hyaluronan with various molecular weights. Interactions in this system are important for the design of the systems for the targeted delivery, especially for the drugs. The experiments were made in water and sodium chloride solution. The significant breakpoint in the ultrasonic velocity showed changes in the system hyaluronan-surfactant.

ABSTRAKT

Tato disertační práce se zaměřuje na fyzikálně-chemické interakce hyaluronanu (molekulové hmotností od 10 do 1750 kDa) s kationickými tenzidy. Pro zkoumání a měření vzájemného působení byla použita technika s názvem ultrazvuková spektroskopie s vysokým rozlišením (HR-US). Při zkoumání interakcí byl též použit denzitometr, a to při měření hustoty a uktrazvukové rychlosti hyaluronanu o různé molekulové hmotnosti v závislosti na vybrané teplotě (25-50 °C). Práce se zaměřuje se na studium kritické micelární (CMC) a agregační (CAC) koncentrace tenzidů v přítomnosti a nepřítomnosti hyaluronanu o různé molekulové hmotnosti. Interakce hyaluronanu s kationickými tenzidy jsou důležité pro systémy s cíleným transportem, zejména léčiv. Měření interakcí bylo prováděno ve vodě a v roztoku chloridu sodného. V získaných datech lze pozorovat významné zlomy v ultrazvukové rychlosti, které nám ukazují změny v systému hyaluronan-tenzid.

KEYWORDS

hyaluronan, hexadecyltrimethylammonium bromide, tetradecyltrimethylammonium bromide, hyaluronan-surfactant system, critical micelle concentration, high-resolution ultrasonic spectroscopy

KLÍČOVÁ SLOVA

hyaluronan, hexadecyltrimethylamonium bromid, tetradecyltrimethylamonium bromid, ktitická micelární koncentrace, systém hyaluronan-tenzid, Ultrazvuková spektroskopie s vysokým rozlišením

KARGEROVÁ, A. *Charakterizace hyaluronanu a jeho interakcí s tenzidy ultrazvukovou spektroskopií a densitometrií*. Brno: Vysoké učení technické v Brně, Fakulta chemická, 2014. 213 s. Vedoucí dizertační práce prof. Ing. Miloslav Pekař, CSc..

STATMENT

I declare that the dissertation thesis has been elaborated by me and that all the quotations from the used literary sources are accurate and complete. The content of dissertation thesis is the property of the Faculty of Chemistry of Brno University of Technology and all commercial uses are allowed only if approved by both the supervisor of thesis and the dean of the Faculty of Chemistry, Brno University of Technology.

.....
Ing. Andrea Kargerová

ACKNOWLEDGEMENTS

I would like to thank my supervisor prof. Ing. Miloslav Pekař, CSc. for all the helpful advices and time he gave me during my whole studies. He motivated me very well and his international contacts helped me to travel in the professional meaning. I very appreciate also the cooperation with prof. Vitaly Buckin and Evgeny Kudryashov and their students at University College in Dublin, in the department of Chemical biology who gave me the opportunity to work with them and to learn a lot about high resolution ultrasonic spectroscopy. They are specialized on the working with this instrument.

I would like to thank Marie Dvořáková for participating on the experiments of density.

My special thanks go to my family and my boyfriend for their help and support.

The support from the COST action CM1101 and the corresponding Czech project No.OC08004 and the Centre for Materials Research at FC BUT, project No.LD12068 and project No. CZ.1.05/2.1.00/01.0012 from ERDF is gratefully acknowledged.

CONTENT

1 INTRODUCTION

Hyaluronan is a natural biopolymer occurring in the human body and it is used as controlled drug delivery transport system, as a material for scaffold in tissue engineering, as a component of a bandage by wound healing processes, as an alternate fluid in human joints, as a space filling matter in plastic surgery and last but not least as a hydration matter in cosmetics.

Hyaluronan is considered as a polymeric carrier which is soluble in water or physiological solution and has specific receptors for the binding to the right molecules, for application in target delivery. Thanks to negative charge on hyaluronan chain we used cationic surfactants. There are existing strong electrostatic interactions between negatively charged hyaluronan carboxyl group and positively charged surfactant head group. Surfactant forms micelles, where a non-polar drug can be inserted. Drug carriers, which could contain hyaluronan, as a target delivery could be medicament for cancer. The thesis investigates the interactions between surfactants and polymer for the possible following application for target delivery.

Theoretical part summarizes the research of hyaluronan and method high resolution ultrasonic spectroscopy. The experimental part is divided in three parts. The first part (preliminary part) studies the behaviour of hyaluronan in water, measurement of pH, preliminary density measurement. The aim of this part of the work is to characterize the dissolution and storage stability of hyaluronan. The second part (experimental part I) is focused on the study of hyaluronan in wide range of molecular weights and as broad range of its concentration. The density and ultrasonic velocity is measured in solutions in temperature range from 25 °C to 50 °C. In the third part (experimental part II), high resolution ultrasonic spectroscopy is used for a detailed study of interactions between hyaluronan and two cationic surfactants tetradecyltrimethylammonuim bromide (TTAB) and hexadecyltrimethylammonuim bromide (CTAB) either in water or in sodium chloride solution at physiological concentration (0.15 M).

2 THEORETICAL PART

2.1 Hyaluronic acid

Hyaluronan (also called hyaluronic acid or hyaluronate) is a carbohydrate, more specifically a mucopolysaccharide, occurring naturally in all the living organisms. The term hyaluronan refers to the polysaccharide in general whether it is in the acid form or the salt form. This term is consistent with the general nomenclature of polysaccharides. The suggestion came in 1986, that is, rather late in the development of the field, by Balazs et al. [1].

The names hyaluronic acid and hyaluronan have been used interchangeably ever since although strictly speaking they have different meanings: hyaluronan is a general term whereas hyaluronic acid and hyaluronate are unambiguously specific for the acid and for the salts, respectively. The salt is very often sodium hyaluronate [2].

2.1.1 History

In 1934, Karl Meyer and John Palmer [3] isolated a previously unknown chemical substance from the vitreous body of bovine eyes and named it hyaluronic acid. They found that the substance contained two sugar molecules, an uronic acid and an amino sugar. The popular name is derived from two words: “hyalos”, which is the Greek word for glassy, and from uronic acid [3]. At that time, they didn’t know how useful and interesting will be this natural macromolecule for our life.

During the 1940s, hyaluronan was isolated from many sources such as the vitreous body, synovial fluids, umbilical cord, skin, and rooster comb and also from streptococci.

In 1972, Hardingham and Muir [4] discovered that hyaluronan interacts with cartilage proteoglycans and serves as the central structural backbone of cartilage. This was the first example of a specific interaction between hyaluronan and a protein, and many more such interactions were discovered during the 1990s.

2.1.2 Chemical structure

The chemical structure of hyaluronan was determined in the 1950s in the laboratory of Karl Meyer. Hyaluronic acid is a polymer of D-glucuronic acid alternating with N-acetyl-D-glucosamine which are linked together through alternating β-1,4 and β-1,3 glycosidic bonds (Figure 1).

In the physiological solutions hyaluronan forms a stiffened and expanded random coil which occupies very large domain. In this solution backbone is stiffened by a combination of the chemical structure of the disaccharide, internal hydrogen bonds and the interactions with the solvent.

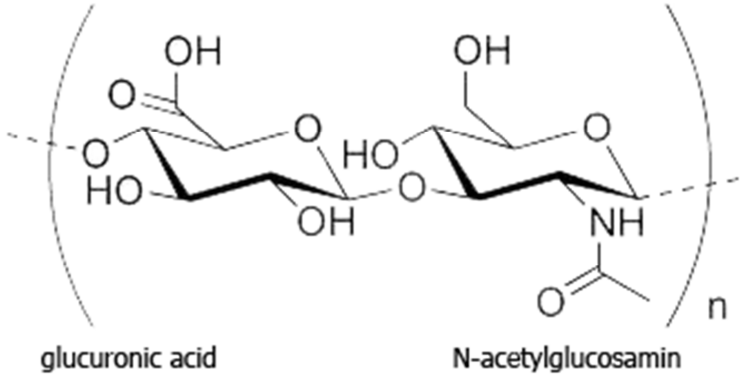

Figure 1. Structure of hyaluronan

The primary structure of hyaluronan has important consequences for the secondary structure in the solution. Glucose in β configuration allows the more space molecules to take equatorial position more advantageous sterically, while the small hydrogen atoms occupy the axial position the less sterically preferred, in the structure. Not only hyaluronan, but other polysaccharides, such as chondroitin, keratan or dermatan occupy in the aqueous solution a similar double-helix as DNA, named "two-fold helix". Hyaluronan is amphiphile because of presence of hydrophilic and hydrophobic regions in the polymer. The small molecules such as water, low molecular weight electrolytes and nutrients can diffuse freely throught the solvent in the domain. The larger molecules such as proteins are partially excluded due to their larger hydrodynamic size in the solution [2].

2.1.3 Production of hyaluronan

In general, hyaluronic acid refers to the acid form and hyaluronate refers to the salt form. These two terms for hyaluronan, however, are often used interchangeably, irrespective of which form is present in a solution. When in the salt form, it is very often sodium hyaluronate.

Commercially produced hyaluronan is isolated either from the animal and the human sources, as an umbilical cord [5] and a rooster comb [6], or from attenuated pathogenic strains of streptococci [7], through a process of fermentation or direct isolation. During the medical application of hyaluronan obtaining from the animal sources to the human body hyaluronan can induce the alergic or even inflammatory reactions. Hence, since 1980s the microbial production is gradually replacing extraction from the animal tissues in the fermentation of group C streptococci, in particular *Streptococcus equi* subsp. *zooepidemicus* [7]-[9] and *Streptococcus equi* subsp. *epui*. Hyaluronan from attenuated streptococci may have the potential to be contaminated by the pathogenic factors. Therefore, the hyaluronan production through the fermentation by GRAS (generally recognized as safe) microbial strains emerged as an attractive alternative. *Bacillus subtilis* [10],[11], S. *thermophilus* [12],[13], *Pasteurella multocida* [14],[15], *Lactococcos lactis* [16] and *Escherichia coli* [17] were used as a host.

Izawa et al. [12] at their work constructed high-hyaluronan-producing recombinant *Streptococcus thermophilus* strains to attain more than 1 g/l production of hyaluronan. The recombinant strain could be an alternative material for medical, cosmetic and food

utilization instead of hyaluronan from conventional pathogenic streptococci. *B. subtilis* does not produce hyaluronidase that could degrade the synthesized hyaluronan. Hyaluronan produced by bacteria has a higher degree of purity than hyaluronan obtained from the animal sources [18]. At present, microbially produced hyaluronan has been approved for the treatment of superficial wounds as well as for the use in the cosmetic industry.

Therefore, the companies specializing in the production of hyaluronan for cosmetic and pharmaceutical use (such as CONTIPRO) cleaner and risk-free biotechnological production. In this company hyaluronic acid is extracted from the cell walls of the bacteria *Streptococcus zooepidemicus*.

Commercially available hyaluronan is produced in the molecular weights ranging from less than 10^6 daltons to as high as 8×10^6 daltons [19],[20].

2.1.4 Occurrence of hyaluronan in living organisms

Hyaluronan is present in all vertebrates, and also in the capsule of some pathogenic bacteria such as *Streptococcus sp.* and *Pasteurella*. It is a component of the extracellular matrices in most tissues, and in some tissues it is a major constituent.

In the human body, hyaluronan occurs in the salt form, hyaluronate. The highest amount of hyaluronan is found in synovial fluid, in umbilical cord and in vitreous humor of the eye, where a transparent hyaluronan gel fills the space between the lens and the retina. More than 50 % of hyaluronan in the human body is found in the skin (the dermis and the epidermis), where it has a lot of important functions, and about 35 % in the muscles/skeleton [21]. Hyaluronan immobilizes water in the tissue and also it can influence the cell proliferation, differentiation and tissue repair. Hyaluronan occurs in lung, kidney, brain, and muscle tissue too.

2.1.5 Biosynthesis and metabolism of hyaluronan

Hyaluronan is a very dynamic tissue component. The half-life of hyaluronan in the skin and the joints is around twelve hours, in the cartilage is normally 2-3 weeks while in thebloodstream it is very short, only a few minutes [22]. This implies that a large amount of hyaluronan is cleaved during one day. The average 70 kg man has approximately 15 g of hyaluronan, 5 g of which are turned over every day. The celullar synthesis and degradation of hyaluronan are unique and highly controlled. The synthesis is usually balanced by catabolism, thereby maintaining a constant concentration in the tissue. The main degradation sites are lymph nodes, where approximately 90 % of hyaluronan is degraded. This process results in a relatively large number of fragments with different molecular weight naturally occurring in the organism.

Hyaluronan belongs to a group of glucosaminoglycans but it differs in many ways from other glucosaminoglycans. Hyaluronan is huge, usually with a molecular weight between 10^3 and 10^4 kDa, comparing with other glycosaminoglycans (15-20 kDa), and an extended length of 2–25 µm. Unlike other glycosaminoglycans, hyaluronan doesn't contain sulfate groups. As shown in the study described in this section, the mechanism of hyaluronan synthesis is unique - hyaluronan is made at the plasma membrane rather than in the Golgi apparatus; it is most likely elongated at the reducing rather than the nonreducing terminus

during synthesis; and it is not covalently linked to a protein backbone during synthesis [18],[23],[24] and [25].

Mechanism of hyaluronan synthesis

Bacteria can synthesize a wide range of biopolymers that serve diverse biological functions and have material properties suitable for numerous industrial and medical applications. Better understanding of the fundamental processes involved in polymer biosynthesis and the regulation of these processes has created the foundation for metabolic and protein-engineering approaches to improve economic-production efficiency and to produce tailor-made polymers with highly applicable material properties. Rehm [29] summarizes the key aspects of bacterial biopolymer production and highlight how a better understanding of polymer biosynthesis and the material properties can lead to increased use of bacterial biopolymers as valuable renewable products.

There are two mechanisms of hyaluronan synthesis, the first for mammalian cells and for streptococci [26],[27], and the second for *Pasteurella* [21],[28].

The most of glucosaminoglycans are made in the Golgi apparatus and they are covalently attached to core proteins and are sulfonated [22],[23],[30], while hyaluronan is synthesized at the plasma membrane as a free linear polymer without any protein core and immediately extruded out of the cell and into the extracellular matrix [31]. The biosynthesis of hyaluronan is naturally regulated by three glycosyltransferases, hyaluronan synthase-1 (HAS1), HAS2, HAS3, located in the plasma membrane [34]. These enzymes elongate hyaluronan by repeatedly adding glucuronic acid and N-acetylglucosamine to the growing chain at the reducing end using substrates UDP-N-acetylglucosamine and UDP-glucuronic acid. Other glucosaminoglycans lengthen at the non-reducing end and require a protein backbone [24],[28],[31]. Described above mechanism of synthesis is for vertebrates and Gram-positive streptoccoci. Gram-negative *Pasteurella* has a different mechanism of hyaluronan synthesis inwhich the chains are elongated at the non-reducing end [15],[21],[28].

The number of repeat units in a completed hyaluronan molecule can reach 10,000 or more, with a molecular mass of ~ 4×10^6 daltons (each disaccharide is ~ 400 daltons) [31].

Degradation

The splitting of the long hyaluronan polymers to the shorter fragments is important in many cellular processes. The resulting short chains are involved in the stimulating cell proliferation, cell migration, participate in the healing process, but also affect such survival different types of cancer cells.

Hyaluronan, as a large molecule, tends to mechanical degradation either by the ultrasonic treatment or by the thermal degradation. Physiologically, hyaluronan can be degraded by oxygen free radicals or enzymatically by hyaluronidases [33].

In mammals, enzymatic degradation of high molecular weight hyaluronan begins in the somatic tissues and continues in the regional lymph nodes, and is effectively endocytosed by the liver [22],[28]. It is then trasported to the lysosomes that contain enzymes responsible for degradation: hyaluronidases (hyase), β-D-glucuronidase and β-N-acetyl-hexosaminidase. Hyaluronidase cleaves the high molecular weight hyaluronan into the smaller oligosaccharides while β-D-glucuronidase and β-N-acetylhexosaminidase

degrade the oligosaccharide fragments by removing nonreducing terminal sugars [31],[34]-[36]. Now there are known six hyaluronidases in mammals: HYAL1, HYAL2, HYAL3, HYAL4, HYALP1 (PHYAL1) and SPAM1 (Sperm adhesion molecule 1, PH-20).

Hyaladherins

The hyaladherins have different functions. Some are matrix components, which bind to hyaluronan to form organized structures extracellularly. To these belong aggrecan, versican, neurocan, brevican, link protein and TSG-6. A second group of hyaladherins are cell surface receptors. To this group belong CD44 on the Figure 2. [23],[37], RHAMM (Receptor for Hyaluronan Mediated Motility), TLR4 (toll-like receptor 4) and laylin. The hyaluronan-endocytosing receptors in liver (stabilin-2) and lymph tissues (lymphatic vascular endothelial hyaluronan receptor - LYVE) also belong to this group. There is also one example of a protein, which binds covalently to hyaluronan, i.e. serum-derived-hyaluronan-binding-protein (SHAP).

The receptors for hyaluronan involved in the binding processes between cells, the interaction of the cells with intercellular matter and the removal of hyaluronan from tissues and blood. The most important receptors for hyaluronan are CD44 and RHAMM.

CD44 is very widely distributed cell-surface glycoprotein in the body and is recognized to be the major cell surface receptor for hyaluronan. CD44 plays a role in immune processes, especially in inflammation and cancer formation [23], CD44 is important for organogenesis and epidermal homeostasis. At the cellular level induces growth, differentiation and maturation, the process of cell attachment and motility, coordinates incoming signals leading to survival or cell death and serves as a protein to which it is collected metaloproteas matrix [37].

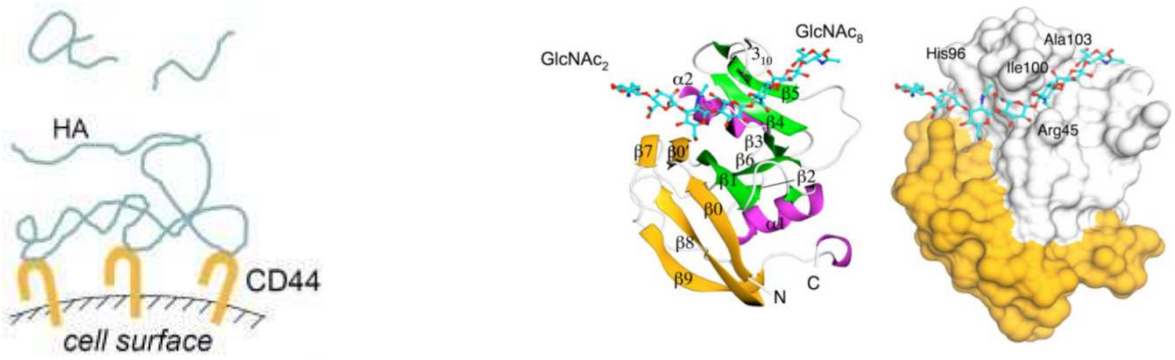

a) b)

Figure 2. a) The interaction of hyaluronan with CD44 on the cell surface [38] b) structure of the molecule CD44 [39].

2.1.6 Medical applications of hyaluronan

Hyaluronan has many physiological and patophysiological functions in organism. Hyaluronan arrange the transportation of ions and nutritive substances. The increased amount of hyaluronan is proved during wound of skin, in cancer cells or in immunity disorder (for example asthma or rheumatoid arthritis).

Thanks to its unique properties, hyaluronan has found many applications in various medical sectors: in rheumatology, ophthalmology, diabetology, pharmaceutical technology and other areas, such as the wound healing or dermal and osteoarthritis treatment [40].

We are using hyaluronic acid even in normal life, outside medical facilities. It is included in the eye drops, where creates a continuous film, which helps dry eye syndrome and insufficient production of tears. There is used in some nasal sprays where moisturize the nasal mucosa. Hyaluronan is also part of the anti-nutritional supplements as nutrition for joints and cartilages [41],[42]. The products containing hyaluronan is widely used in the pharmaceutical and cosmetic industries. It is used in preparations for shaving, night creams against wrinkles and acne, the cleansing water, in the preparations after sunbathing or hair loss. Hyaluronan is very often used in eye surgery and in ophthalmology because of viscoelastic properties, in addition to improving the properties of eye drops [18],[43].

The application as well the function of hyaluronan in organism is determined by different molecular weight of hyaluronan [68]. High molecular weight hyaluronan (MW > 1000 kDa) is used in medicine in wound healing [73] while low molecular weight hyaluronan (200-1000 kDa) binds to proteins in extracelural matrix and on cell surfaces, which is part of the receptors for many cellular processes so it is used as a drug delivery system [79] and treatment of cancer [55] or it can be found in cosmetic products. Very low molecular weight hyaluronan (10-200 kDa), other group of polysaccharides, is used for diabetic and chronic wound healing [79].

Schiraldi et al. [44] describe different fields of the application of linear, derivatized [74] and crosslinked of hyaluronan [51]. The hyaluronan derivatives (hydrogels [75]-[77], hylans) are used in tissue engineering for make of scaffolds [78] because they are highly non-immunogenic and non-antigenic [22],[43],[44]. The latest research in the direction of hyaluronan is its use as a potential carrier of bioactive substances, which would ensure the targeted delivery of drugs in the patient's body [44]. It makes use of a large number of interactions with different receptors, the best known is CD44 [45],[46]. The interactions between hyaluronan and CD44 have different physiological functions in the body of organisms, such as leukocyte activation and growth, differentiation and cell migration. There is very intensively exploring the possibility of using hyaluronan as part of a targeted drug cancer, because cancer cells contain high concentrations of hyaluronan. The research is performed with drugs such as paclitaxel [47], doxorubicin [45], diclofenac [48],[49] or gentamicin, thrombin, interferon or serotonin [43].

Recently hyaluronan is subject for research in the treatment of cancer and as a marker of many diseases including cancer, rheumatoid arthritis and pathology liver [51],[53]-[55].

Hyaluronan in targeted drug delivery

The patients with cancer increase and the research is focused on the development of carriers of cytostatics as targeted drug delivery. The cytostatic drugs in chemotherapy form have the nonspecific effect and many side effects such as nausea and vomiting, temporary hair loss, damage of immune and nervous system, cardiovascular disorders, some permanent damage of organs such as the kidney or liver. They interfer cancer cells mainly rapidly proliferating tissues but they damage healthy cells also which is other of the side effect of the treatment.

The target delivery of cytostatic drugs exactly to the cancer cells can prevent these side effects. The target carrier of drug has to be biocompatible, biodegradable and nontoxic.

Cancer of epithelial origin is associated with excessive activity of receptor CD44, which binds hyaluronan. Hyaluronan is used as a carrier and a ligand for liposomes and nanoparticles, these substances transported to the cells, which are largely activated CD44 receptor [56]. Hyaluronan is a highly hydrophilic biopolymer with massive hydration shell and lots of potent drugs are hydrophobic hence hyaluronan must be chemically modified (hydrophobized), can be used hylans, or interact with some substances which can form any hydrophobic space for solubilizing of these drugs. In second case it can be used surfactants forming micelles where drug is in the core of the micelle with hydrophobic domain which is suitable for drug solubilization and micelle is electrostatically bound to the core of a hydrophilic hyaluronan chain. Hyaluronan can interact with cell receptors and thus, the complex of hyaluronan and the hydrophobic domain is able to enter the cancer cell and release the drug inside. The complex can find just the cancer cells with no influence on the healthy cells because hyaluronan specifically binds to CD44 receptor. In this case, dose of the cytostatic can be lower and the effect of the treatment is bigger then in the case of chemotherapy.

2.2 Surfactants

2.2.1 Definition of surfactants

A surfactant, a surface active agent, is characterized by its tendency to adsorb at the surfaces and at the phase interfaces. It reduces surface or interfacial energy and therefore spontaneously concentrated in the interface. Because the surfactants reduce the surface tension of the solvents, they facilitate the dissolution and removal of impurity. Therefore surfactants are often used in cleaning and washing products. A well-known example of surfactant is soap.

The surfactants are amphiphilic; the molecule of the surfactant is consisting of two parts, one is soluble in a liquid (the hydrophilic part) and the other is insoluble (the hydrophobic part) (Figure 3). The hydrophilic one or polar moiety is called head and hydrophobic or nonpolar moiety is named tail. The surfactant head can be charged (anionic or cationic), dipolar (zwiterionic) or non-charged (nonionic). Hydrophobic part can be branched or linear and mostly consists of a carbon chain with the length of chain between 8-18 carbon atoms). The rate of branching, the position of the polar groups and the length of chain are important parameters of the physiological properties of the surfactant [52],[56].

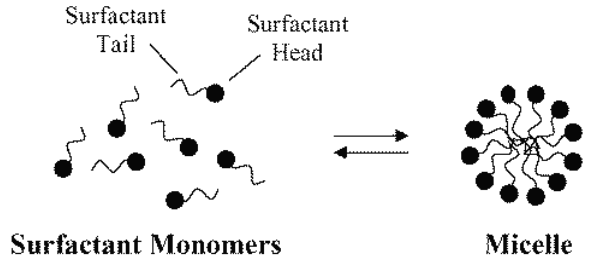

Figure 3. Free surfactant and formation of micelle [56].

The nonpolar part causes the molecule is only slightly soluble in water, while the polar portion extensively reacts with water. For solubilization of the substance in water, it has to contain strongly hydrophilic group and that there was an association, molecule has to have a sufficiently long hydrocarbon chain. The hydrophobic portion of micelles is directed to the cluster and the polar group is directed into the solvent [58].

The classification of the surfactants is made on the basis of the charge of the polar head group, ionic and nonionic. The ionic surfactants are divided into anionic, cationic and zwiterionic (sometimes called amphoteric). Most of the anionic surfactants have sodium ion, but there are also other, lithium, potassium, calcium and protonated amines. The cation ion is usually halide or methyl sulfate. Nitrogen atom is basis of cationic surfactants, either amine or quaternary ammonium salt [52],[56].

2.2.2 Micelles and critical micelle concentration

The surfactant, which is presented at low concentrations in a system, absorbs onto surfaces or interfaces significantly and there is changing the surface or interfacial free energy. The surfactants usually act to reduce the interfacial free energy, although there are occasions when they are used to increase it. When the surfactant molecules are dissolved in water at concentrations above the critical micelle concentration (CMC) they form aggregates known as micelles. In a micelle, the hydrophobic parts are directed to the cluster in order to minimize their contact with water, and the polar groups remain into the solvent in order to maximize their contact with water (Figure 3) [58]. All of these result in minimal contact between water molecules and hydrophobic parts of surfactant molecules. The size and shape of the micelles depends on the concentration, temperature, molecular structure of the surfactant and the character of the intermolecular forces, including hydrophobic, steric, electrostatic, hydrogen bonding, and van der Waals interactions. The radius of these micelles is approximately equal to the length of surfactant molecules. The aggregation number is defined as the number of molecules forming a micelle. The value of number is mostly between 50 and 150 and increases with the hydrocarbon chain length and decreases with the size of the area, which one polar group occupies on the surface of the micelle. The increasing of the hydrocarbon chain length or the adding of salt degreases the critical micelle concentration and increases aggregation number, while raising the temperature increases the critical micelle concentration and decreases aggregation number [56],[58].

If the content of the surfactants in the solution is growing, the concentrations of spherical micelles increase and there is gradually changing shape of the micelle. Hydrocarbon chains begin to orient parallel to each other and there are formed cylindrical micelles, which can produce hexagonal liquid crystals at higher concentrations; in even greater concentrations are made up laminar shapes called McBain micelles which are composed of two layers of the surfactants, which are facing each other hydrocarbon chain and polar groups directed out. Increasing of the content of the surfactants in the solution (in reducing content of water) decreases mobility of micelles and it leads to their associate, especially end parts, and creates dimensional network structure of coagulation - the gel [56].

Harley micelles which are formed in the aqueous medium were discussed. The surfactants may also create micelles in non-polar solvents, e.g. in hydrocarbons, benzene, cyclohexane, chloroform etc. They are called reverse micelle and have opposite orientation, their heads are

oriented in the hydrophilic cores and the nonpolar tails are hydrophobic and are oriented to the solvent. The aggregation number of these micelles is not greater than 10 [58],[59].

The critical micelle concentration (CMC) can be determined by the change in the physicochemical properties, such as surface tension, conductivity – in case of ionic surfactants, osmotic pressure, detergency, etc. [60]. These properties are plotted as a function of surfactant concentration (or its logarithm, in case of surface tension). The break in the curve of each property corresponds to the critical micelle concentration and the formation of micelles is from that point [56],[58],[59].

2.2.3 Micelle solubilization

An important property of micelles, which is associated with the construction of the micelles, is solubilization, the ability to increase the solubility of low soluble substances in water.

There are a number of possible locuses of solubilization for a drug in a micelle, e.g. on the surface of the micelle, between the hydrophilic head groups of micelles, in the layer between the hydrophilic groups and the first few carbon atoms of the hydrophobic group or in the inner core of the micelle for the solubilization of completely insoluble hydrophobic drugs [57].

2.3 Polymer-surfactant systems

Hyaluronan can interact with

other polymers or with the surfactants, depending on it is forming either micelle polymer [44],[57] or polymer-surfactant systems [61],[63].

The surfactants and water-soluble polymers have a wide application. The products contain one or more polymers together with one or more surfactants. They can be used to achieve different effects - colloidal stability, emulsifical, flocculation and structural properties. The surfactants with polymers can be found in various products such as cosmetics, paints, detergents, food and manufacturing of pharmaceuticals and pesticides.

The effect of the polymer on the surface tension of water solution varies according to surfactant concentrations. At a certain concentration, break will be on curve of the surface tension and there is reached approximately constant value. Then there is the concentration area, where is possible to find a constant value of surface tension. Finally there is a decrease to the value measured without the polymer.

The widespread method for characterization the system polymer-surfactant is surface tension measurement. It is based on the fact that surfactantslower surface tension of the solution and the break point on the surface tension curve against concentration is observed at critical aggregation concentration (CAC). The complex behaviour of such a system is shown in Figure 4.

The concentration dependence of surface tension in the presence of polymer is shown in Figure 5. At the certain concentration, called critical association concentration (CAC), the surfactant starts to associate to the polymer. Consequently, there is no observed futher increase in surfactant activity and no further reduction in surface tension. Because the polymer is saturated with the surfactant, the activity and the concentration

of unimer units of the surfactant begins to rise again and there is observed the reduction of surface tension, until the value of the critical micelle concentration. After this point the surface tension is constant and micelles begin to form [52],[63],[81].

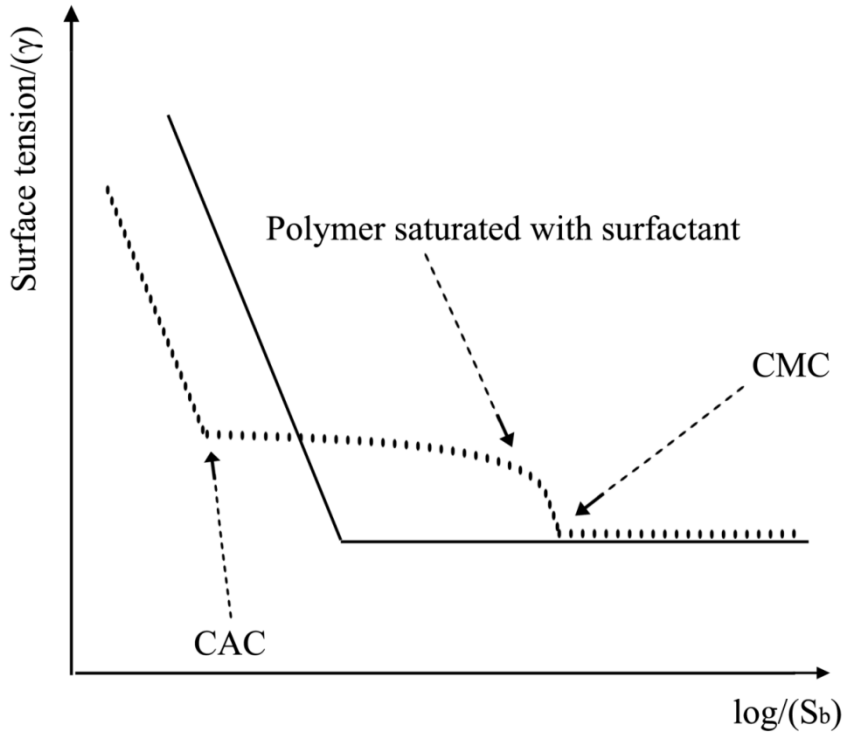

Figure 4. Schematic plott of surface tension against log(bulk surfactant concentration). Surfactant solution with the polymer - dotted line, the curve containing a surfactant only -solid line. Critical aggregation concentration (CAC) and critical micelle concentration (CMC) [63].

The binding study of polymer-surfactant solutions (ionic surfactant and nonionic homopolymer) are describes in Figure 5. At low concentrations of the surfactant there is no agregation in any concentration of polymer (I). Above a critical agregation concentration (CAC), agregation is increased to surfactant concentration which increases linearly with the polymer concentration (II). Upon further increasing the concentration of the surfactant is an association of saturated (III). In Area IV are clusters of the surfactant on the polymer chain and free micelles [52].

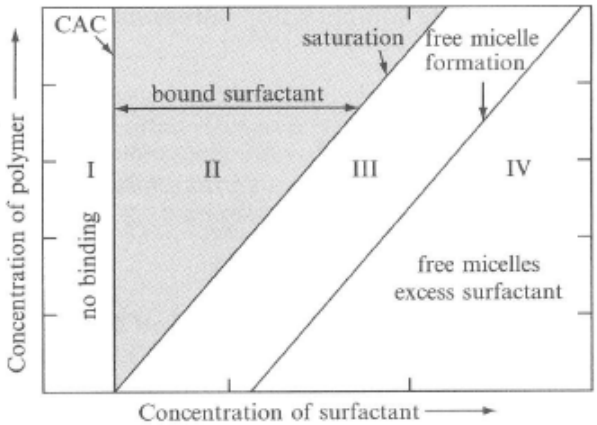

Figure 5. Agregation of homopolymer and surfactant in the different concentration [52].

Polymer–surfactant interactions

There are two alternative theoris of mixed polymer-surfactant solutions, in this case negatively charged hyaluronan with cationic surfactant. One describes the interaction in terms of an association or a binding of the surfactant to the polymer, and the second in terms of micellization of surfactant on or near the polymer chain. Both descriptions are useful and overlapping each other. The aggregates take the form of surfactant micelles attached to the polymer chains and this structure is called the "pearl necklace model" (Figure 6). In the presence of the polymer, chemical potential is lower and the polymer micelle formation begins at lower concentration (critical aggregation concentration) than without polymer (critical micelle concentration) (Figure 4) [52],[60],[63],[81].

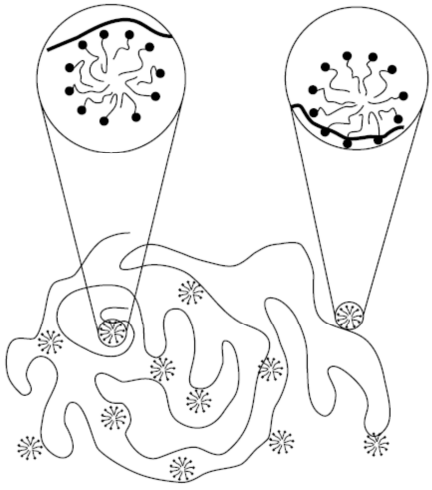

Figure 6. Pearl-necklace model of a polymer-surfactant association [52].

Added surfactant strongly reacts with the hydrophobic groups of the polymer, leading to increased links between polymer chains, thereby increasing the viscosity. It is proved to hydrophobic modified celulose ether (HM-EHEC), surfactant SDS significantly increases the viscosity for HM-EHEC, but the unmodified EHEC increases only slightly. When the content of surfactant is increased, the effect of viscosity is lost. For the purpose of cross-linking must be sufficiently high number of polymer hydrophobe per micelle.

At higher concentrations of the surfactant, the only one polymer hydrophobe in a micelle and all cross-linking effects disappear. Thus self-association of hydrophobe modified water-soluble polymer can be strengthened or weakened, depending on the stoichiometry. Viscosity can also be affected by electrostatic bonds. The adding of the opposite charged surfactant into the solution of modified hydrophobic polyelectrolyte gives a much higher viscosity than nonionic surfactants or similarly charged surfactants. By increasing the temperature there is an induced gelation, and by cooling, gel melts. This effect can also be achieved in a mixture of nonionic surfactant and hydrophobically modified water-soluble polymer [52].

The use of polymer-surfactant system is based on different effects, such as overseeing the phase behaviour or regulating of interphase properties. Polymer-surfactant systems have some advantages compared with other drug carriers. For example, micelles can be obtained easy and reproducible way and specific ligands can be attached to their outer surface in order to optimize the controlled releasing and specificity of pharmacological effect. In this thesis, as a polymeric carriers is used hyaluronan which is soluble in water or physiological solution and has specific receptors for the binding to the right molecules, for application of target delivery. Micelles, on the other hand, offer a core/shell structure, where drug can be inserted [57].

Drug carriers should be stable in vivo for sufficiently long periods of time without provoke any biological reactions. Release of the drug should be started after contact with target tissues/cells and the components of the carrier (surfactant molecules) should be easily removed or biodegradable, in the case of hyaluronan, from the body when the therapeutic function of drug is completed [57],[82].

2.4 High resolution ultrasonic spectroscopy (HR-US)

There are many spectroscopic analytical methods for the characterization of liquid samples. Most of them measure parameters of waves propagating through the analyzed sample. The classical spectroscopy methods (UV, VIS, IR, NMR etc.) are based on monitoring interactions of electromagnetic radiation with observed sample. These methods are employing in the ultraviolet, visible and infrared range frequencies. Ultrasonic spectroscopy is simply spectroscopy employing sound waves. In particular, it uses a high frequency acoustical wave (similar or higher to those used by dolphins for communication and bats for navigation), frequencies 20-100 kHz. We usually observed changes in this radiation evoked by its pass of the sample in ultrasonic spectroscopy. The greatest advantage of ultrasonic waves is that they can penetrate most materials, including those that are opaque to electromagnetic waves.

The relationships between a material's properties and acoustical characteristics have been studied for a long time and ultrasonic techniques have been used in non-destructive testing and imaging for decades. Taking advantage of ultrasonic to detection is known especially in field of medicine and defectoscopy of constructions or materials. Technical progress, when there are available high resolution ultrasonic spectrometers, have made possible expressively spread spectrum of ultrasonic application in colloid chemistry.

2.4.1 Basic principles of ultrasonic spectrometer

Ultrasonic wave is a wave of longitudinal deformations where compressions and decompressions occur in the direction of the propagation of the wave.

The molecules respond through the intermolecular forces (intermolecular repulsion and attraction) reflecting the micro-elasticity of the sample. High resolution ultrasonic spectroscopy is technique that can measure these intermolecular forces directly.

Ultrasonic spectrometry is based on detecting interactions of ultrasonic wave with studied sample. There are two parameters which are measured - ultrasonic velocity (speed of sound) and ultrasonic attenuation.

Velocity of ultrasonic wave is determined by local elasticity and density of the medium. Elasticity is usually dominating and extremely sensitive to molecular organization and intermolecular interactions. Effect of the density and the elasticity can be illustrated as follows: solids have the strongest interactions between the molecules followed by liquids and gases. Therefore solids are more rigid (have higher elastic modulus) compared with liquids and gases. For this reason sound travels faster in solids than it does in liquids and gases. Ultrasonic velocity decreases in the order solids > liquids > gases. In short, wave travels faster in more rigid medium [68],[69].

Amplitude of ultrasonic wave is usually decreased after travelling through some medium; an ultrasonic wave loses its energy. Ultrasonic attenuation is a measure of this lost. Attenuation is determined by the energy losses in compressions and decompressions in ultrasonic waves, which include absorption and scattering contributions (Figure 7).

In the homogenous samples (Figure 7) source of attenuation is able to illustrate as anoscillation of the equilibrium position of the chemical process A + B <=> AB. In compression period of transporting wave the reactants are like compressed in direct formation of products. In decompression period it leads to the relaxation to the equilibrium state causes absorption of energy. In these cases the measurements of the attenuation allows observing the kinetics of fast chemical reactions and particle sizing in emulsions and suspensions.

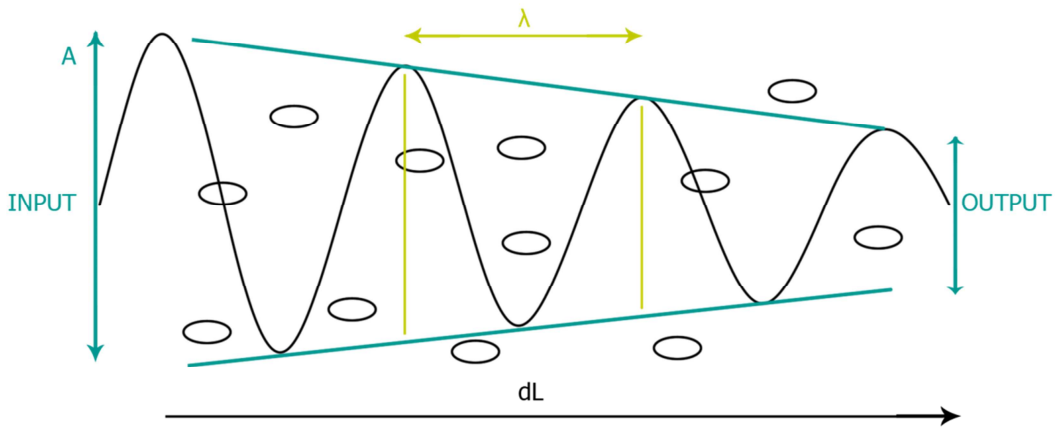

Figure 7. Attenuation in the sample.

In the heterogonous samples attenuation is a result of ultrasonic scattering on dispersed particles. Thus measurement of attenuation is basic for the determination of colloid particle sizing in emulsions and suspensions and their distribution. Scattering of ultrasonic wave on particles results in a decrease of the amplitude of the wave (ultrasonic attenuation) and the dispersion of the ultrasonic velocity. The contribution of the ultrasonic scattering is determined by the volume fraction of dispersed particles. The ultrasonic wave loses its amplitude (energy) because of scattering effects.

As measurements of attenuation do not require high temperature stability of the sample, they can be performed in large samples. That is why attenuation was the parameter responsible for the largest portion of past ultrasonic applications in research, such as the kinetics of fast chemical reactions and particle sizing in emulsions and suspensions.

The application of ultrasonic velocity requires high resolution of the measurements, which cannot be achieved in large samples because of the difficulty of controlling the temperature. It is because of the difficulty in resolving both sets of information that scientists tended to belong to research groups working on the measurement of either attenuation or velocity and adjusted their instruments for the best performance in the selected area [69].

2.4.2 HR-US

High resolution ultrasonic spectroscopy (HR-US) is a new technique for material analysis based on the measurements of parameters of ultrasonic waves propagating through samples. This technique is based on the measurements of velocity and attenuation on acoustical waves at high, ultrasonic frequencies propagating through materials. This technique allows direct and non-destructive measurements without formation of derivatives or changing state of sample. Advantage of this technique is the ability of ultrasonic waves to propagate through optically non-transparent materials. The analyzed sample can be highly coloured or even opaque.

When we speak about ultrasonic spectroscopy with high resolution we have in mind measurement of velocity that is measured with high resolution. Faculty of chemistry in Brno University of Technology has this spectrometer from Irish company Ultrasonic Scientific which developed technology enabling improved resolution in measurements of ultrasonic velocity a few degrees. Whereas traditional equipments measure velocity with resolution about 0.1 m/s high resolution apparatus achieves 0.0001 m/s resolution, i.e. about 10^{-5}% in common aqueous solutions. Attenuation, other parameter of measuring with HR-US, is measured in classical resolution (0.2 %) and we need more concentrated solution for its measurement. Range of applicability of high resolution ultrasonic spectrometer isn't only given itself resolution but also variability of measurement modes. In additional to measurements of velocity and attenuation of ultrasonic it is able to measurement in various modes – kinetic, titration or programmed temperature.

Standard measurements in spectrometer are performed as comparative, i.e. measurements take place simultaneously in reference cell filled up e.g. by pure disperse media, and in sample cell containing the sample. The difference between the two measured values (sample and

reference) is used for evaluation. Moreover it is possible to run the measurement at several selected frequencies of ultrasonic.

Which major techniques are used for high-resolution ultrasonic measurements? There are two main methods for precision measurements of ultrasonic velocity and attenuation. The pulse technique, the so-called sing around method, is the first method. In this case the ultrasonic velocity is determined through direct or indirect measurements of the time of propagation of the transmitted ultrasonic pulse through a liquid. The ultrasonic attenuation is determined from the change of amplitude of the pulse [65],[67]. The second method is the resonator technique; know also as the fixed-path interferometer. In this method, the ultrasonic cell forms an acoustic resonator. The ultrasonic velocity is determined through the measurements of frequency or the wavelength of the ultrasonic in the resonance. The ultrasonic attenuation is obtained from the energy losses in the resonance.

Measuring principles

In this technique the ultrasonic parameters of the liquids are obtained through the measurements of resonance characteristics of acoustic resonators. The construction of a resonator cell involves two main elements, the resonator chamber, where the acoustic resonance is formed, and the piezotransducers, which excite and detect the ultrasonic vibrations. An illustration of a plane parallel type resonator is given in Figure 8.

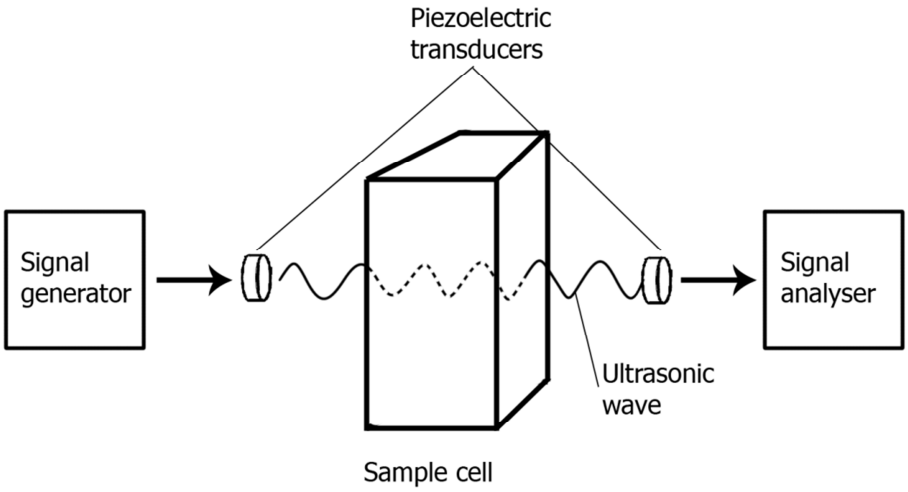

Figure 8. The basic principle of high-resolution ultrasonic spectroscopy.

A signal generator produces an electronic signal which causes the transducer to vibrate. This vibration sends a mechanical wave travelling in the direction of the second piezotransducer. At the frequencies corresponding to a whole number of half wavelength between the piezotransducers, a resonance occurs, resulting in an increase in the amplitude of the signal detected at the receiving piezotransducer. In an ideal resonator, where the effects of diffraction, non-ideal reflection and others can be neglected, the resonance condition can be expressed by the relationship

$$n\lambda_n/2 = L \quad (1)$$

where n is any whole number – ID number of peak, λ_n is the ultrasonic wavelength in the sample at the n^{th} resonance and L is the distance between the piezotransucers. The wavelength (λ) is determined by the value of ultrasonic velocity (u) and frequency (f):

$$\lambda_n = u/f_n \tag{2}$$

where f_n is the frequency at the maximum of the n^{th} resonance. The combination of above equations gives the relationship between the change of the ultrasonic velocity (δu) and the corresponding shift of the frequency of the n^{th} resonance (δf_n):

$$\delta u/u = \delta f_n/f_n \tag{3}$$

The absolute value of the ultrasonic velocity can be obtained from the frequencies of any two n^{th} and $(n-1)^{th}$ resonances:

$$u = 2L(f_n - f_{n-1}) \tag{4}$$

The distance between the piezotransducers (L) can be determined from the measurements of ($f_n - f_{n-1}$) for the resonator filled with a liquid with a known value of ultrasonic velocity. [85]

High resolution ultrasonic spectroscopy allows direct probing of microstructural organisation and intermolecular forces in a variety of colloidal systems. Ultrasonic wave is a wave of oscillating pressure and associated longitudinal deformation travelling through sample. Molecules in the sample respond to oscillating deformations through inter-molecular repulsive (compression) and attractive (decompression) forces reflecting the measured elasticity of the sample. Elasticity is the major contributor to the first characteristic measured in this technique, ultrasonic velocity. Propagating through the medium, the ultrasonic wave loses its energy and is subjected to a scattering process, which causes ultrasonic attenuation. Attenuation (or attenuation coefficient), the second measured parameter, is determined by the reduction in amplitude of an ultrasonic wave which has travelled a known distance through a medium per unit travelled distance. The major contributors to attenuation are fast chemical relaxation and microstructure of non-homogeneous samples. The high resolution refers primarily to the measurement of velocity and is achieved by parallel measurements of ultrasound propagation in sample and reference cells. The reference cell is filled with the pure solvent (water or NaCl solution in our case).

2.4.3 Benefits of ultrasonic analysis

High resolution ultrasonic spectroscopy has major advantages over many other conventional methods. HR-US probes the elastic characteristics of materiasl, which are extremely sensitive to interemolecular elastic characteristics of materials, which are extremely sensitive to intermolecular interactions. So the ultrasonic method is used to analysis of a broad range of molecular processes, which can not be analysed or are difficult to analyse with other techniques [71]. At optical techniques concentrated dispersions have to be diluted in order to achieve sufficient optical transparency and avoid multiple scattering. In HR-US, ultrasonic waves can propagate through concentrated dispersions. Also ultrasonic can propagate through a broad range of samples including opaque materials, it possible to measure the speed of enzymatic reactions in aqueous solutions as well as in blood or tomato juice, samples where traditional spectroscopy fails. It can analyse chemical reactions, transitions and seconds

without optical markers, meaning that the reaction or system can be studied in its natural state-processes as fast as 10^{-5} to 10^{-7}.

Modern ultrasonic cells do not have any cavities or sharp corners allowing for easy filling, refilling, cleaning and sterilization. We can measure even aggressive liquids such as organic solvents, acids and bases and others. Semi-solid cells are also available for samples such as biological tissues, gels, toothpaste, waxes, pastes, creams etc.

Other advantage is necessary small volume samples (about 1 ml) for standard measurement; it is possible to provide even cells for very small volume (about 30 μl), cells for semi-solid materials such as gels otherwise cells for measurement in increased pressure or automatic titrating doser.

Ultrasonic spectroscopy is non-destructive method and allows us to obtain information about the high frequency and the sample keeps intact. Small or no claims to modification of the samples is other advantage of this method.

The construction of modern ultrasonic cells allows controlled stirring of the sample. It also allows the measurement of ultrasonic velocity and ultrasonic attenuation in the course of titration, useful for the analysis of ligand binding, adsorption of molecules on the surface of particles in colloid systems and complex formation phenomenon.

The measurements are performed in short measuring time, on small volumes (from 4 ml down to 30 μl.). Except pure measurements of velocity and attenuation of ultrasonic it is possible to do measurements in kinetic, titration or temperature modes and to use high-resolution ultrasonic spectrometers in HPLC and similar applications. Because the ultrasonic velocity and attenuation can be measured simultaneously at different wavelengths as a function of time the instrument can be used for the analysis of the kinetics of chemical reactions and processes, such as the analysis of enzymatic activity.

The measurements are completely computer controlled and results are presented in a graphical and digital format.

2.4.4 Application of high resolution ultrasonic spectroscopy

Ultrasonic analysis can now be easily performed in chemistry, physics, biotechnology, pharmaceuticals [89], food [90], biotechnology, agriculture, environmental control, medicine, oil, petroleum and gas industries [91]. The users of high-resolution ultrasonic spectrometers can measure chemical reactions [92], composition analysis [93], conformational transitions in materials, aggregation [94] and gelatinisation [95], crystallisation [71], particle and droplet sizing [96], phase transitions, adsorption on particle surfaces, stability of compounds such as emulsions and suspensions [97],[98], micelle formation [99] and measurements of the critical micelle concentration, composition analysis or ligand binding [85],[87]. Fakhari et al. [88] used HR-US 102 for assessment differences in hyaluronan nanoparticle compressibility. The 17kDa hyaluronan nanoparticles showed a significantly lower differential wave velocity compared to the 1500 kDa hyaluronan nanoparticles, which was indicative of higher nanoparticle compressibility.

2.5 Densitometer DSA 5000M

In 1967, the company Anton Paar GmbH presented the first digital density meter for liquids and gases. It was the first instrument to employ the oscillating U-tube principle by Dr. Hans Stabinger and Prof. Hans Leopold for density determination. The instrument can measure density and ultrasonic velocity simultaneously. Using of density measurement, the machine can do a precise density and concentration measurement of food, beverages, sugar, oleum, hydrochloric, phosphoric, nitric, boric acid, sodium hydroxide, ammonia, sulfuric acid up to 90 %, hydrogen peroxide, glucose, ethanol, hydrocarbons, fuels, lubricants and liquefied petroleum gas. By the using of sound velocity measurement, the machine can do a precise sound velocity and concentration measurement of food, beverages, sugar, alkalis, solvents, emulsions, reaction monitoring, sulfuric acid above 90 %, oleum, acetic acid, sodium hydroxide, potassium hydroxide solution, oil in refrigerants, acids in particular measuring ranges, phase separation, interphase detection. Density meter in the regime combined density and sound velocity measurement can do precise concentration measurement of food, beverages, mixture sucrose/inverted sugar/water, formaldehyde/methanol/water, sodium chloride/sodium hydroxide/water, concentration of sulfuric acid and oleum, emulsions and reaction monitoring.

The density measurements are based on the oscillating U-tube principle. The density (ρ) of the sample liquid is calculated from the frequency period τ of the oscillating U-tube filled with the sample liquid using the equation:

$$\rho = A \cdot \tau^2 - B \tag{5}$$

where A and B are the apparatus constants which incorporate the factors of volume, mass, and elastic modulus of the oscillating tube. Their values are determined by calibrating with two substances, water and air, of the precisely known densities, ρ_1 and ρ_2.

U-shaped glass tube (Figure 9) is electronically excited to harmonic oscillation at its characteristic frequency. The period of oscillation (the characteristic frequency change) is dependent on thedensity of the sample in the tube. Therefore, by measuring the period of oscillation, the density or density-related values can be calculated to a high level of accuracy.

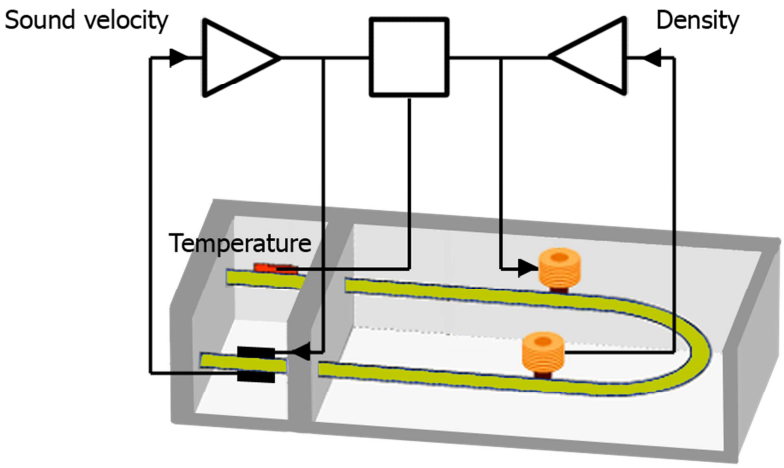

Figure 9. A scheme of U-shape glass tube of density meter DSA 5000M.

The sample flowes perpendicular to a sound signal during density and sound velocity measurement. The speed of sound is measured between a transmitter and a receiver and temperature compensation is achieved using an integrated Pt 1000 temperature sensor.

In view of the high dependence of density and ultrasonic velocity on the temperature, the measuring cell has to be accurately thermostatted using integrated Peltier thermostat with Pt 1000 temperature sensor. The sample flows continuously through the vibrating U-tube sensor. The characteristic frequency of vibration is measured and the separate evaluation unit instantly translates the signal into a density value.

3 STATE OF ART

3.1 Hyaluronan and density meausurement

The solution properties of hyaluronan are well documented, particularly with respect to the chain structure and size, rheology, and electrolyte-related properties. Rinaudo [101] states that there is nothing much remarkable in the behaviour of hyaluronan in solution. It is a typical semi-flexible polyelectrolyte with the properties dependent on the concentration and on the molecular weight. Even at low concentrations the zero shear viscosity is high and the complex viscosity remains non-newtonian which contribute to much higher apparent molecular weight of entangled hyaluronan chains. The review [102] summarizes the studies of hydrodynamic properties of hyaluronan in neutral aqueous solutions in the presence of physiological NaCl concentration as the expected behaviour of a high molecular weight linear semi-flexible polymer. The dependence of the intrinsic viscosity on hyaluronan molecular weight follows the predicted change from short extended chains to longer chains coiled into spheres as the molecular weight increases. The unusual high viscosity of hyaluronan solutions arises from the huge hydrodynamic volume and also from transient interchain interactions. The significant nonideality found for hyaluronan solutions could be predicted by simple models for hydrodynamic interactions between polymer chains.

The studies on the density of hyaluronan solutions are scarce. Gómez-Alejandre et al. [103] measured the density of high molecular weight hyaluronan (1.5 MDa) either in water at different pH or in the presence of several inorganic salts. In water and in $CaCl_2$ solution they also determined the effect of temperature. Their main interest was the determination of the partial specific volume at infinite dilution and the density data were not analyzed and discussed. Some density data are reported in the paper [104] but its main aim was the study of viscosimetric behaviour of hyaluronan in aqueous and water-alcohol solutions. Only single hyaluronan sample of high molecular weight (1.43 MDa) was used in this work and the density was reported for five concentration points at 20 °C and 50 °C. No analysis of density data was given.

García-Abuín et al. [104] studied the influence of the polymer concentration, temperature, electrolyte presence and use of co-solvents on the rheological behaviour of hyaluronan water solutions. Vibrating tube densitometer and a sound analyser Anton Paar DSA 5000 was used for the measurement of the density and sound speed of hyaluronan. They discuss the dependence of density and the speed of sound on concentration of hyaluronan and on the temperature. The value of the density and of the speed of sound increases with the concentration of hyaluronan. This behaviour might indicate slight interactions among the polymer-solvent and polymer-polymer molecules. They measured the influence of the temperature on the density value and the sound speed too, in the range of temperature 10-50 °C. The value of the density decreases and the value of the sound speed increases with the rise of temperature.

The effects of temperature and concentration on carboxymethylcellulose [109], chitosan [110] and polyethylene glycol [111]-[113] have been studied by density measurements. Some authors calculated apparent molar volumes or adiabatic compressibility from the measured densities and ultrasonic velocities for study of interactions of glycine

with polyethylene glycol [114], study of system β-cyclodextrin-alkyltrimethylammonium bromides [115] or chitosan [110]. In our work the adiabatic compressibility of the aqueous solution of hyaluronan was calculated from the density and ultrasonic velocity data which are obtained by measuring at oscillating-U-tube densimeter and it have been compared with other works [106] [108].

Our interest in density data of hyaluronan solutions comes from the studies of hyaluronan and its interactions measured by means of high resolution ultrasonic spectroscopy. The ultrasonic measurements are usually accompanied by the measurements of density in order to enable the calculations of compressibility from ultrasonic velocity and density. There are several studies on ultrasonic propagation in hyaluronan solutions. The speed of sound of hyaluronan with molecular weight 1.43 MDa is reported in ref [104] for the density and is not further analysed. Suzuki and Uedaira [105] and Davies et al. [106] used compressibilities for the study of hyaluronan hydration.

3.2 Polymer-surfactant systems

Surfactants and water soluble polymers have very broad ranges of applications [48],[116]. The main types of the polymer-surfactant interactions can be relatively weak interactions between the polymer chains and the surfactant groups or strong electrostatic interactions between oppositely charged polyelectrolytes and surfactant head groups. The kinetics of surfactant binding onto polymers, as relaxation times, and the thermodynamic quantities controlling polymer-surfactant interactions, is presented and discussed in the reference [117]. There is used lot of biopolymers as cellulose [117],[118], carboxymethylcellulose [119],[120], chitosan [118],[128], DNA [122]-[125], gelatin or lysozyme [126],[127].

Bao et al. [119] studied the interactions between surfactants and polysaccharides in the aqueous solutions. They used different six combinations of neutral, positively and negatively charged polysaccharides as methylcellulose, chitosan and κ-carrageenan with anionic (SDS) and cationic (CTAB) surfactants.

Hyaluronan is a very hydrophilic polymer surrounded by a massive hydration shell. Due to the presence of dissociable (carboxyl) group on its basic unit, hyaluronan has a character of a polyelectrolyte. At physiological pH, the carboxyl groups are predominantly ionized, the hyaluronan behaves like a polyanion and can interact with or associate cationic counterions to maintain charge neutrality. Hyaluronan interactions with positively charged surfactants were thus studied as a specific case of polyelectrolyte-surfactant interactions [52]. Hyaluronan-surfactant complexes containing hydrophobic domains formed by surfactant molecules and bound to hyaluronan chain can also be a potential carrier system for water-insoluble pharmaceutics agents. A series of papers by Swedish research groups provided a detailed study on phase behaviour of systems containing water, hyaluronan, alkyl trimethylammonium bromides (tetradecyl derivative was the most studied type) and salt (mostly NaBr) [61],[62],[129],[130]. Binding of surfactant to hyaluronan was detected for surfactants with alkyl chain consisting from at least ten carbon atoms. The binding was found to be considerably weaker than for most other carboxyl-containing polyelectrolytes, due to the low linear charge density of hyaluronan. Thalberg with Lindman [61],[62] studied interactions between hyaluronan and alkyltrimethylammonium bromide of various chain lengths (8, 9, 10, 12, 14 and 16 carbons in the alkyl group) by phase separation, conductivity

and NMR self-diffusion. Their results indicate that there is needed certain minimum concentration of surfactant for marked formation of hyaluronan-surfactant complexes. Below this concentration, the only general electrostatic interactions take place. The binding of surfactant to hyaluronan was detected for surfactants with least ten carbons in the alkyl chain. In the case of the surfactants with shorter chain then 10 carbons in alkyl chain, there is energetically preferred formation of free micelles to binding surfactant to hyaluronan. Their results of measuring showed that very low concentrations of surfactant suffice to binding surfactant to hyaluronan. The value of concentration of surfactant is bellow critical micelle concantration of certain surfactant. With the growing number of carbons in alkyl chain, the value of concentration of surfactant decrease.

Most of the authors used cationic surfactants because of the negatively charged hyaluronan chain. System tetradecyltrimethylammonium bromide-hyaluronan in water and salt (NaCl, NaBr) was published in papers [61],[84],[118].

The aim of the reference [131] was to obtain additional information on hyaluronan-surfactant interactions in solutions with physiological salt concentration (0.15 M NaCl) by tensiometry and fluorescence probe technique. Reference [131] found effect of low (90 kDa) and high (1400 kDa) molecular weight hyaluronan on the critical micelle concentration as determined by pyrene and surface tension methods. They used non-ionic (Tween 20, Octyl-β-$_{D}$-glucopyranoside) anionic (SDS), cationic (TTAB, CTAB, CTAT) and zwitterionic (Cetylbetaine, Betadet THC2) surfactants. The dependence of surface tension on surfactant concentration in the physiological solution showed no or small effect of hyaluronan (of any molecular weight) on the surface activity and particularly on the micellization. The value of the critical micelle concentration was practically not affected by the addition of hylauronan in tensiometry measurement. Fluorescence results showed, that althought the presence of sodium chloride may supress interactions between oppositely charged polyelectrolyte and surfactant, the interactions are still present in some hyaluronan-surfactant systems. The greatest influence of hyaluronan was observed on Tween 20 and hexadecyltrimethylammonium bromide. In the presence of hyaluronan, the critical micelle concentration was significantly decreased in Tween 20 and increased in the case of CTAB in comparing in the absence of hyaluronan. For both surfactants the micellization region was substantially broadened in comparing without hyaluronan.

The interactions of hyaluronan with dodecyldimethylamine oxide (DDAO) and another dimeric surfactant (dimeric quarternary ammonium surfactant 12-8-12, 12 carbon atoms in the chain, 8 carbon atoms in the spacer) was studied in [132],[133]. From a light scattering measurements of hyaluronan in aqueous sodium chloride solution have been calculated molecular weight, second virial coefficient, radius of gyration, and hydrodynamic radius.

Pisárčik [132] with his colegues calculated the number of positive charge of dimeric surfactant unit per one negatively charged hyaluronate disaccharidic unit in hyaluronan-surfactant complex. First they calculated the number n_{ps} of dimeric surfactant units in hyaluronan aggregate as

$$n_{ps} = \left(M_{ps} - M_{p}\right)/M_{s0} \tag{6}$$

where M_{ps} is the molecular weight of hyaluronan-surfactant complex, M_{p} is the molecular weight of hyaluronan without surfactant addition, and M_{s0} is the molecular weight of surfactant dimer.

The number of disaccharide unit n_p

$$n_p = M_p/M_{p0} \quad (7)$$

where M_{p0} is the molecular weight of one disaccharide unit of hyaluronan (390.3 g/mol). Then they could calculate the ratio n - number of positive charge of dimeric surfactant unit per one negatively charged hyaluronate disaccharidic unit in hyaluronan-surfactant complex as follows

$$n = 2n_{ps}/n_p. \quad (8)$$

There is a slight excess of positive surfactant charges per one negatively charged disaccharidic unit in the region around critical micelle concentration and the hyaluronan-surfactant complex is not far from electroneutrality. The excess adsorption of surfactant is observed at high surfactant concentrations.

3.2.1 Polymer-surfactant systems studied by HR-US

There are not many references about interactions of cationic surfactant with hyaluronan measured by means of high resolution ultrasonic spectroscopy. The main reference for this thesis is an article by Buckin et al. [125], where they worked with DNA polymer and cationic surfactant (C_{12}TAB). The complexes of cationic surfactant with DNA play important role in the construction of liposomal genetic delivery systems. They studied the complex formation by using combination of high-precision ultrasonic velocity and density measurements.

Buckin et al. [125] used the high resolution ultrasonic spectrometry to study the DNA interactions with cationic surfactants. Combining ultrasonic data with measurements of density they found a high value of the effect of surfactant binding to DNA on compressibility. This could not be explained by hydration changes only. It was considered as an indicator of the formation of micelle-like aggregates of surfactants on the DNA surface with a highly compressible core.

They obtained the compressibility effect in the micelle formation for three surfactants (C_{12}TAB, C_{14}TAB and C_{16}TAB). The compressibility in the formation of C_{12}TAB micelles in the solution was very close to the compressibility in the binding of C_{12}TAB to DNA. The C_{12}TAB molecules form structures on the DNA surface with the intrinsic compressibility closed to the compressibility of C_{12}TAB micelles in the solution and in the binding of C_{12}TAB to DNA, demonstrated the formation of micelles-like aggregates of C_{12}TAB molecules on the DNA surface. They expressed ultrasonic measurement as the concentration increment of ultrasonic velocity (A) which was determined by the relation:

$$A=(u-u_0)/(u_0 c\rho_0) \quad (9)$$

where u and u_0 were ultrasonic velocities in the solution and pure solvent, respectively, c was the concentration of the solute in mol/g, and ρ_0 was the density of water at 25 °C in g/cm^3, 0.997047 g/cm^3. In case of micelle formation, where depend of the concentration increment of ultrasonic velocity on the concentration of the surfactants in water was studied, the concentration increment of ultrasonic velocity was constant at low surfactant concentration which corresponds to the monomer form of surfactant. Above the critical micelle concentration, the value of the concentration increment of ultrasonic velocity

decreased as a result of the micelle formation. In the case of binding of surfactant with DNA, where was done the dependences of the concentration increment of ultrasonic velocity of DNA (A_{DNA}) on concentration of dodecyltrimethylammonium bromide in sodium bromide solution, the value of A_{DNA} at low surfactant concentration in the solution. The concentration increment of ultrasonic velocity decreased in the concentration range 0.5-2 mmol/l of the surfactant which indicated the binding of the surfactant to DNA. At concentration of surfactant above 2 mmol/l, there was a plateau in graph as a result of the saturation of all binding sites on the DNA surface. The polymer is completely saturated by the surfactant micelles and there is complex polymer-surfactant and free micelles in the system.

From the measurement of density has been calculated the apparent molar volume.

$$\Phi_v = M/\rho - (\rho - \rho_0)/(\rho_0 \rho\, c) \tag{10}$$

where ρ is the density of the solution and M is the molecular weight of the solute.

The values of the apparent molar adiabatic compressibilities of the surfactant and DNA ($(\Phi_{kS})_S$) were determined from the values of the concentration increment of ultrasonic velocity (A) and the values of the apparent molar volume (Φ_v). Then it can be calculated the compressibility effect in the binding of surfactant with DNA.

$$(\Phi_{kS})_S = 2\beta_{so}\,(\Phi_v - A - M/2\rho_0) \tag{11}$$

where β_{so} is the coefficient of adiabatic compressibility of the solvent.

In case of low molecular weight solutes, there are no cavities in their structure; the intrinsic compressibility, Km, is determined by the compressibility of covalent bonds and van derWaals radii. Km is small and negligible. For high molecular weight molecules, such as globular proteins and also for molecular aggregates, such as micelles or liposomes, the contribution of the value of the internal compressibility can be significant.

Kudryashov et al. [134] analysed the apparent adiabatic compressibility of surfactants in the free form in solution and in a micelle as a function of the surfactant length. They obtained the apparent molar adiabatic compressibility, Φ_{kS}, and the apparent molar volume, Φ_v, for a series of alkyltrimethylammonium bromides, C_8TAB, C_{10}TAB, C_{12}TAB, C_{14}TAB, and C_{16}TAB, from the ultrasonic measurement using high resolution ultrasonic spectroscopy. Because of high precision of ultrasonic technique it is possible to analyse the concentration behaviour of the apparent molar adiabatic compressibility of long surfactants near the critical micelle concentration, below and above critical micelle concentration.

They found out that values of the apparent molar adiabatic compressibility of alkyltrimethylammonium bromides in a micelle state, $(\Phi_{kS})_{mic}$, are large and positive for all of the surfactants.

$$\Phi_v = V_m + \Delta V_h \tag{12}$$

$$\Phi_{kS} = K_m + \Delta K_h \tag{13}$$

where Vm is the intrinsic volume of the solute molecule, Km is the intrinsic molar adiabatic compressibility of this solute volume; ΔV_h and ΔK_h represent, respectively, the difference between volume and compressibility of the hydration shell of a solute and volume and compressibility of the bulk water.

From the experimental data of Buckin et al. [135] as well as of Kudryashov et al. [134], the values of apparent molar adiabatic compressibilities of the surfactant in the micelle formation increase with the length of carbon chain, from C_{12}TAB to C_{16}TAB. The compressibility effect in the binding of C_{12}TAB molecules to DNA is nearly the same as the compressibility effect of the micelle formation, caused by that the hydration contribution to the effect of binding is small. At low concentrations of surfactant, in the dependence of the apparent molar volume, Φ_v, on the concentration of the surfactant, the value of Φ_v is constant which means that the surfactant is in the momomer form. At concentrations above critical micelle concentration, the value of the apparent molar volume increases as a result of the micelle formation [89],[134].

For the determination of the critical micelle concentration and of the micelle formation, Buckin et al. [125] introduced the concentrantion increment of ultrasonic velocity (A). Main experiment observable in the ultrasonic measurements is determined by the Equation (9).

The concentrantion increment of ultrasonic velocity is constant at low surfactant concentration, which means that the surfactant is in the monomer state. By adding of surfactant to the solution, the micelles begin to form from the value of critical micelle concentration.

Different surfactants have different concentration increment of ultrasonic velocity and different value of critical micelle concentration. The value of concentration increment of ultrasonic velocity, A, increases with the lengh of carbon chain and critical micelle concentration is lower for the surfactants with a chain legth of 12-16 carbon atoms [125],[135].

The reference [99] demonstrates the potential of high resolution ultrasonic spectroscopy in evaluating aggregation-degaggregation behaviour of self-assemling polymer Poloxamer. The results shows that polymer aggregation process can be successfully monitored using both ultrasonic parameters of sound speed and attenuation. The sound attenuation data were able to identify both transitions of the micellization and the gelation. Both parameters were in very good agreement with differential scanning calorimetry (DSC).

Andreatta et al. [137] used high resolution ultrasonic spectroscopy for determination of the critical nanoaggregate concentration of asphaltenes and of the critical micelle concentration of ionic surfactant (CTAB, SDS) and nonionic surfactant (Tween 80, Brij 35) in both water and organic solvents (toluen). They determinated critical micelle concentration of the mentioned surfactants by the measuring of ultrasonic velocity. The comparison of ultrasonic curves for ionic surfactants in water with nonionic surfactants in water showed very different behaviour. From the density measurements they calculated the apparent specific volumes of surfactants and of asphaltene nanoaggregate. The combination of high resolution ultrasonic spectroscopy and densitometer allows calculating the compressibility of the monomers and the micelles.

Hickey et al. [138] published an analysis of the phase diagram and microstructural transitions in a microemulsion system containing phospholipid in which titration arrangement with the detection of ultrasound parameters was used. They demonstrated that break points (points of abrupt changes in slope) on dependences of ultrasonic velocity on the concentration of titrant are located on phase boundaries and can be used to construct phase diagram. Knowledge of other physical parameters of the microemulsion system enabled to make also

a quantitative characterization of various detected microphases or the state of water. Similar study on compositionally different microemulsion system was published by the same group later [139]. Singh and Yadav [141] investigated interactions between poly(N-vinyl-2-pyrrolidone) and sodium dodecyl sulphate using a less sensitive ultrasound equipment operating at single frequency [141]. Ultrasonic velocity as a function of the surfactant concentration exhibited several breaks which were attributed to different molecular organization in the system – for instance, the formation of premicelle associates or their binding to the polymer chain. The authors also noted that ultrasound titration did not substantiated previous claims based on conductivity or viscosity data.

4 AIM OF THE WORK

This thesis is focused on the study of physico-chemical interactions of hyaluronan whose molecular weight is from 10 to 1750 kDa with cationic surfactants. These interactions are studied by means of using uncommon technique named high resolution ultrasonic spectroscopy (HR-US). The densitometry measurement is the indispensable complement to ultrasonic technique enabling to calculate compressibility from ultrasonic velocity and density. The interactions in these systems are important especially for the design of drug delivery systems to human body; the study of the system surfactant-hyaluronan could be possible using as new carrier systems for drug delivery.

In the theoretical part of the thesis, there is mapping the current state of knowledge in the carrier system based on the interaction polyelectrolyte-surfactant. This part is focused on hyaluronan, surfactants and surfactant-hyaluronan system and also in methods using for the discovery of these systems. The previous knowledge of density and ultrasonic measurement of polymers and surfactant-hyaluronan system is summarized in the state of the art. The working out of the theroretical part and the state of the art is basis for the experimental part. The first aim of the experimental part is basic study of hyaluronan in the dependence on its molecular weight and on elevated temperature (25-50 °C) by measuring of density and of ultrasonic velocity with densitometer DSA 5000M. The second aim is to determine the critical micelle concentration and critical aggregation concentration of the surfactants in the absence and in the presence of hyaluronan of different molecular weight and study interactions between surfactants and hyaluronan by means of method high resolution ultrasonic spectroscopy.

This thesis should conduce to recognition applications of surfactants in combination with hyaluronan for using in drug delivery. The results are discussed with regard to the molecular weight of hyaluronan and its concentration. Other aspects are surfactant alkyl chain length and two solution media (water, sodium chloride).

5 PRELIMINARY EXPERIMENTS

First results of my working with hyaluronan are given in this chapter. I started with measurement of pH to find out if there are any changes in the values of pH in the system surfactant-hyaluronan. The measurement of density was the other experiment. It was asked a question: does the age of hyaluronan solution influence density measurement?

The dissolution of hyaluronan depends on many factors, such as temperature, speed of the rotation, concentration of final solution, molecular weight of hyaluronan, the way of the adding of the powder sample and a few others. The aim of present part of the work is to characterize the dissolution and the storage stability of hyaluronan.

5.1 Materials and methods

Hyaluronan of several molecular weights was obtained from Contipro Biotech (Czech Republic). It is produced biotechnologically and extracted from the cell walls of the bacteria *Streptococcus zooepidemicus*. This producer offers a broad range of molecular weights in predefined range of molecular weights. The following products were used in this study: 10-30 kDa, 110-130 kDa, 300-500 kDa and 1500-1750 kDa; particular molecular weights (determined by the producer using SEC-MALS) of particular samples from each range used in this study are given in Table 1. The surfactant hexadecyltrimethylammonium bromide (CTAB) with p.a. 99.0% (Lot number 059K0041 BCBC4707V) was purchased from Sigma Aldrich, tetradecyltrimethylammonium bromide TTAB p.a. 98% (Lot number: 1377175 117K0732) and sodium bromide of p.a. 99.0% purity from Fluka and sodium chloride (NaCl) of p.a. 99.5% purity was obtained from Lachner.

Table 1. Molecular weights of hyaluronan used in the preliminary experiments.

Product name	M_w*	Batch number
kDa	kDa	
10-30	15	208-250
	17	211-589
90-130	116	210-493
	137	211-234
300-500	421	208-125
1500-1750	1730	210-636
1750-2000	1800	211-180

* weight-average molecular weight provided by the supplier and obtained by SEC-MALS analysis.

Ultrapure deionized water from PURELAB water purification system (Option R7/15; ELGA, Great Britain) was used for the preparation of all samples. Hyaluronan solutions were prepared at concentration 1000 mg/l (0.1% w/w) by dissolving powder hyaluronan in water, 0.15 M NaBr or 0.15 M NaCl in closed vessels. The solution was stirred for 48 hours at room temperature to ensure the complete dissolution. The solutions of surfactants were prepared by dissolving solid surfactant (TTAB or CTAB) in water or solutions of 0.15 M NaBr and 0.15 M NaCl. 1 ml of 0.05% w/w sodium azide per 100 ml of solution was used

for stabilization of solutions. The measurements of pH were run on pH meter (S220 SevenCompact, Mettler Toledo, USA).

Densitometer DMA 4500 (Anton Paar, Austria) was used for density measurements, the accuracy of density measurement of 0.00005 g/cm^3. The samples were degassed using the syringe and then was injected to the apparature and the density measurement was started. It had to be ensured that the U-tube was properly filled and that no gas bubbles were present.

The temperature was controlled with integrated Pt 1000 temperature sensor. The density measurements of each molecular weight range, at each concentration were made at least in triplicates. The concentration ranges of samples are given in Table ST7 in Supplementary information.

5.2 Results and discussion

5.2.1 Measurement of pH

The solution of hexadecyltrimethylammonium bromide (25 µl) was added using pipette to the solution (10 ml) of hyaluronan (90-130 kDa and 1500-2000 kDa) or to 0.15 M NaCl to get concentration range of surfactant CTAB (0-0.104 mmol/l) (Table ST1 in Supplementary information). The value of pH was written down after addition and stabilization of every addition. The value of pH does not change expressively with addition of CTAB.

The measurement of pH, as a base for titration hyaluronan by surfactant measured in experimental part II, is in Table ST2 and Table ST3 in Supplementary information. TTAB or CTAB dissoluble in water or sodium chloride was injected to pure solvents or hyaluronan solution (90-130 kDa and 1500-2000 kDa) in water or 0.15 M NaCl. The solutions were prepared without sodium azide.

The value of pH in hyaluronan-surfactant solution with different concentration of surfactant did not change during addition of CTAB to hyaluronan solution so it did not have influence to our results.

5.2.2 Density measurements of hyaluronan solution

Hyaluronan with the molecular weight 70-90 kDa and 1500-2000 kDa were used for the measurement of density of concentrated solution of hyaluronan and the system hyaluronan-CTAB. It was measured the concentration series of hyaluronan in water and titration of hyaluronan by CTAB in NaBr solution. The measurements were performed during 30 days. The hyaluronan solutions (0.05; 0.1; 0.2; 0.4; 0.8 and 1% w/w) were measured with densitometer DMA 4500. The samples after 48 hours of dissolving were named the first day of the measurement. The measurements of density were done on 1st, 2nd, 3rd, 7th, 14th, 21th and 30th day. The data from this measurement are in Table ST5 in Supplementary information, where it is seen that there are no differences in the values of density in the course of time. The density increases linearly with the increasing concentration of hyaluronan.

The concentration series of hyaluronan-surfactant solutions were prepared in the concentration range of surfactant CTAB (0-0.049 mmol/l) and were measured

1st-30th day at 25 °C with densitometer DMA 4500. The density slightly increased with the rising concentration of CTAB and the values are not different neither in molecular weight of hyaluronan nor in the various days of measurements (Table ST6 in Supplementary information).

Other measurements were performed with four molecular weights of hyaluronan (10-30, 90-130, 300-500 and 1500-2000 kDa) where were distinguished the dependence of density on concentration of hyaluronan solutions with sodium azide measured at 25 °C by means of densitometer Anton Paar DMA 4500. The concentration range of density was measured at all four molecular weights of hyaluronan. In case of the lowest molecular weight, hyaluronan 10-30 kDa, the range was to 2 g/l of hyalururonan, in hyaluronan 110-130 kDa was to 1.5 g/l, in hyaluronan 300-500 kDa was 1 g/l and the upper concentration of the range of the highest molecular weight hyaluronan (1500-2000 kDa) was 0.5 g/l. The data are seen in Figure 10 and in Table ST7 in Supplementary information where it is seen that the curves of hyaluronan with four different molecular weights lie in the same values of density.

The dependence of density on concentration of hyaluronan solution with sodium azide is linear, the density increases with concentration of hyaluronan. There is not any difference in the molecular weight of hyaluronan; value of density is similar at all molecular weights of hyaluronan at certain concentration, Table ST7 in Supplementary information.

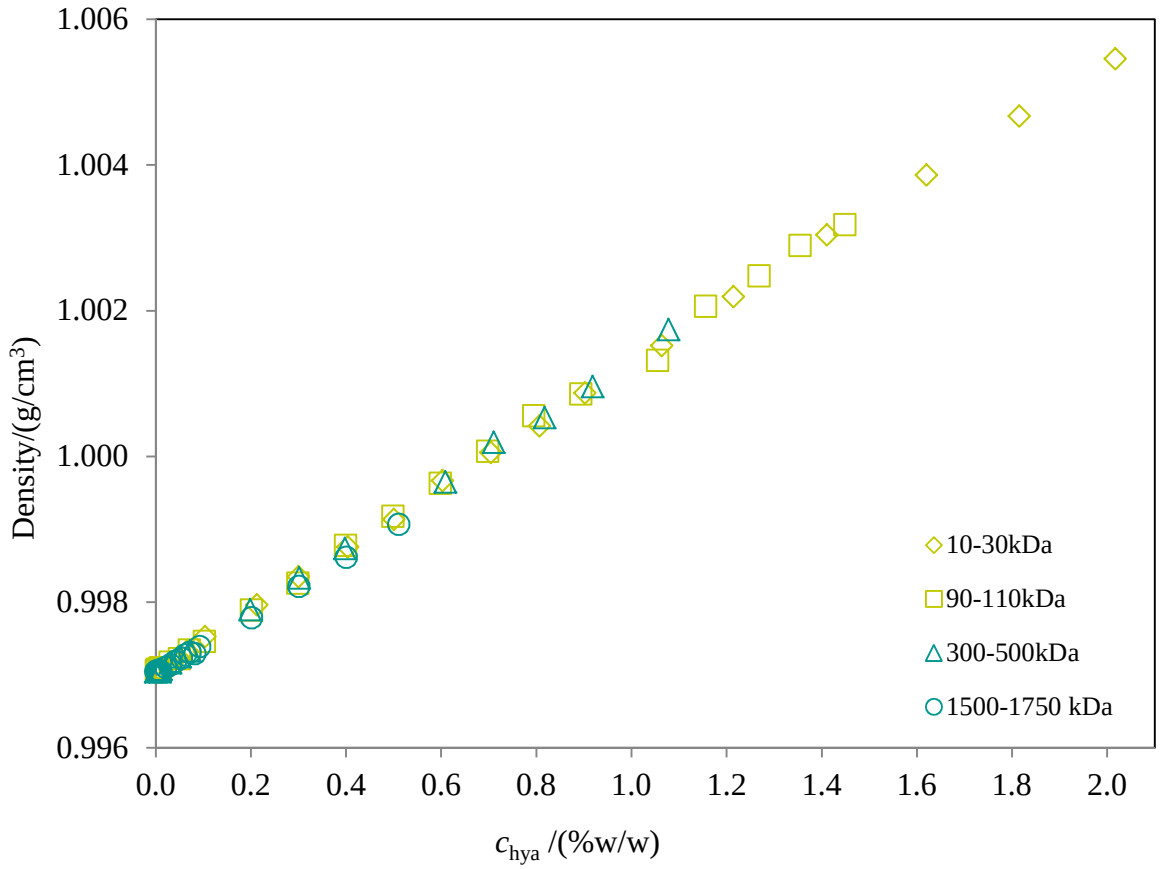

Figure 10. Density of hyaluronan of four molecular weigths with sodium azide measured with DSA 4500.

First experiments were performed with sodium azide which was used as a stabilizer. However the results are almost the same in the presence and in the absence of azide. As emerged from the measurement of density, it is not a good idea to add another substance which can change the interaction in the titration experiment measured by means of high resolution ultrasonic spectroscopy. We prepared the samples without sodium azide for other experiments in Experimental part I and II and the solutions were used only three days after the preparation.

5.3 Conclusions

The addition of CTAB to pure solvents and to hyaluronan solution in various solvents did not change the value of pH. This means that results from the titration in high resolution ultrasonic spectroscopy are not affected by changing pH but are results of the hyaluronan-surfactant interaction.

These preliminary results were done with sodium azide as a stabilizer of solutions. It was found out that the results with and without sodium azide were very close. Other experiments were done without sodium azide (Experimental part I and II). Sodium azide could disturb or change the results of very precise and clear measurements in HR-US. The addition of sodium azide did not bring much better stability of the solutions. Therefore the samples without sodium azide were used in shorter time (three days after dissolving) in order to perform high resolution ultrasonic spectroscopy not interfering with sodium azide.

As resulted from the density measurements of different ages of hyaluronan solution, there were no changes in the values of density in different days which could be caused by the progresive hyaluronan dissolution of measurement so subsequent measurements where realized after 24 hours of preparing of the solutions.

6 EXPERIMENTAL PART I – MEASUREMENT OF DENSITY AND ULTRASONIC VELOCITY OF HYALURONAN SOLUTIONS

Before the characterization of hyaluronan-surfactant system the thesis investigated the basic characteristics of hyaluronan solutions of various concentrations of hyaluronan and in different solvents (water or 0.15 M NaCl). The main method used was thedensitometry by means of densitometer DSA 5000M. Hyaluronan was characterized by the measurement of density and ultrasonic velocity and from these parameters were calculated the specific molar volume and the compressibility. In this study we used a wide range of hyaluronan molecular weights and as broad range of its concentration as possible to measure the density of solutions and the ultrasonic velocity in solutions in details. From the measured data the additional parameters like the partial specific volume, the compressibility or the hydration number were calculated.

6.1 Materials and methods

Hyaluronan of several molecular weights was obtained from Contipro Biotech (Czech Republic). It is produced biotechnologically and extracted from the cell walls of the bacteria *Streptococcus zooepidemicus*. This producer offers a broad range of molecular weights in predefined range of molecular weights. Following products were used in this study: 10-30, 110-130, 300-500 and 1750-2000 kDa); the average molecular weights (determined by the producer using SEC-MALS) of particular samples from each range used in this study are given in Table 2. The selected concentration range of hyaluronan solution was dependent on the molecular weight and was selected in order to enable the sample injection into the densitometer without problems (not too high viscosity and no entrapment of bubbles). The hyaluronan solutions were prepared at the concentration ranges reported in Table 5 by dissolving the original hyaluronan powder slowly in water or in 0.15 M NaCl in a closed vessel. The surfactant hexadecyltrimethylammonium bromide (CTAB) was get from Sigma Aldrich, tetradecyltrimethylammonium bromide (TTAB) was obtained from Fluka and sodium chloride (NaCl) from Lachner. Hyaluronan was fully soluble in water and time of dissolving depends on the molecular weight of hyaluronan. The solutions with low molecular weights of hyaluronan (10-30 kDa and 90-130 kDa) were stirred for 24 hours; the solutions with the high molecular weights of hyaluronan (300-500 kDa and 1500-1750 kDa) were stirred for 48 hours at room temperature to ensure the complete dissolution. The surfactant solutions were prepared by dissolving of surfactant powder (TTAB, CTAB) in water or 0.15 M NaCl. The solutions were prepared by weighing their components. Ultrapure deionized water from PURELAB water purification system was used for the preparation of all samples. PURELAB Option R7/15 was from ELGA (Great Britain). Ideal temperature for working with aqueous CTAB solution is around 30 °C. Under temperature 25 °C, there is cristalization of solution CTAB in water (Figure 11).

Table 2. Molecular weights of hyaluronan used in the experimental part I.

Product name	M_w*	Batch number
kDa	kDa	
10-30	17	211-589
	16	211-263
	15	212-2069
90-130	137	211-234
	101	212-1214
	116	212-2859
300-500	430	212-2082
	458	213-3809
1500-1750	1800	211-180
	1697	212-1271
	1644	212-2298

* weight-average molecular weight provided by the supplier and obtained by SEC-MALS analysis.

Figure 11. Cristalization of CTAB in water.

6.1.1 Densitometer DSA 5000M

The density of the liquid samples was measured using densitometer DMA 4500 or DSA 5000M Anton Paar with the accuracy of density 0.00005 g/cm^3 and 0.000005 g/cm^3, respectively. DSA 5000M is equipped with a density cell and a sound velocity cell with the temperature-controlled by a buil-in Peltier thermostat. There were measured the ultrasonic velocity and the density simultaneously in temperature regime (25-50 °C, heating rate 0.5 °C/min) as well as in kinetic (constant temperature of 25 °C) modes with density meter DSA 5000M. The sample is heated or cooled and after the stabilization at elevated temperature (after one or five degrees of Celsius) the density of the sample was measured. In kinetic regime, temperature was set to 25 °C and after the stabilization at this temperature the sample was measured within the interval of 3 minutes.

The temperature was measured in cell by the high-precision platinum thermometer. Patented reference oscillator built into the measuring cell provided that one adjustment (with water and air) at 20 °C was sufficient for measurements for the whole temperature range. The calibration of densitometers was performed at 20 °C using air and water in the density measuring interval from 0 to 3 g/cm^3 and in the sound velocity measuring interval from

1000 to 2000 m/s. The goal of a calibration is to validate the accuracy of the density and ultrasonic velocity measurement. To calibrate the instrument, measure a certified standard liquid and compare the result to the reference value indicated in the calibration certificate of the standard. The physical properties (density, ultrasonic velocity) of the liquid density standards should be similar to those of the samples.

After a water check (measurement of water and check with the calibrate value of the standard liquid), the degassed sample (5 ml) was carefully filled into the measuring cell using the syringe and left in holder for several minutes to equilibrate at desired temperature before the measurement was started. It had to be ensured that the U-tube was properly filled and that no gas bubbles were present. The samples were degassed using the syringe and then samples were injected into U-shaped borosilicate glass tube that was excited electronically to vibrate at its characteristics frequency. The sample flowed continuously through a single combined sensor measuring the speed of sound and the density simultaneously. Density and velocity measurements of each molecular weight range, at each concentration and for each temperature were repeated at least in triplicates. The data fitting and the statistical analyses were made with QC.Expert 3.3 software (TriloByte, Czech Republic).

Figure 12. Densitometer DSA 5000M from Anton Paar.

6.2 Results and discussion

Density and ultrasonic velocity of water and 0.15 M NaCl was measured in the temperature range 25-50 °C in chapter 6.2.1. The density (6.2.2) and ultrasonic velocity (6.2.3) data of hyaluronan solutions were used for calculation of volume characteristics and compressibility (6.2.4). The results are summarized also in the scientific paper *(In press)* (Chapter 13.1).

6.2.1 Density and ultrasonic velocity of pure solvents

Ultrapure water, water with sodium azide and 0.15 M NaCl was measured by means of densitometer DSA 5000M and compared with value of density and ultrasonic velocity of water from literature [142] in the temperature range 20-55 °C. The density and ultrasonic velocity of water and sodium chloride solution are in accordance with the literature (Table 3).

The density decreases with increasing temperature and the ultrasonic velocity increases (Figure 13). The values of density and ultrasonic velocity of sodium chloride solution are higher with increasing temperature compared to those of water and the difference of density values of water and 0.15 M NaCl is higher than that of ultrasonic velocity values. The density values of water with sodium azide are slightly bigger then in water without azide.

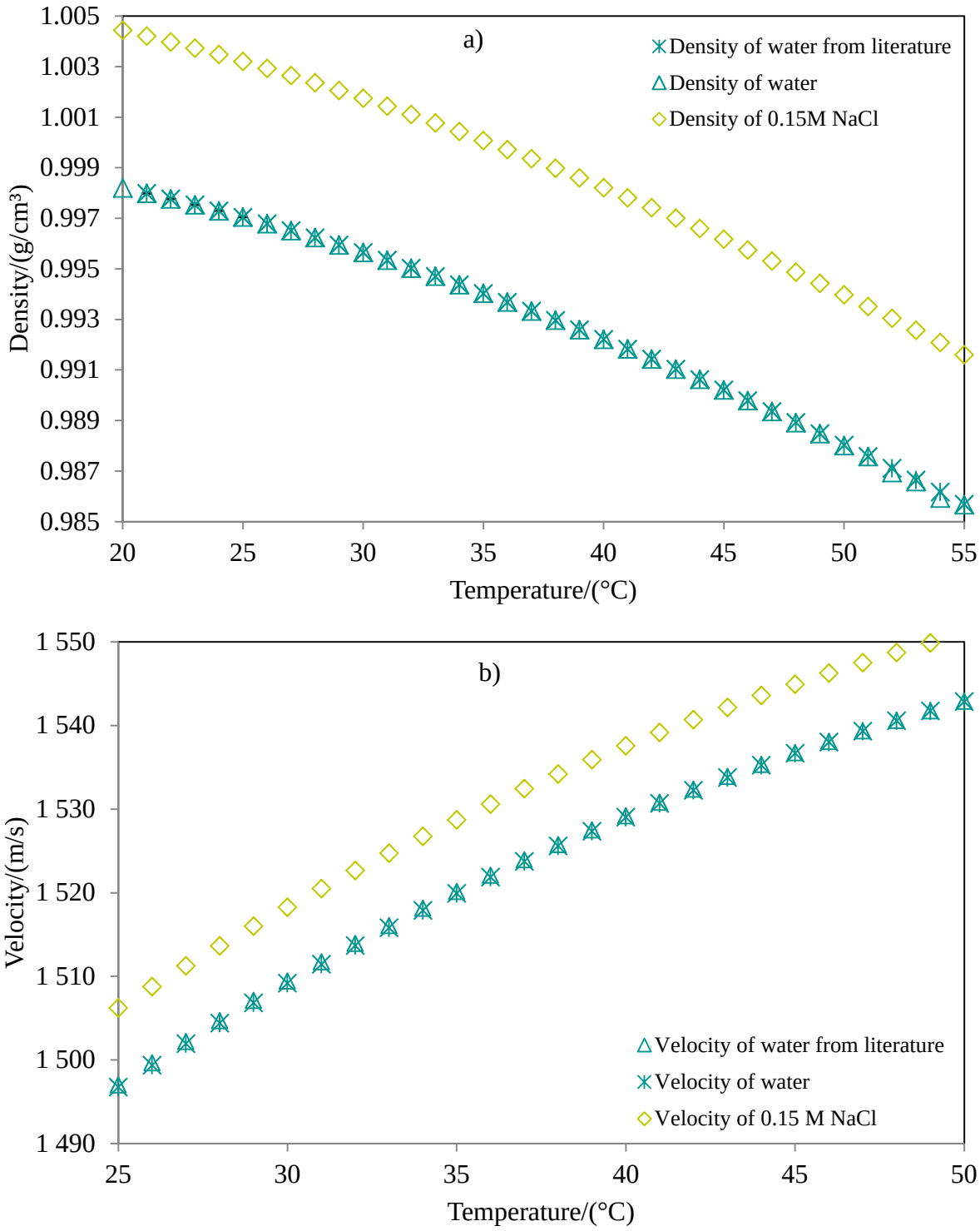

Figure 13. The dependence of density (a) and ultrasonic velocity (b) of water and 0.15 M NaCl on temperature (20-55 °C) measured with DSA 5000M. Density and velocity of water from literature [142].

Table 3. *Density and ultrasonic velocity of water and 0.15 M NaCl.*

T	$\rho_{(literature)}$	ρ_{water}	$\rho_{water\ NaN3}$	$\rho_{0.15\ M\ NaCl}$	$v_{(literature)}$	v_{water}	$v_{0.15\ M\ NaCl}$
°C	g/cm³	g/cm³	g/cm³	g/cm³	m/s	m/s	m/s
20	0.998203	0.998196		1.004434	1482.66	1482.58	1492.58
21	0.997991	0.997988		1.004209	1485.69	1485.50	1495.39
22	0.997769	0.997768		1.003974	1488.63	1488.42	1498.17
23	0.997537	0.997535		1.003728	1491.50	1491.27	1500.91
24	0.997295	0.997295		1.003473	1494.29	1494.04	1503.59
25	0.997043	0.997044	0.997368	1.003207	1497.00	1496.75	1506.21
26	0.996782	0.996784	0.997111	1.002932	1499.64	1499.38	1508.76
27	0.996511	0.996514	0.996840	1.002649	1502.20	1501.93	1511.23
28	0.996232	0.996234	0.996561	1.002357	1504.68	1504.41	1513.64
29	0.995943	0.995946	0.996270	1.002056	1507.10	1506.83	1515.99
30	0.995645	0.995650	0.995973	1.001747	1509.44	1509.17	1518.26
31	0.995339	0.995343	0.995666	1.001429	1511.71	1511.45	1520.48
32	0.995024	0.995028	0.995350	1.001103	1513.92	1513.66	1522.63
33	0.994700	0.994706	0.995027	1.000769	1516.05	1515.80	1524.71
34	0.994369	0.994374	0.994694	1.000429	1518.12	1517.88	1526.74
35	0.994029	0.994034	0.994354	1.000078	1520.12	1519.90	1528.69
36	0.993681	0.993687	0.994007	0.999720	1522.06	1521.85	1530.59
37	0.993325	0.993331	0.993650	0.999354	1523.93	1523.74	1532.42
38	0.992962	0.992967	0.993285	0.998980	1525.74	1525.56	1534.19
39	0.992591	0.992595	0.992913	0.998597	1527.49	1527.33	1535.90
40	0.992212	0.992217	0.992533	0.998206	1529.18	1529.03	1537.55
41	0.991826	0.991830	0.992148	0.997811	1530.80	1530.67	1539.14
42	0.991432	0.991436	0.991753	0.997415	1532.37	1532.25	1540.67
43	0.991031	0.991035	0.991350	0.997009	1533.88	1533.77	1542.14
44	0.990623	0.990626	0.990942	0.996595	1535.33	1535.24	1543.57
45	0.990208	0.990210	0.990525	0.996176	1536.72	1536.65	1544.93
46	0.989786	0.989783	0.990103	0.995747	1538.06	1538.00	1546.24
47	0.989358	0.989356	0.989673	0.995312	1539.34	1539.30	1547.50
48	0.988922	0.988915	0.989237	0.994871	1540.57	1540.55	1548.71
49	0.988480	0.988476	0.988792	0.994422	1541.74	1541.72	1549.86
50	0.988030	0.988004	0.988343	0.993969	1542.87	1542.86	1550.95
51	0.987575	0.987570	0.987887	0.993507	1543.93	1543.93	1552.00
52	0.987113	0.986945	0.987423	0.993041	1544.95	1544.96	1553.00
53	0.986644	0.986581	0.986955	0.992569	1545.92	1545.95	1553.95
54	0.986170	0.985929	0.986480	0.992088	1546.83	1546.87	1554.85
55	0.985688	0.985663	0.985998	0.991604	1547.70	1548.03	1555.70

The error bars of density and velocity: 0.0000007 g/cm^3 and 0.0000006 m/s.

$\rho_{(literature)}$, $v_{(literature)}$ – the values of density and ultrasonic velocity got from [142].

6.2.2 Density of hyaluronan solutions

The concentration range of density and ultrasonic velocity was measured at all four molecular weights of hyaluronan. The concentration range was dependent on the molecular weight and was selected in order to enable sample injection into the densitometer without problems (not too high viscosity and no entrapment of bubbles). In case of lowest molecular weight, hyaluronan 10-30 kDa, the highest concentration that could be used was to 2 % w/w of hyalururonan, in hyaluronan 110-130 kDa was to 1.5 % w/w, in hyaluronan 300-500 kDa was 1 % w/w and the upper concentration of the range of the highest molecular weight hyaluronan was 0.5% w/w. Fukada et al. [108] measured density of aqueous solutions of sodium hyaluronate with molecular weight 1.4×10^6 at 25 °C. These data of the measured density are collected in Table ST8-Table ST11 in Supplementary information.

The density increases with the increasing concentration and decreases with the increasing temperature. The dependence of density on concentration of hyaluronan is shown in Figure 14 and the influence of the temperature on the density is seen in Figure 15. The effect of the temperature is much more perceptible than the effect caused by concentration of hyaluronan. The temperature dependences were slightly curved the reason of what was the temperature effect on the density of pure solvents (see in Figure 13).

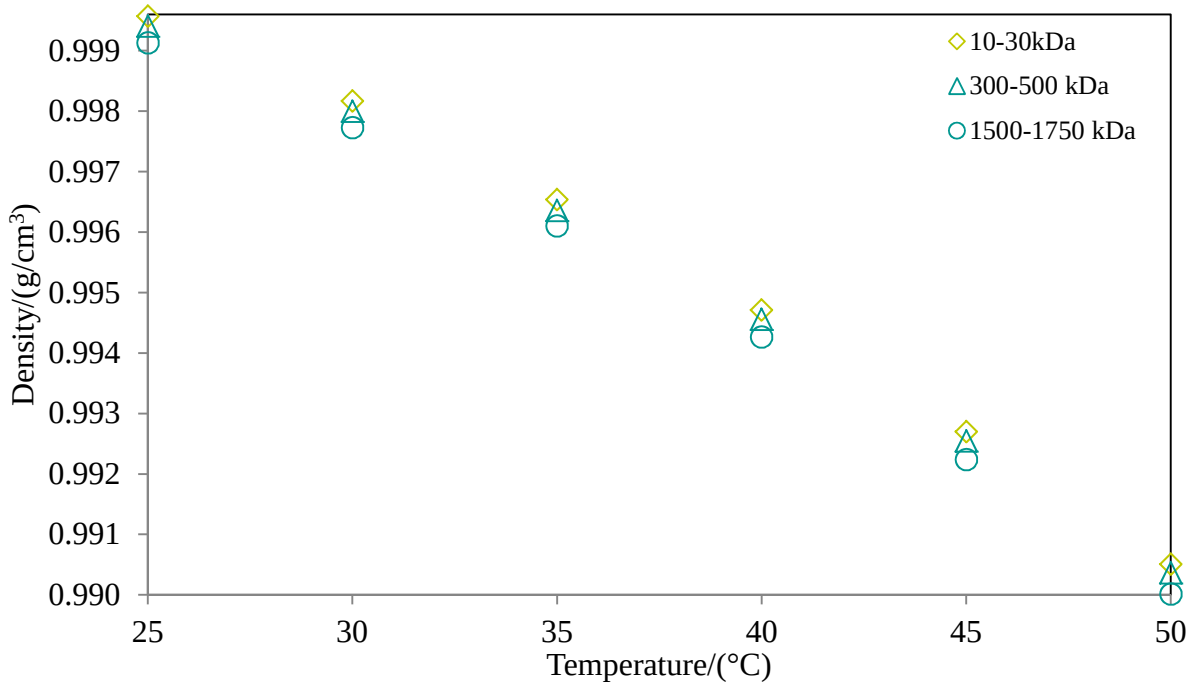

Figure 14. The temperature dependence of density of hyaluronan solution on concentration 5 g/l (0.5% w/w) of three molecular weights (10-30 kDa, 300-500 kDa and 1500-1750 kDa) in water.

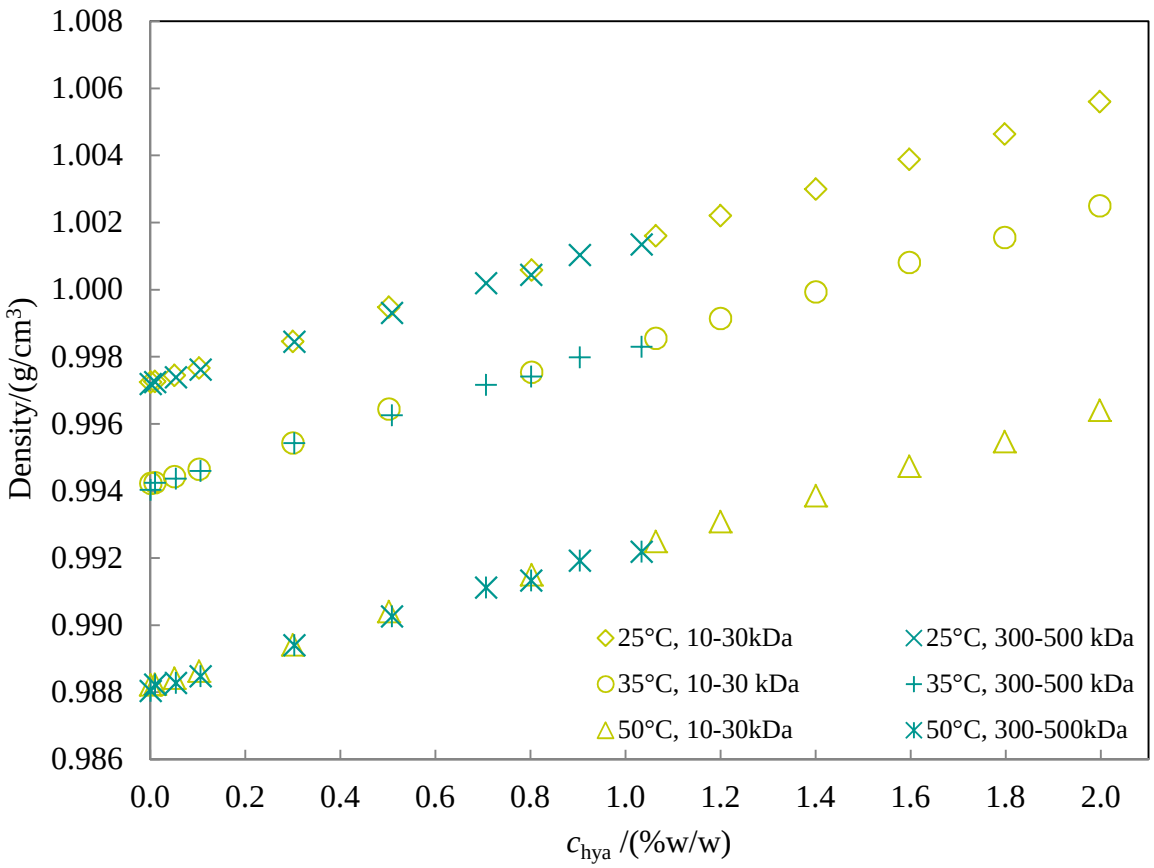

Figure 15. The temperature and concentration dependence of density of hyaluronan solutions (10-30 kDa and 300-500 kDa) in water.

The density-concentration-temperature data were fitted for each molecular weight by two models – linear and quadratic in temperature – to compare the effect of including the slight curvature into the fitting equation. The latter model is called the quadratic model henceforth. The model equations are as follows:

linear: $\rho = a_0 + a_w c_w + a_t t$

quadratic: $\rho = a_0 + a_w c_w + a_t t + a_{tt} t^2$

where ρ is the density of hyaluronan solution in g/cm^3, c_w is the concentration of hyaluronan in grams per kilogram of solution, t is the temperature in °C and a_i denotes the (fitted) parameters. The results of regression fits were evaluated on the basis of following characteristics: multiple correlation coefficient (R), coefficient of determination (R^2), predicted coefficient of determination (R_p), mean quadratic error of prediction (*MEP*), and Akaike information criterion (*AIC*). These characteristics are collected in Table ST16 in Supplementary information for the solutions in water and show that the quadratic model fits better the data. Fitting results obtained for the data measured in NaCl solution lead to very similar conclusions. The parameters of quadratic models are given in Table 4 and the parameters of linear models in Table ST17 in Supplementary information for the sake of completeness.

Table 4. Parameters of quadratic models and their standard deviation for hyaluronan solutions of different molecular weights.

$M_{w\,hya}$ kDa	solvent	a_0 g/cm^3	a_w kg/cm^3 10^{-4}	a_t g/cm^3°C 10^{-5}	a_{tt} g/cm^3(°C)^2 10^{-6}
10-30	water	1.00152 ± 8 × 10^{-5}	4.1 ± 0.025	-7.2 ± 1.1	-3.9 ± 0.15
110-130		1.00124 ± 39 × 10^{-5}	4.0 ± 0.031	-5.8 ± 2.1	-4.1 ± 0.28
300-500		1.00149 ± 26 × 10^{-5}	4.1 ± 0.032	-7.6 ± 1.4	-3.8 ± 0.19
1500-1750		1.00110 ± 9 × 10^{-5}	3.8 ± 0.023	-6.1 ± 0.5	-4.0 ± 0.06
10-30	NaCl	1.00795 ± 20 × 10^{-5}	4.1 ± 0.013	-9.2 ± 1.1	-3.7 ± 0.15
110-130		1.00806 ± 22 × 10^{-5}	4.0 ± 0.018	-9.1 ± 1.2	-3.7 ± 0.16
300-500		1.00800 ± 16 × 10^{-5}	4.3 ± 0.019	-9.3 ± 0.9	-3.7 ± 0.12
1500-1750		1.00786 ± 16 × 10^{-5}	4.2 ± 0.044	-8.8 ± 0.9	-3.8 ± 0.11
10-1750	water	1.00131 ± 17 × 10^{-5}	4.1 ± 0.013	-6.6 ± 0.9	-4.0 ± 0.12
10-1750	NaCl	1.00797 ± 17 × 10^{-5}	4.1 ± 0.009	-9.1 ± 0.6	-3.7 ± 0.08

Because the molecular weight did not show appreciable effect on the density (Figure 16) the whole set of data over all molecular weights was fitted by one common equation. In this way a single equation was obtained which can serve for a reasonable estimate of density of hyaluronan solution at the desired concentration and temperature which fall within their ranges used in this work and with hyaluronan molecular weight within the range from 10 up to 1750 kDa. The statistical characteristics of this overall fit are given at the bottom of Table ST16 in Supplementary information and corresponding model parameters in the last two rows of Table 4. Parametres of linear models of experiment with 0.15 M NaCl are in Supplementary information in Table ST17.

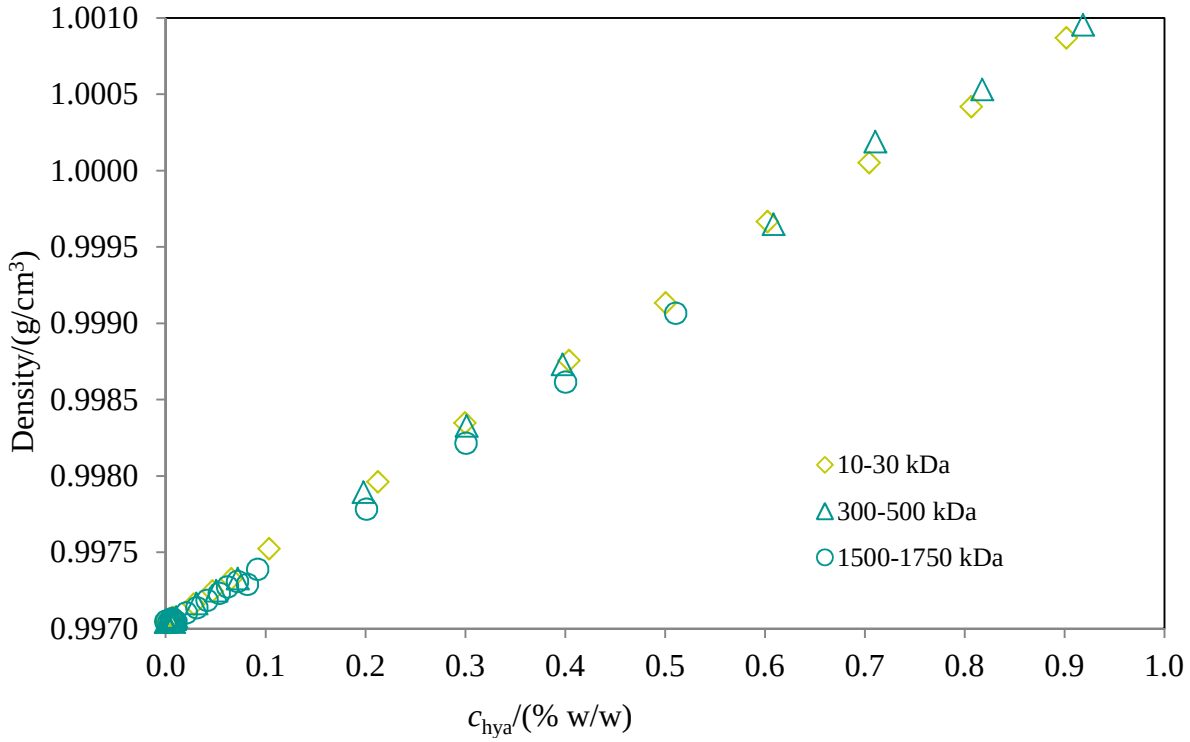

Figure 16. The dependence of density on concentration of hyaluronan at 25 °C. The hyaluronan water solution of three molecular weights (10-30 kDa, 300-500 kDa and 1500-1750kDa) in water.

These results can be additionaly used in the linear and quadratic equations to calculate directly density of hyaluronan solution at certain hyaluronan concentration and temperature (applicable for both water and 0.15 M NaCl environment) without a very time-consuming measurement:

$\rho_{H_2O} = 1.00662+0.00041c_w-0.00036t$

$\rho_{NaCl} = 1.01297+0.00041c_w-0.00037t$

$\rho_{H_2O} = 1.00131+0.00041c_w-0.00007t+0.000004t^2$

$\rho_{NaCl} = 1.00797+0.00041c_w-0.00009t+0.000004t^2$

6.2.3 Ultrasonic velocity of hyaluronan solutions

Ultrasonic velocity is the second parameter measured in densitometer DSA 5000M. These data of measured ultrasonic velocity are collected in Table 5 and in Table ST19-Table ST26 in Supplementary information. The ultrasonic velocity increases with hyaluronan concentration linearly as for many other solutions of low concentration [70], see the example in Figure 17. The dependence on temperature at given concentration also increases but is slightly curved what corresponds to the temperature dependence of ultrasonic velocity in water. The molecular weight of hyaluronan practically has no effect on the concentration line of hyaluronan (Figure 17).

Table 5. Ultrasonic velocity of hyaluronan in water at the temperature range 25-50 °C.

		Velocity (m/s)					
$M_{w\,hya}$	c_{hya}	25 °C	30 °C	35 °C	40 °C	45 °C	50 °C
kDa	%w/w						
10-30	1.99766	1503.81	1515.75	1526.18	1535.03	1542.41	1548.48
	1.79772	1503.47	1515.36	1525.77	1534.64	1542.06	1548.07
	1.59727	1502.71	1514.64	1525.08	1533.97	1541.39	1547.44
	1.40052	1502.10	1514.04	1524.50	1533.42	1540.86	1546.92
	1.19948	1501.33	1513.30	1523.79	1532.73	1540.19	1546.28
	1.06383	1500.74	1512.73	1523.24	1532.21	1539.70	1545.84
	0.80249	1499.94	1511.97	1522.51	1531.51	1539.02	1545.15
	0.50190	1498.78	1510.86	1521.45	1530.49	1538.04	1544.21
	0.29972	1498.06	1510.21	1520.85	1529.92	1537.51	1543.70
	0.10273	1497.31	1509.43	1520.08	1529.18	1536.79	1543.03
	0.05067	1497.51	1509.70	1520.39	1529.49	1537.12	1543.35
	0.01010	1497.12	1509.29	1519.96	1529.08	1536.72	1542.95
	0.00102	1496.67	1509.04	1519.74	1528.87	1536.50	1542.72
	0.00000	1496.92	1509.16	1519.84	1528.95	1536.56	1542.78
90-130	1.53305	1502.53	1514.48	1524.93	1533.85	1541.28	1547.33
	1.39485	1502.09	1514.04	1524.52	1533.44	1540.88	1546.94
	1.31501	1501.75	1513.71	1524.20	1533.14	1540.59	1546.67
	1.20050	1501.31	1513.29	1523.78	1532.73	1540.20	1546.29

	1.10684	1500.99	1513.04	1523.56	1532.53	1540.01	1546.11
	1.06436	1500.62	1512.63	1523.15	1532.13	1539.62	1545.72
	0.80103	1500.04	1512.08	1522.63	1531.64	1539.15	1545.28
	0.50070	1498.89	1510.96	1521.55	1530.59	1538.15	1544.32
	0.30335	1498.17	1510.27	1520.87	1529.94	1537.52	1543.71
	0.10587	1497.52	1509.65	1520.30	1529.38	1536.99	1543.20
	0.05178	1497.28	1509.41	1520.06	1529.15	1536.81	1542.99
	0.01067	1497.06	1509.25	1519.99	1529.10	1536.71	1542.94
	0.00104	1496.75	1509.11	1519.81	1528.93	1536.55	1542.78
	0.00000	1496.92	1509.16	1519.84	1528.95	1536.56	1542.78
	1.03400	1500.90	1512.98	1523.50	1532.44	1539.90	1545.72
	0.90393	1500.49	1512.49	1523.01	1531.99	1539.48	1545.53
	0.80197	1500.15	1512.16	1522.69	1531.68	1539.19	1545.24
	0.70684	1499.72	1511.74	1522.30	1531.31	1538.83	1544.96
	0.50888	1498.98	1511.04	1521.61	1530.64	1538.17	1544.23
300-500	0.30317	1498.16	1510.24	1520.84	1529.90	1537.47	1543.65
	0.10595	1497.54	1509.68	1520.32	1529.40	1537.00	1543.03
	0.05397	1497.26	1509.39	1520.03	1529.12	1536.59	1542.81
	0.01036	1497.15	1509.28	1519.93	1529.03	1536.65	1542.88
	0.00106	1497.14	1509.26	1519.92	1528.82	1536.43	1542.65
	0.00000	1496.92	1509.16	1519.84	1528.95	1536.56	1542.78
	0.51056	1498.92	1510.99	1521.58	1530.61	1538.16	1544.31
	0.39971	1498.83	1510.89	1521.49	1530.55	1538.12	1544.28
	0.29776	1498.43	1510.53	1521.16	1530.25	1537.84	1544.07
	0.19948	1497.82	1510.01	1520.65	1529.74	1537.35	1543.56
	0.10757	1497.57	1509.70	1520.34	1529.42	1537.03	1543.23
1500-1750	0.09241	1497.53	1509.67	1520.30	1529.39	1536.99	1543.21
	0.07231	1497.56	1509.70	1520.34	1529.44	1537.05	1543.27
	0.05354	1497.50	1509.63	1520.28	1529.38	1536.99	1543.22
	0.01027	1497.23	1509.38	1520.03	1529.13	1536.74	1542.95
	0.00103	1496.70	1509.07	1519.79	1528.96	1536.67	1543.05
	0.00000	1496.96	1509.26	1519.96	1529.08	1536.71	1542.94

As already noted by [104] the effect of temperature is more significant than the effect of concentration (Figure 18). The negligible effect of hyaluronan molecular weight (Figure 18) is indicative of the principal role of hyaluronan basic disaccharide unit in determining the properties of hyaluronan solutions – its molar amount at a given hyaluronan mass concentration is independent on the molecular weight.

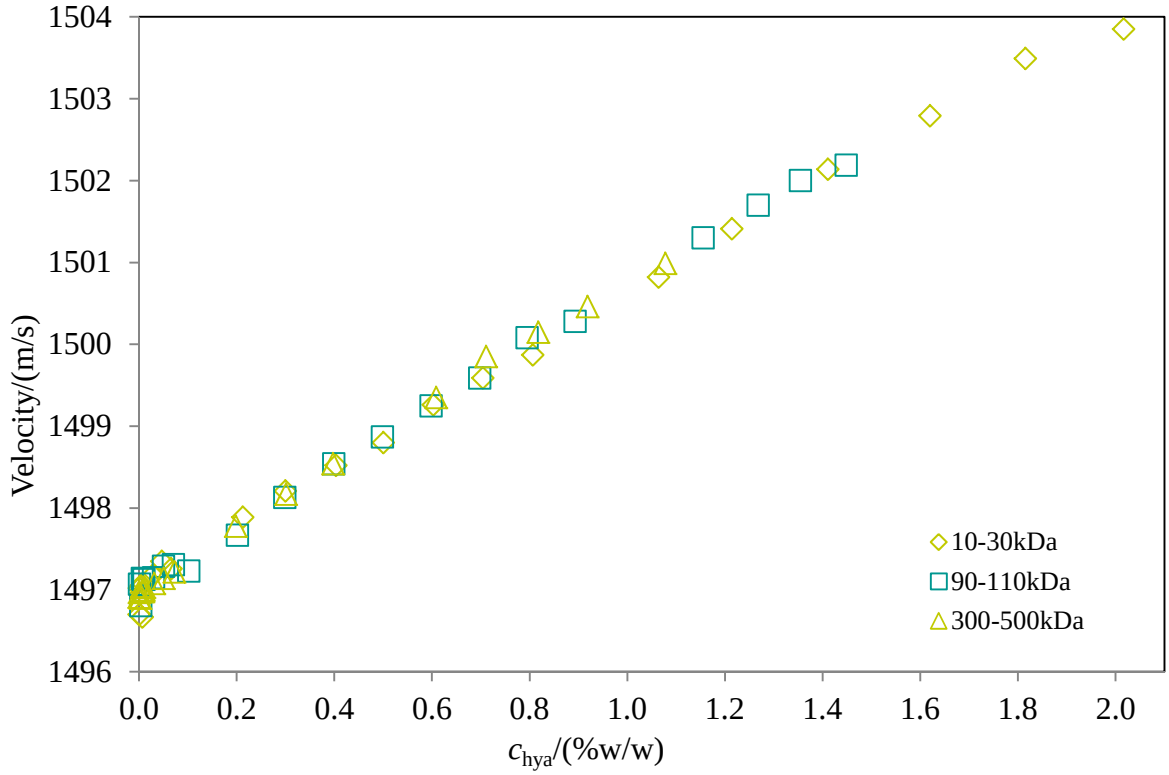

Figure 17. The dependence of velocity on concentration of hyaluronan at 25 °C. The hyaluronan water solution of three molecular weights (10-30, 90-130 and 300-500 kDa) in water.

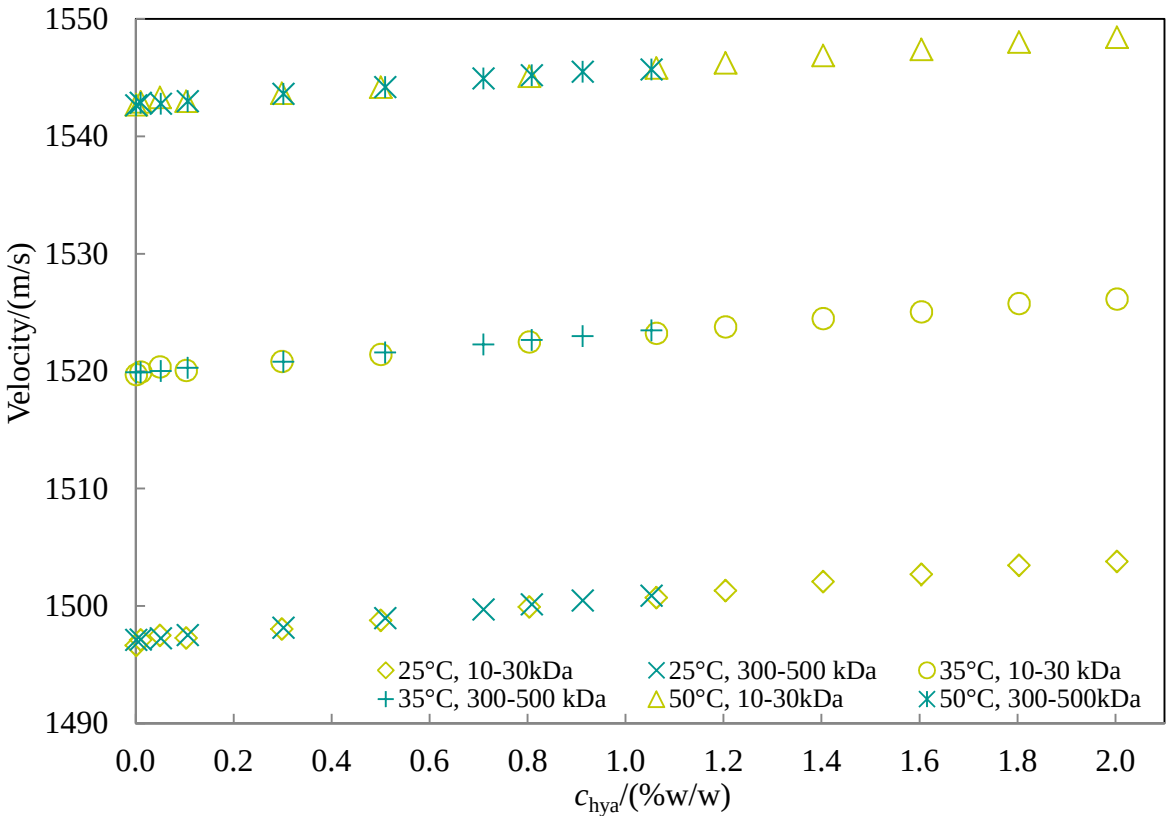

Figure 18. The temperature and concentration dependence of velocity of hyaluronan solutions (10-30 kDa and 300-500 kDa) in water.

The velocity-concentration-temperature data were fitted for hyaluronan with molecular weight 10-1750 kDa by quadratic model (explanation is above). The results of regression fits were evaluated on the basis of following characteristics: multiple correlation coefficient (R), coefficient of determination (R^2), predicted coefficient of determination (R_p), mean quadratic error of prediction (MEP), and Akaike information criterion (AIC). These characteristics are collected Table ST27 in Supplemenatry information for hyaluronan in range of molecular weight 10-1750 kDa. The parameters of quadratic models are given in Table 6.

Table 6. Parameters of quadratic models and their standard deviation for hyaluronan solution.

$M_{w\,\mathrm{hya}}$	Solvent	a_0	a_w	a_t	a_{tt}
kDa		g/cm^3	kg/cm^3 10^{-2}	g/cm^3°C	g/cm^3(°C)^2
10-1750	water	1415 ± 0.24	31.7 ± 0.19	4.06 ± 0.013	-0.29
10-1750	NaCl	1426 ± 0.27	32.5 ± 0.21	3.96 ± 0.015	-0.29

These results can be additionaly used in the quadratic equations to calculate directly ultrasonic velocity of hyaluronan solution at certain hyaluronan concentration and temperature (applicable for both water and 0.15 M NaCl environment) without a very time-consuming measurement:

$v_{H_2O} = 1.415+0.0031c_w+4.06t-0.29t^2$
$v_{NaCl} = 1426+0.0032c_w+3.96t-0.29t^2$

Ultrasonic velocity measured with high resolution ultrasonic spectroscopy

In this chapter it is compared concentration curve of hyaluronan measured in various instruments and also by different performance of measuring solutions. The concentration series of hyaluronan at 25 °C was measured also by HR-US 102 and HR-US 102 T, where the same concentration curve of hyaluronan was obtained Figure 19 and Figure 20. The hyaluronan solutions (90-130 kDa) with concentration 1; 0.5; 0.2 and 0.1 % w/w were titrated by water and ultrasonic velocity was measured by means of HR-US 102T. The titration curves were plotted in Figure 19. The ultrasonic velocity linearly increased with increasing concentration of hyaluronan.

The same experiment with hyaluronan (10-30 kDa, 90-130 kDa, 300-500 kDa and 15001750 kDa) were measured in HR-US 102 (Figure 20), but kinetic regime of HR-US 102 was used, not titration one. Method HR-US is described in Experimental part II. The samples of different molecular weights were prepared at the concentration range which is seen in Table ST28-Table ST31 in Supplementary information and then put to the machine and measured in two hours every sample. At one time the sample was measured at seven frequencies, where is seen that ultrasonic velocity did not change with frequency, Table ST28-Table ST31 in Supplementary information.

The same values of ultrasonic velocity were measured both with densitometer DSA 5000M, and with ultrasonic spectrometer HR-US 102 and HR-US 102T.

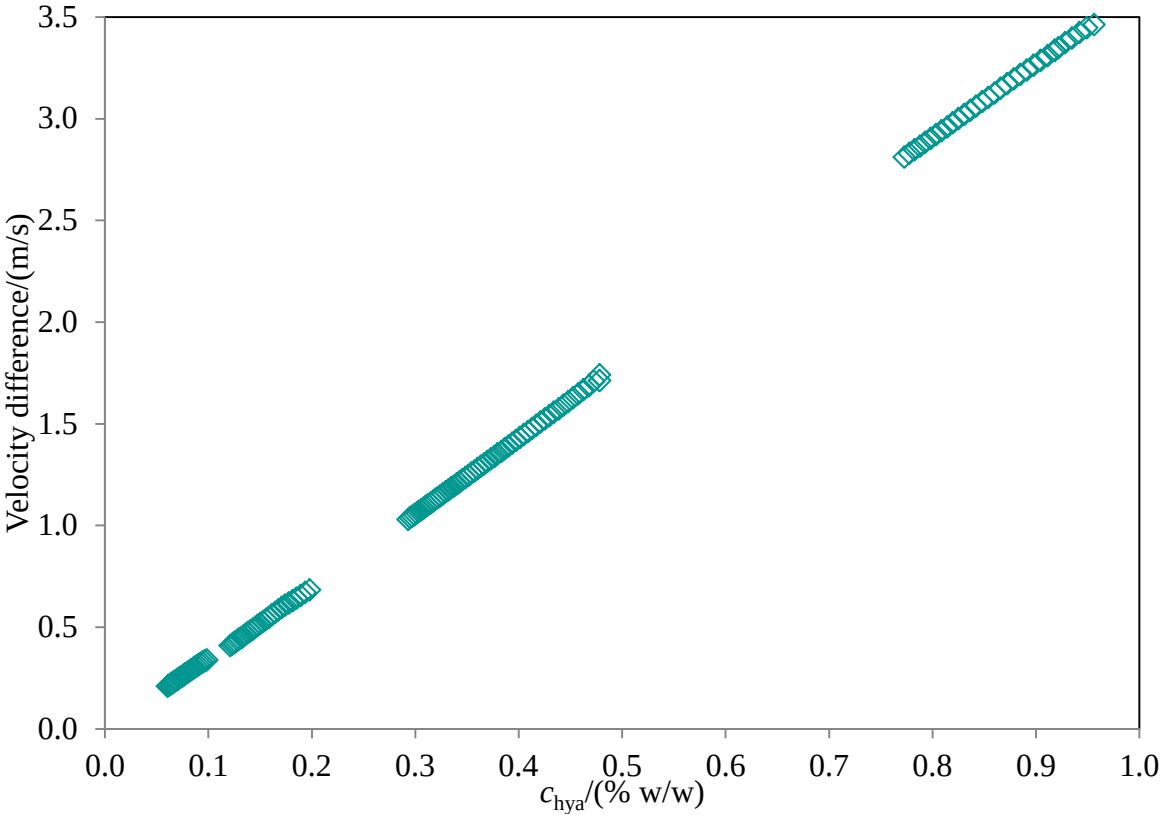

Figure 19. The concentration line of hyaluronan 90-130 kDa measured by means of HR-US 102T in titration regime at 25 °C, at frequency 15 MHz.

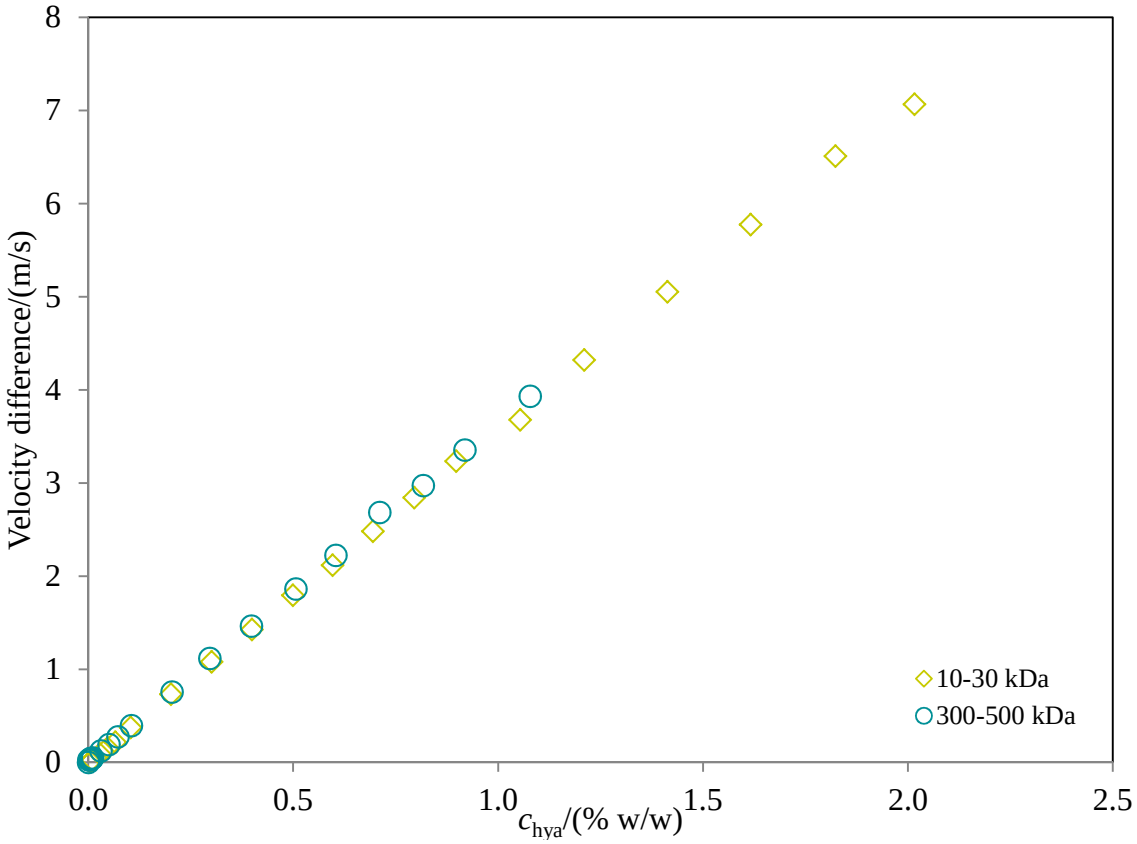

Figure 20. The concentration line of hyaluronan 10-30 and 300-500 kDa measured by means of HR-US 102 at 25 °C, at frequency 15 MHz.

6.2.4 Calculated parameters – volume characteristics, compressibility and hydration numbers

Apparent and partial specific volumes were calculated from density data including their extrapolated values to infinite dilutions. Measurement of ultrasonic velocity in the same solutions under the same conditions enabled to calculate compressibility and its dependence on concentration and temperature. Compressibility was used to estimate hydration numbers.

Volume characteristics

The measurements of density are usually used to calculate the volume characteristics of the solution and solvent. The apparent specific volume is frequently reported characteristic, which is defined as the difference between the solution and solvent volumes per unit solute mass; in our case:

$$V_{app} = (V - V_0)/m_{hya} \tag{14}$$

(V is the solution and V_0 the solvent volume, m_{hya} is the hyaluronan mass in the solution). Expressing volumes in terms of densities the following relationships can be derived to calculate the apparent specific volume from measured densities:

$$V_{app} = m_0\,(\rho_0 - \rho)/(\rho\,\rho_0\,m_{hya}) + 1/\rho \tag{15}$$

$$V_{app} = (m_0/m_{hya})\,(1/\rho - 1/\rho_0) + 1/\rho \tag{16}$$

where m_0 is the solvent mass in the solution, ρ_0 is the solvent and ρ the solution density. Both expressions gave identical values of V_{app} within the measurement precision of our data, as expected.

In thermodynamics, the effects of mixture components on mixture properties are rigorously described by partial quantities. They are defined as partial derivatives of a mixture property expressed as a function of relevant variables. In our case, the mixture property is the volume and the variable is the hyaluronan (solute) mass keeping other variables (temperature, pressure) constant. The partial specific volume is then defined as follows:

$$\overline{V}_{sp,hya} = \partial V / \partial m_{hya}\,;\ \ T,p=\text{const.} \tag{17}$$

This definition can be expressed in terms of measured density using the solute mass fraction (w_{hya}):

$$\overline{V}_{sp,hya} = \frac{1}{\rho} + (m_0 + m_{hya})\,\frac{\partial(1/\rho)}{\partial w_{hya}}\,\frac{\partial w_{hya}}{\partial m_{hya}} \tag{18}$$

Evaluating the second of the two partial derivatives, the final expression for calculating the partial specific volume from experimental data is obtained:

$$\overline{V^{\circ}}_{sp,hya} = \frac{1}{\rho}\left[1 - \frac{(1-w_{hya})}{\rho}\,\frac{\partial\rho}{\partial w_{hya}}\right] \tag{19}$$

Note that this calculation requires the slope of the dependence of the solution density on hyaluronan mass fraction.

Gómez-Alejandre et al. [103] calculated hyaluronan partial specific volumes according to the following equation:

$$\bar{v}^0_{\mathrm{sp,hya}} = \frac{1}{\rho_0}\left[1 - \frac{1}{\rho_0}\left(\frac{\partial\rho}{\partial w_{\mathrm{hya}}}\right)^0\right] \tag{20}$$

where $\bar{v}^0_{\mathrm{sp,hya}}$ is the hyaluronan partial specific volume at infinite dilution (we will call it the limiting partial specific volume here) and the derivative indexed by 0 is the limiting slope of the indicated dependence. This equation was called the rigorous relation but its justification is given neither in [103] nor in Fabre et al. [143] and to which the former refers. However, this equation can be arrived at as the zero-concentration limit of the partial specific volume, Equation (19), when $\rho \to \rho_0$, $w_{\mathrm{hya}} \to 0$, and the slope goes to its limiting value calculated at the point of zero mass fraction.

The values of the apparent and partial specific volumes are summarized in Table ST18 in Supplementary information. The apparent specific volume was calculated using the averages of the measured solvent and solution densities and of the corresponding hyaluronan masses. Its value and standard deviation were sensitive to measurements errors, particularly at low concentrations (and higher temperatures) where the solution density was very close to the solvent density. This is quite common situation [144],[145] sometimes attributed also to the effect of dissolved gases in low concentrated samples [144]. Therefore only the values of V_{app} with the relative standard deviation not exceeding ca 20% are reported. The partial specific volume was calculated according to Equation (19) using the averaged densities, averaged hyaluronan mass fractions and the slope of the straight line determined by fitting all experimental points. The values of the partial specific volume were determined much more reliably with the relatively standard deviation below 2% and at more consistent trends with concentration or temperature. Nevertheless, the numerical values of the averages of the two specific volumes were comparable and not too much different.

The partial specific volume (Figure 21) slightly increases with increasing hyaluronan concentration which can be expected due to the increasing role and number of interactions with the solvent and inter-chain contacts. Analogical conclusions can be made also for the apparent specific volume. A moderate increase is observed also with the temperature growth; here the data for the partial specific volume are more conclusive. This is expected and could be explained by the expansion of hyaluronan coils due to the increased mobility at elevated temprature. effect of hyaluronan molecular weight on the specific volume was not detected. Thus the hyaluronan partial specific volume in water typically ranges, depending on concentration, between 0.587 and 0.594 cm^3/g at 25 °C and between 0.597 and 0.604 cm^3/g at 50 °C. The influence of temperature and molecular weight of hyaluronan is shown in Figure 21.

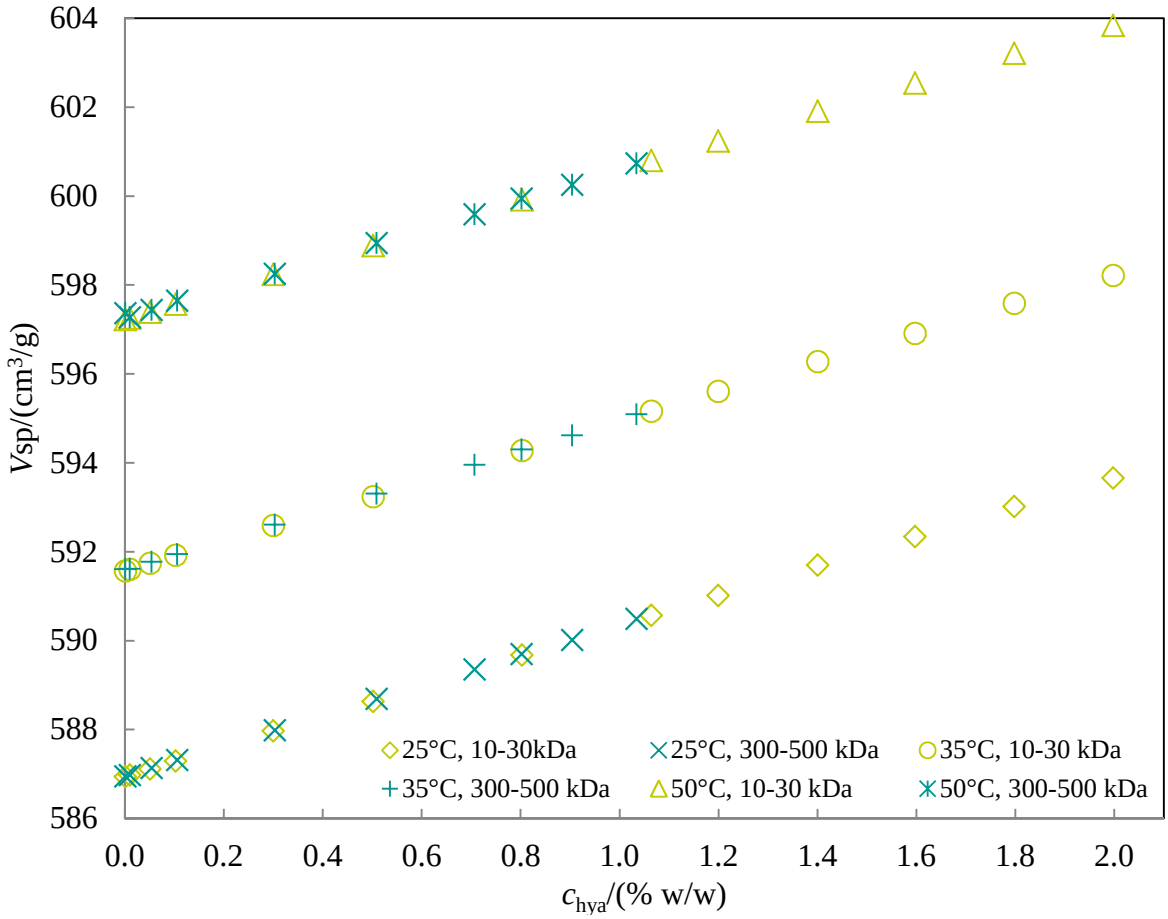

Figure 21. The temperature and concentration dependence of partial specific volume of hyaluronan solutions (10-30 kDa and 300-500 kDa) in water.

Partial or apparent (specific, molar, molal) quantities are typically extrapolated to zero concentration to obtain a value which is supposed to be free of the effects of solute-solute interactions. The extrapolated value should thus reflect only the solute-solvent interactions [148]. The extrapolation of the apparent specific volume is usually problematic due to the high uncertainty and nonlinearity of data at very low concentrations. Only the linear part of data at reasonably higher concentrations is used to be extrapolated, see e.g. [144] or [145],[145]; the same procedure was used in this work. The dependence of the partial specific volume on hyaluronan concentration was linear and the extrapolation thus was without problems. Equation (20) is, in fact, also a kind of the extrapolation to the infinite dilution. Due to the linearity of partial specific volume versus hyaluronan concentration the limiting partial specific volume ($\bar{v}^0_{sp,hya}$) calculated from this equation is numerically equal to the extrapolated value of the partial specific volume ($\bar{V}_{sp,hya}$); the latter has much lower standard deviation (owing to the fitting procedure). All the zero concentration volumes together with their dependence on temperature are shown in Table 7 and in Table ST18 in Supplementary information. The values slightly increase with temperature and the extrapolated apparent specific volume is somewhat lower than its partial counterparts. Durchschlager and Zipper [146] as well as Davies et al. [106] reported the value 0.556 cm^3/g for the extrapolated partial specific volume of sodium hyaluronate at 25 °C with no other experimental details. Gómez-Alejandre et al. [103]

determined the limiting partial specific volume of sodium hyaluronate of a molecular weight of 1500 kDa and it changed from 0.512 cm^3/g at 25 °C to 0.561 cm^3/g at 40 °C. Our values are somewhat higher; due to the lack of original data in the referenced works it is difficult to discuss these differences, we can only point to a narrower concentration range used in ref. [103] and to Haxaire et al. [149] who reported the density of (solid) hyaluronan to be 1.61 g/cm^3 which gives the specific volume of 0.621 cm^3/g. Further, Perkins et al. [147] determined the value of the hyaluronan partial specific volume, 0.58 cm^3/g, which is in excellent agreement with our results.

Table 7. Extrapolated partial specific volume of hyaluronan of different molecular weights dissolved in water.

T / °C	$\bar{V}^0_{sp,\mathrm{hya}}$ / 10^{-3} cm^3/g			
	10-30 kDa	90-130 kDa	300-500 kDa	1500-1750 kDa
25	587	587	587	587
30	589	589	589	589
35	592	592	592	592
40	594	594	594	594
45	596	595	595	595
50	597	597	597	597

* standard deviation was less then $5\times10^{-5} cm^3/g$.

Compressibility and hydration numbers

The compressibility (β) was calculated from measured density (ρ) and ultrasonic velocity (u) using the well-known equation, usually called Laplace equation:

$$u=\frac{1}{\sqrt{\beta\rho}} \tag{21}$$

$$\beta=\frac{1}{\rho u^2} \tag{22}$$

where density is in kg/m^3 and ultrasonic velocity in m/s.

Because both the density and the velocity increase with hyaluronan concentration the compressibility of hyaluronan solutions is a decreasing function of concentration at all temperatures; however the decrease is only mild (Table ST19-Table ST22). More concentrated solutions are thus slightly tougher, more rigid what can be explained by increased amount of hydrated structures, increasing excluded volume effects and perhaps also by interchain interactions.

The compressibility decreases also with growing temperature at given hyaluronan concentration and, once again, the effect of temperature is more significant than the effect of concentration (Figure 22). In a typical liquid the compressibility increases with temperature as the structure becomes more open. The decrease of the compressibility with elevated temperature is among the peculiar properties of liquid water. In fact, the adiabatic compressibility of water decreases up to 64 °C where it has a minimum.

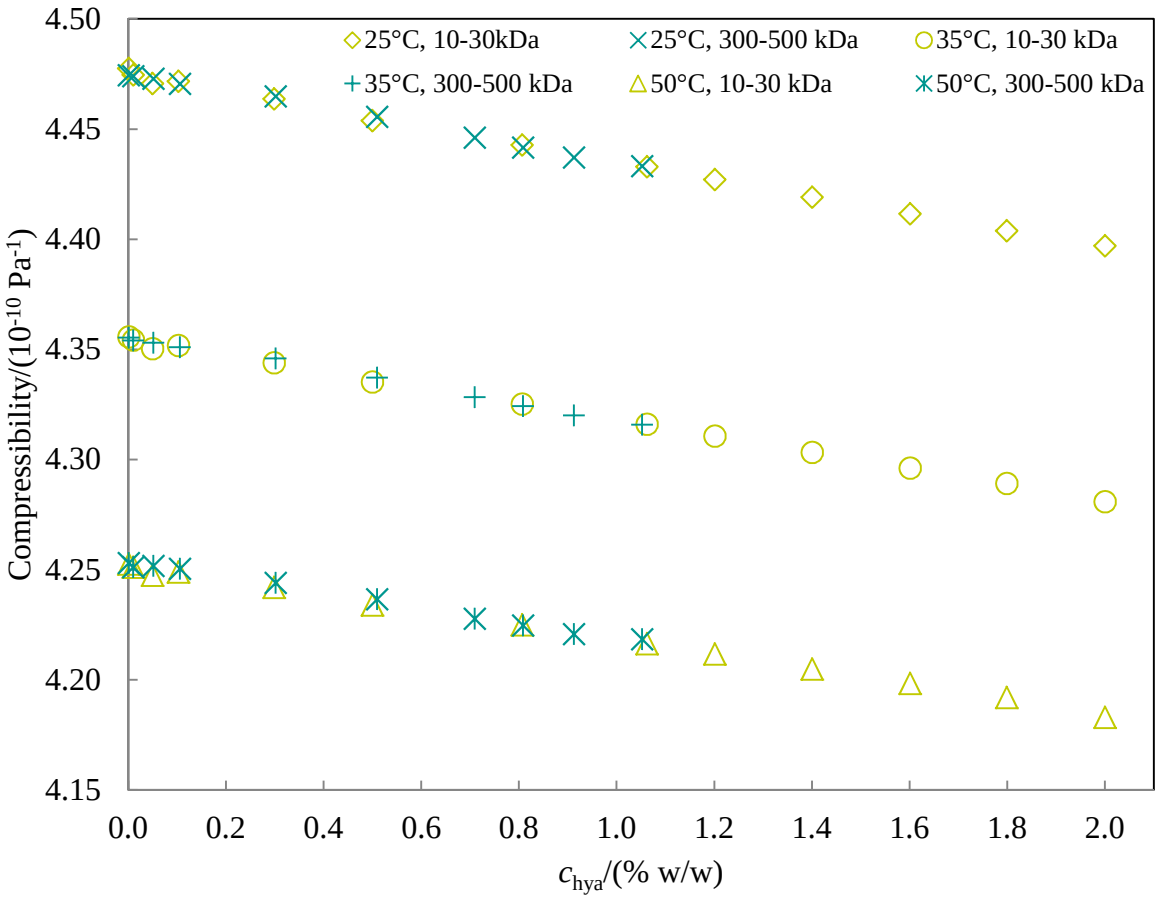

Figure 22. The temperature and concentration dependence of compressibility of hyaluronan solutions (10-30 kDa and 300-500 kDa) in water.

Hyaluronan does not disturb this peculiar property of liquid water. The effect of hyaluronan weight is negligible in compressibility.

The compressibility can be used to estimate the hydration numbers, i.e. the number of water molecules in hydration shell. An overview of acoustic methods for the determination of hydration numbers was published recently [152]. Here the simple and general Pasynski method was applied which gives the following equation to calculate hydration numbers (n_h):

$$n_{H_2O} = \frac{m_{H_2O}}{M_{H_2O}} \tag{23}$$

$$n_{dimer} = \frac{m_{hyaluronan}}{401.299} \tag{24}$$

$$n_h = \left(\frac{n_{H_2O}}{n_{dimer}}\right) * \left(1 - \frac{\beta_{sample}}{\beta_{H_2O}}\right) \tag{25}$$

where m_{H_2O} is mass of water, M_{H_2O} is the molecular weight of water, β_{H_2O} and β_{sample} are the compressibility of water and sample, respectively. n_{H_2O} and n_{dimer} are the molal concentration of water and the dimer of hyaluronan, respectively. The molecular weight of one disacharide unit of hyaluronan is 401.299 g/mol.

The Pasynski method assumes zero compressibility of water molecules in hydration shells and simple additivity of compressibility with respect to number of (compressible) molecules. Resulting hydration numbers should better be considered as estimates than exact true values; any acoustic method involves similar assumptions [152] and should be used preferably for comparison purposes within a series of similar samples. The hydration numbers are given in Table ST19-Table ST22 in Supplementary information and are very weakly dependent on temperature and hyaluronan concentration. Mostly they decrease with increasing temperature and concentration which is typical for the hydration numbers calculated by this method. No effect of the hyaluronan molecular weight could be observed. The hydration numbers in water are around 20. Haxaire et al. [150] determined hydration numbers up to about 30 depending on the moisture content in the atmosphere hydrating hyaluronan films. Hydration numbers of about 20 were observed at the very high moisture content, in relative units at almost 95% moisture.

Suzuki and Uedaira [105] used different and rather complex methods arriving at the hydration numbers of about 9 or 18 (for potassium hyaluronate) depending on the level of complexity of the method and its presumptions. The value 9 is reported as an averaged value also by Davies et al. [107] who used yet another calculation method which should determine the number of water molecules directly interacting with hydrated substrate.

6.2.5 Effect of NaCl on density, velocity and calculated parameters

The experiments and the obtained or calculated data from the measurements with sodium chloride solution are in Supplementary information in Table ST12-Table ST16, Table ST23-Table ST26, Figure SF1-Figure SF4, Table ST18. The addition of NaCl resulted in different numerical values of measured densities or ultrasonic velocities (Table ST12-Table ST16 and Table ST23-Table ST26 in Supplementary information) but did not change their dependence on concentration or temperature. The dependences of density and ultrasonic velocity on concentration of hyaluronan (of all four molecular weights) in sodium chloride solution have the same linear curve as the coincident experiments in water.

Only the linear curves of density and velocity, which increase with rising concentration of hyaluronan, are shifted to the higher volume then in water. The value of density and velocity for water and pure NaCl at 25 °C, are 0.997212, 1.003211 g/cm^3 and 1496.99, 1506.42 m/s, respectively. The examples of density and velocity dependence in two different solutions are plotted in Figure 23 and Figure SF5 in Supplementary information. The numerical difference is rooted in the difference of pure solvents – in the density of water and NaCl solution and in ultrasonic velocity in these two media.

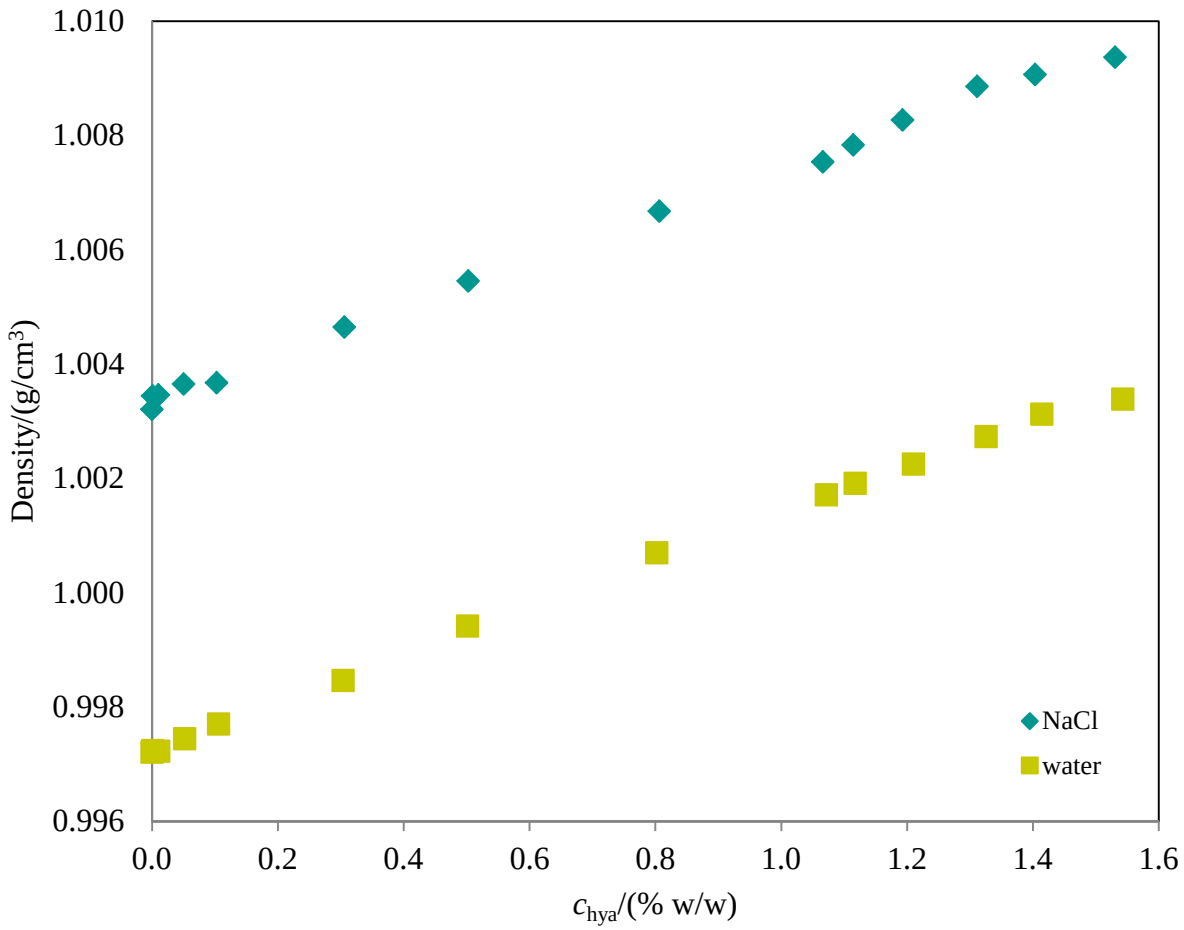

Figure 23. The dependence of density on concentration of hyaluronan with molecular weight 90-130 kDa at water and at 0. 15 M NaCl at 25 °C, measured with DSA 5000M.

In Figure 24 and Figure SF6 in Supplementary information, density and ultrasonic velocity curves of sodium chloride solutions are moved to curves of water for a certain temperature and there is seen that sodium chloride has no influence on the dependence of density and ultrasonic velocity on concentration of hyaluronan. The points of shifted sodium chloride curves of both parameters ($\rho_{NaCl,M}$, $u_{NaCl,M}$) lie at the same values of density or ultrasonic velocity of concentration line of hyaluronan in aqueous solutions in the desired temperature. The following equations recalculates density and ultrasonic velocity of sodium chloride ($\rho_{NaCl,M}$, $u_{NaCl,M}$) for the zero point of aqueous solutions:

$$\rho_{\mathrm{NaCl,M}} = \frac{\rho_{\mathrm{NaCl,\,S}}}{\frac{\rho_{\mathrm{water}}}{\rho_{\mathrm{NaCl}}}} \tag{26}$$

$$u_{\mathrm{NaCl,\,M}} = \frac{\rho_{\mathrm{NaCl,S}}}{\frac{u_{\mathrm{water}}}{u_{\mathrm{NaCl}}}} \tag{27}$$

where ρ_{water}, ρ_{NaCl}, $\rho_{NaCl,S}$ are density of water, pure sodium chloride and sample in sodium chloride solution, respectively. u_{water}, u_{NaCl}, $u_{NaCl,S}$ are velocity of water, pure sodium chloride and sample in sodium chloride solution, respectively. After recalculated parameters in sodium chloride solutions the both curves (of water and 0.15M NaCl) could be compared. If this

difference is accounted for by proper shifting of concentration or temperature dependences, common curves are obtained for both solvents as illustrated in Figure 24 for density and in Figure SF6 in Supplementary information for velocity.

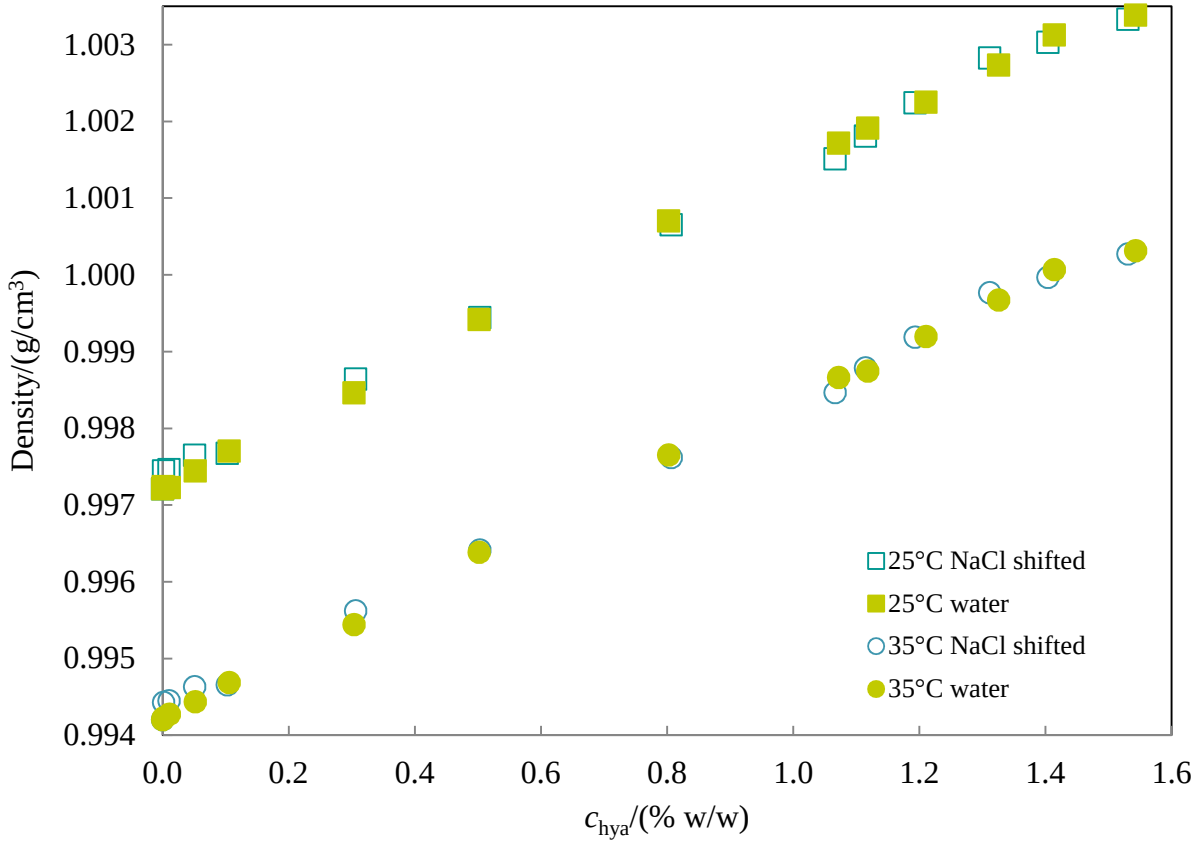

Figure 24. The effect of NaCl on the density of hyaluronan with molecular weight 90-130 kDa measured at 25 °C by DSA 5000M, where the curves of NaCl are shifted to the first point of water curves.

The partial volumes determined in 0.15 M NaCl for hyaluronan of the two lower molecular weights (10-30 kDa and 90-130 kDa) are comparable with corresponding values in water (Figure SF3). Increasing hyaluronan molecular weight causes some differences in partial volumes – those determined in sodium chloride solution are lower than corresponding values in water (Figure 25).

The values of compressibility of concentrated line of hyaluronan in 0.15 M NaCl are lower than in water (Figure 26), which means the formation of compact structure in 0.15 M NaCl. The difference is 0.08 10^{-10} Pa^{-1} at whole curve, the values for very low diluted hyaluronan are 4.39 10^{-10} Pa^{-1} and 4.47 10^{-10} Pa^{-1} in 0.15 M NaCl and in water, respectively. But the trend in both solutions is the same, the compressibility decreases with increasing concentration of hyaluronan.

Hydration numbers are comparable in both solvents. The reference [103] reported increased limiting partial volume of hyaluronan in NaCl solution and rationalized this finding by the formation of more open structures in the presence of added small ions. Again, due to

the lack of original data in that reference it is difficult to discuss this difference but our compressibility measurements do not support the idea of more open structures.

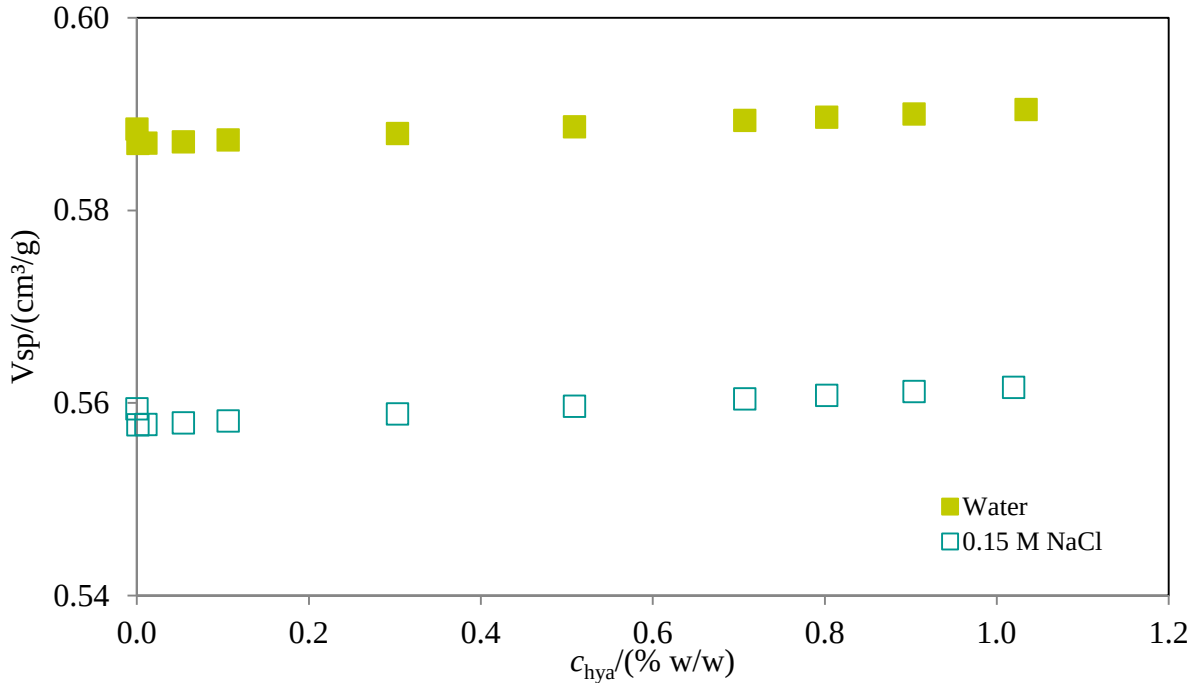

Figure 25. Comparison of partial specific volume in water and 0.15 M NaCl of hyaluronan with molecular weight 300-500 kDa at 25 °C measured by means of DSA 5000M.

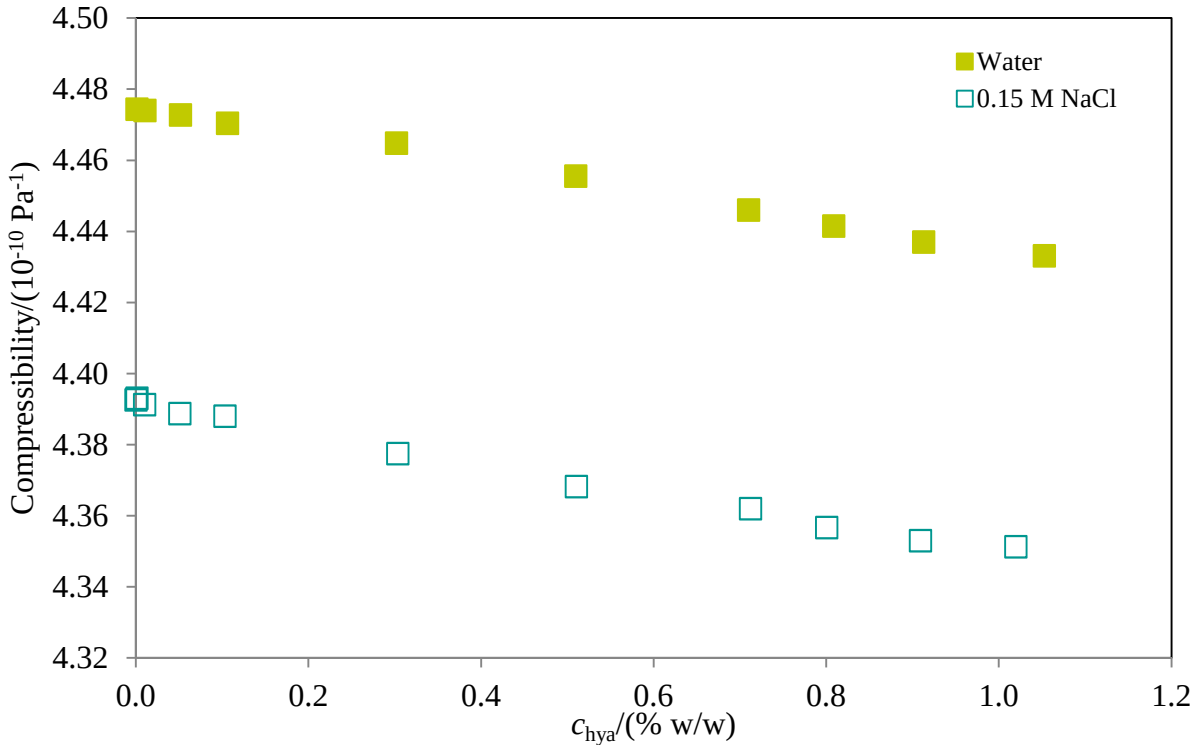

Figure 26. Comparison of compressibility in water and 0.15 M NaCl of hyaluronan with molecular weight 300-500 kDa at 25 °C measured by means of DSA 5000M.

6.3 Conclusions

The density of hyaluronan solutions in water or in 0.15 M NaCl was linearly dependent on the concentration at any used temperature and increased with the concentration. Increasing temperature decreased the density of a solution of given concentration; the temperature dependence was slightly curved and slightly deviated from linearity. The molecular weight of hyaluronan had negligible effect. Therefore all the data through all molecular weights, concentrations and temperatures used could be satisfactorily fitted with a single equation (one for each solvent); linear in concentration and quadratic in temperature. The equation can be used for reliable estimate of the density of hyaluronan solutions in the concentration range 0-2% w/w, the molecular weight range 10-1750 kDa and the temperature range 25-50 °C.

Ultrasonic velocity of hyaluronan solutions in water or in 0.15 M NaCl was linearly dependent on the concentration at any used temperature and increased with the concentration. Increasing temperature increased ultrasonic velocity of a solution of given concentration; the temperature dependence was slightly curved and slightly deviated from linearity.

The densities were used to calculate several specific volume characteristics. The hyaluronan partial specific volume in water typically ranges, depending on concentration, between 0.587 and 0.594 cm^3/g at 25 °C and between 0.597 and 0.604 cm^3/g at 50 °C; in sodium chloride solution the values are slightly lower. The ultrasonic velocity was primarily used to calculate the compressibility. The compressibility decreased with both the hyaluronan concentration and the temperature, the influence of the temperature was stronger.

The hydration numbers determined from the compressibility data were typically about 20 and only slightly dependent on concentration. The addition of NaCl caused the changes in numerical values of measured or calculated quantities but did not change the character of their concentration or temperature behaviour. There is negligible effect of molecular weight on all measured or calculated properties.

7 EXPERIMENTAL PART II – HYALURONAN-SURFACTANT SYSTEMS

The aim of this chapter is study of the system hyaluronan-surfactant in concentration of 15 mg/l and 1000 mg/l of hyaluronan in water and sodium chloride solution. These systems were investigated mainly with high resolution ultrasonic spectroscopy.

First part of the chapter is focused on pure cationic surfactants: tetradecyltrimethylammonium bromide and hexadecyltrimethylammonium bromide, and determination of the critical micelle concentration.
Method high resolution ultrasonic spectroscopy was further used for a detailed study of interactions between hyaluronan and two cationic surfactants tetradecyltrimethylammonium bromide (TTAB) and hexadecyltrimethylammonium bromide (CTAB) in water and in sodium chloride solution. This part of the work is summarized in 7.2.3.

Figure 27. High resolution ultrasonic spectroscopy (HR-US 102T) from Ultrasonic Scientific.

7.1 Materials and methods

Hyaluronan was obtained from Contipro Biotech (Czech Republic) where is extracted from the cell walls of the bacteria *Streptococcus zooepidemicus*. This producer offers a broad range of molecular weight in predefined range of molecular weight. Following hyaluronan products were used in this study: 10-30 kDa, 110-130 kDa, 300-500 kDa and 1750-2000 kDa; concrete molecular weight (determined by the producer using SEC-MALS) of particular samples from each range used in this study are given in Table 8. Surfactant hexadecyltrimethylammonium bromide (CTAB) and tetradecyltrimethylammonium bromide (TTAB) (Figure 28) were purchased from Fluka and sodium chloride (NaCl) from Lachner.

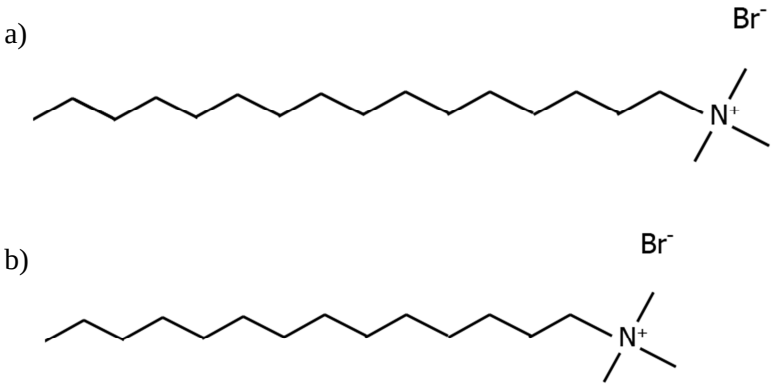

Figure 28. Specification of surfactants a) CTAB and b) TTAB

Table 8. Molecular weights of hyaluronan used in the experimental part II.

Product name	M_w *	Batch number
kDa	kDa	
10-30	17	211-589
	16	211-263
	15	212-2069
90-130	116	210-493
	137	211-234
	101	212-1214
	116	212-2859
	117	213-3842
300-500	421	208-125
	430	212-2082
	458	213-3809
1500-1750	1730	210-636
	1800	211-180
	1697	212-1271
	1644	212-2298

* weight-average molecular weight provided by the supplier and obtained by SEC-MALS analysis.

Hyaluronan solutions were prepared at concentration 1000 mg/l and 15 mg/l by dissolving powder hyaluronan in water or in 0.15M NaCl in closed vessel. Hyaluronan is very hydroscopic and must be protected from moisture during weighing. The solution was stirring for 24 hours at room temperature to ensure the complete dissolution. Ultrapure deionized water from a Millipore water purification system (Option R7/15; ELGA, Great Britain) was used for the preparation of all samples.

7.1.1 High resolution ultrasonic spectroscopy

Ultrasonic wave is a wave of oscillating pressure and associated longitudinal deformation travelling through the sample. Molecules in the sample respond to oscillating deformations through inter-molecular repulsive (compression) and attractive (decompression) forces reflecting the measured elasticity of the sample. Thr elasticity is the major contributor to the first characteristic measured in this technique, ultrasonic velocity. Propagating through the medium, the ultrasonic wave loses its energy and is subjected to a scattering process, which causes ultrasonic attenuation. Attenuation (or attenuation coefficient), the second measured parameter, is determined by the reduction in amplitude of an ultrasonic wave which has travelled a known distance through a medium per unit travelled distance. The major contributors to attenuation are fast chemical relaxation and microstructure of non-homogeneous samples. The high resolution refers primarily to the measurement of velocity and is achieved by parallel measurements of ultrasound propagation in sample and reference cells. The reference cell is filled with the pure solvent (water or sodium chloride solution in our case).

All ultrasonic measurements were performed on high resolution ultrasonic spectroscopy within one of the following three regimes: kinetic, temperature and titration regimes. In this chapter, these regimes are described in details.

The kinetic regime was used in experimental part I and II. The ultrasonic cell 1 was filled with a solution and cell 2 was filled with water. The measurement was started ten minutes after filling the cells. The measurement was running for two hours. The contribution of the hyaluronan was subtracted using the baseline (measuring when in both cells were water).

The second example of ultrasonic measurements is used for evaluation of thermal stability [94],[98] and effects of thermal history. This analysis is done with the temperature ramp regime, which allows measurement when the temperature is changing with a programmed speed. The measurements were done in temperature range from 25 °C to 50 °C with the temperature ramp rate 0.5 °C/min. The temperature in the cell was monitored by the incorporated thermometer. Temperature regime was used in the experimental part II.

In this chapter the main using of HR-US 102T was the titration regime for the characterization of system hyaluronan-surfactant. The titration profiles for ultrasonic velocity and attenuation were measured at 25 ºC; at frequency range 2.5-17.5 MHz using HR-US 102T. The sample ultrasonic cell was closed with a stopper, which incorporated a line for injection of titrant. The measuring cell was filled with hyaluronan solution using a calibrated 1 ml Hamilton syringe. The exact amount of the solution in the cell was determined by weighing the syringe before and after filling. The titration accessory of HR-US 102T was equipped with 50 µl Hamilton syringe which was used for the dosage of the titrant. The reference cell was filled with the same amount of water. Measurements were continuously performed while the sample in the measuring cell was titrated with surfactant (CTAB or TTAB). Solution of TTAB and CTAB in water and in 0.15 M NaCl was used as a titrant. The titrant solution was injected to the sample automatically in 2-µl steps by the computer-controlled titration accessory of ultrasonic spectrometer. The stirring was activated before each addition of surfactant and continued until no further change in the ultrasonic velocity and attenuation occurred, indicating that stabilization after the titrant addition had

been reached. Following this stirring was stopped, stability of the measured values and attenuation was confirmed (5 to 10 minutes without stirring approximately) and next portion of surfactant was added.

It was used the resonance mode, measurements of ultrasonic velocity and attenuation was performed with high precision. The longitudinal ultrasonic wave, generated by the vibrations of one wall of the ultrasonic cell (first wall), of a particular frequency propagates through the sample toward the opposite (second) wall. The opposite wall reflects the wave back toward the first wall, which also reflects the wave back to the opposite wall and so on.

Every titration measurement has three parts: measurement of water, titration 1 – measurement of the baseline (titration into the water/0.15 M NaCl), titration 2 – titration into sample (hyaluronan). Before every measurement water was measured for two hours check that the known value for water was in agreement with previous measurement of water. If it is not so, the cells have to be cleaned again and refilled with water to start the measurement.

Titration 1: measurement of the baseline (titration into water)

Both cells contain water and the titrant (surfactant) was added to cell one by titration regime. The HR-US program with present frequency channels (peaks) was started first. After the several minutes required for the measurement of initial values, the titration scenario was started. The ultrasonic velocity and the attenuation were measured upon the automatic titration of CTAB solution into the water and the data were collected.

Titration 2: titration into sample

The sample cell was washed with water and then dried using dry air. After drying the sample cell was filled with 1 ml of degassed sample of hyaluronan. The frequencies of the peaks with the same peak number (peak ID) as in buffer were found and the measurement was started. Cell one contained sample (hyaluronan) and cell two contained water. The 50 µl syringe of titration accessory was loaded with 35 µl of titrant solution using the same Program Steps as those used for Titration 1. The ultrasonic velocity and attenuation in the solution of hyaluronan was measured up on the automatic titration with the solution of surfactant using the same procedure as for Titration 1.

Before every measurement baseline correction was done. The same measurements in titration regime were performed for sample cell loaded at time zero with deionised water or with 0.15M NaCl. Ultrasonic velocity and attenuation profiles measured in water or in 0.15M NaCl were subtracted from corresponding profiles in hyaluronan sample, in order to remove the effect of temperature fluctuations and fine differences in the resonance of the cells on measured values of ultrasonic parameters

The measured data were processed using Titration Analysis software (Ultrasonic Scientific, Ireland) which also includes a correction for dilution. All ultrasonic spectra were acquired by adding surfactant to the solution, with stepwise concentration increases. A quantitative dilution was performed for each point in the curve which is the average of 8-10 values of ultrasonic attenuation in the time of relaxation (10 minutes) after three minutes of stirring. One titration measurement typically took 22 hours. Each measurement was done minimally three times and the values were averaged.

The measurement of pure water lasting minimally 30 minutes was done before every measurement at all regimes of HR-US. The values of water were compared to previous

measurement and if the results were not close, the cell had to be cleaned again very well. The value of water is given in the table of software HR-US so it is the reason of importance of measurement of water in the accuracy of the relative measurements of ultrasonic velocity. In references [153],[154],[155] ultrasonic velocity in water was extensively measured as a function of temperature. The density, heat capacity and many other physicochemical quantities were published in numerous papers and tables but high precision data of ultrasonic velocity in water are available only in original papers [153],[154].

Setting of HR-US instrument

Relative velocity/attenuation (*U1, N1*) is difference between velocity/attenuation in sample and in the reference media (water). Velocity/attenuation difference (*U12, N12*) is difference between velocity/attenuation in the cell 1 and cell 2. Differential plot is plot of the differences of the relevant parameters between cell 1 and cell 2.

$$f_{n+1}\text{-}f_n = \frac{u}{2L} \tag{28}$$

Determination of approximate value of ultrasonic velocity knowing the cell length (L):

$$u = 2L(f_{n+1}\text{-}f_n) \tag{29}$$

Determination of approximate value of ultrasonic velocity knowing the difference between two successive peaks ($f_{n+1} - f_n$) in the reference liquid (Δf_{ref}) and in sample (Δf_{sample}).

$$u \cong 2u_{ref}\frac{\Delta f_{sample}}{\Delta f_{ref}} \tag{30}$$

Determination of ultrasonic velocity in unknown media using the frequency shift of a peak relative to a reference medium (the shift shall be much smaller than the frequency of the peak)

$$\frac{\Delta u}{u} = \frac{\Delta f_n}{f_n} \leftrightarrow \frac{u_{unkonwn} - u_{reference}}{u_{reference}} = \frac{f_{n\ unkown} - f_{n\ reference}}{f_{n\ reference}} \tag{31}$$

Determination of peak ID - peak number (n):

$$n = \frac{f_n}{f_{n+1} - f_n} \tag{32}$$

the frequency difference between two successive peaks f_{n+1} and f_n.

The determination of ultrasonic velocity is based on the measurement of frequency of peak produced in measured sample. The ultrasonic attenuation is related to the width of this peak. It had to have to perform a frequency scan to find the positions of these peaks.

Because the resonances are not ideal and depend also on the materials of which ultrasonic cells are built, resonance peaks in some frequency ranges may not be suitable for measurements of ultrasonic velocity and attenuation in sample. Amplitude/frequency scan allows the user to see the available peaks. The both cells were filled with degassed water or with sodium chloride solution and the HR-US spectrometer was switched to the Amplitude/frequency scan mode in HR-US software. The frequency scan is performed

in every solvent and in every different instrument of HR-US or when the certain instrument is fixed or transported.

The typical ultrasonic spectrum of water and 0.15 M NaCl are shown in Figure 29 and Figure 30, the amplitude of the output signal is shown as a function of the frequency of the acoustical signal. Amplitude/frequency scan allows seeing the available peaks for measuring of the sample. The spectral regions for example at frequencies around 4, 7 and 10 MHz were avoided in all of our experiments.

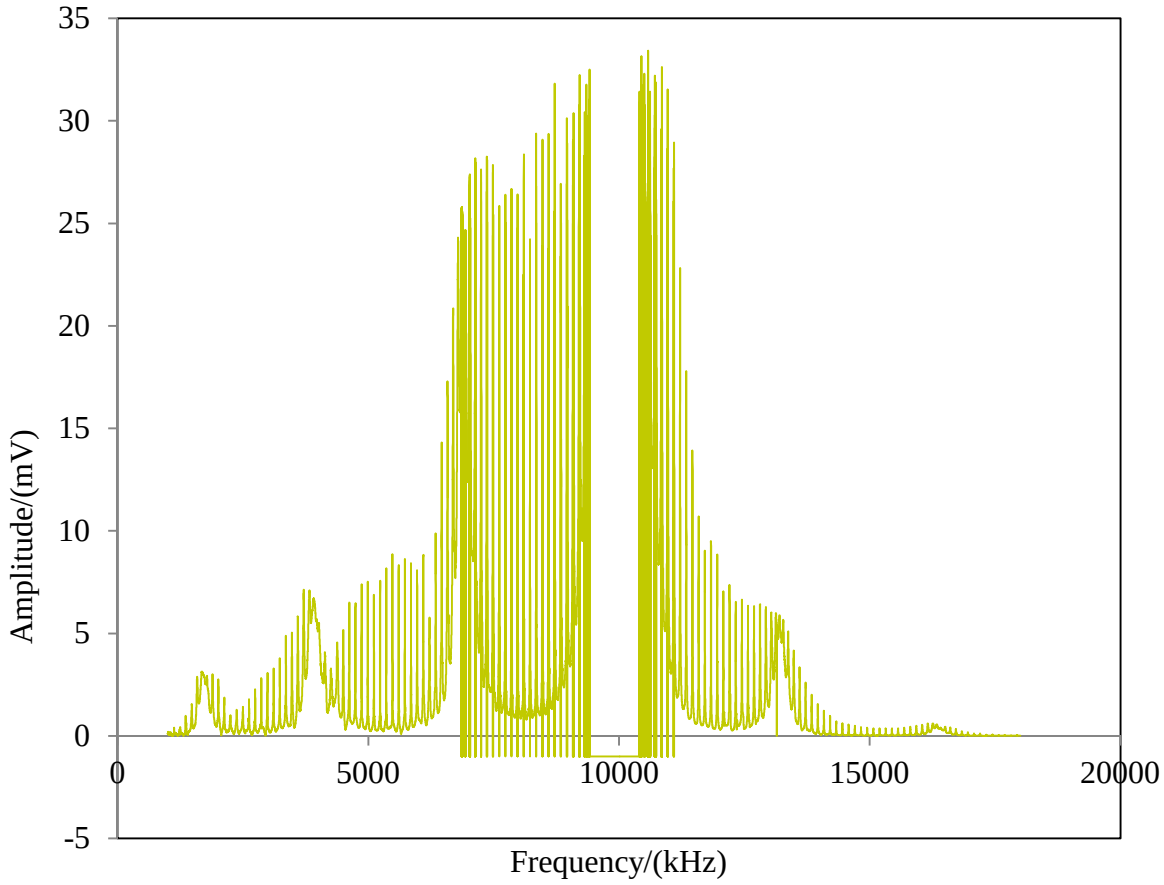

Figure 29. Ultrasonic spectrum of water at 25 °C.

It has to be selected the resonant peaks for our measurements in the eight frequency ranges. It is important to write down the resonant frequency and ID number of peak. The ID number (*n*) tells how many half ultrasonic wavelengths can be placed between the walls of ultrasonic cells and each peak has its unique number. ID number has to be the same for each measurement. That peaks move during the analysed chemical process or a temperature ramp so it has to be control that the peak leave in the recommended frequency ranges (Table 9).

Table 9. The recommended frequency ranges of water for HR-US spectrometer.

Frequency range	Amplitude of the input signal
2.4 – 3.0 MHz	1V
4.6 – 5.8 MHz	0.4 V
7.7 – 8.6 MHz	0.16 V
11.6 – 12.7 MHz	0.4 V
14.5 – 15.7 MHz	4 V
17.1 – 20.0 MHz	4 V

Because resonances are not ideal and depend also on the materials of which ultrasonic cells are built, resonance peaks in some frequency ranges may not be suitable for measurements of ultrasonic velocity and attenuation in the sample. So it is necessary to do frequency scan before every new measurement of new material or solution. The frequency scan of 0.15 M NaCl is in Figure 30. In choosing of peak is important to think that the peak will be shifted in temperature ramp or during titration so it is good to give peak in the middle of the recommended frequency range and of course the peak has to look good, without other small peaks. Also the peak number of the peak´s frequency (F_0) and the peak number of the frequency of the reference media must be the same. Several of the sharp ultrasonic resonances are shown in Figure 31 at frequency range 7700-8400 kHz. Each of these peaks has a peak number, which can be calculated by dividing the frequency of the peak by the frequency difference between neighbouring peaks (equation 32).

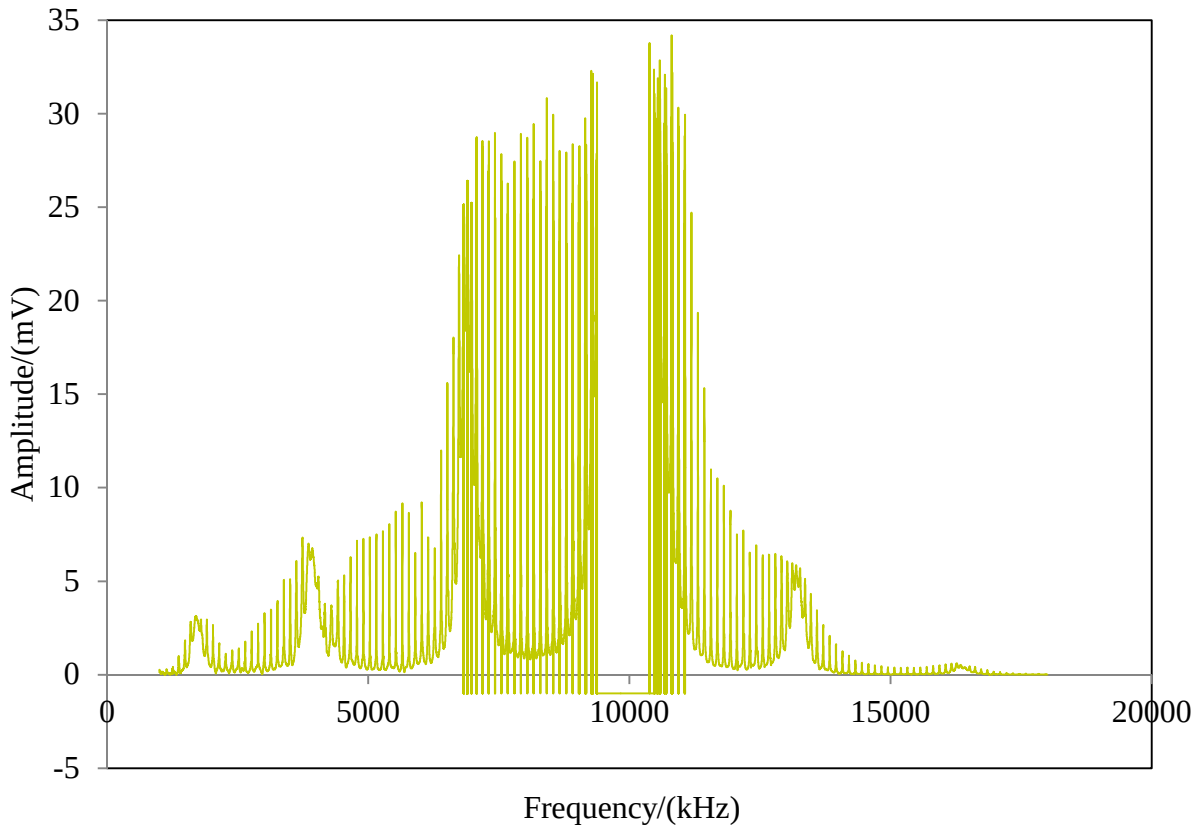

Figure 30. Ultrasonic spectrum of 0.15 M NaCl at 25 °C.

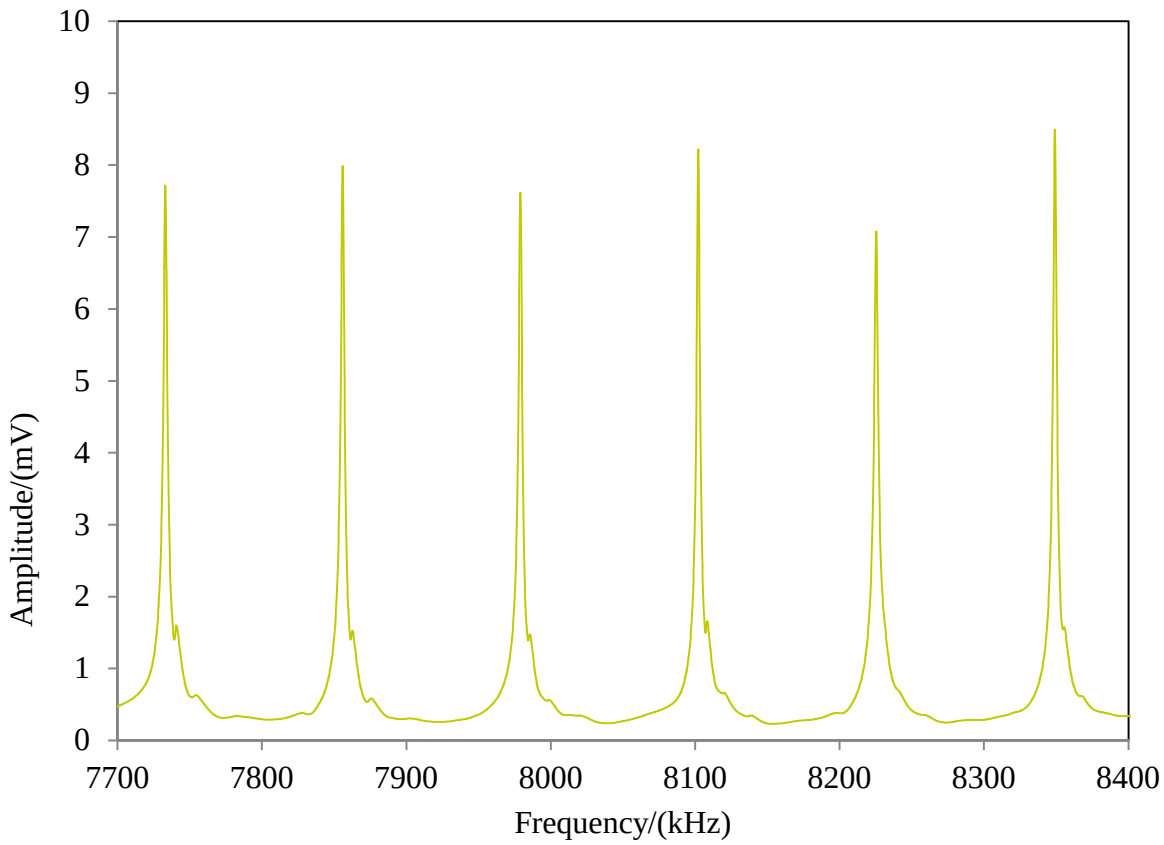

Figure 31. Ultrasonic spectrum of water at frequency range 7700-8400 kHz at 25 °C.

The correct input voltage must be chosen. Amplitude of the input signal should be adjusted for each frequency range (recommended voltage for water is in Table 9). The chosen peak should have maximum amplitude around 15 mV. If amplitude of peak is lower than 6 mV, the input voltage must be increased in proportion to the required amplitude range. If the amplitude of the peak is greater than 20 mV or it has "overloaded", it was reduced the input voltage in proportion to the required amplitude range. An overload occurs when the amplitude of the chosen peak has exceeded the maximum measurable peak amplitude; for water that is 30 mV.

Differential measurement is used for eliminate the effect of small temperature variations on the measured values of ultrasonic velocity. In this type of measurements one of the cells contains an analysed sample and the second cell contains a liquid (water, buffer, reference sample etc.), which has similar dependence (slope) to the analysed sample of ultrasonic velocity versus temperature. Because both cells are controlled by the same temperature controller, the effect of small temperature variations of the temperature controller (0.01 °C approximately) will be excluded (minimized) from the velocity difference (difference between ultrasonic velocity in the cell 1 and cell 2). It is necessary explain some terms as differential and relative parameters or what it is phase and bandwidth. Differential plot is plot of the differences of the relevant parameter between cell 1 and cell 2. Relative velocity/attenuation is difference between velocity/attenuation in the sample and the reference media. The "phase" is the angular relationship between the input and output signal to and from the cell and is gave in units of degrees. The HR-US spectrometer creates

a mechanical wave within the analysis cell and the peak produced is what is analysed. The ultrasonic attenuation is calculated from the "bandwidth" (the width of the peak, measured across a point equal to the maximum amplitude divided by the square root of 2) at which this peak occurs.

In setting of measurements were gave amplitude 1 and phase accumulation 3.

7.1.2 Densitometer DSA 5000M

The princip of measurement of densitometer is described in detail in Experimental I. In this chapter, densitometer was used for characterization of surfactants where was measured density and ultrasonic velocity in temperature ramp 20-50 °C. Our interest in density data of hyaluronan solutions with solutions of surfactants comes from the studies of hyaluronan and its interactions with surfactants measured by means of high resolution ultrasonic spectroscopy. The ultrasonic measurements are usually accompanied by the measurements of density in order to enable the calculations of compressibility from ultrasonic velocity and density.

7.2 Results and discussion

Density and ultrasonic velocity of surfactants (TTAB and CTAB) were measured in the temperature range 25-50 °C (chapter 7.2.1). The critical micelle concentration of surfactants both in water and sodium chloride solution was determined by HR-US in chapter 7.2.2. The binding of surfactants to hyaluronan chain either in water or in sodium chloride solution is described in chapter 7.2.3. The results are summarized also in a scientific paper which is prepared for publication (chapter 13.2).

High resolution ultrasonic spectrometer gives as output the difference in velocity or attenuation measured between the sample and reference cells, i.e. the difference between the value in the sample and in water or in 0.15 M NaCl in our case. Data are therefore reported in terms of velocity difference – *U12* (attenuation difference – *N12*).

7.2.1 Characterization of surfactants

The solutions of surfactants (100 mM CTAB and 50 mM TTAB) in water or 0.15M NaCl were examined with densitometer DSA 5000M. The parameters, density and ultrasonic velocity, were used for the determination of temperature dependences of surfactants in temperature range 20-55 °C (Figure 32, Table ST34, Table ST35 and Figure SF7 in Supplementary information).

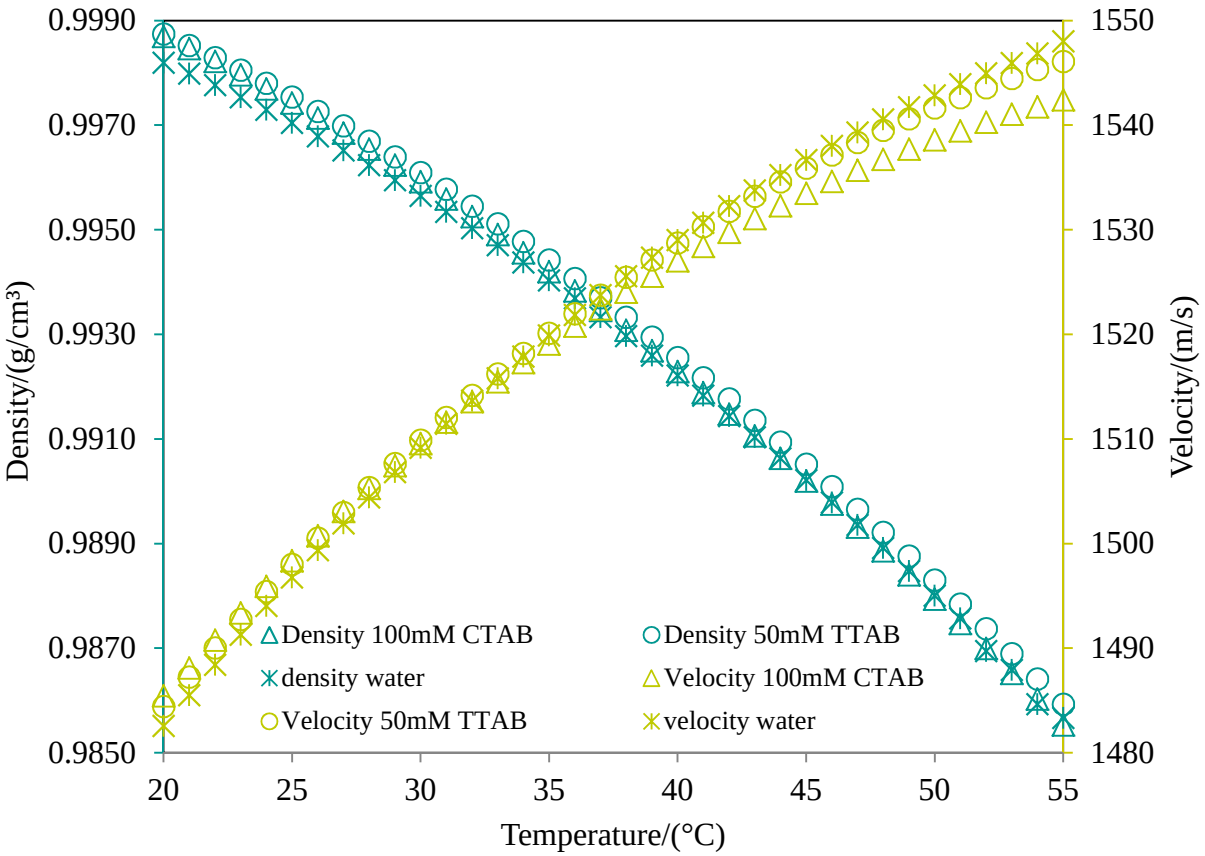

Figure 32. The density and velocity dependence of surfactants CTAB and TTAB on temperature measured with DSA 5000M.

7.2.2 The critical micelle concentration in water and 0.15 M NaCl

The critical micelle concentration is an important parameter for the development of products and processes containing surfactants. The critical micelle concentration of alkyltrimethylammonium bromides with different long alkyl chain were studied using tensiometric, fluorimetric [131], and calorimetric [157],[159], viscometric and conductometric [160],[161],[162] methods. In our work as well as in other works [134],[125],[136], the critical micelle concentration was studied by measurement of density and ultrasonic velocity.

First, titrations with pure surfactants in water or 0.15 M NaCl were performed for the purpose of verification and comparison. Critical micelle concentrations and compressibility could be obtained and compared with literature. Further, the titration profiles in the absence of hyaluronan provided the base for investigation of its effect caused by the interactions with surfactants. The measured velocity profiles are shown in Figure 33 and Figure 34. The velocity increases with increasing surfactant concentration due to the increasing number of relatively rigid surfactant molecules and especially due to their hydration shells composed of less compressible water molecules [156]. The increase is linear and the point of abrupt change of the slope determines the critical micelle concentration. In water, the slope behind the critical micelle concentration is close to zero while in the NaCl solution it is still positive but smaller than below this concentration. The decreased slope is a combined result of the formation of micelles with compressible core, the release of hydration water from

surfactant monomers, and the formation of new hydration shells around micelles. In the salt solution also the chloride ions are incorporated into micellization forming more rigid micelle structures and their increasing number causes the continuous velocity increase observed behind the critical micelle concentration. In the salt solution also the chloride ions are incorporated into micellization forming more rigid micelle structures and their increasing number causes the continuous velocity increase observed behind the critical micelle concentration. The critical micelle concentrations were determined from the intersection of two straight-line segments fitting the ultrasonic velocity versus concentration plots and are close to the values given in the [157] [162].

At low surfactant concentration (below the critical micelle concentration) the value of ultrasonic velocity increases linearly which corresponds to the monomer form of the surfactant. Above the critical micelle concentration, the concentration of ultrasonic velocity is constant as a result of the micelle formation. Figure 33 gives water and Figure 34 gives sodium chloride solution ultrasonic velocity versus surfactant concentration. The measured values of ultrasonic velocity and attenuation for corresponding concentration of surfactants are in Table ST36 in Supplementary information.

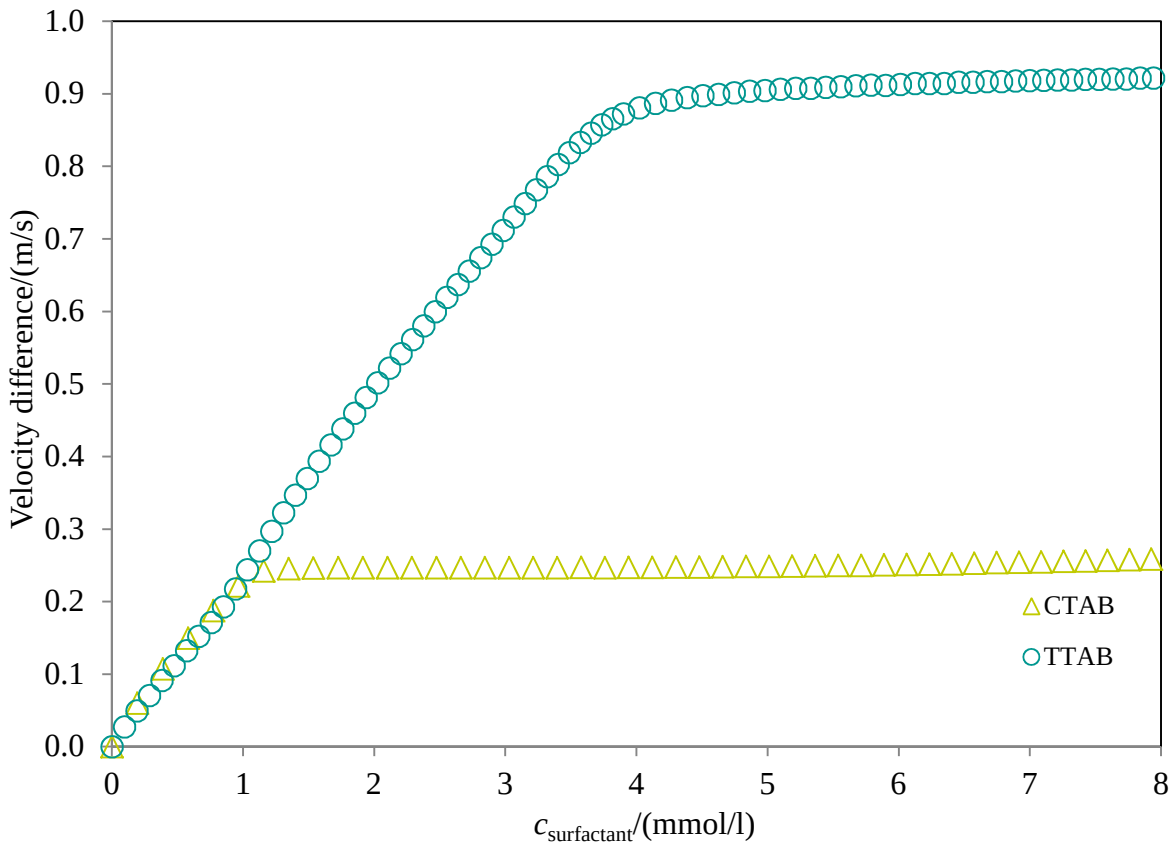

Figure 33. The determination of the critical micelle concentration of surfactants TTAB and CTAB in water at 25 °C, at frequency 15MHz.

We used the concentration of 0.15 M of sodium chloride because of presence of this concentration in the human body, the system surfactant-hyaluronan could be used as a drug delivery.

Beyer et al. [157] dissolved alkyltrimethylammonium bromides with different alkyl chain lengths, namely dodecyltrimethylammonium bromide (DTAB), tetradecyltrimethylammonium bromide (TTAB), and hexadecyltrimethylammonium bromide (CTAB) in 0.1 M sodium chloride solution and studied thermodynamic characterization of the micellization of these cationic surfactants, as a function of temperature using isothermal titration calorimetry (ITC).

Table 10. The critical micelle concentration, CMC, of the surfactants TTAB and CTAB in water and sodium chloride solution at 25 °C measured by means of HR-US 102T, comparing with the CMC from literature [137],[164].

Surfactant/environment	CMC mmol/l (this work)	CMC mmol/l [references]
TTAB/water	3.7	3.7 [164], 3.7 [134] , 3.5 [160], 3.8 [115], 3.7 [125], 3.7 [136]
CTAB/water	1.0	0.9 [115],[125],[134],[135],[157],[160], 1.0 [164]
TTAB/0.15M NaCl	0.58	0.52 [131]
CTAB/0.15M NaCl	0.07	0.06 [131]

In water and below the critical micelle concentration the velocity profiles of both surfactants are very close. In the micelle state the velocity in the TTAB system is several times higher than in CTAB. The TTAB micelles are thus less compressible than the CTAB micelles which correspond to previous determinations of the apparent adiabatic compressibility of alkyltrimethylammonium bromides [134] and was attributed to the structure of the internal core of micelles which was found to be close to that in pure hydrocarbon liquids. Similar situation was observed comparing the two velocity profiles in NaCl solution. As expected, salt did not penetrated into the micelle core and affected only the micelle surface composed of polar groups and their hydration which resulted in increasing velocity within the post-micelle concentration region of both surfactants. Increasing the salt concentration reduces the electrostatic repulsion between the charged groups and therefore favours the aggregation process inducing a decrease of critical micelle concentration. The measured values of ultrasonic velocity and attenuation for corresponding concentration of surfactants are in Table ST36 in Supplementary information.

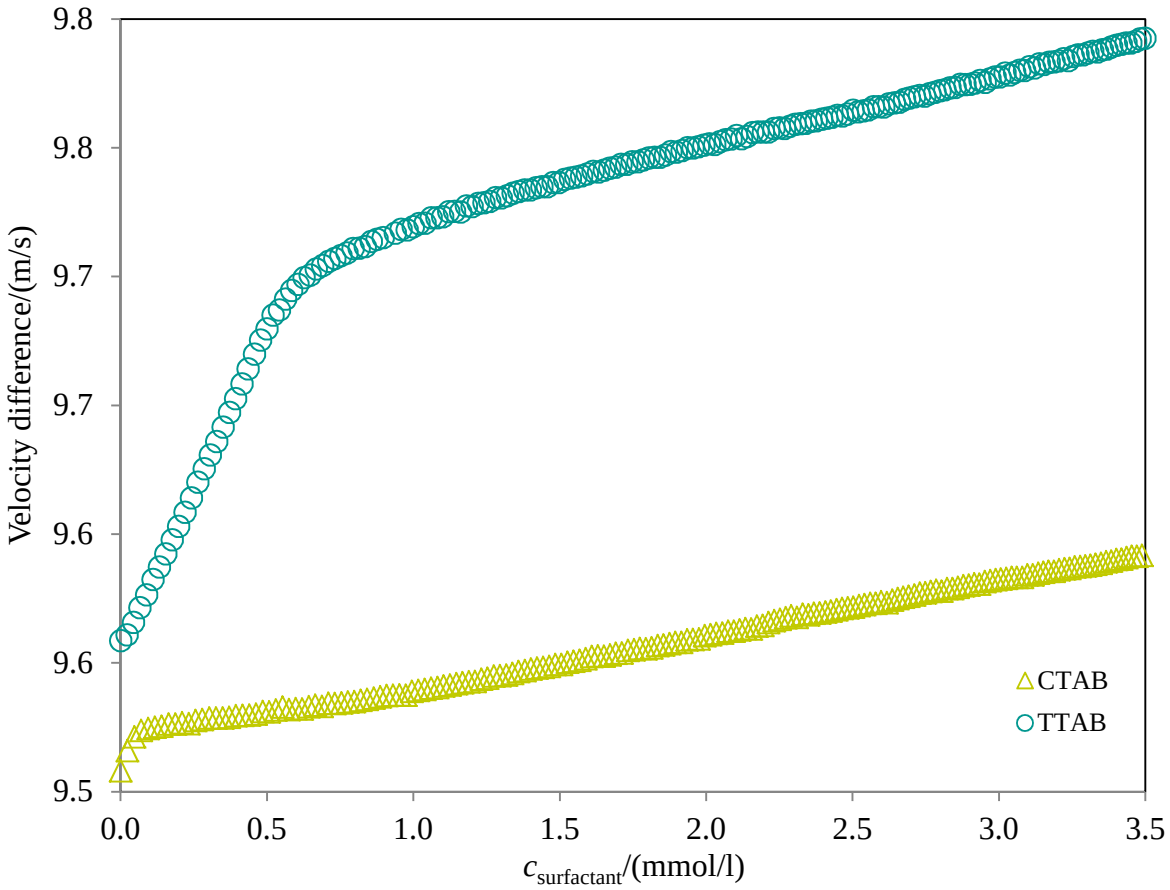

Figure 34. The determination of the critical micelle concentration of the surfactants TTAB and CTAB in sodium chloride solution at 25 °C, at frequency 15 MHz.

Compressibility of the surfactants in water and 0.15 M NaCl

The compressibility was calculated from the equation 22. There are the noticeable changes in compressibility during micelization; the compressibility descreases to the critical micelle concentration and above critical micelle concentration the compressibility is constant (Figure 35).

Kudryashov et al. [134] showed dependence of the values of apparent molar adiabatic comppresibility as a function of the number of the alkyl groups where the apparent molal adiabatic compressibility decreases with the alkyl chain. Zielisnky et al. [163] the apparent adiabatic compressibility of the surfactant in the monomeric forms decreases with the number of carbon atoms of alkyl chain. On the otherwise the apparent compression of the surfactant in the micelle forms increases.

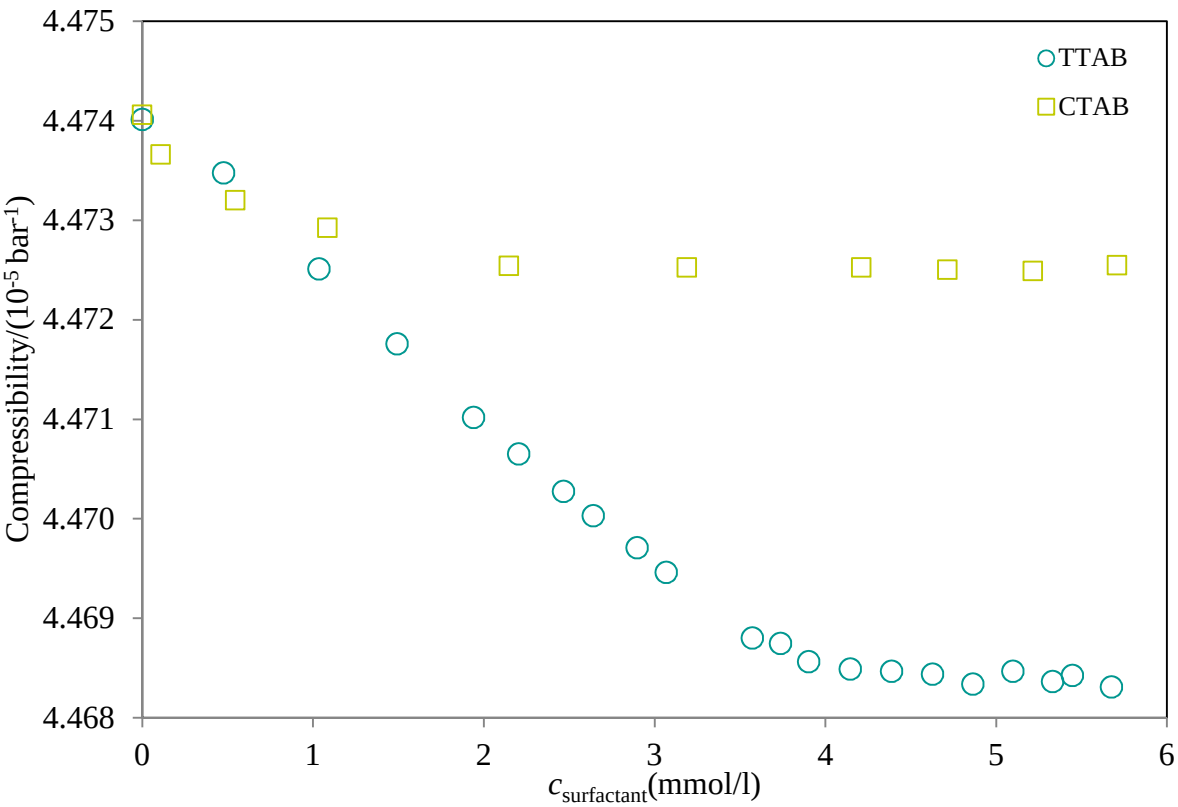

Figure 35. Adiabatic compressibility of surfactants TTAB and CTAB in water.

7.2.3 Binding of the surfactant to hyaluronan in water and 0.15 M NaCl

Binding of surfactant to hyaluronan chain is observed mainly by technique high resolution ultrasonic spectroscopy, but it was also investigated by densitometer DSA 5000M. Data from densitometer were used for the calculation of compressibility.

Titration of hyaluronan solution hyaluronan by TTAB in water

The ultrasonic cell was filled with hyaluronan solution and titrant (surfactant) was injected stepwise in the solution and then the reference cell was filled with water/0.15 NaCl. Ultrasonic parameters (velocity, attenuation) of the solution were constantly monitored and the contribution of the titrant was subtracted using the reference cell data. The curve on the screen of the monitor represents a change in ultrasonic velocity and attenuation caused by the binding of surfactant with polymer. Figure SF9 (in Supplementary information) shows the dependence of ultrasonic velocity and attenuation on concentration of surfactant TTAB during the titration of hyaluronan solution by TTAB. The titration of water by surfactant TTAB is in Figure SF8 in Supplementary information. In these two figures the significant breakpoint is seen both in velocity and in attenuation profile. Titration curve of water was shifted to to first point of curve of hyaluronan solution (Figure 36) for better comparing.

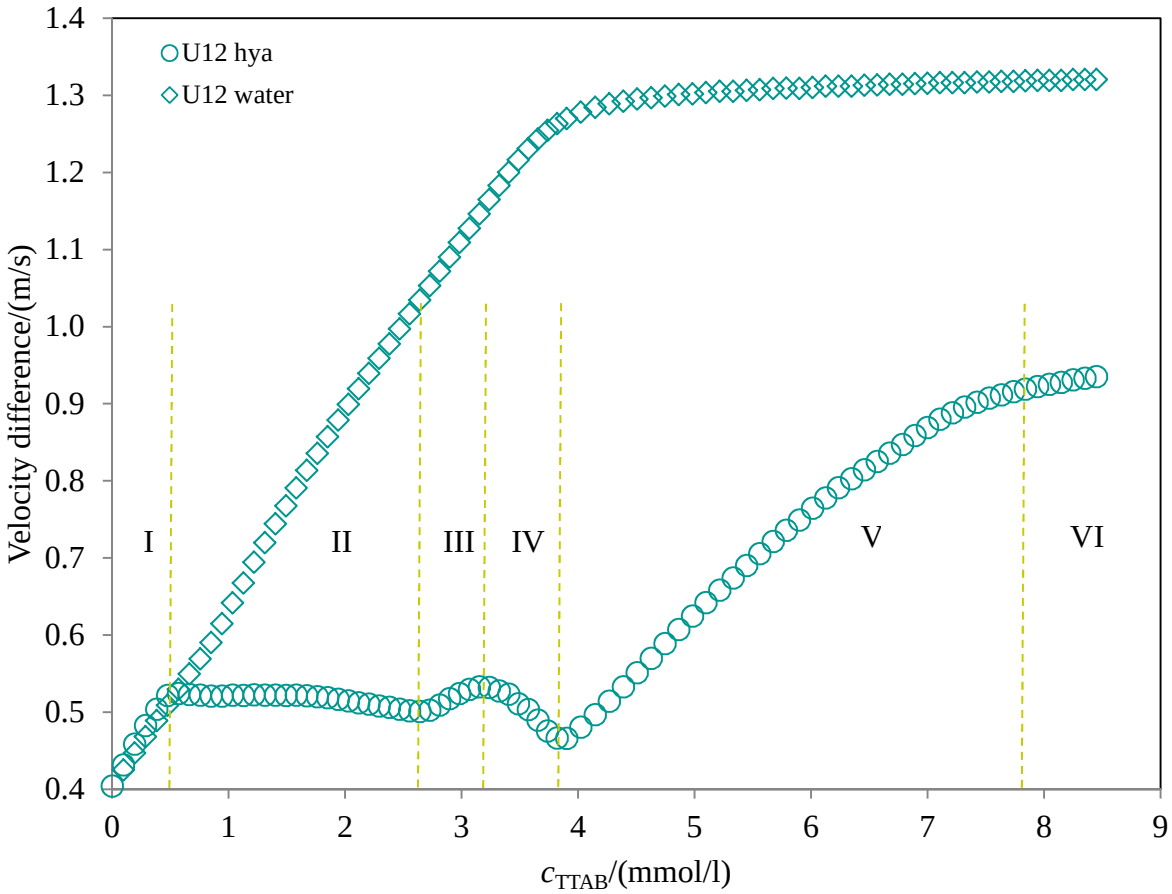

Figure 36. The velocity titration profile of hyaluronan of concentration 1000 mg/l and molecular weight of 300-500kDa and titration velocity profile of water with TTAB, at frequency 15 MHz. The titration curve of water is shifted to fisrt point of hyaluronan curve.

Figure 36 compares ultrasonic velocity titration curves obtained during the TTAB titration into water or hyaluronan solution (300-500 kDa, initial concentration of 1 g/l). The curve for the titration in water clearly shows the two parts corresponding to pre-micelle and post-micelle states. On the other hand, up to six parts can be found for the titration profile measured in hyaluronan solution (Table 11). The first part is practically identical to the corresponding pre-micelle part of the titration profile obtained in water. Visually, this part corresponds to clear solution; the charge ratio is well below one (see in Table 11). In this part no effect of added hyaluronan is thus observed which should be a result of the prevailing presence of free surfactant molecules; some single surfactant molecules could be loosely bound to hyaluronan without changing their compressibility.

In the second part the increase of ultrasonic velocity with the surfactant concentration stops at the presence of hyaluronan. On contrary, a very slight velocity decrease is observed. This part resembles the post-micelle part of the titration profile in water. Progressive opalescence up to milky clouding was observed visually. The charge ratio approaches one closely to the end of part II. Ultrasonic practically does not “see” the addition of surfactant molecules into the system. In this part binding of surfactant on hyaluronan in the form of micelles should prevail. Because the surfactant concentration is still below its normal

critical micelle concentration the micellization process is induced by the presence of hyaluronan, mainly by electrostatic interactions between oppositely charged groups on hyaluronan and surfactant. Two opposite effects contribute to the almost constant ultrasonic velocity in the second part. The formation of compressible micelles together with the release of the less compressible molecules of hydration water from the interaction sites decrease the velocity. Formation of new and rigid hydration shell on emerged micelles increases the velocity. The former effect thus more than compensates the latter.

The third part is characterized by re-increase of ultrasonic velocity upon the addition of surfactant. This part is somewhat similar to the pre-micelle part of the titration profile in water (with smaller slope). At the end of this part (around the local maximum of ultrasonic velocity) formation of macroscopic phase separated particles was observed visually. The charge ratio is slightly above one (around 1.2-1.3) (Table 11). In this part the binding of surfactant in the form of micelles is finished, free (unbound) surfactant molecules probably appear in the solution, electrostatic repulsion is removed and phase separation progresses to macroscopic level. Both the free surfactant molecules and rigid phase separated particles contribute to the velocity increase.

In part IV the velocity decreases this time more steeply than in the part II. The system progressively clarifies with increasing concentration of surfactant. In the same time the number of macroscopic separates decreases and at the end of part IV only a few particles can be observed. The decrease of velocity is thus attributable to the decreased size and number of phase separated particles which are more rigid than the liquid medium. Part IV ends when the surfactant concentration corresponds to its normal critical micelle concentration.

The velocity increases again during part V with a slope approximate to the slope of pre-micelle part of the titration profile in water. The increase goes on in part VI but with much lower slope similar to that of the post-micelle part of the titration profile in water. Visual inspection reveals no special changes or behaviour in both parts just slightly opalescent appearance. Due to the surfactant concentration formation of standard micelles should be expected in both parts. In part V the formed micelles probably interact with the previously formed hyaluronan-TTAB complexes, dissolve the macroscopically separated particles and form rather rigid structures apparently of microgel type which increase the ultrasonic velocity. When the interactions are completed part VI begins where mainly new free micelles are formed.

The measurement of ultrasonic attenuation is much less sensitive. From the transition between part I and II the attenuation is continuously increasing up to the transition between part III and IV (Figure 37). Then it steeply decreases in part IV and finally stays practically constant. Increasing attenuation indicates increasing heterogeneity of the system and formation of bigger particles scattering the ultrasonic wave. The step decrease corresponds to the dissolution of such particles and clarificiation of the system. Constant attenuation is found where no substantial heterogeneity evolves, i.e. when only really microscopic phase separation or structures are found.

Table 11. TTAB concentrations at the boundaries of the different parts identified in the velocity titration profile and corresponding charge ratio TTAB/hyaluronan.

		Water			0.15 M NaCl		
M_w	Part	c_{TTAB}	c_{hya}	TTAB/HYA	c_{TTAB}	c_{hya}	TTAB/HYA
kDa		mmol/l	g/l		mmol/l	g/l	
10-30	I	0.37	0.99	0.2	0.61	0.99	0.2
	II	3.00	0.94	1.3			
	III	3.98	0.92	1.7			
	IV	4.61	0.91	2.0			
	V	6.25	0.88	2.9			
90-130	I	0.35	0.99	0.1	0.92	0.98	0.4
	II	2.00	0.95	0.9			
	III	2.62	0.93	1.1			
	IV	2.99	0.92	1.3			
	V	7.19	0.83	3.5			
300-500	I	0.48	0.99	0.2	3.15	0.94	1.4
	II	2.73	0.95	1.2			
	III	3.15	0.94	1.4			
	IV	3.90	0.92	1.7			
	V	8.35	0.84	4.0			
1500-1750	I	0.38	0.99	0.2	4.9	0.90	2.2
	II	2.71	0.95	1.2			
	III	3.04	0.94	1.3			
	IV	3.99	0.93	1.7			
	V	8.39	0.83	4.0			

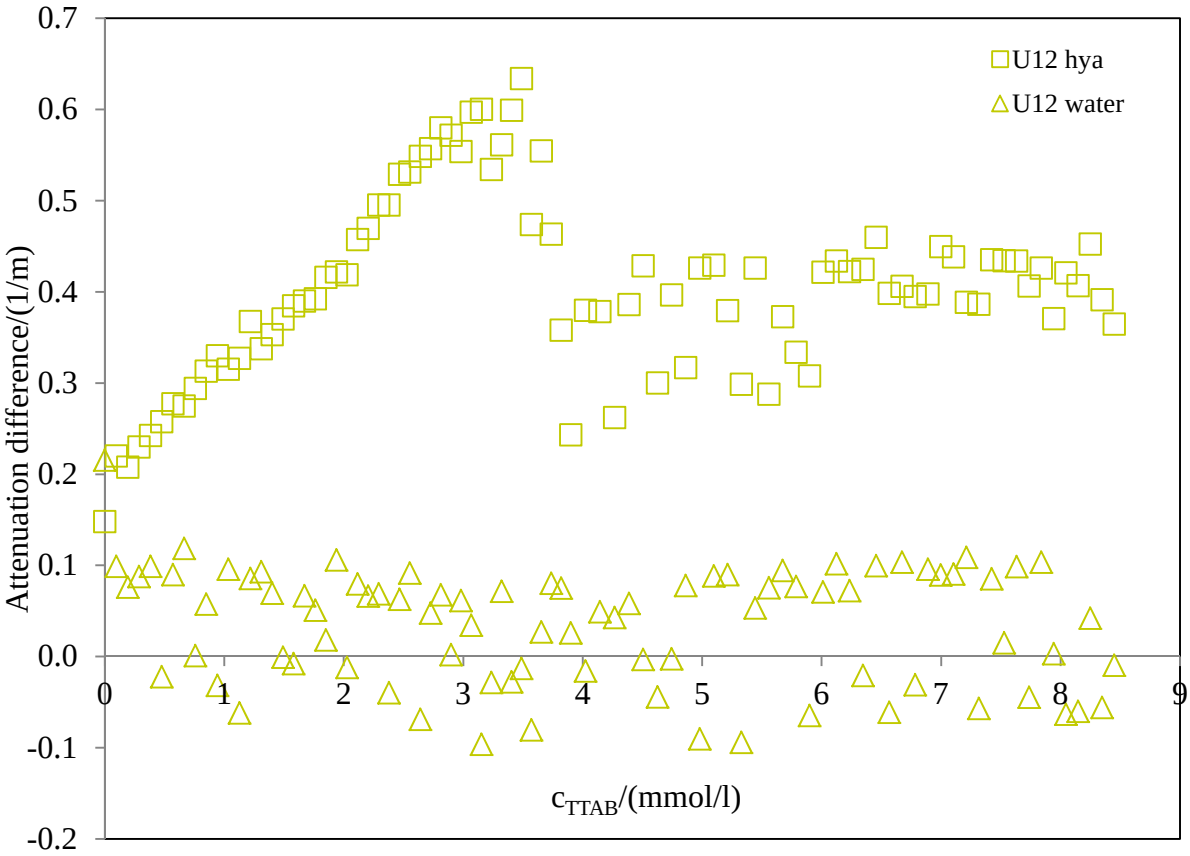

Figure 37. The attenuation titration profile of hyaluronan of concentration 1000 mg/l and molecular weight of 300-500kDa and the attenuation titration profile of water with TTAB, at frequency 15 MHz. The titration curve of water is shifted to the fisrt point of hyaluronan curve.

The charge ratio surfactant/hyaluronan corresponds to the ratio of concentration of charges on the surfactant molecule and hyaluronan. The ratio of charges gives the information about the possible free or occupied hyaluronan charged groups. Hyaluronan has one negative charge per one disaccharide unit and surfactants TTAB and CTAB have one positive charge in their structure. The concentration of charges on hyaluronan chain was calculated as follows:

$$\frac{\text{concentration of hyaluronan in the solution (g/l)}}{\text{weight of one disaccharide unit (g/mol)}} = \text{concentration of disaccharide units (mol/l)},$$

where the weight of one disaccharide unit is 401.299 g/mol.

Afterwards, the charge ratio surfactant/hyaluronan was calculated as the ratio of molar surfactant concentration and concentration of disaccharide units. The charge ratio surfactant/hyaluronan increased with rising concentration of surfactant, example is in Figure 38.

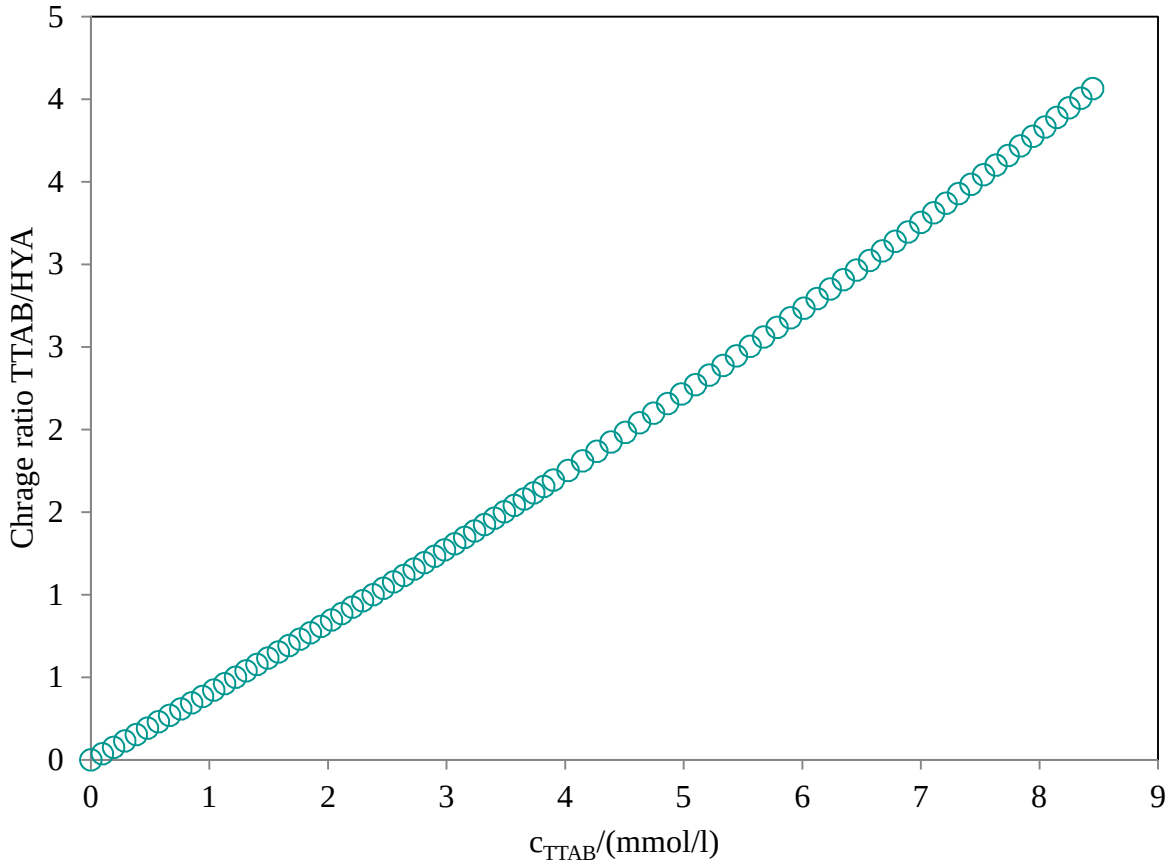

Figure 38. Dependence of charge ratio TTAB/hyaluronan on concentration of surfactant TTAB. Hyaluronan 1000 mg/l 300-500 kDa in water.

Titration measurement in HR-US 102T was done in four molecular weights of hyaluronan and at eight frequencies in range 2.5-17.5 MHz. Effect of hyaluronan molecular weight on the velocity titration profiles was very small (Figure SF10 in Supplementary information). The shapes were retained, small differences were found in the values of the surfactant concentration corresponding to the boundaries between neighboring parts but they should be caused mainly by experimental uncertainities. The effect on the values of attenuation (Figure 39) was stronger – the higher the molecular weight the higher the value of attenuation difference. This should be a result of more intensive ultrasonic scattering on more complex coiled structures formed from chains of higher molecular weight. The differences in the shapes of attenuation profiles were small.

In contrast to velocity, attenuation values were dependent on the frequency of ultrasonic which is typical for systems containing micro-heterogeneities capable of relaxation upon ultrasonic propagation [138],[139],[140]. Depending on the mechanism of relaxation ultrasonic waves of different frequency may be scattered to different amount. However, the curved shapes of attenuation profiles and their locations on the concentration axis were not affected by the frequency as is illustrated on typical example in Figure 39.

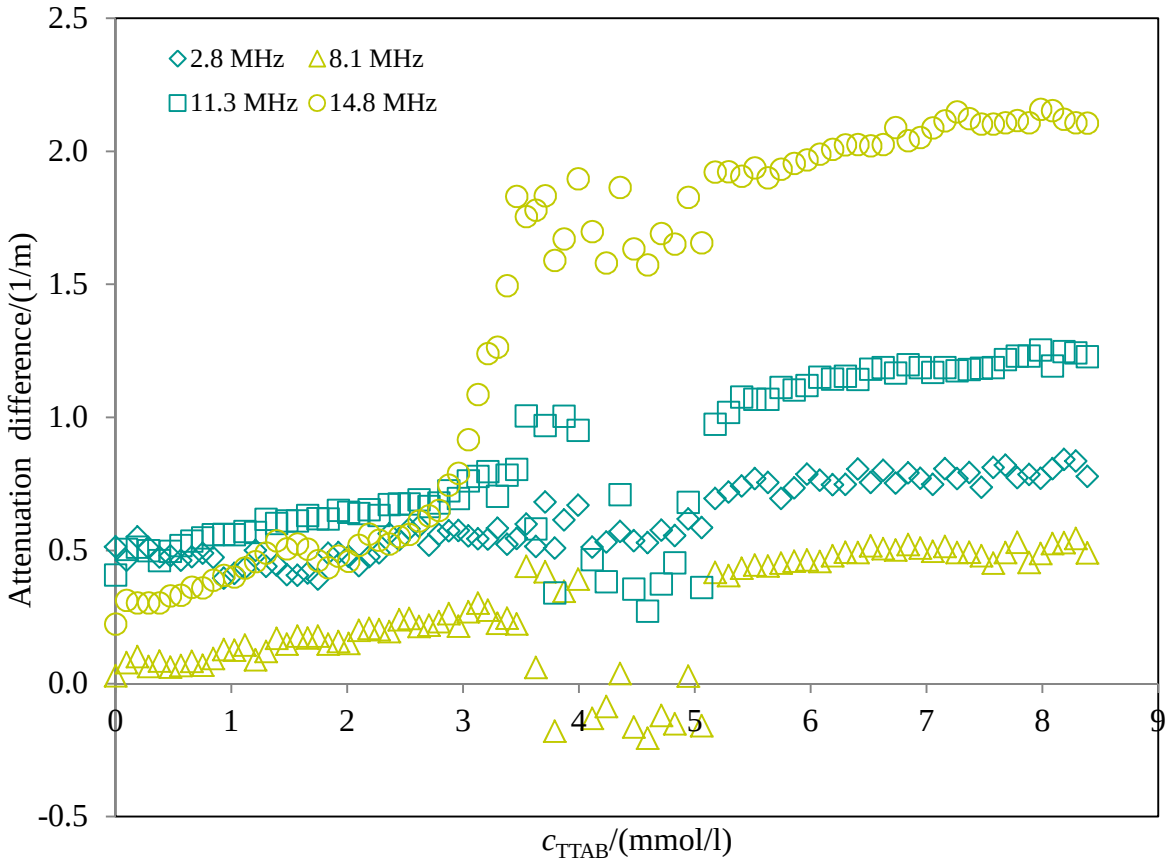

Figure 39. The effect of frequency on ultrasonic attenuation profile of hyaluronan-TTAB system in water, at 25 °C, at frequencies 2.8-14.8 MHz. Hyaluronan 1000mg/l 300-500 kDa.

Ultrasonic velocity measured with DSA 5000M

The binding of surfactant to hyaluronan chain was investigated also by densitometer DSA 5000M. The breakpoint is seen only in low molecular weights of hyaluronan (10-30 kDa and 110-130 kDa). During measuring of high molecular weights of hyaluronan (300-500 kDa and 1500-1750 kDa) the precipitate was seen in very low concentration of surfactant and there is not seen negligible breakpoint, the densitometer is not accurate, the error is big for the very near point of concentration line of surfactant. Example of surfactant binding to hyaluronan from densitomer is in Figure 40.

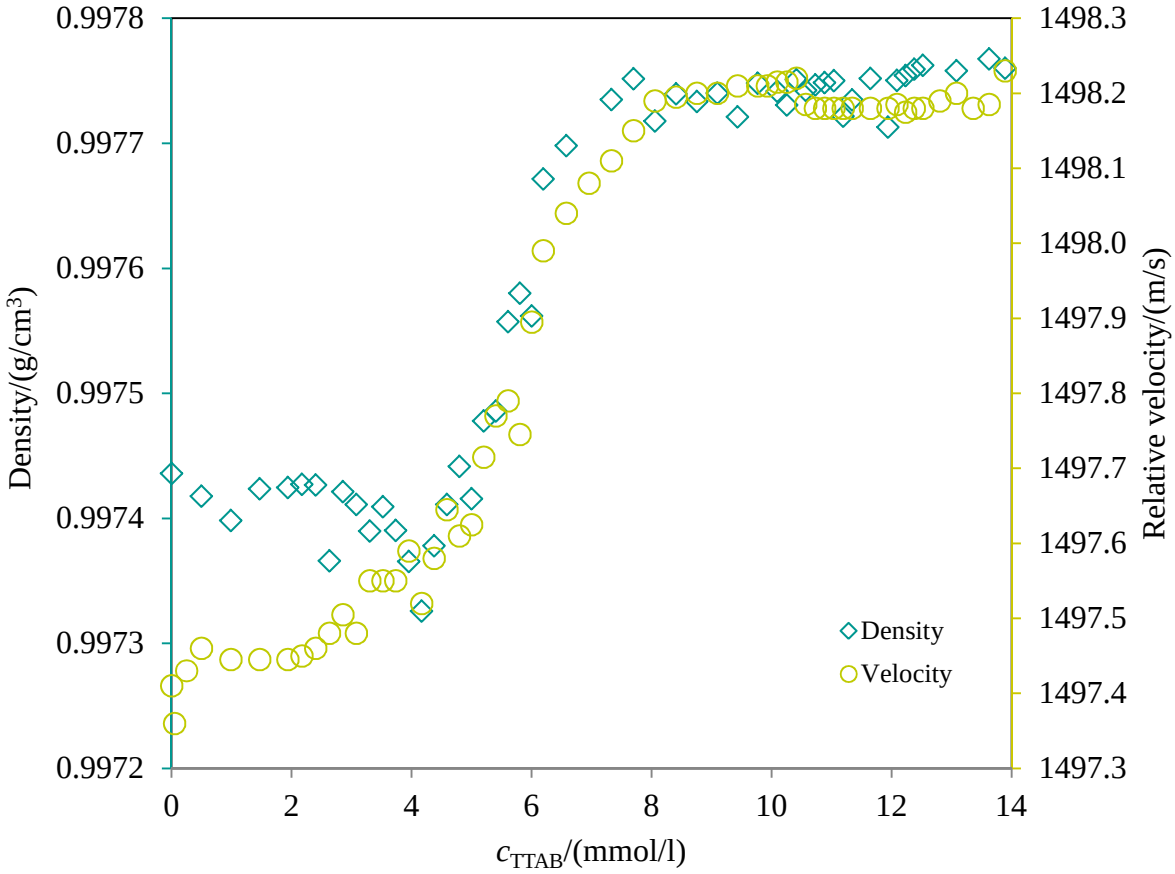

Figure 40. Binding of surfactant TTAB to hyaluronan chain (1000 mg/l, 90-110 kDa, in water) measured by means of densitometer DSA 5000M.

Titration of hyaluronan solution by CTAB in water

Figure SF13 (in Supplementary information) shows the dependence of ultrasonic velocity and attenuation on the concentration of surfactant CTAB during the titration of hyaluronan solution by CTAB. The titration of water by surfactant CTAB is in Figure SF12 in Supplementary information. In these two figures the significant breakpoint is seen both in velocity and in attenuation profile. Titration curve of water was shifted to to first point of curve of hyaluronan solution (Figure 42) for better comparing. CTAB interacts with hyaluronan from the first adding of surfactant.

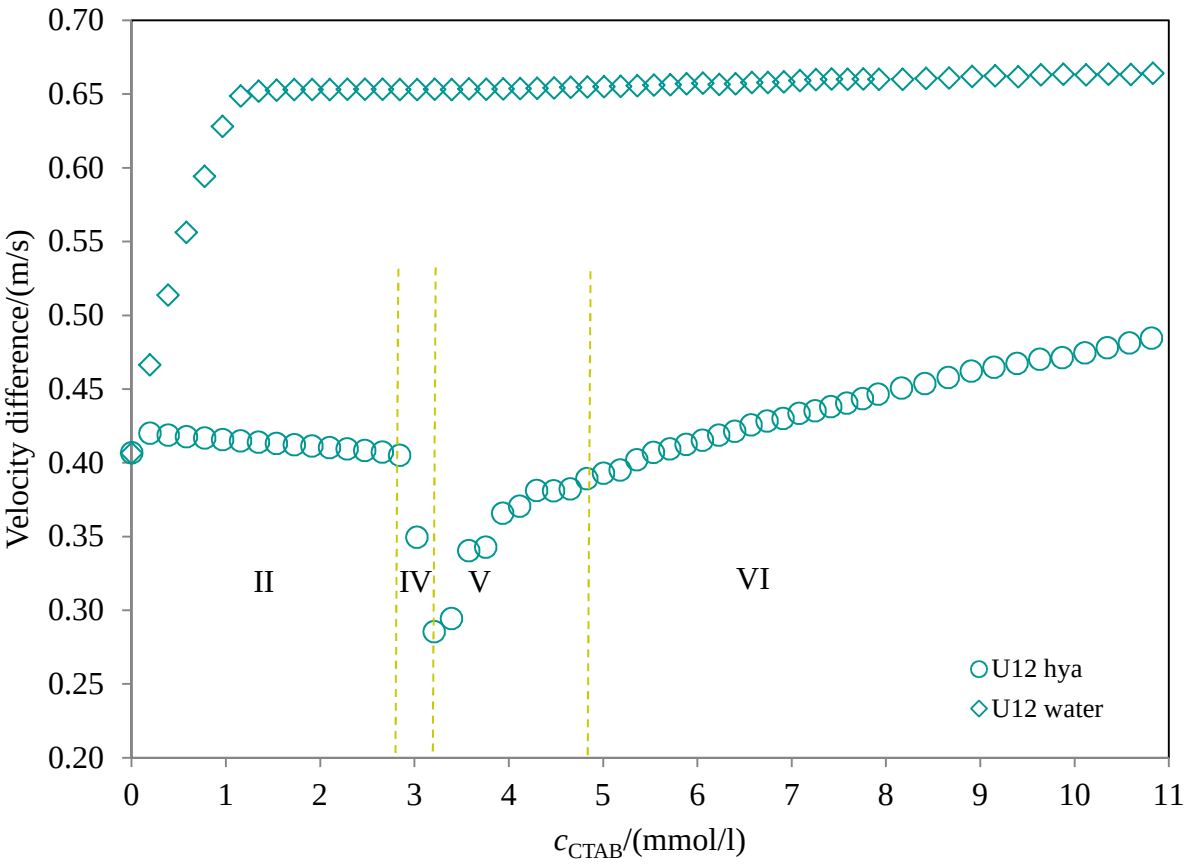

Figure 42. The velocity titration profile of hyaluronan of concentration 1000 mg/l and molecular weight of 300-500kDa and the velocity titration profile of water with CTAB, at frequency 15 MHz. The titration curve of water is shifted to first point of hyaluronan curve.

Titration profiles measured with CTAB are obviously different from those with TTAB. Some parts are missing in the velocity profile (Figure 42) and from this point of view the CTAB profile is simpler. On the basis of changes of the profile slope including its sign it is reasonable to assume that parts I and III are missing, and part V extends through much shorter concentration interval. The titration curve in the hyaluronan solution is from the first point different from that obtained in pure water. In comparison to TTAB, CTAB interacts with hyaluronan at much lower surfactant concentration, consequently, part I was not observed. Part II is characterized also by the evolution of turbidity and extends to concetrations well above the normal critical micelle concentration but it terminates also around the equivalent charge ratio (Table 12). Visible macroscopic phase separation occurs

here only in part IV and the steep velocity decrease in this part is mainly a result of particle setting out of the detection volume. The missing part III is probably a result of stronger cooperativity of CTAB binding on hyaluronan; perhaps no free surfactant molecules can be present in this case.

The precipitated particles were progressively dissolved during part V changing from precipitates through clot structures or swelled flocs to almost clear system in part VI where also the formation of free standard micelles can be expected.

It is also interesting that the velocity difference measured in the TTAB-hyaluronan system approaches the values measured for TTAB micelle system and the values are very close for both systems starting at TTAB concentration of about 8 mmol/l. On contrary the velocity difference in the CTAB-hyaluronan system is always higher than in corresponding hyaluronan-free solutions. CTAB thus forms complexes with hyaluronan which are more rigid, less compressible than CTAB micelles whereas the opposite is found for TTAB.

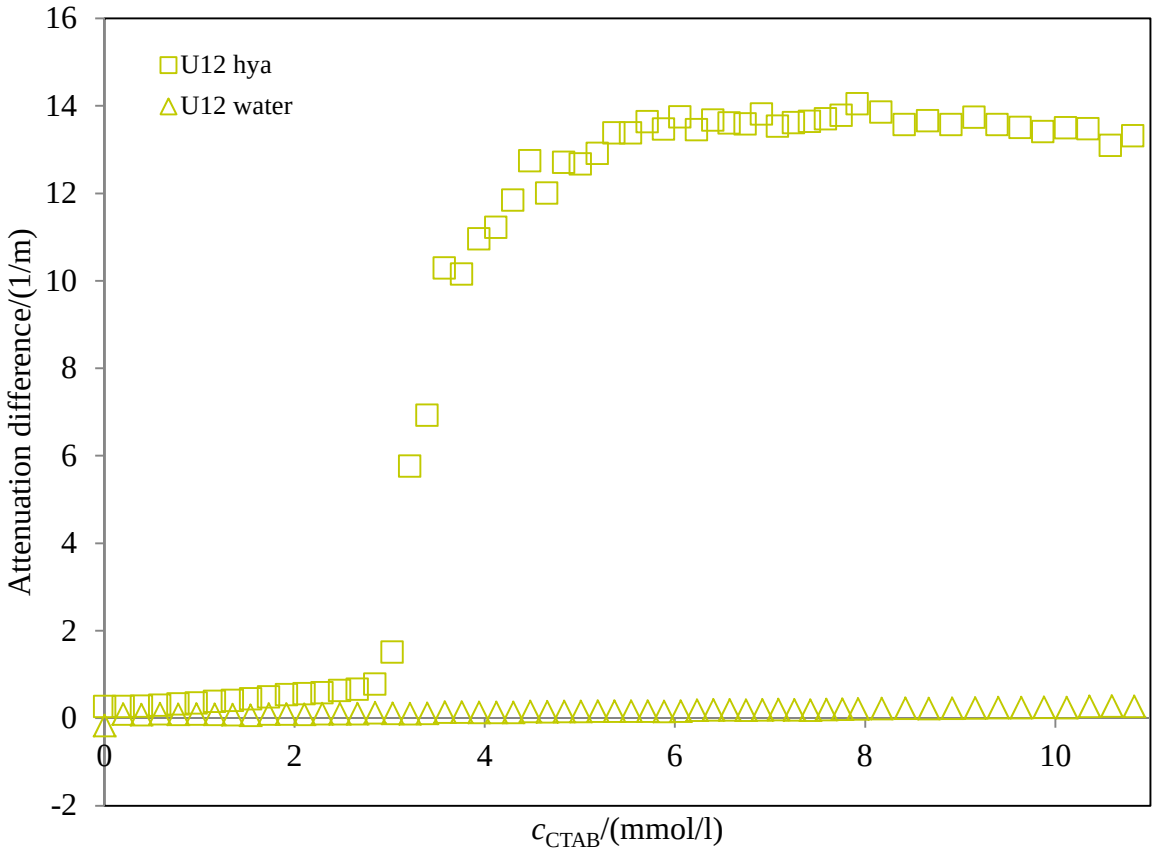

Figure 43. The attenuation titration profile of hyaluronan of concentration 1000 mg/l and molecular weight of 300-500kDa and the attenuation titration curve of water with CTAB, at frequency 15 MHz. The titration curve of water is shifted to first point of hyaluronan curve.

The titration profile of ultrasonic attenuation measured for CTAB is also different from that for TTAB (Figure 43). It continuously and slightly increases up to the boundary between parts II and IV (remember the missing part III). Then it sharply increases (in contrast to the system with TTAB) up to the boundary between parts V and VI. In the part VI it continues to increase at first, but with lower slope, and then is essentially constant. The sharp increase

reflects the increased heterogeneity due to the phase separation. The relatively high final value of attenuation, comparing to TTAB system, shows more heterogenous structure capable of more intensive scattering of ultrasonic wave formed probably by rather rigid and translucent micro-gel or nano-gel particles.

Table 12. CTAB concentrations at the boundaries of the different parts identified in the velocity titration profile and corresponding charge ratio CTAB/hyaluronan.

		Water			0.15 M NaCl		
M_w	Part	c_{CTAB}	c_{hya}	CTAB/HYA	c_{CTAB}	c_{hya}	CTAB/HYA
kDa		mmol/l	g/l		mmol/l	g/l	
10-30	I						
	II	2.29	0.98	0.9	3.08	0.97	1.3
	III						
	IV	2.85	0.97	1.2			
	V	5.88	0.94	2.5			
90-130	I						
	II	2.47	0.97	1.0	1.13	0.99	0.5
	III						
	IV	2.85	0.97	1.2			
	V	4.84	0.95	2.0			
300-500	I						
	II	2.84	0.97	1.2	3.13	0.97	1.4
	III						
	IV	3.21	0.97	1.3			
	V	4.11	0.96	1.7			
1500-1750	I						
	II	2.66	0.97	1.1	5.16	0.95	2.2
	III						
	IV	3.03	0.97	1.3			
	V	5.36	0.95	2.3			

The effect of hyaluronan molecular weight on the shape of all measured velocity titration profiles was very small. The shapes were retained, some differences were found in the values of the surfactant concentration corresponding to the boundaries between neighboring parts and in the velocity values within the same part of the profile. The differences are seen particularly in parts III-VI and should be ascribed to the effects of differences in conformations of hyaluronan chains of different molecular weight [102]. On average, the two preparations of lower molecular weight differed from the two preparations of higher molecular weight which gave very similar profiles. The effect on the values of attenuation was stronger – the higher the molecular weight the higher the value of attenuation difference. This should be a result of more intensive ultrasound scattering on more complex coiled structures formed from chains of higher molecular weight. The differences in the shapes of attenuation profiles were small. Visually, the smaller the hyaluronan molecular weight the less perceptible opacity was observed.

Titration measurement in HR-US 102T was done in four molecular weights of hyaluronan and at eight frequencies in range 2.5-17.5 MHz. Effect of hyaluronan molecular weight on the velocity titration profiles was very small (Figure SF14 in Supplementary information). The shapes were retained, small differences were found in the values of the surfactant concentration corresponding to the boundaries between neighboring parts but they should be caused mainly by experimental uncertainities. The effect on the values of attenuation (Figure 44) was stronger – the higher the molecular weight the higher the value of attenuation difference. This should be a result of more intensive ultrasound scattering on more complex coiled structures formed from chains of higher molecular weight. The differences in the shapes of attenuation profiles were small.

In contrast to velocity (Figure SF11), attenuation values were dependent on the frequency of ultrasonic which is typical for systems containing micro-heterogeneities capable of relaxation upon ultrasonic propagation [138]-[140]. Depending on the mechanism of relaxation ultrasonic waves of different frequency may be scattered to different amount. However, the curved shapes of attenuation profiles and their locations on the concentration axis were not affected by the frequency as is illustrated on typical example in Figure 44.

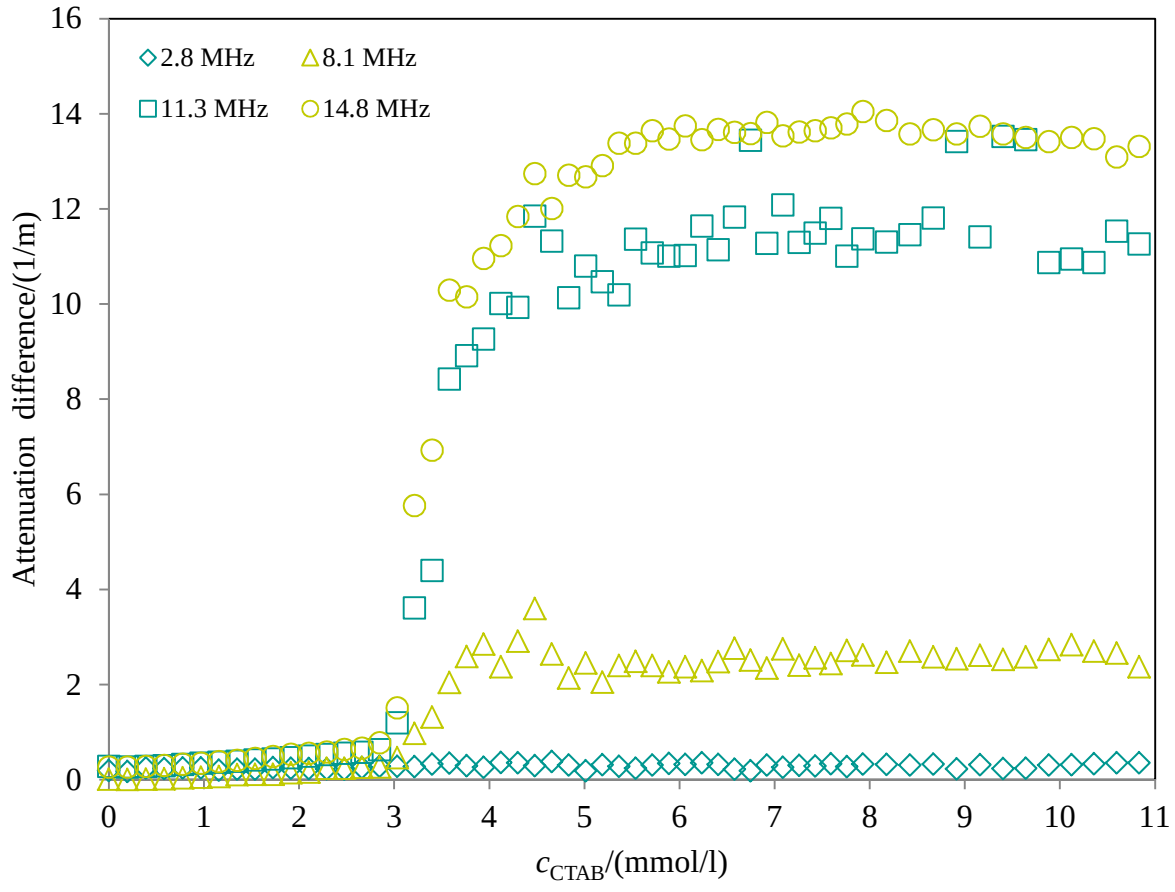

Figure 44. The effect of frequency on ultrasonic attenuation profile of hyaluronan-CTAB system in water, at 25 °C, at frequencies 2.8-14.8 MHz. Hyaluronan 1000mg/l 300-500 kDa.

The effect of ultrasonic frequency on both velocity and attenuation titration profiles is very similar for TTAB and CTAB (Figure 39, Figure 44, Figure SF15).

The titration of hyaluronan solution by TTAB in sodium chloride solution

The measurement of the solution of hyaluronan in 0.15 M NaCl was done the same way as the measurement in water but results are different. The breaks in the curves of the plot are not so noticeable; in case of hyaluronan solution with the molecular weight 10-30 kDa (Figure SF19 in Suppplementary information) the curve is linear without any breakpoint. The interactions of the system hyaluronan-surfactant in 0.15 M NaCl are so slight. In case of hyaluronan 90-110 kDa (Figure SF20 in Suppplementary information), the critical micelle concentration and range of the binding of the surfactant to the polymer is noticeable. In the experiment with hyaluronan 300-500 kDa (Figure SF21 in Suppplementary information) and 1500-1750 kDa (Figure SF22 in Suppplementary information) is noticeable break in the curve of ultrasonic velocity and expressive change in the trend of the curve of the attenuation.

Figure SF19 (in Supplementary information) shows the dependence of ultrasonic velocity and attenuation on concentration of surfactant TTAB during the titration of hyaluronan solution by TTAB. The titration of sodium chloride solution by surfactant TTAB is in Figure SF18 in Supplementary information. Titration curve of sodium chloride was shifted to first point of curve of hyaluronan solution (Figure 45) for better comparing.

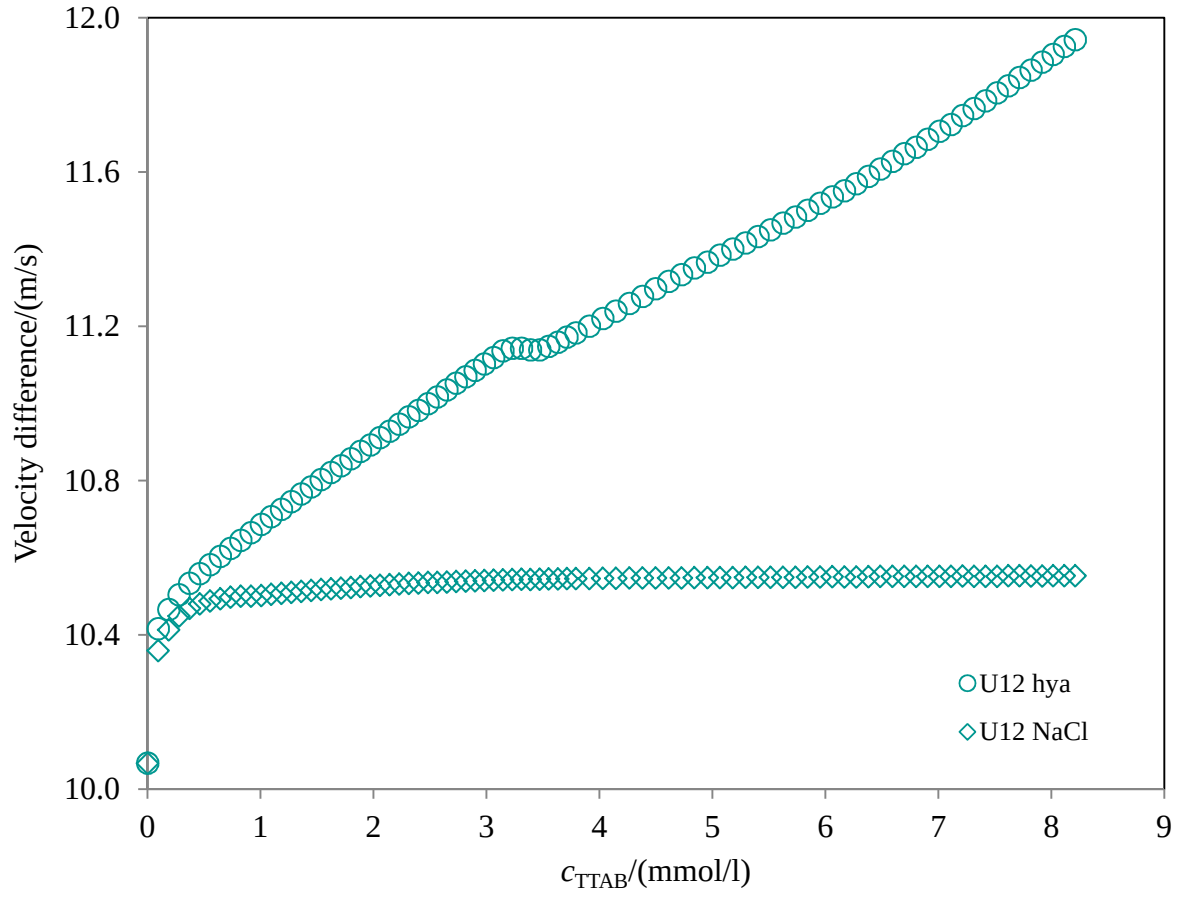

Figure 45. The velocity titration profile of hyaluronan of concentration 1000 mg/l and molecular weight of 300-500kDa and titration curve of water with TTAB in 0.15M NaCl, at frequency 15 MHz. The titration curve of 0.15 M NaCl is shifted to first point of hyaluronan curve.

The titration profiles were significantly changed by the presence of NaCl at the concentration of 0.15 M (the physiological concentration). Ultrasonic titrations of both surfactants into NaCl solution (without hyaluronan) confirmed the well-known decrease of critical micelle concentration in about one order of magnitude (Figure 34, Figure SF18 and Figure SF23 in Supplementary information). In case of TTAB the titration profiles at the absence and presence of hyaluronan practically coincide at low surfactant concentrations (and show a linear dependence of the ultrasonic velocity on the surfactant concentration) which is the same observation as for the titrations in water. However, in the NaCl solution this coincidence survives up to the critical micelle concentration and even then the velocity increases at the presence of hyaluronan though with apparently somewhat smaller slope. This continuous increase is interrupted by a short interval of almost constant velocity which corresponds to the steep increase in the ultrasonic attenuation and to the visual observation of several macroscopically phase-separated particles dispersed in a milky system. The charge ratio at the start point of this increase is about 1.3 (Table 11). It is interesting that this short interval occurs at surfactant concentrations close to critical micelle concentration in water. The system is clear before and cloudy or milky after this interval.

The ultrasonic attenuation of TTAB-hyaluronan-NaCl system does not almost change up to the start of the short region of constant velocity where it sharply increases (Figure SF16 in Supplementary information). The sharp increase continues behind the region of constant velocity and then the attenuation progressively levels off and finally increases only moderately but continuously. In fact, the start of only moderate increase of attenuation corresponds to a weak bend on the velocity titration profile. The increased attenuation reflects the formation of heterogeneities – microaggregates of hyaluronan-surfactant complexes. The effect of ultrasound frequency is similar as described above – the velocity values are unaffected in contrast to the values of attenuation.

In contrast with the titrations in water the effect of hyaluronan molecular weight was much more obvious in the presence of NaCl. The velocity profile for the lowest molecular weight (10-30 kDa) is linear (Figure SF19 in Supplementary information), the attenuation is constant and the sample clear throughout the whole range of applied surfactant concentration. Because the velocity is systematically increasing in presence of hyaluronan this should not directly indicate that no interactions between hyaluronan and surfactant are detected. Further, only below the critical micelle concentration (0.584 mmol/l, TTAB) the profiles measured at the presence and at the absence (Figure SF18 in Supplementary information) of hyaluronan coincide. Progressive formation of rigid, very small structures which do not scatter ultrasonic waves should be expected. The velocity profile measured for the molecular weight of 110-130 kDa (Figure SF20 in Supplementary information) shows instead of the short interval of almost constant velocity a broader interval of “ïnflexing” behaviour during which also the attenuation markedly increases and opacity is developer. For the highest molecular weight (1500-1750 kDa) the constant velocity interval and corresponding sharp increase of attenuation are shifted to higher surfactant concentrations (5-6 mmol/l) (Figure SF22 in Supplementary information).

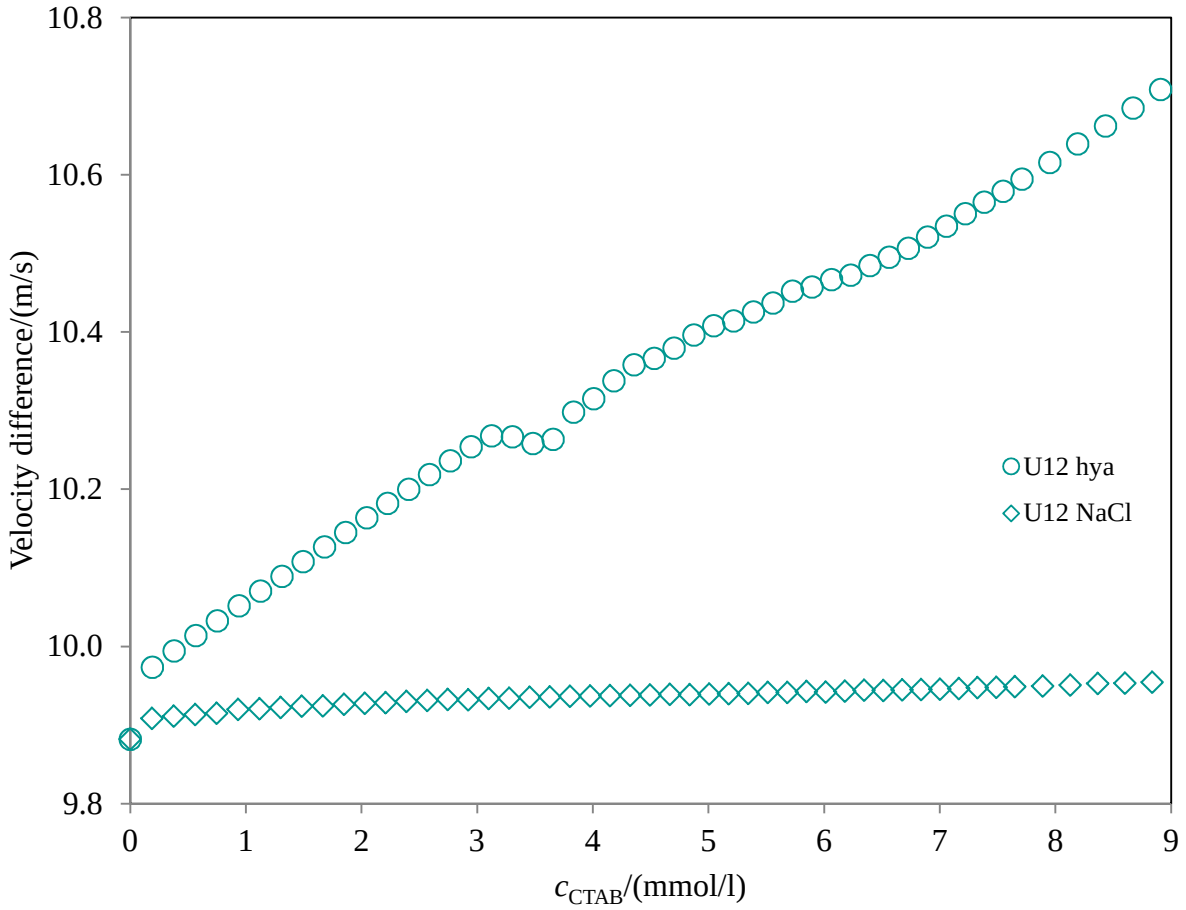

Figure 46. The velocity titration profile of hyaluronan of concentration 1000 mg/l and molecular weight of 300-500kDa and titration curve of water with CTAB in 0.15M NaCl, at frequency 15 MHz. The titration curve of 0.15 M NaCl is shifted to first point of hyaluronan curve.

The shapes of titration profiles for CTAB in hyaluronan-NaCl system are much closer to those for TTAB than it was observed in water. The velocity increases before the critical micelle concentration (Figure 46) but is higher than in the absence of hyaluronan, the slope of this increase is smaller behind this concentration and a narrow interval of almost constant velocity appears at much higher surfactant concentration than is the critical micelle. CTAB concentration corresponding to this constant interval is very similar as for TTAB as well as the charge ratio which is here around 1.3 (Table 12). Thus electrostatic interactions control this behaviour. The re-increase of the velocity behind this interval is clearly (in contrast to TTAB) composed from at least two more or less linear branches intersecting around the CTAB concentration of 6 mmol/l. The initial increasing part corresponds visually to a clear system, during the constant interval some flakes or flocs and evolution of turbidity can be observed. After this interval the system is cloudy.

The attenuation reflects the changes in velocity (Figure SF17 in Supplementary information). Before the short region of constant velocity the attenuation increases moderately then sharply within this region and even behind it. Then it remains essentially constant up to the bend mentioned in the preceding paragraph which appears around the CTAB concentration

of 6 mmol/l and above this concentration it increases again. The effect of ultrasonic frequency is still the same as given above.

Due to the higher velocity and increasing attenuation at low CTAB concentrations in presence of hyaluronan it cannot be excluded that the surfactant interacts with CTAB in NaCl solution even in its normal pre-micelle region forming some more rigid structures. It can not be concluded that micelle structures bound to hyaluronan are formed at this stage but taking into account the smaller slope of velocity increase during the normal post-micelle region (at CTAB concentration between ca 1 and 3 mmol/l) single surfactant or "minimicelle" binding should be prefered. The steep increase of attenuation reflects increasing heterogeneity in the system which results in separation of macroscopic particles (the flakes). The interval of almost constant attenuation corresponds to re-dissolving of big particles by the excess of surfactant and is followed by progressive formation of rigid (increasing velocity) microheterogeneous (increasing attenuation in cloudy system) structures probably of microgel type as can supposed due to the increased slope of the velocity profile (from the CTAB concentration of 6-7 mmol/l).

The effect of hyaluronan molecular weight is much more obvious in the presence of NaCl (Figure 47 and Figure 48) than measurements in water. The velocity profile for the lowest molecular weight (10-30 kDa) is practically linear (Figure SF24 in Supplementary information), there is small change in attenuation and the sample clear throughout the whole range of applied surfactant concentration. Because the velocity is systematically increasing in presence of hyaluronan this should not directly indicate that no interactions between hyaluronan and surfactant are detected. Further, only below the critical micelle concentration (0.071 mmol/l CTAB) the profiles measured at the presence and at the absence of hyaluronan coincide. The velocity profile measured for the molecular weight of 110-130 kDa (Figure SF25 in Supplementary information) shows instead of the short interval of almost constant velocity a broader interval of "ïnflexing" behaviour during which also the attenuation markedly increases and opacity is developed. For hyaluronan 300-500 kDa (Figure SF26 in Supplementary information) and for the highest molecular weight (1500-1750 kDa) the constant velocity interval and corresponding sharp increase of attenuation are shifted to higher surfactant concentrations, in case of 1500-1750 kDa to concentration 5-7 mmol/l (Figure SF27 in Supplementary information). Again, frequency affects the values of attenuation (not the shape of profiles).

Our results suggest that in case of very low molecular weight hyaluronan in presence of salt, the surfactant cation may replace the polysaccharide counterion forming very small and phase non-separating structures of separate surfactant molecules bound to the biopolymer chain. An increased molecular weight of the hyaluronan leads to the formation of larger and coiled ball-like biopolymer structures with surfactant molecules bound preferably on their surface. The higher the structure, the larger its surface and the higher surfactant amount is needed to induce (micro)phase separation.

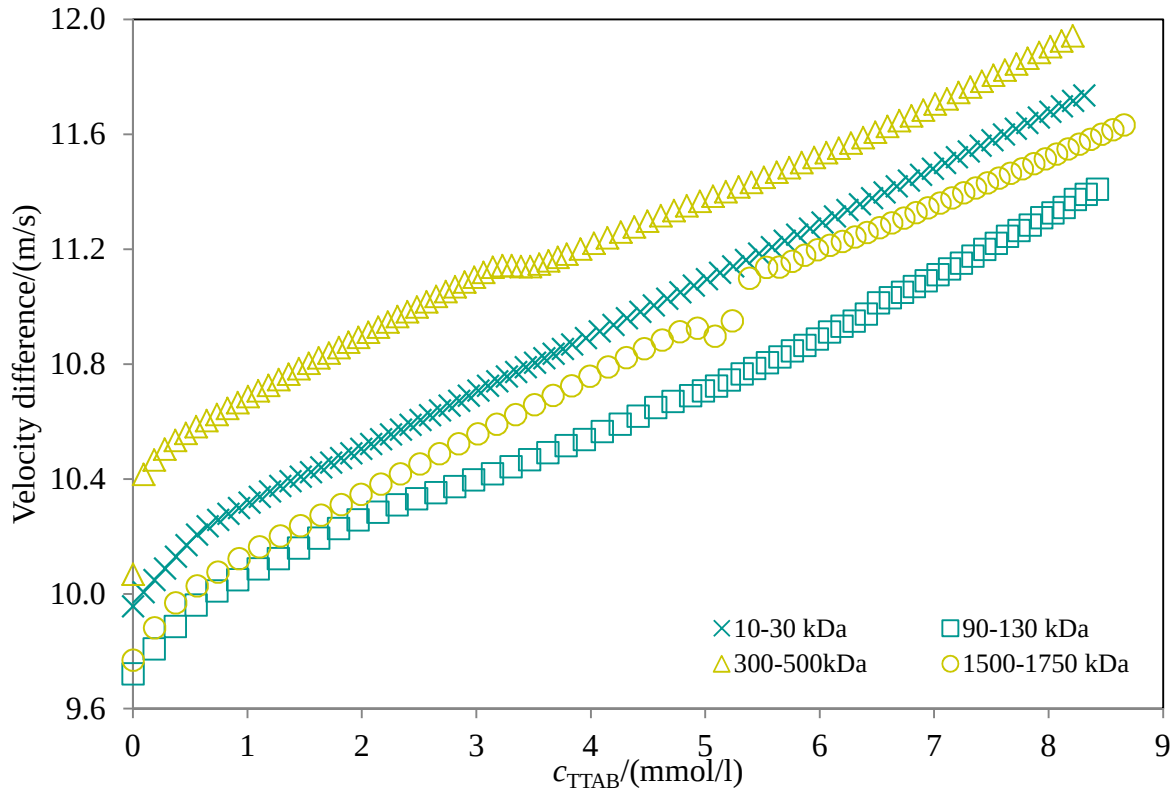

Figure 47. The effect of molecular weigh of hyaluronan on ultrasonic velocity profile of hyaluronan-TTAB system in 0.15 M NaCl, at 25 °C, at frequencies 15 MHz. Hyaluronan 1000 mg/l.

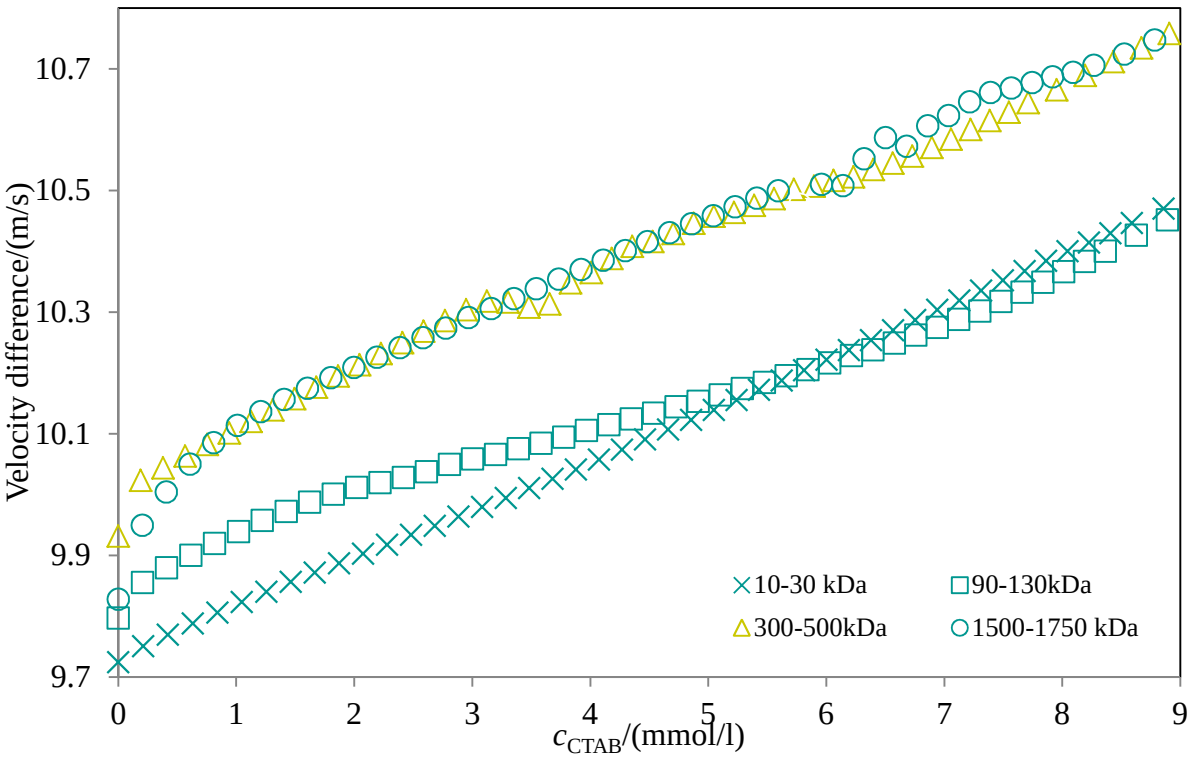

Figure 48. The effect of molecular weigh of hyaluronan on ultrasonic velocity profile of hyaluronan-CTAB system in 0.15 M NaCl, at 25 °C, at frequencies 15 MHz. Hyaluronan 1000 mg/l.

Comppresibility of the binding of surfactant to hyaluronan

The adiabatic compressibility was calculated in the system hyaluronan-TTAB in 0.15M NaCl with hyaluronan with molecular weight max 300 kDa. Density of the higher molecular weight in the system hyaluronan-surfactant was not possible to measure because of occurred precipitation.

The compressibility in hyaluronan solution in NaCl decreases slowly when compared to the solution without addition of hyaluronan, so it proves the interaction between surfactant and hyaluronan and it shows no free surfactant micelles in the bulk solution (Figure SF28 in Supplementary information).

Visual observation of titrations

Visual observation of titrated systems was realized outside of the machine, in a test-tube with upper and bottom stirrer with the same steps of titration program as is performed in the machine. The observation was used for systems hyaluronan (10-1750 kDa) with CTAB or TTAB in water and 0.15 M NaCl.

Due to good solution stirring, precipitates and aggregates were dispersed uniformly in the bulk solution. This behaviour did not influence the ultrasonic measurement. Then, the stirring was turned off and the sedimentation of precipitates took place. At this point, the data were collected, thus, the value of the ultrasonic velocity is not influenced by the present (sedimented) precipitation.

It can be concluded that the size of precipitates increased with increasing molecular weight of hyaluronan (in both water and 0.15 M NaCl). In addition, the precipitates in water solutions were better to identify and it was more compact white aggregate that it was observed in NaCl solutions. The aggregates in NaCl solution were smaller and it was difficult to see them in samples with low molecular weight of hyaluronan in the whole concentration range. The most intensive formation of aggregates corresponds to the break point on the titration curve (parts III – V). In the case of TTAB in NaCl solution with hyaluronan molecular weight 10-30 kDa the sample behaved like without precipitates and it was clear and no turbid. Then, in the part VI, the sample became clear (with CTAB only with weak turbid character) which was caused by the dissolved precipitates. Further, it was observed that the samples with CTAB in water solution showed first opacity character wright after the first addition of CTAB into the hyaluronan solution. It is in contrast to the situation with TTAB were the first opacity character was observed at higher TTAB concentration (from part II).

Examples of the photos from the visual observation are in Figure 49.

a)

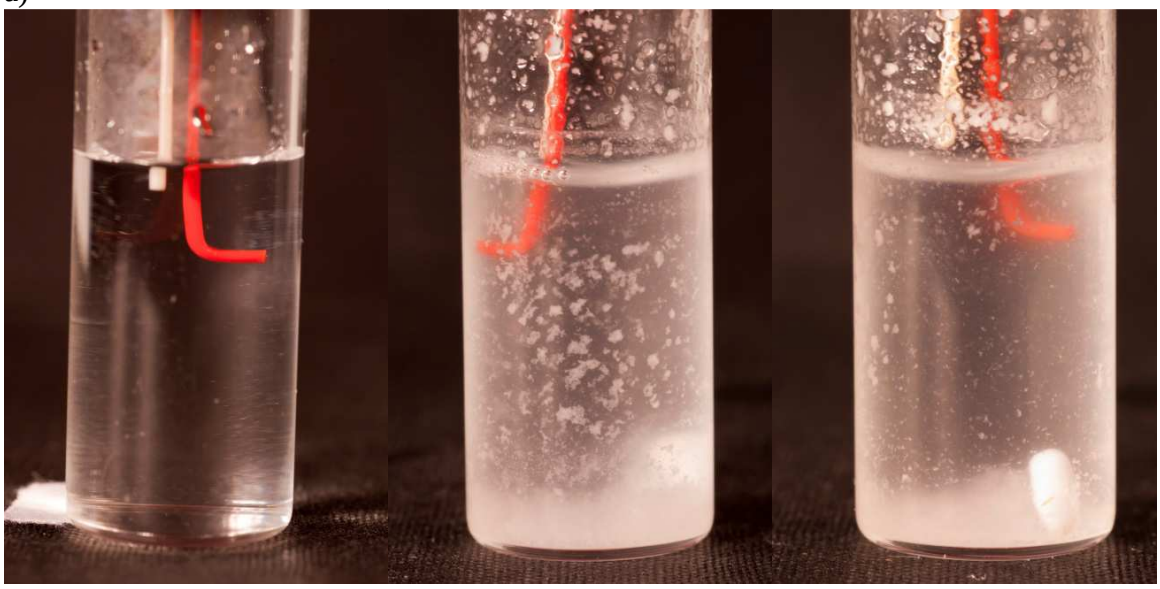

b)

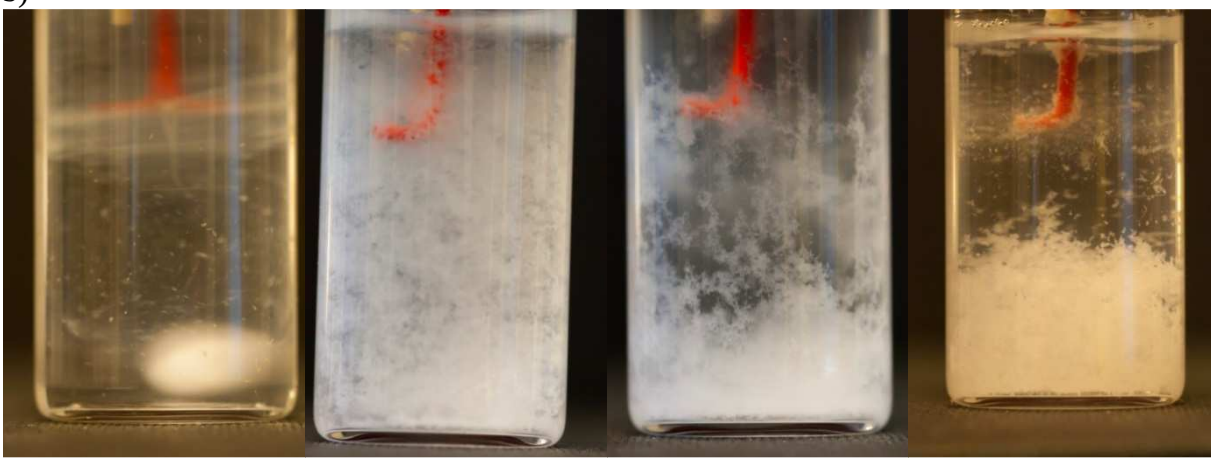

c)

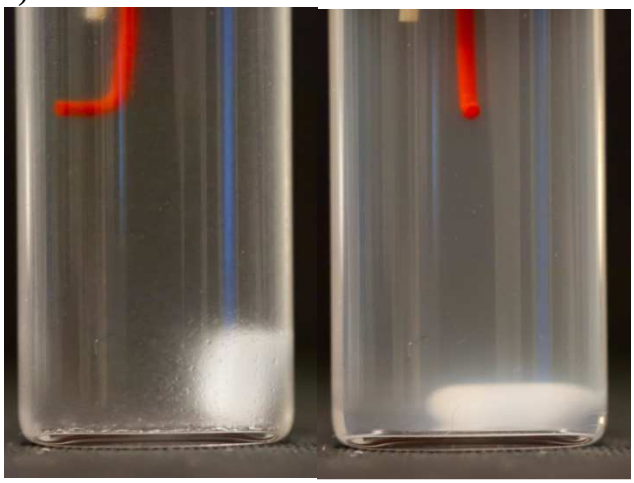

Figure 49. Visual observation of titrations in a test-tube. Titration of hylauronan solution in water by $_{a)}$ *TTAB, by* $_{b)}$ *CTAB. Titration of hylauronan solution in 0.15 M NaCl by TTAB* $_{c)}$*.*

Stop-titrations

Previous results in this chapter describe the kinetic regime and the titration curves are obtained for the wide concentration range. The question appears – what will happen with the curve shape whether the titration is stopped at chosen surfactant concentration and the data of ultrasonic velocity are still being collected. We are interested whether the data will be in agreement with the previsously described results (titration curve without any plateau region). As is shown in Figure 50, the experiment with the same sample was performed three times and the titration was stopped at different surfactant concentrations with further data collection. The measurement of one experimental point during titration took 10 minutes. This is much shorter time than used in previous measurements of phase diagrams [62] or fluorescence studies of hyaluronan-surfactant systems [131].

Previous studies in this thesis were based on mixing all components at a time and letting the system stand for 24 hours at least. To test potential time development of our systems several control stopped-titrations were realized. Titration was stopped at three preselected points of titration profile and ultrasonic parameters were measured during following 13 hours. When the titration stopped in part II or IV no further change in the parameters was observed. After stopping the titration in part V a slight decrease of the velocity was detected (around 6% during 13 hours) which is attributable to slow sedimentation of microgel particles Figure 50 and Figure 51. Stopped titrations confirmed that dynamics and kinetics of hyaluronan-surfactant interactions were adequately recorded during ultrasonic titrations and potential progressive changes in ultrasonic parameters would be caused by progressive separation (sedimentation) of aggregates formed during titration.

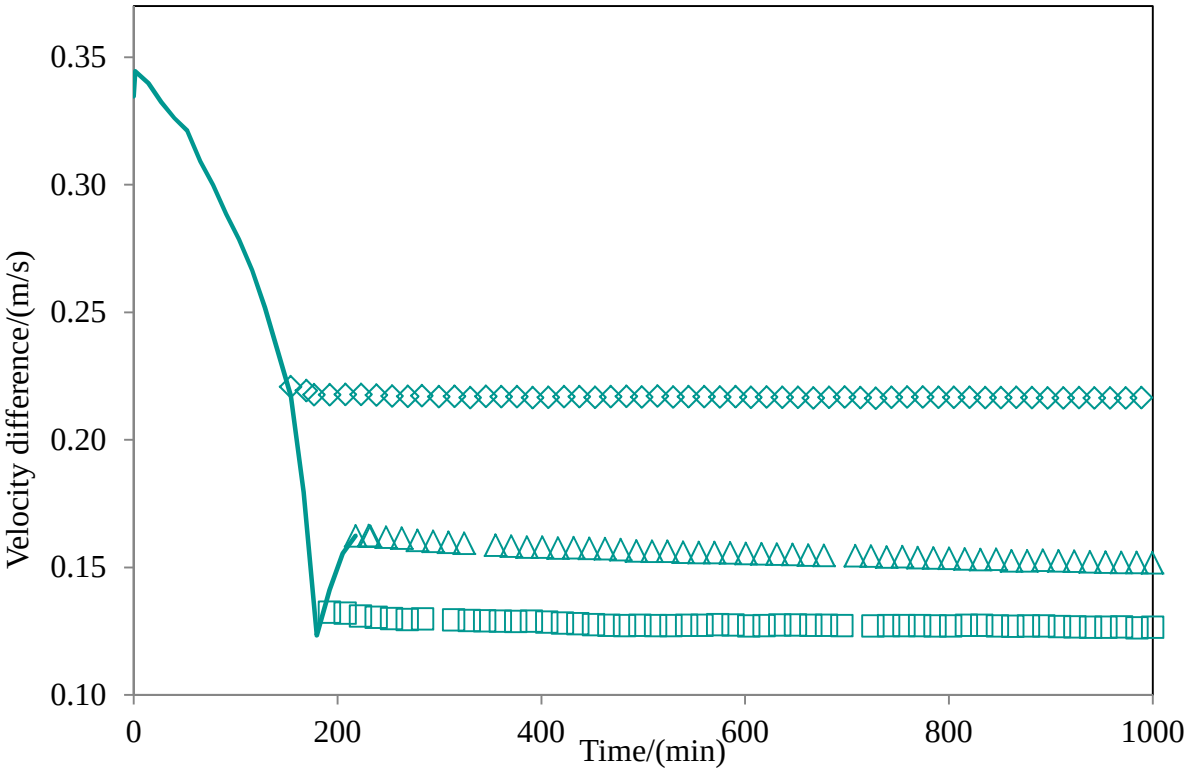

Figure 50. Titration profiles of stop titrations of hyaluronan (1500-1750 kDa by CTAB). Solid line illustrates velocity of the original titration and points correspond to velocity of three stop-titrations in the phase II-V.

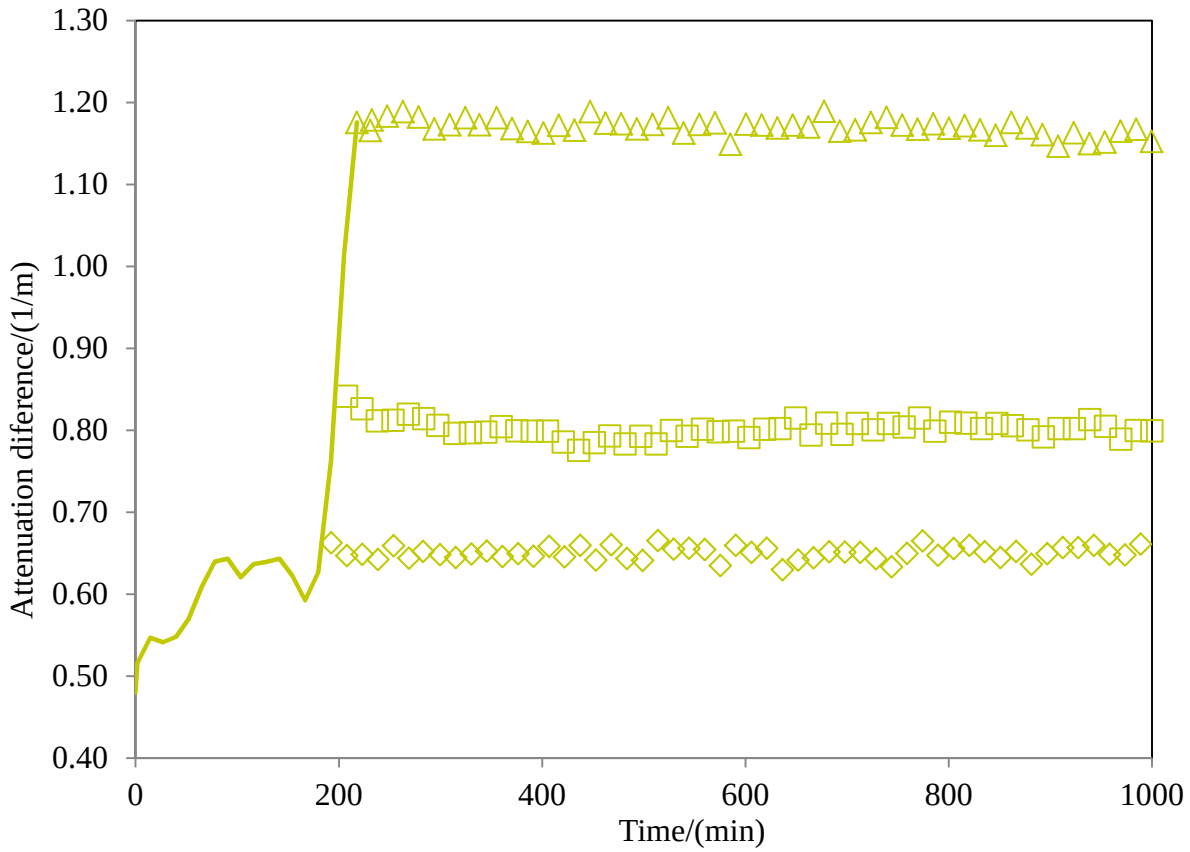

Figure 51. Titration profiles of stop titrations of hyaluronan (1500-1750 kDa by CTAB). Solid line illustrates attenuation of the original titration and points correspond to attenuation of three stop-titrations in the phase II-V.

Titration of hyaluronan 15 mg/l by CTAB

The inspiration in choosing of low hyaluronan concentration 15 mg/l is described in ref. [158] where the interaction of low concentrated hyaluronan (molecular weight 650 kDa) and CTAB was studied by fluorescence probe technique with pyrene as a probe. At such a diluted hyaluronan concentration the fluorescence technique revealed formation of clear systems hyaluronan-micelle-like aggregates at surfactant concentration well bellow its ctitical micelle concentration. In this work hyaluronan with molecular weight 90-130 kDa and 1500-1750 kDa was used for the experiment with concentration of hyaluronan 15 mg/l.

The micelles begun to form already at concentration of CTAB 0.02 mmol/l. The phase separation is from the concentration of CTAB 0.1 mmol/l. Curve with absence hyaluronan (titration of water by CTAB) was plotted to the curve with presence of hyaluronan (titration of hyaluronan 15 mg/l by CTAB) in Figure 52 where is shown that hexadecyltrimethylammonium bromide interacts with hyaluronan immediately from first addition of surfactant. There are seen interactions even in very dilute concentrations of hyaluronan, these results are in agreement with fluorescence measurements.

Investigation of hyaluronan-CTAB interactions by fluorescence spectroscopy [131] revealed that at very low hyaluronan concentrations the binding of the surfactant in the micelle form is induced by the presence of hyaluronan, at concentrations below the normal critical micelle concentration. The resulting system was clear but when the charge ratio CTAB: hyaluronan

was around 3 (Table 13), a small amount of gel phase was separated on the walls of vial. The high resolution ultrasonic spectroscopy confirmed this behaviour but at the same time showed that ultrasonic titration profiles are simpler than at high hyaluronan concentration. From the beginning of titration the ultrasonic velocity increases linearly with the surfactant concentration both in water and in very diluted hyaluronan solution in water but is lower in the presence of hyaluronan (Figure 52). This should indicate binding of surfactant to biopolymer, probably in the form of single chains – the release of hydration water from binding sites as well as the reduced hydration shell of bound surfactant molecules in comparison to their free state in water decrease the velocity. Formation of bound micelles is indicated by the interval of almost constant velocity – the explanation is similar as of the part II in titration of hyaluronan 1000 mg/l. The completion of binding results in another increase of velocity with a slope which is very close to the slope obtained for titration in water in the pre-micelle region – the monomeric form of the titrating surfactant prevails in this stage. Separation of the gel phase is not seen on the attenuation profile due to the very low concentration in this case.

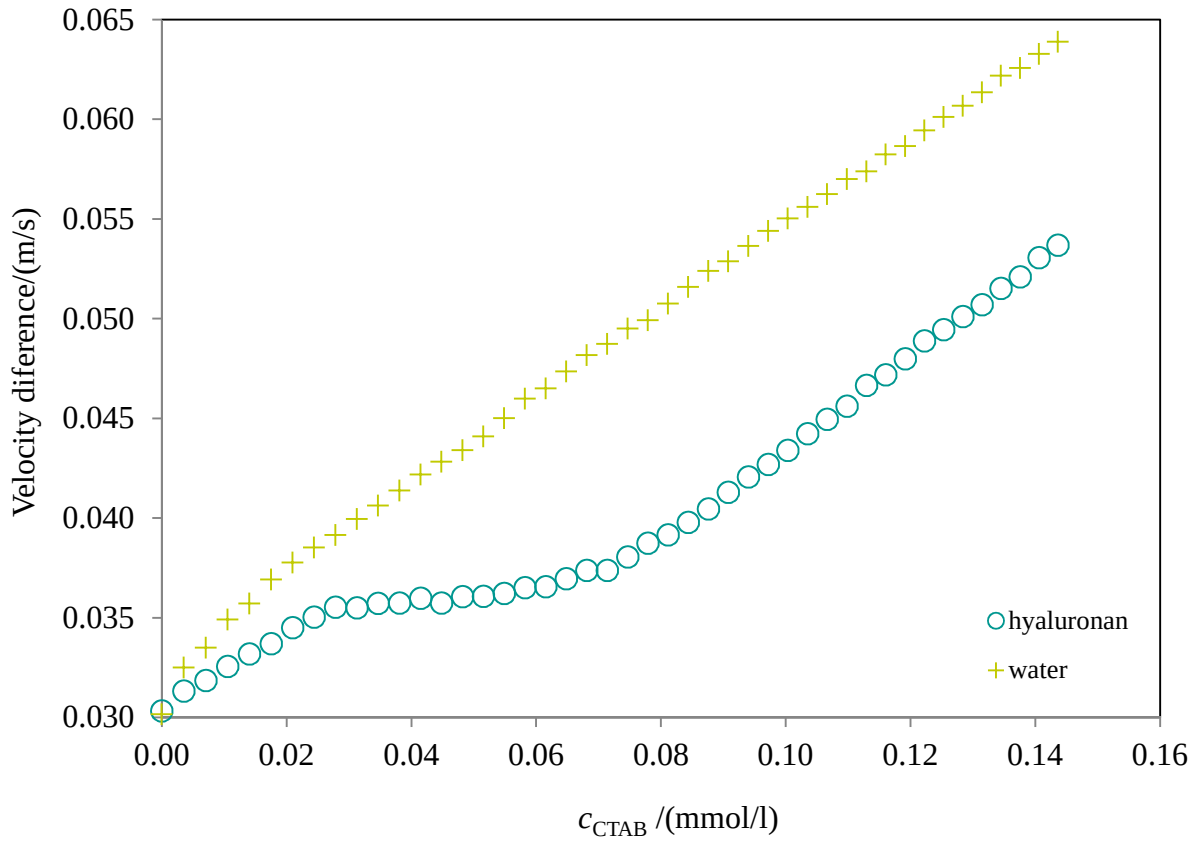

Figure 52. Ultrasonic titration profile of hyaluronan of the concentration 15 mg/l andmolecular weight of 90-130 kDa and ultrasonic titration profile of water with surfactant CTAB of concentration 2mM in water. The change in ultrasonic velocity in solution caused by addition of the surfactant is plotted as function of concentration of surfactant. The titration curve of water is shifted to first point of hyaluronan curve.

The stop-titration of hyaluronan of concentration 15 mg/l was done, the experiment is described in previous chapter. Titration was stopped at three preselected points of titration profile and ultrasonic parameters were measured during following 13 hours. When the titration stopped in the concentration range of surfactant 0.08-0.12 mmol/l no further change in the parameters was observed. Stopped titrations confirmed that dynamics and kinetics of hyaluronan-surfactant interactions were adequately recorded during ultrasonic titration.

Table 13. CTAB concentrations at the boundaries of the different parts identified in the velocity titration profile and corresponding charge ratio CTAB/hyaluronan.

M_w kDa	Part	c_{CTAB} mmol/l	c_{hya} g/l	Charge ratio CTAB/HYA
90-130	II	0.03	0.01	0.8
	IV	0.07	0.01	2.0
1500-1750	II	0.02	0.01	0.7
	IV	0.07	0.01	2.0

Interactions hyaluronan-TTAB measured with DSA 5000M

System hyaluronan-TTAB was performed by means of densitometer Anton Paar 500M or by means of HR-US 102T. The binding of surfactant to hyaluronan was measured in HR-US 102 T with titration regime and in case of densitometer were prepared concentration line and then every sample with different concentration was measured in desnitometer. The results from both methods are compared in this chapter. The measurement of ultrasonic velocity in high resolution ultrasonic spectroscopy was more precisely than in densitometer DSA 5000M. There are seen changes in velocity in the dependence on concentration of TTAB measured by means of HR-US 102T and densitometer 5000M (Figure 53).

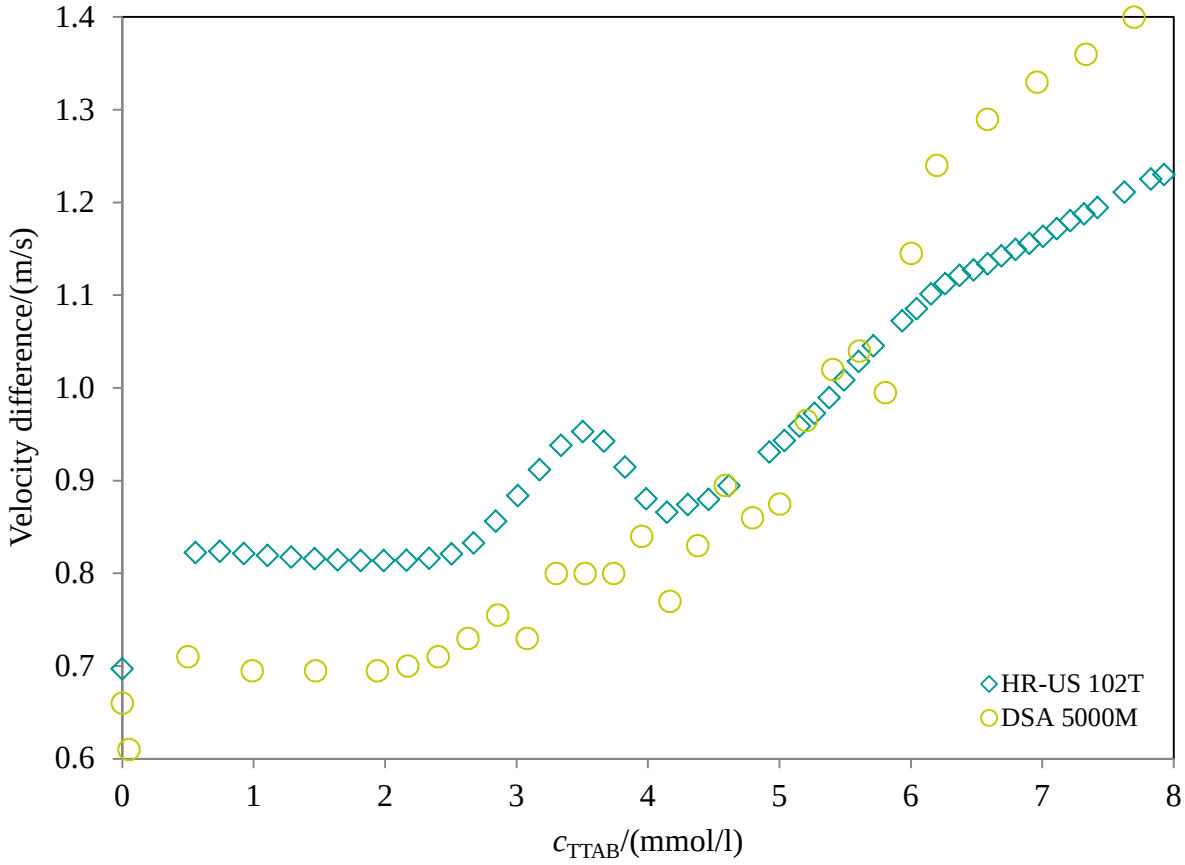

Figure 53. Dependence of velocity of hyaluronan of concentration 1000 mg/l and molecular weight of 300-500kDa with surfactant TTAB in water measured by means of densitometer DSA 5000M and HRUS 102T.

In case of measurement in densitometer DSA 5000M, the velocity is measured as relative velocity and in the case in HR-US 102T it was measured as velocity difference. The curves are very various. The breakpoint in curve from HR-US measurement is very clear. The breakpoint was observed at all four molecular weights as with TTAB and CTAB. The same measurements were done in densitometer, but the breakpoint is noticeable only in low molecular weights of hyaluronan (10-30 kDa and 90-130 kDa). Example of dependence of density and ultrasonic velocity is shown in Figure 54. During the measuring of high molecular weights of hyaluronan (300-500 kDa and 1500-1750 kDa) the precipitate was seen in very low concentration of surfactant TTAB and there is not seen

negligible breakpoint, the densitometer is not accurate, the error is big for the very near point of concentration line of surfactant. The measurement with TTAB gave better results than in case of CTAB. In using CTAB small breakpoint were seen in low molecular weight of hyaluronan and any breakpoint in high molecular weight of hyaluronan.

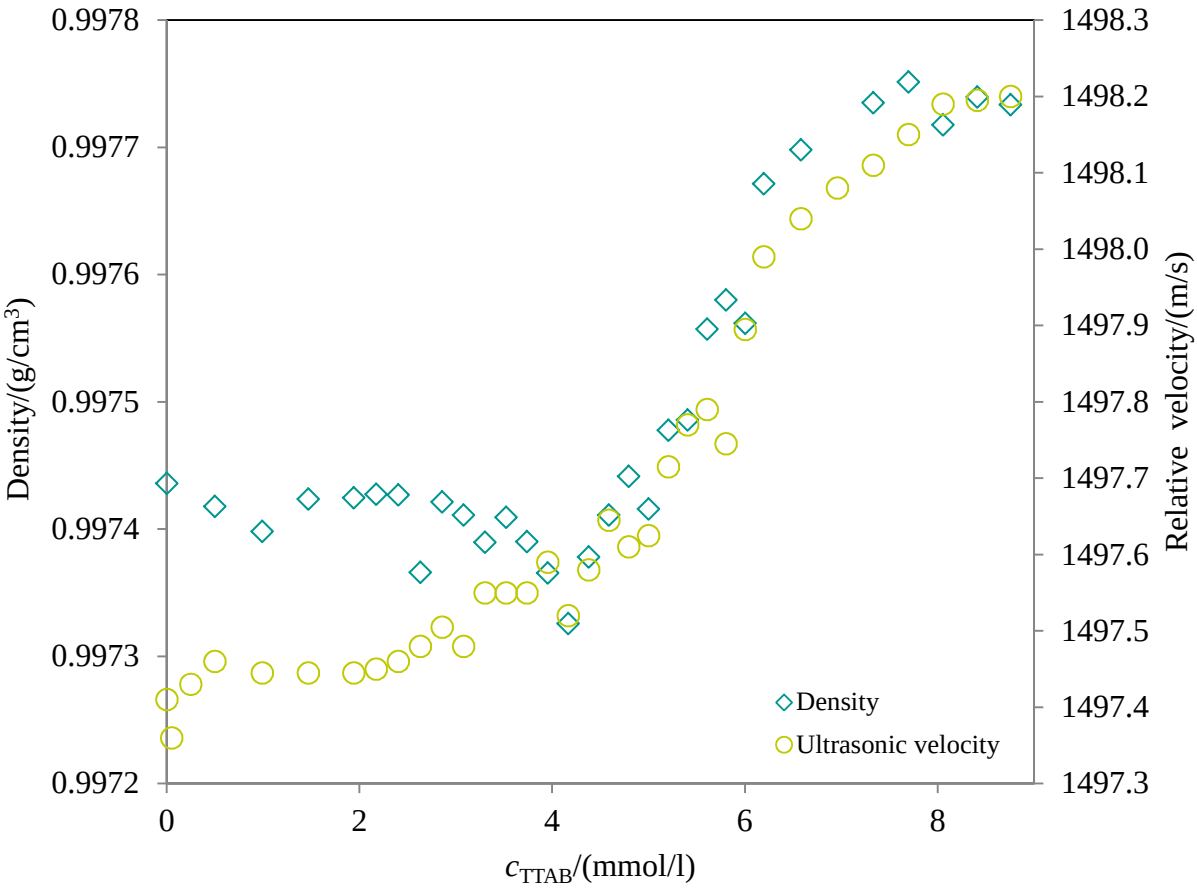

Figure 54. Dependence of density and velocity of hyaluronan of concentration 1000 mg/l and molecular weight of 300-500kDa with surfactant TTAB in water measured by means of DSA 5000M.

7.3 Conclusions

The critical micelle concentrations were determined by measurement of the ultrasonic velocity and the values are close to the values given in the literature. In water and below the critical micelle concentration the velocity profiles of both surfactants are very close. In the micelle state the velocity in the TTAB system is several times higher than in CTAB. Similar situation was observed comparing the two velocity profiles in NaCl solution. The titration profiles in the absence of hyaluronan provided the base for investigation of its effect caused by the interactions with surfactants.

The ultrasonic velocity titration curve by surfactant TTAB in water clearly shows the two parts corresponding to pre-micelle and post-micelle states. On the other hand, up to six parts can be found for the titration profile measured in hyaluronan solution. The titration curve in case of CTAB is devided to four parts and the curve in the hyaluronan solution is from the first point different from that obtained in pure water.

In contrast with the titrations in water the effect of hyaluronan molecular weight was much more obvious in the presence of NaCl for both surfactants. The velocity profile for the lowest molecular weight (10-30 kDa) is practically linear. In case of TTAB, attenuation is constant; there is small negligible break in case of CTAB. The sample clear throughout the whole range of applied surfactant concentration. Because the velocity is systematically increasing in presence of hyaluronan this should not directly indicate that no interactions between hyaluronan and surfactant are detected. The velocity profile measured for the molecular weight of 110-130 kDa shows instead of the short interval of almost constant velocity a broader interval of “ïnflexing” behaviour during which also the attenuation markedly increases and opacity is developed. For the highest molecular weight (1500-1750 kDa) the constant velocity interval and corresponding sharp increase of attenuation are shifted to higher surfactant concentrations (4-7 mmol/l).

The ultrasonic attenuation was not changed, was constant in titration of hyaluronan 15 mg/l by CTAB. It can mean microphase separation with very low concentration of separated particles and also small sensitivity of instrument HR-US. In case of titration of hyaluronan 1000 mg/l by CTAB, ultrasonic attenuation changes noticeable and it is result of macrophase separation with sufficient concentration of separated particles. There are seen interactions even in very dilute concentrations of hyaluronan, these results are in agreement with fluorescence measurements.

Vision of the interactions between hyaluronan and surfactant are depicted in Figure 55. The binding of surfactant to hyaluronan is portrayed in Figure 55. At low surfactant concentration its free monomers bind to the hyaluronan chain; later, with increasing surfactant concentration the micelles are formed and electrostatically bind to the chain. At the very high surfactant concentration, the free surfactant micelles are formed in the bulk solution because the hyaluronan chain is already fully occupied by previously formed micelles.

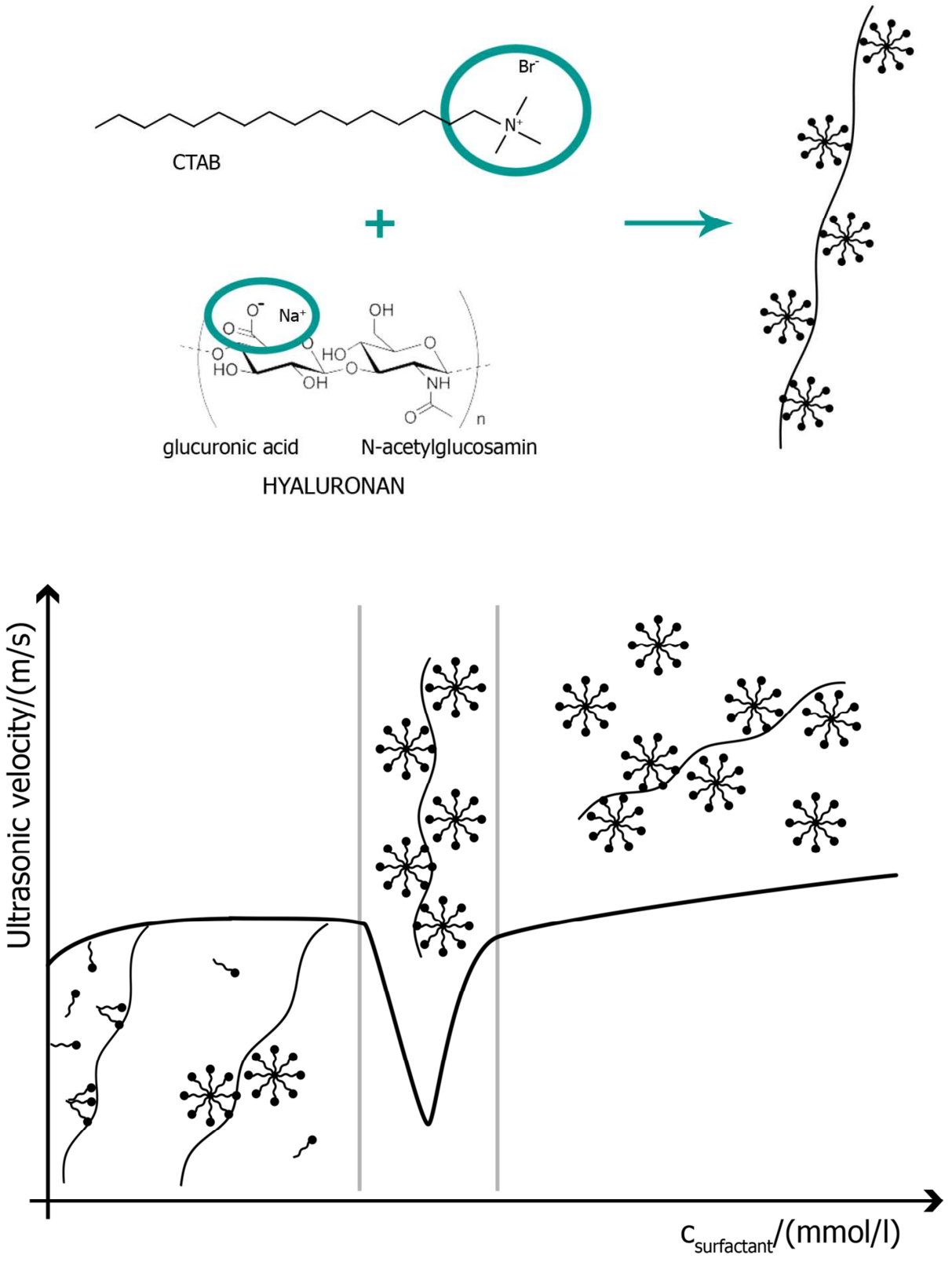

Figure 55. Illustration of the interactions between hyaluronan and surfactant CTAB in water.

8 CONCLUSION

The experimental part was divided to three parts. The first part (preliminary part) followed up behaviour of hyaluronan in water, measurement of pH and preliminary density measurement. The aim of this part was to characterize the dissolution and storage stability of hyaluronan. The value of pH all measured solutions did not change with adding of surfactant. Sodium azide could not be used for preparation of hyaluronan solution because the stability is the same in the presence and absence of azide. So the samples without sodium azide were used in shorter time (three days after dissolving). As emerged from the density measurements of different ages of hyaluronan solution, there were no changes in the values of density in different days of measurement so measurements were performed in first day.

The second part (experimental part I) was focused on the study of hyaluronan in wide range of molecular weights and as broad range of its concentration. Density and ultrasonic velocity were measured in solutions in temperature range 25-50 °C by means of densitometer DSA 5000M.

The density and ultrasonic velocity of hyaluronan solutions in water or in 0.15 M NaCl was linearly dependent on the concentration at any used temperature and both quantities increased with the concentration. Increasing temperature decreased density and increased ultrasonic velocity of a solution of given concentration; the temperature dependence was slightly curved and slightly deviated from linearity. Therefore all the data through all molecular weights, concentrations and temperatures used could be satisfactorily fitted with a single equation (one or each solvent and each quantity); linear in concentration and quadratic in temperature. The equation can be used for reliable estimate of the density and ultrasonic velocity of hyaluronan solutions in the concentration range 0-2% w/w, the molecular weight range 10-1750 kDa and the temperature range 25-50 °C. The densities were used to calculate several specific volume characteristics. The hyaluronan partial specific volume in water typically ranges, depending on concentration, between 0.587 and 0.594 cm^3/g at 25 °C and between 0.597 and 0.604 cm^3/g at 50 °C; in sodium chloride solution the values are slightly lower. The ultrasonic velocity was primarily used to calculate the compressibility. The compressibility decreased with both the hyaluronan concentration and the temperature, the influence of the temperature was stronger. The hydration numbers determined from the compressibility data were typically about 20 and only slightly dependent on concentration. The addition of NaCl caused the changes in numerical values of measured or calculated quantities but did not change the character of their concentration or temperature behaviour. There is negligible effect of molecular weight on all measured or calculated properties.

In the third part (experimental part II), high resolution ultrasonic spectroscopy was used for a detailed study of interactions between hyaluronan and two cationic surfactants tetradecyltrimethylammonuim bromide (TTAB) and hexadecyltrimethylammonium bromide (CTAB) either in water or in sodium chloride at physiological concentration (0.15 M).

The same values of ultrasonic velocity were measured both with densitometer DSA 5000M, and with ultrasonic spectrometer HR-US 102 and HR-US 102T.

Our results suggest that in the case of very low molecular weight hyaluronan in the presence of salt, the surfactant cation may replace the polysaccharide counterion forming very small and phase non-separating structures of separate surfactant molecules bound to the biopolymer

chain. An increased molecular weight of the hyaluronan leads to the formation of larger and coiled ball-like biopolymer structures with surfactant molecules bound preferably on their surface. The higher the structure, the larger its surface and the higher surfactant amount is needed to induce (micro)phase separation.

The results clearly show differences in interactions of TTAB and CTAB with hyaluronan in water. Taking into account the molecular structure of these surfactants the differences should be caused by little bit longer alkyl chain of CTAB. In other words, besides the electrostatic contribution also the hydrophobic interactions play an important role especially in the case of CTAB which has longer hydrophobic tail. For example, hydrophobic component supports interactions at very low surfactant concentration. Ultrasonic titration profiles revealed that the behaviour of hyaluronan-surfactant system is more complex than simple one-phase or two-phase behaviour with a sharp boundary as could be inferred from phase diagrams. In the phase separation region several transitions were observed on the ultrasonic velocity profiles which reflect formation of colloidal structures of different rigidity. The number of detected transitions was richer for TTAB therefore increasing importance of the hydrophobic interaction contribution simplifies the details of phase separation behaviour.

In water there is no significant effect of hyaluronan molecular weight similarly as in the previous studies on phase diagrams [62]. Thus the basic disaccharide unit and its interaction abilities are relevant for hyaluronan interactions with oppositelly charged surfactants whereas specific conformations or coil shapes of the biopolymer chain of various lengths are not so important. In the presence of sodium chloride at the concentration of 0.15 M the effect of molecular weight is appreciable. Salts should suppress the electrostatic interactions and this was reflected in much simpler titration profiles and less rich behaviour in two-phase region. However, the titration profiles measured in the NaCl solution were much closer for both surfactants than in water. Probably, the more collapsed conformations supposed to exist in the presence of electrolyte as compared to conformations in water prevented the access of surfactant molecules to the polyelectrolyte interaction sites and consequently restricted (cooperative) interactions between surfactant alkyl chains. In other words, the effect of salt on hydrophobic interactions was mediated by sterical reasons.

The measured values of the ultrasonic velocity had the same values from the HRUS 102, HRUS 102T and DSA 5000M.

High-resolution ultrasonic spectroscopy in titration regime enabled to reveal details of interactions between hyaluronan and oppositely charged surfactants. Due to its high sensitivity much more in-depth picture on interactions could be obtained when compared to other methods. Up to six different regions could be identified in a narrow interval of surfactant concentration corresponding to different states of hyaluronan-surfactant complexes formed by the interactions. These regions differed primarily in the shape of the dependence of ultrasonic velocity on surfactant concentration values of which are determined by the compressibility of structures formed in the system. The richness of titration profiles was depressed in salt solution where essentialy only two principal regions were observed. On the other side, the effect of hyaluronan molecular weight on the position of boundary between regions was more significant in the presence of salt. Very important effect on titration profiles in water had the length of the surfactant hydrophobic tail.

Besides electrostatic also hydrophobic interactions are relevant for determining the behaviour of hyaluronan-surfactant systems and properties of formed complexes (aggregates).

The series of papers by Swedish research groups [61],[62] provided a detailed study on phase behaviour of systems containing water, hyaluronan, alkyl trimethylammonium bromides (static experiment). This thesis investigated directly study of interactions hyaluronan-surfactant (dynamic experiment). HR-US is very the excellent method for measurement of the interactions polymer-surfactant with very excellent results and resolutions which is seen from the comparison of measurement in DSA 5000M and in HR-US.

The other contribution to this thesis is particularly in detailed study of attributes of different samples of hyaluronan. Thus is thought the different molecular weights and concentration of hyaluronan, its behaviour in water and 0.15 M NaCl and at different temperature.

System hyaluronan-TTAB and hyaluronan-CTAB as dynamic experiment were performed in this thesis and in article (13.2.) for the first time.

Our results of density and ultrasonic velocity and subsequently calculated parameters are published in this broad range for the first time.

Other experiments could be done in temperature around 37 °C.

9 REFERENCES

[1] BALAZS, Endre A., Torvard C. LAURENT, Roger W. JEANLOZ. Nomenclature of hyaluronic acid. *Biochemical Journal.* 1986, vol. 235, issue 3, pp. 903.

[2] HARGITTAI, István, Magdolna HARGITTAI, Philip A. BAND, Bryan TOOLE, Philip A. BAND. Molecular structure of hyaluronan: an introduction. *Structural Chemistry*. 2008, vol. 19, issue 5, pp. 425-440.

[3] MEYER, Karl, John W. PALMER. The polysaccharide of the vitreous humor. *Journal of Biology and Chemistry.* 1934, vol. 107, pp. 629-634.

[4] HARDINGHAM, Timothy E., Roger J.F. EWINS, Helen MUIR. Cartilage proteoglycans. Structure and heterogeneity of the protein core and the effects of specific protein modifications on the binding to hyaluronate. *Biochemical Journal.* 1976, vol. 157, pp. 127–143.

[5] LAGO, Guilermo, Loida ORUÑA, Jose A. CREMATA, Carlos PERÉZ, Gabriel COTO, Efren LAUZAN, John F. KENNEDY. Isolation, purification and characterization of hyaluronan from human umbilical cord residuem. *Carbohydrate Polymers.* 2005, vol. 62, pp. 321-326.

[6] SWANN, David A., James B. CAULFIELD, Philip A. BAND. Studies on hyaluronic acid V. Relationship between the protein content and viscosity of rooster comb dermis hyaluronic acid. *Connective Tissue Research.* 1975, vol. 4, issue 1, pp. 96-105.

[7] RANGASWAMY, Vidhya a Dharmendra JAIN. An efficient process for production and purification of hyaluronic acid from Streptococcus equi subsp. zooepidemicus. *Biotechnology Letters*. 2008, vol. 30, pp. 493-496.

[8] PATIL, Kanchankumar P., Deepak K. PATIL, Bhushan L. CHAUDHARI, Sudhir B. CHINCHOLKAR. Production of hyaluronic acid from Streptococcus zooepidemicus MTCC 3523 and its wound healing activity. *Journal of Bioscience and Bioengineering*. 2011, vol. 111, pp. 286-288.

[9] HUANG, Wei-Chih, Shu-Jen CHEN, Teh-Liang CHEN. Modeling the microbial production of hyaluronic acid. *Journal of the Chinese Institute of Chemical Engineers*. 2007, vol. 38, pp. 355-359.

[10] WIDNER, B., R. BEHR, S. Von DOLLEN, M. TANG, T. HEU, A. SLOMA, D. STERNBERG, P. L. DEANGELIS, P. H. WEIGEL a S. BROWN. Hyaluronic Acid Production in Bacillus subtilis. *Applied and Environmental Microbiology*. 2005, vol. 71, issue 7, pp. 3747-3752.

[11] JIA, Yuning, Jing ZHU, Xiaofei CHEN, Dongyang TANG, Ding SU, Wenbing YAO, Xiangdong GAO. Metabolic engineering of Bacillus subtilis for the efficient biosynthesis of uniform hyaluronic acid with controlled molecular weights. *Bioresource Technology*. 2013, vol. 132, pp. 427-431.

[12] IZAWA, Naoki, Masaki SERATA, Toshiro SONE, Takeshi OMASA, Hisao OHTAKE, Nguyen H. K. TU, Phi T. T. TRANG. Hyaluronic acid production by recombinant Streptococcus thermophilus. *Journal of Bioscience and Bioengineering*. 2011, vol. 111, issue 6, pp. 665-670.

[13] DON, Mashitah Mat, Noor Fazliani SHOPARWE. Kinetics of hyaluronic acid production by Streptococcus zooepidemicus considering the effect of glucose. *Biochemical Engineering Journal*. 2010, vol. 49, issue 1, pp. 95-103.

[14] DEANGELIS, P. L. Identification and molecular cloning of a unique hyaluronan synthase from Pasteurella multocida. *Journal of Biological Chemistry*. 1998, vol. 273, issue 14, pp. 8454-8458.

[15] DEANGELIS, P. L. Molecular directionality of polysaccharide polymerization by the Pasteurella multocida hyaluronan synthase. *Journal of Biological Chemistry*. 1999, vol. 274, issue 37, pp. 26557–26562.

[16] CHIEN, Liang-Jung, Cheng-Kang LEE. Hyaluronic acid production by recombinant Lactococcus lactis. *Applied Microbiology and Biotechnology*. 2007, vol. 77, issue 2, pp. 339–346.

[17] MAO, Zichao, Hyun-Dong SHIN, Rachel CHEN. A recombinant E. coli bioprocess for hyaluronan synthesis. *Applied Microbiology and Biotechnology*. 2009, vol. 84, issue 1, pp.63–69.

[18] RAH, Marjorie J., Endre A. BALAZS. A review of hyaluronan and its ophthalmic applications. *Optometry - Journal of the American Optometric Association*. 2011, vol. 82, issue 1, pp. 38-43.

[19] CHEN, W. Y., E. MARCELLIN, J. HUNG, L. K. NIELSEN. Hyaluronan molecular weight is controlled by UDP-N-acetylglucosamine concentration in Streptococcus zooepidemicus. *Journal of Biological Chemistry*. 2009, vol. 284, issue 27, pp. 18007-18014.

[20] ARMSTRONG, David C., Michael R. JOHNS. Culture conditions affect the molecular weight properties of hyaluronic acid produced by Streptococcus zooepidemicus. *Applied and environmental microbiology*. 1997, vol 63, issue 7, pp. 2759-2764.

[21] CHONG, Barrie Fong, Lars M. BLANK, Richard MCLAUGHLIN a Lars K. NIELSEN. Microbial hyaluronic acid production. *Applied Microbiology and Biotechnology*. 2005, vol. 66, issue 4, pp. 62-69.

[22] BREKKE, John H.; THACKER, Kipling. Hyaluronan as a biomaterial. An introduction to biomaterials, 2005, pp. 219-240.

[23] TOOLE, B. P., Mark G. SLOMIANY, Bryan P. TOOLE. Hyaluronan-CD44 interactions in cancer: paradoxes and possibilities. *Clinical Cancer Research*. 2009, vol. 15, issue 24, pp. 7462-7468.

[24] FRASER, J. R. E., T. C. LAURENT, U. B. G. LAURENT. Hyaluronan: its nature, distribution, functions and turnover. *Journal of Internal Medicine*. 1997, vol. 242, issue 1, pp. 27–33.

[25] VOLPI, Nicola, Juergen SCHILLER, Robert STERN, Ladislav SOLTES, Tracey J. BROWN, Natalie K. THOMAS, Paul H WEIGEL, Carl T MCGARY, Janet A WEIGEL, Teruzoh MIYOSHI, Akio OKAMOTO, Paul L. DEANGELIS. Role, metabolism, chemical modifications and applications of hyaluronan: Mechanistic studies and biotechnological applications. *Current Medicinal Chemistry*. 2009, vol. 16, issue 14, pp. 1718-1745.

[26] HUBBARD, Caitlin, Joshua T. MCNAMARA, Caleigh AZUMAYA, Mehul S. PATEL, Jochen ZIMMER, Naoki ITANO. The hyaluronan synthase catalyzes

the synthesis and membrane translocation of hyaluronan. *Journal of Molecular Biology*. 2012, vol. 418, 1-2, pp. 558-562.

[27] AMADA, Takashi, Takeru KAWASAKI. Microbial synthesis of hyaluronan and chitin: New approaches. *Journal of Bioscience and Bioengineering*. 2005, vol. 99, issue 6, pp. 521-528.

[28] *Biopolymers for medical and pharmaceutical applications: Hyaluronan*. 1st ed. Weinheim: Wiley-VCH, 2005. ISBN 3-527-31154-8. p. 617-644

[29] REHM, Bernd H. A., Nicolaus BARBARA, Anzelmo GIANLUCA, Poli ANNARITA. Bacterial polymers: biosynthesis, modifications and applications. *Nature Reviews Microbiology*. 2010, vol. 8, issue 8, pp. 578-592.

[30] LEE, Janet Y, Andrew P SPICER. Hyaluronan: a multifunctional, megaDalton, stealth molecule. *Current Opinion in Cell Biology*. 2000, vol. 12, issue 5, pp. 581-586.

[31] WNEK, Gary E. and Gary L. BOWLIN. Encyclopedia of biomaterials and biomedical engineering . New York: Marcel Dekker, 2004, p. 779–789. ISBN 978-0-8247-5562-1.

[32] NEČAS, Jiří, Lenka BARTOŠÍKOVÁ, Pavel BRAUNER, Jozef KOLÁŘ. Hyaluronic acid (hyaluronan): a review. *Veterinární medicína*. 2008, vol. 53, issue. 8, pp. 397-411.

[33] LAPČÍK, Lubomír, Lubomír LAPČÍK, Stefaan De SMEDT, Joseph DEMEESTER, Peter CHABREČEK. Hyaluronan: Preparation, structure, properties, and applications. *Chemical Reviews*. 1998, vol. 98, issue 8, pp. 2663-2684.

[34] WEIGEL, Paul H., Vincent HASCALL, Markku TAMMI. Hyaluronan synthases. *Journal of Biological Chemistry*. 1997, vol. 272, issue 22, pp. 13997-14000.

[35] STERN, Robert, Mark J. JEDRZEJAS. Hyaluronidases: Their genomics, structures, and mechanisms of action. *Chemical Reviews*. 2006, vol. 106, issue 3, pp. 818-839.

[36] GIRISH, K.S., K. KEMPARAJU. The magic glue hyaluronan and its eraser hyaluronidase: A biological overview. *Life Sciences*. 2007, vol. 80, issue 21, pp. 1921-1943.

[37] LESLEY, Jayne, Vincent C. HASCALL, Markku TAMMI, Robert HYMAN. Hyaluronan Binding by Cell Surface CD44. *Journal of Biological Chemistry*. 2000, Vol. 275, pp. 26967–26975.

[38] WOLNY, P. M., S. BANERJI, C. GOUNOU, A. R. BRISSON, A. J. DAY, D. G. JACKSON, R. P. RICHTER. Analysis of CD44-Hyaluronan Interactions in an Artificial Membrane System: Insights into the distinct binding properties of high and low molecular weight hyaluronan. *Journal of Biological Chemistry*. 2010, vol. 285, pp. 30170-30180.

[39] BANERJI, Suneale, Alan J WRIGHT, Martin NOBLE, David J MAHONEY, Iain D CAMPBELL, Anthony J DAY, David G JACKSON. Structures of the CD44-hyaluronan complex provide insight into a fundamental carbohydrate-protein interaction. *Nature Structural*. 2007, vol. 14, pp. 234-239.

[40] FAKHARI, A., C. BERKLAND. Applications and emerging trends of hyaluronic acid in tissue engineering, as dermal filler and in osteoarthritis treatment. *Acta Biomaterialia*. 2013, vol. 9, issue 7, pp. 7081–7092.

[41] PARK, Hyejin, Bogyu CHOI, Junli HU, Min LEE. Injectable chitosan hyaluronic acid hydrogels for cartilage tissue engineering. *Acta Biomaterialia*. 2013, vol. 9, issue 1, pp. 4779–4786.

[42] MUZZARELLI, Riccardo A., Francesco GRECO, Alberto BUSILACCHI, Vincenzo SOLLAZZO, Antonio GIGANTE. Chitosan, hyaluronan and chondroitin sulfate in tissue engineering for cartilage regeneration: A review. *Carbohydrate Polymers*. 2012, vol. 89, issue 3, pp. 723-739.

[43] LARSEN, Nancy E., Endre A. BALAZS, M. PRABAHARAN a M. PRABAHARAN. Drug delivery systems using hyaluronan and its derivatives. *Advanced Drug Delivery Reviews*. 1991, vol. 7, pp. 279-293.

[44] SCHIRALDI, Chiara; LA GATTA, Annalisa; DE ROSA, Mario. Biotechnological production and application of hyaluronan. *Biopolymers*, 2010, 20: 387-412. JIN Y., T. UBONVAN, D. KIM. Hyaluronic acid in drug delivery systems. *Journal of Pharmaceutical Investigation.* 2010, vol. 40, pp. 33-43.

[45] VERCRUYSSE, Koen P., Glenn D. PRESTWICH. Hyaluronate derivatives in drug delivery. *Critical Reviews™ in Therapeutic Drug Carrier Systems*. 1998, vol. 15, issue 5, pp. 513-555.

[46] AVILA, LUIS Z., GA GIANOLIO, P.A. KONOVICZ. Drug delivery and medical applications of chemically modified hyaluronan. *Carbohydrate Chemistry, Biology and Medical Applications*, 2008, pp. 333-357.

[47] LIU, Yanhua, J. SUN, W. CAO, J. YANG, H. LIAN, X. LI, Y. SUN. Dual targeting folate-conjugated hyaluronic acid polymeric micelles for paclitaxel delivery. *International journal of pharmaceutics*, 2011, vol. 421, issue 1, pp. 160-169.

[48] BROWN M. B., S.A. JONES. Hyaluronic acid: a unique topical vehicle for the localized delivery of drug to the skin. *European Academy of Dermatology and Venerology* 2005, vol. 19, pp. 308-318.

[49] J. KENNEDY, G.O. PHILIPS, P. A. WILLIAMS, V. HASCALL. Hyaluronan: Biomedical, Medical and Clinical Aspects. 2002, Woodhead Publishers, Cambridge, pp. 249–256.

[50] PRESTWICH, Glenn D. Hyaluronic acid-based clinical biomaterials derived for cell and molecule delivery in regenerative medicine. *Journal of Controlled Release*. 2011, vol. 155, issue 2, pp. 193-199.

[51] BURDICK, Jason A., Glenn D. PRESTWICH. Hyaluronic acid hydrogels for biomedical applications. *Advanced Materials*. 2011, vol. 23, issue 12, pp.41–56.

[52] HOLMBERG, Krister. *Surfactans and polymers in aqueous solution*. 2nd ed. Chichester, 2003, xvi. ISBN 04-714-9883-1.

[53] DELPECH, B., N. GIRARD, P. BERTRAND, M.-N. COUREL, C. CHAUZY, A. DELPECH. Hyaluronan: fundamental principles and applications in cancer. *Journal of Internal Medicine*. 1997, vol. 242, issue 1, pp. 41-48.

[54] STERN, Robert. Hyaluronan metabolism: a major paradox in cancer biology. *Pathologie Biologie*. 2005, vol. 53, issue 7, pp. 372-382.

[55] ALANIZ, Laura, Manglio RIZZO, Mariana G. GARCIA, Flavia PICCIONI, Jorge B. AQUINO, Mariana MALVICINI, Catalina ATORRASAGASTI, Juan BAYO, Itziar ECHEVERRIA, Pablo SAROBE, Guillermo MAZZOLINI. Low molecular weight

hyaluronan preconditioning of tumor-pulsed dendritic cells increases their migratory ability and induces immunity against murine colorectal carcinoma. *Cancer Immunology, Immunotherapy*. 2011, vol. 60, issue 10, pp. 1383-95.

[56] KARBOWNIK, Micha S., NOWAK, Jerzy Z. Hyaluronan: Towards novel anti-cancer therapeutics. *Pharmacological Reports*. 2013, vol. 65, pp. 1056-1074.

[57] RANGEL-YAGUI Carlota Oliveira, Adalberto PESSOA, Leoberto Costa TAVARES. Micelle solubilization of drugs. *Journal of Pharmaceutical Sciences* 2005, vol. 8, pp. 147-163.

[58] CHEVALIER, Y, T ZEMB, Avinoam BEN-SHAUL, William M. GELBART, J. ROUCH, P. CHABRAT, P. TARTAGLIA, D. LANGEVIN. The structure of micelles and microemulsions: Structure and phase transitions in micelle solutions. *Reports on Progress in Physics*. 1990, vol. 53, issue 3, pp. 327-349.

[59] MOULIK S.P.: Micelles: self-organized surfactant assemblies. *Current Science* 1996, vol. 71, pp. 368-376.

[60] MATA, Jitendra, Dharmesh VARADE, Prashant BAHADUR, Bryan C. SMITH, Lu-Chien CHOU, Bin LU a ZAKIN. Aggregation behaviour of quaternary salt based cationic surfactants. *Thermochimica Acta* 2005, vol. 428, pp. 147–155.

[61] THALBERG, Kyrre, Bjoern LINDMAN. Interaction between hyaluronan and cationic surfactants. *The Journal of Physical Chemistry*. 1989, vol. 93, issue 4, pp. 1478-1483.

[62] THALBERG, Kyrre, Björn LINDMAN and Gunnar KARLSTRÖM. Phase diagram of a system of cationic surfactant and anionic polyelectrolyte: tetradecyltrimethylammonium bromide-hyaluronan-water. *The Journal of Physical Chemistry*. 1990, vol. 94, no. 10, p. 4289–4295. ISSN 0022-3654.

[63] BELL, Christopher G., Christopher J. W. BREWARD, Peter D. HOWELL, Jeffery PENFOLD, Robert K. THOMAS. Macroscopic modeling of the surface tension of polymer−surfactant systems. *Langmuir*. 2007, vol. 23, issue 11, pp. 6042-6052.

[64] KOGAN, Grigorij, Ladislav ŠOLTÉS, Robert STERN, Peter GEMEINER. Hyaluronic acid: a natural biopolymer with a broad range of biomedical and industrial applications. *Biotechnology Letters*, 2007, Vol. 29, pp. 17-25.

[65] KAATZE, Udo, V KUHNEL, K MENZEL, S SCHWERDTFEGER. Ultrasonic spectroscopy of liquids. Extending the frequency range of the variable sample length pulse technique. *Measurement Science and Technology*. 1993, vol. 4, issue 11, pp. 1257-1265.

[66] KAATZE, U.; LAUTSCHAM, K.; BRAI, M. Acoustical absorption spectroscopy of liquids between 0.15 and 3000 MHz: II. Ultrasonic pulse transmission methods. *Journal of Physics E: Scientific Instruments*, 1988, vol. 21, pp. 103-107.

[67] KAATZE, Udo, Frieder EGGERS, Karl LAUTSCHAM. Ultrasonic velocity measurements in liquids with high resolution-techniques, selected applications and perspectives. *Measurement Science and Technology*. 2008, vol. 19, issue 6.

[68] PEKAŘ M., J. KUČERÍK, D. Šmejkalová. Nové možnosti ultrazvukové spektroskopie v koloidní chemii, *CheMagazín* 2005, vol. 1, pp. 12-14.

[69] www.ultrasonic-scientific.com cited 10.3.2013

[70] POVEY, Malcolm J. *Ultrasonic Techniques for Fluids Characterization*. San Diego: Academic Press, 1997. ISBN 01-256-3730-6.

[71] TIAN Zhen, BING Nai Ci, XIE Hong Yong. High-resolution ultrasonic spectroscopy for crystallization process. *Advanced Materials Research* 2012, vol. 508, issue 146.

[72] MIZRAHY, Shoshy, Sabina Rebe RAZ, Martin HASGAARD, Hong LIU, Neta SOFFER-TSUR, Keren COHEN, Ram DVASH, Dalit LANDSMAN-MILO, Maria G.E.G. BREMER, S. Moein MOGHIMI a Dan PEER. Hyaluronan-coated nanoparticles: The influence of the molecular weight on CD44-hyaluronan interactions and on the immune response. *Journal of Controlled Release* 2011, vol. 156, issue 2, pp. 231-238.

[73] ANILKUMAR, T. V., Jaser MUHAMED, Anumol JOSE, Arun JYOTHI, P. V. MOHANAN, Lissy K. KRISHNAN. Advantages of hyaluronic acid as a component of fibrin sheet for care of acute wound. *Biologicals*. 2011, vol. 39, issue 2, pp. 81-88.

[74] SCHANTÉ, Carole E., Guy ZUBER, Corinne HERLIN, Thierry F. VANDAMME. Chemical modifications of hyaluronic acid for the synthesis of derivatives for a broad range of biomedical applications. *Carbohydrate Polymers*. 2011, vol. 85, issue 3, pp. 469-489.

[75] XU, Keming, Fan LEE, Shu Jun GAO, Joo Eun CHUNG, Hirohisa YANO, Motoichi KURISAWA. Injectable hyaluronic acid-tyramine hydrogels incorporating interferon-α2a for liver cancer therapy. *Journal of Controlled Release*. 2013, vol. 166, issue 3, pp. 203-210

[76] PALUMBO, Fabio Salvatore, Giovanna PITARRESI, Calogero FIORICA, Salvatrice RIGOGLIUSO, Giulio GHERSI, Gaetano GIAMMONA. Chemical hydrogels based on a hyaluronic acid-graft-α-elastin derivative as potential scaffolds for tissue engineering. *Materials Science and Engineering: C*. 2013, vol. 33, issue 5.

[77] PALUMBO, Filippo CALASCIBETTA, Calogero FIORICA, Mauro Di STEFANO a Gaetano GIAMMONA. Medicated hydrogels of hyaluronic acid derivatives for use in orthopedic field. *International Journal of Pharmaceutics*. 2013, vol. 449, issue 1-2, pp. 84-94.

[78] COLLINS, Maurice N., Colin BIRKINSHAW. Hyaluronic acid based scaffolds for tissue engineering—A review. *Carbohydrate Polymers*. 2013, vol. 92, issue 2, pp.1262-1279.

[79] XIE, Yan, Zee UPTON, Sean RICHARDS, Simone C. RIZZI, David I. LEAVESLEY. Hyaluronic acid: Evaluation as a potential delivery vehicle for vitronectin. *Journal of Controlled Release*. 2011, vol. 153, issue 3, pp. 225-232.

[80] MISRA, Suniti, Shibnath GHATAK, Neha PATIL, Prasad DANDAWATE, Vinita AMBIKE, Shreelekha ADSULE, Deepak UNNI, K. Venkateswara SWAMY, Subhash PADHYE. Novel dual cyclooxygenase and lipoxygenase inhibitors targeting hyaluronan–CD44v6 pathway and inducing cytotoxicity in colon cancer cells. *Bioorganic*. 2013, vol. 21, issue 9, pp.2551-9.

[81] CHIAPPISI, Leonardo, Ingo HOFFMANN, Michael GRADZIELSKI. Complexes of oppositely charged polyelectrolytes and surfactants – recent developments in the field of biologically derived polyelectrolytes. *Soft Matter*. 2013, vol. 9, issue 15, pp. 3896-3909.

[82] TORCHILIN, Vladimir P., Eva ROBLEGG, Reas ZIMMER. Structure and design of polymeric surfactant-based drug delivery systems. *Journal of Controlled Release*. 2001, vol. 73, issue 2-3, pp. 137-172.

[83] JONES, Marie-Christine. Polymeric micelles – a new generation of colloidal drug carriers. *European Journal of Pharmaceutics and Biopharmaceutics*. 1999, vol. 48, issue 2, pp. 101-111.

[84] HERSLOEF, Aasa, Lars Olof SUNDELOEF, Katarina EDSMAN. Interaction between polyelectrolyte and surfactant of opposite charge: hydrodynamic effects in the sodium hyaluronate/tetradecyltrimethylammonium bromide/sodium chloride/water system. *The Journal of Physical Chemistry*. 1992, vol. 96, issue 5, pp. 2345-2348.

[85] BUCKIN, Vitaly, Cormac SMYTH: High-resolution ultrasonic resonator measurements for analysis of liquids, *Seminars in Food Anaysis*. 1999, vol. 4, pp. 113-130.

[86] BUCKIN, Vitaly, Evgeny KUDRYASHOV, S. R. REN, P. R. WILLIAMS, M. I. VALIČ, J. STEPIŠNIK. Ultrasonic shear wave rheology of weak particle gels. *Advances in Colloid and Interface Science*. 2001, vol. 401, pp. 89-90.

[87] SARVAZYAN, A. Ultrasonic velocimetry of biological compounds. *Annual Review of Biophysics and Biomolecular Structure*. 1991, vol. 20, issue 1, pp. 321-342.

[88] FAKHARI, Amir, Quang PHAN, Santosh V. THAKKAR, C. Russell MIDDAUGH, Cory BERKLAND. Hyaluronic acid nanoparticles titrate the viscoelastic properties of viscosupplements. *Langmuir*. 2013, vol. 29, issue 17, pp. 5123-5131.

[89] KUDRYASHOV, Evgeny, Cormac SMYTH, Breda O´DRISCOLL, Vitaly BUCKIN. High resolution ultrasonic spectroscopy for the analysis of raw material and formulations used in pharmaceutical Industry. *Pharmaceutical Technology Europe*. 2005, vol. 1.

[90] CORREDIG, Milena, Marcela ALEXANDER, DALGLEISH. The application of ultrasonic spectroscopy to the study of the gelation of milk components. *Food Research International*. 2004, vol. 37, issue 6, pp. 557-565.

[91] HOE, Susan, Paul M. YOUNG, Philippe ROGUEDA, Daniela TRAINI. Determination of reference ultrasonic parameters for model and hydrofluoroalkane propellants using high-resolution ultrasonic spectroscopy. *AAPS PharmSciTech*. 2008, vol. 9, issue 2, pp. 605–611.

[92] RESA, Pablo, Vitaly BUCKIN. Ultrasonic analysis of kinetic mechanism of hydrolysis of cellobiose by β-glucosidase. *Analytical biochemistry*. 2011, vol. 415, issue 1, pp.1-11.

[93] BUCKIN, Vitaly, B. I. KANKIYA, Dionisios RENTZEPERIS, Luis A. MARKY. Mg2+ recognizes the sequence of DNA through its hydration shell. *Journal of the American Chemical Society*. 1994, vol. 116, issue 21, pp. 9423-9429.

[94] OCHENDUSZKO, Agnieszka, Vitaly BUCKIN. Real-time monitoring of heat-induced aggregation of β-lactoglobulin in aqueous solutions using high-resolution ultrasonic spectroscopy. *International Journal of Thermophysics*. 2010, vol. 31, issue 1, pp. 113-130.

[95] LEHMANN, L., Evegeny Kudryashov, Vitaly Buckin. Ultrasonic monitoring of the gelatinisation of starch. *Trends in Colloid and Interface Science XVI*. Springer Berlin Heidelberg. 2004, pp.136-140.

[96] MCCLEMENTS, D. J. Principles of ultrasonic droplet size determination in emulsions. *Langmuir*. 1996, vol. 12, issue 14, pp. 3454-3461.

[97] SMYTH, Cormac, Evgeny KUDRYASHOV, Breda O´DRISCOLL, Vitaly BUCKIN. High-resolution ultrasonic spectroscopy for analysis of industrial emulsions and suspensions. *Journal of the Association for Laboratory Automation.* 2004, vol. 9, issue 2, pp. 87-90.

[98] LIU, Jinru, Marcela ALEXANDER, Edita VERESPEJ, Milena CORREDIG. Real-time determination of structural changes of sodium caseinate-stabilized emulsions containing pectin using high resolution ultrasonic spectroscopy. *Food Biophysics*. 2007, vol. 2, issue 2-3, pp. 67-75.

[99] CESPI, Marco, Giulia BONACUCINA, Giovanna MENCARELLI, Stefania PUCCIARELLI, Gianfabio GIORGIONI, Giovanni F. PALMIERI. Monitoring the aggregation behaviour of self-assembling polymers through high-resolution ultrasonic spectroscopy. *International Journal of Pharmaceutics*. 2010, vol. 388, issue 1, pp. 274-279.

[100] MORRISSEY, S.; CRAIG, E.; BUCKIN, V. Does the structure of surfactant complexes on the DNA surface depend on the nucleotide sequence? *Trends in Colloid and Interface Science XIV.* Springer Berlin Heidelberg, 2000, pp. 201-208.

[101] RINAUDO, Marguerite. Polyelectrolyte properties of a plant and animal polysaccharide. *Structural Chemistry*. 2009, vol. 20, issue 2, pp. 277-289..

[102] COWMAN, Mary K., Shiro MATSUOKA, Naoki ITANO, Katia HAXAIRE, Eric BUHLER, Michel MILAS, Serge PEREZ, Marguerite RINAUDO, R.-H. MIKELSAAR, Bryan TOOLE, ROBERT E. CANFIELD, CHRISTIAN B. ANFINSEN. Experimental approaches to hyaluronan structure. *Carbohydrate Research*. 2005, vol. 340, issue 5, pp. 311-378.

[103] GÓMEZ-ALEJANDRE, S, E Sánchez de la BLANCA, C Abradelo de USERA, M.F REY-STOLLE, I HERNÁNDEZ-FUENTES. Partial specific volume of hyaluronic acid in different media and conditions. *International Journal of Biological Macromolecules*. 2000, vol. 27, issue 4, pp. 287-290.

[104] GARCÍA-ABUÍN, A., D. GÓMEZ-DÍAZ, J.M. NAVAZA, L. REGUEIRO a I. VIDAL-TATO. Viscosimetric behaviour of hyaluronic acid in different aqueous solutions. *Carbohydrate Polymers*. 2011, vol. 85, issue 3, pp. 500-505.

[105] SUZUKI, Yasuko; Hisashi UEDAIRA. Hydration of potassium hyaluronate. *Bulletin of the Chemical Society of Japan*. 1970, vol. 43, pp. 1892-1894.

[106] DAVIES, A., J. GORMALLY, E. WYN-JONES, D.J. WEDLOCK, G.O. PHILLIPS. A study of factors influencing hydration of sodium hyaluronate from compressibility and high-precision densimetric measurements. *Biochemical Journal*. 1983, vol. 213, pp.363-369.

[107] DAVIES, A., J. GORMALLY, E. WYN-JONES, D.J. WEDLOCK, G.O. PHILLIPS. A study of hydration of sodium hyaluronate from compressibility and high precision densitometric measurements. *International Journal of Biological Macromolecules*. 1982, vol. 4, issue 7, pp. 436-438.

[108] FUKADA, K., E. SUZUKI, T. SEIMIYA. Density and compressibility measurements of a highly viscous polyelectrolyte solution: a study on aqueous solutions of sodium hyaluronate. *Colloid*. 1999, vol. 277, issue 2, pp.242-246.

[109] CANCELA, M.A., E. ÁLVAREZ, R. MACEIRAS. Effects of temperature and concentration on carboxymethylcellulose with sucrose rheology. *Journal of Food Engineering*. 2005, vol. 71, issue 4, pp. 419-424.

[110] RAO, KSV Krishna, Yong-IlLEE, Changdae KIM. Thermodynamic and physicochemical properties of chitosan in water+ formic acid mixtures at different temperatures. *Asian Chitin Jurnal*. 2011, vol. 7, issue 1, pp. 43-50.

[111] ZAFARANI-MOATTAR, Mohammed Taghi, Shokat SARMAD. Volumetric and ultrasonic studies of the poly(ethylene glycol) methacrylate 360 alcohol systems at 298.15 K. *Journal of Chemical*. 2006, vol. 51, issue 3, pp. 968-971.

[112] SASAHARA, K., M. SAKURAI, K. NITTA. Volume and compressibility changes for short poly(ethylene glycol)-water system at various temperatures. *Colloid*. 1998, vol. 276, issue 7, pp. 643-647.

[113] HANKE, Elke, Ulrike SCHULZ, Udo KAATZE. Molecular interactions in poly(ethylene glycol) - water mixtures at various temperatures: density and isentropic compressibility study. *ChemPhysChem*. 2007, vol. 8, issue 4, pp. 553-560.

[114] SAHIN, Melike, Zerin YESIL, Merve GUNEL, Sadife TAHIROGLU, Erol AYRANCI. Interactions of glycine with polyethylene glycol studied by measurements of density and ultrasonic speed in aqueous solutions at various temperatures. *Fluid Phase Equilibria*. 2011, vol. 300, issue 1, pp.155-161.

[115] GONZÁLEZ-GAITANO, Gustavo, A. CRESPO, G. TARDAJOS. Thermodynamic investigation (volume and compressibility) of the systems β-cyclodextrin n-alkyltrimethylammonium bromides water. *The Journal of Physical Chemistry B*. 2000, vol. 104, issue 8, pp. 1869-1879.

[116] GODDARD, E. D.; ANANTHAPADMANABHAN, K. P. Applications of polymer-surfactant systems. *Surfactant science series*, 1998, vol. 77, pp. 21-64.

[117] MESA, Camillo La. Binding of surfactants onto polymers: a kinetic model. Colloids and surfaces A: *Physicochemical and Engineering Aspects*. 1999, vol. 160, issue 1, pp. 37-46.

[118] BISWAS, S. C., D. K. CHATTORAJ. Polysaccharide-surfactant interaction. Adsorption of cationic surfactants at the cellulose-water interface. *Langmuir*. 1997, vol. 13, issue 17, pp. 4505-4511.

[119] BAO, Hongqian, Lin LI, Leong Huat GAN, Hongbin ZHANG. Interactions between ionic surfactants and polysaccharides in aqueous solutions. *Macromolecules*. 2008, vol. 41, issue 23, pp. 9406–9412.

[120] BISWAS, S. C., L. DUBREIL, D. MARION. Interfacial behaviour of wheat puroindolines: monolayers of puroindolines at the air-water interface. *Colloid*. 2001, vol. 279, issue 6, pp. 607–614.

[121] SARDAR, Najam, Mohammad KAMIL a KABIR-UD-DIN. Solution behaviour of anionic polymer sodium carboxymethylcellulose (NaCMC) in presence of cationic gemini/conventional surfactants. *Colloids and Surfaces A: Physicochemical and Engineering Aspects*. 2012, vol. 415, pp. 413-420.

[122] RUDIUK, Sergii, Kenichi YOSHIKAWA, Damien BAIGL. Enhancement of DNA compaction by negatively charged nanoparticles: Effect of nanoparticle size and surfactant chain length. *Journal of Colloid and Interface Science*. 2012, vol. 368, issue 1, pp. 372-377.

[123] BONINCONTRO, A., S. MARCHETTI, G. ONORI, A. ROSATI. Interaction cetyltrimethylammonium bromide–DNA investigated by dielectric spectroscopy. *Chemical Physics*. 2005, vol. 312, issue 1, pp. 55-60.

[124] DIAS, Rita S., Josef INNERLOHINGER, Otto GLATTER, Maria G. MIGUEL, Björn LINDMAN, S. M. MEL'NIKOV, V. G. SERGEYEV, K. YOSHIKAWA. Coil-globule transition of DNA molecules induced by cationic surfactants: dynamic light scattering study. *The Journal of Physical Chemistry B*. 2005, vol. 109, issue 20, pp. 10458-10463.

[125] BUCKIN, Vitaly, Evgeny KUDRYASHOV, Siobhan MORRISSEY, Kenneth DAWSON, Tatiana KAPUSTINA. Do surfactants form micelles on the surface of DNA? *Progress in Colloid and Polymer Science*. 1998, vol. 110, pp. 214-219.

[126] CHATTERJEE, A., S.P. MOULIK, P.R. MAJHI, S.K. SANYAL. Studies on surfactant–biopolymer interaction. I. Microcalorimetric investigation on the interaction of cetyltrimethylammonium bromide (CTAB) and sodium dodecylsulfate (SDS) with gelatin (Gn), lysozyme (Lz) and deoxyribonucleic acid (DNA). *Biophysical Chemistry*. 2002, vol. 98, issue 3, pp. 313–327.

[127] TAYLOR, D.J.F., R.K. THOMAS, J. PENFOLD. Polymer/surfactant interactions at the air/water interface. *Advances in Colloid and Interface Scienc*e. 2007, vol. 132, issue 2, pp. 69-110.

[128] BORUAH, Bornali, Palash M. SAIKIA a Robin K. DUTTA. Binding and stabilization of curcumin by mixed chitosan–surfactant systems: A spectroscopic study. *Journal of Photochemistry and Photobiology A: Chemistry*. 2012, vol. 245, pp. 18-27.

[129] HERSLOEF, Aasa, Lars Olof SUNDELOEF, Katarina EDSMAN. Interaction between polyelectrolyte and surfactant of opposite charge: hydrodynamic effects in the sodium hyaluronate/tetradecyltrimethylammonium bromide/sodium chloride/water system. *The Journal of Physical Chemistry*. 1992, vol. 96, issue 5.

[130] BJORLING, Mikael, Asa HERSLOEF-BJORLING, Peter STILBS. An NMR self-diffusion study of the interaction between sodium hyaluronate and tetradecyltrimethylammonium bromide. *Macromolecules*. 1995, vol. 28, issue 20, pp. 6970–6975.

[131] HALASOVÁ, Tereza, Jitka KROUSKÁ, Filip MRAVEC, Miloslav PEKAŘ. Hyaluronan-surfactant interactions in physiological solution studied by tensiometry and fluorescence probe techniques. *Colloids and Surfaces A: Physicochemical and Engineering Aspects.* 2011, vol. 391, issue 1, pp. 25–31.

[132] PISÁRČIK, Martin, Toyoko IMAE, Ferdinand DEVÍNSKY, Ivan LACKO, Vittorio DEGIORGIO, Mario CORTI. Aggregates of sodium hyaluronate with cationic and aminoxide surfactants in aqueous solution – light scattering study. *Colloids and Surfaces A: Physicochemical and Engineering Aspects*. 2001, issue 183-185, pp. 471-486.

[133] PISÁRČIK, Martin, Toyoko IMAE, Ferdinand DEVÍNSKY, Ivan LACKO, D. BAKOŠ. Aggregation properties of sodium hyaluronate with alkanediyl-α, ω-bis(dimethylalkylammonium bromide) surfactants in aqueous sodium chloride solution. *Journal of Colloid and Interface Science.* 2002, vol. 228, issue 2, pp. 207-212.

[134] KUDRYASHOV, Evgeny, Tatiana KAPUSTINA, Siobhan MORRISSEY, Vitaly BUCKIN, Kenneth DAWSON. The compressibility of alkyltrimethylammonium bromide micelles. *Journal of Colloid and Interface Science*. 1998, vol. 203, issue 1, pp. 59-68

[135] BUCKIN, Vitaly, Evgeny KUDRYASHOV, Siobhan MORRISSEY, Cormac SMYTH, Breda O´DRISCOLL. High-resolution ultrasonic spectroscopy for analysis of biocolloids. *International Labmate.* 2002, vol. 27, issue 2, pp.23-26.

[136] ZIELIŃSKI, Ryszard, Shoichi IKEDA, Hiroyasu NOMURA, Shigeo KATO. Adiabatic compressibility of alkyltrimethylammonium bromides in aqueous solutions. *Journal of Colloid and Interface Science*. 1987, vol. 119, issue 2, Pp. 398–408.

[137] ANDREATTA, Gaëlle, Neil BOSTROM, Oliver C. MULLINS. High -Q ultrasonic determination of the critical nanoaggregate concentration of asphaltenes and the critical micelle concentration of standard surfactants. *Langmuir*. 2005, vol. 21, issue 7, pp. 2728–2736.

[138] HICKEY, Sinead, M. Jayne LAWRENCE, Sue A. HAGAN, Vitaly BUCKIN. Analysis of the Phase Diagram and Microstructural Transitions in Phospholipid Microemulsion Systems Using High-Resolution Ultrasonic Spectroscopy. *Langmuir*. 2006, vol. 22, issue 13, pp. 5575-5583.

[139] HICKEY, Sinead, Sue A. HAGAN, Evgeny KUDRYASHOV, Vitaly BUCKIN, Brian L. PHILLIPS, R. James KIRKPATRICK, Yuehui XIAO, John G. THOMPSON. Analysis of phase diagram and microstructural transitions in an ethyl oleate/water/Tween 80/Span 20 microemulsion system using high-resolution ultrasonic spectroscopy. *International Journal of Pharmaceutics*. 2010, vol. 388, issue 1, pp. 5575-5583.

[140] PAVLOVSKAYA, G., D.J. MCCLEMENTS, M.J.W. POVEY. Ultrasonic investigation of aqueous solutions of a globular protein. *Food Hydrocolloids*. 1992, vol. 6, issue 3, pp. 253-262.

[141] ANAND, K., O. P. YADAV, P. P. SINGH. Ultrasonic investigation of the behaviour of sodium dodecyl sulphate in aqueous poly(N-vinyl-2- pyrrolidone). *Colloid*. 1992, vol. 270, issue 12, pp. 1201-1207.

[142] HAYNES W.M., D.R. LIDE, T.J. BRUNO, *CRC Handbook of Chemistry and Physics*, 93rd ed. CRC Press, Boca Raton, London, New York, 2012.

[143] FABRE, M.J., L.H. TAGLE, L. GARGALLO, D. RADIC, I. HERNANDEZ-FUENTES. Partial specific volume and specific refractive index increment of some poly(carbonate)s and poly(thiocarbonate)s. *European Polymer Journal*. 1989, vol. 25, issue 12, pp. 1315-1317.

[144] KAULGUD, M.V., DHONGE S.S. Apparent molal volumes and apparent molal compressibilities of some carbohydrates in dilute aqueous solutions at different temperatures. *Indian Journal of Chemistry*. 1988, vol. 27A, issue 1, pp. 9-11.

[145] SURDO, Antonio Lo, Charles SHIN, Frank J. MILLERO. The apparent molal volume and adiabatic compressibility of some organic solutes in water at 25°. *Journal of Chemical*. 1978, vol. 23, issue 3, pp. 197-201.

[146] DURCHSCHLAG H., P. ZIPPER. Calculation of the partial volume of organic compounds and polymers. *Progress in Colloid & Polymer Science*, 1994, vol. 94, pp. 20–39.

[147] PERKINS, Stephen J., Andrew MILLER, Timothy E. HARDINGHAM, Helen MUIR. Physical properties of the hyaluronate binding region of proteoglycan from pig laryngeal cartilage. *Journal of Molecular Biology*. 1981, vol. 150, issue 1.

[148] JUNQUERA, Elena, Dania OLMOS, Emilio AICART. Carbohydrate–water interactions of p-nitrophenylglycosides in aqueous solution. Ultrasonic and densitometric studies. *Physical Chemistry Chemical Physics*. 2002, vol. 4, issue 2, pp. 352-357.

[149] HAXAIRE, K., Y. MARÉCHAL, M. MILAS, M. RINAUDO. Hydration of polysaccharide hyaluronan observed by IR spectrometry. I. Preliminary experiments and band assignments. *Biopolymers*. 2003, vol. 72, issue 1, pp. 10-20.

[150] HAXAIRE, K., Y. MARÉCHAL, M. MILAS, M. RINAUDO. Hydration of hyaluronan polysaccharide observed by IR spectrometry. II. Definition and quantitative analysis of elementary hydration spectra and water uptake. *Biopolymers*. 2003, vol. 72, issue 3, pp. 149-161.

[151] MARÉCHAL, Y., M. MILAS, M. RINAUDO. Hydration of hyaluronan polysaccharide observed by IR spectrometry. III. Structure and mechanism of hydration. *Biopolymers*. 2003, vol. 72, issue 3, pp. 162-173.

[152] BURAKOWSKI, Andrzej, Jacek GLIŃSKI. Hydration numbers of nonelectrolytes from acoustic methods. *Chemical Reviews*. 2011, vol. 112, issue 4, pp. 2059-2081.

[153] GROSSO, V. A. Del., C.V. MADER. Speed of sound in pure water. *The Journal of the Acoustical Society of America*. 1972, vol. 52, issue 5B, pp. 1442-1446.

[154] KROEBEL, W., K.H. MAHRT. Recent results of absolute sound velocity measurements in pure water and sea water at atmospheric pressure. *Acta Acustica united with Acustica*. 1976, vol. 35, issue 11, pp. 154-164.

[155] FUJII, Ken-ichi. Accurate measurements of the sound velocity in pure water by combining a coherent phase-detection technique and a variable path-length interferometer. *The Journal of the Acoustical Society of America*. 1993, vol. 93, issue 1, pp. 276-282.

[156] BUCKIN, V.A., B.I. KANKIYA, A.P. SARVAZYAN, H. UEDAIRA. Acoustical investigation of poly(dA).poly(dT), poly[d(A-T)].poly[d(A-T)], poly(A) . poly(U) and DNA hydration in dilute aqueous solutions. *Nucleic Acids Research*. 1989, vol. 17, issue 11, pp. 4189-4203.

[157] BEYER, Katja, Dag LEINE, Alfred BLUME. The demicellization of alkyltrimethylammonium bromides in 0.1M sodium chloride solution studied by isothermal titration calorimetry. *Colloids and Surfaces B: Biointerfaces*. 2006, vol. 49, issue 1, pp. 31-39.

[158] STIBORSKÝ, F. Studium agregace v systému biopolymer-tenzid za nízkých koncentrací tenzidu. Brno: Vysoké učení technické v Brně, Fakulta chemická, 2010. 36 s. Vedoucí bakalářské práce Ing. Filip Mravec, Ph.D.

[159] STODGHILL, Steven P., Adam E. SMITH, John H. O'HAVER. Thermodynamics of micellization and adsorption of three alkyltrimethylammonium bromides using isothermal ittration calorimetry. *Langmuir*. 2004, vol. 20, issue 26, pp. 11387-1392.

[160] MOSQUERA, Victor. A study of the aggregation behaviour of hexyltrimethylammonium bromide in aqueous Solution. *Journal of Colloid and Interface Science*. 1998, vol. 206, issue 1, pp. 66–76.

[161] PERGER, Tine-Martin, Marija BEŠTER-ROGAČ. Thermodynamics of micelle formation of alkyltrimethylammonium chlorides from high performance electric conductivity measurements. *Journal of Colloid and Interface Science*. 2007, vol. 313, issue 1, pp. 288-295.

[162] RAY, G. Basu, I. CHAKRABORTY, S. GHOSH, S. P. MOULIK, R. PALEPU. Self-aggregation of alkyltrimethylammonium bromides (C 10 -, C 12 -, C 14 -, and C -16 TAB) and their binary mixtures in aqueous medium: A critical and comprehensive assessment of interfacial behaviour and bulk properties with reference to two types of micelle formation. *Langmuir*. 2005, vol. 21, issue 24, pp. 10958-10967.

[163] ZIELIŃSKI, Ryszard, Shoichi IKEDA, Hiroyasu NOMURA, Shigeo KATO. Temperature dependence of adiabatic compressibility of aqueous solutions of CTAB. *Journal of the Chemical Society, Faraday Transactions 1*. 1988, vol. 84, issue 1, pp. 151-163.

[164] ZIELIŃSKI, Ryszard, Shoichi IKEDA, Hiroyasu NOMURA, Shigeo KATO. Effect of temperature on micelle formation in aqueous solutions of alkyltrimethylammonium bromides. *Journal of Colloid and Interface Science*. 1989, vol. 129, issue 1, pp. 175-184.

10 LIST OF ABBREVATIONS AND SYMBOLS

List of used abbrevations

Abbrevation	*Meaning of the abbreviation*
HR-US	high resolution ultrasonic spectroscopy
NMR	nuclear magnetic resonance
TTAB	tetradecyltrimethylammonium bromide
CTAB	hexadeycltrimethylammonium bromide
NaCl	sodium chloride
NaBr	sodium bromide
NaN_3	sodium azide
$CaCl_2$	calcium chlorid
CMC	critical micelle concentration
CD44	type of hyaluronan receptor
RHAMM	type of hyaluronan receptor
C_8TAB	octyltrimethylammonium bromide
C_9TAB	nonyltrimethylammonium bromide
C_{10}TAB, DeTAB	decyltrimethylammonium bromide
C_{12}TAB, DTAB	dodecyltrimethylammonium bromide
C_{14}TAB, TTAB	tetradecyltrimethy lammonium bromide
C_{16}TAB, CTAB	hexadecyltrimethylammonium bromide
CTAT	hexadecyltrimethyammonium p-toluenesulfonate
SDS	sodium dodecyl sulfate

List of used symbols

Used physical parameters are in following table.

Symbol	*Meaning of the symbol*	*Unit*
pH	pH value	
t	temperature	°C
f	frequency	Hz
A	amplitude	V
L	cell length	cm
M_w	molecular weight	Da (Dalton)
c	molar concentration	mol/l, mmol/l
w	mass concentration	g/l, mg/l
w/w	concentration ratio – mass versus mass	%
m	weight	kg
M	molecular weight	kg/mol
ρ	density	g/cm^3
ρ_0	density of water	g/cm^3
a_o	regression parameter	g/cm^3
a_w	regression parameter	kg/cm^3
a_t	regression parameter	$g/cm^3°C$
a_{tt}	regression parameter	$g/cm^3(°C)^2$
c_w	concentration of hyaluronan	g/kg
R	multiple correlation coefficient	
R^2	coefficient of determination	
R_p	predicted coefficient of determination	
MEP	mean quadratic error of prediction	
AIC	Akaike information criterion	
v, u	ultrasonic velocity	m/s
N	ultrasonic attenuation	1/m
V_{app}	apparent specific volume	cm^3/g
V^0_{app}	limiting apparent specific volume	cm^3/g
$\bar{V}_{sp,hya}$	partial specific volume	cm^3/g
$\bar{v}^0_{\mathrm{sp,hya}}$	limiting partial specific volume	cm^3/g
β	compressibility	10^{-10} Pa^{-1}
$U12$	velocity difference	m/s
$N12$	attenuation difference	1/m

11 LIST OF PUBLICATIONS AND ACTIVITIES

Impacted publications:

KARGEROVÁ, A., M. PEKAŘ. Densitometry and ultrasound velocimetry of hyaluronan solutions in water and in sodium chloride solution. *Carbohydrate Polymers*. 2014.

KARGEROVÁ, A.; PEKAŘ, M. High resolution ultrasonic spectroscopy for measuring of interactions of hyaluronan with surfactants contribution. hyaluronan with surfactants contribution. *Chemistry is life*. 2012. pp. 316-321. ISBN: 978-80-214-4545- 8.

KLUČÁKOVÁ, M.; BACHRATÁ, R.; KARGEROVÁ, A. Comparison of complexation properties of humic acids and simple organic ligands. In *X. Workshop of Physical Chemists and Electrochemists 2010.* pp.124-125. ISBN: 978-80-7375-396- 2.

KLUČÁKOVÁ, M.; KARGEROVÁ, A.; NOVÁČKOVÁ, K. *Conformational Changes in Aqueous Solutions of Humic Acids. Chemical Letters* Brno: Czech Chemical Society, 2011, pp. 896-897.

KLUČÁKOVÁ, M.; KARGEROVÁ, A.; NOVÁČKOVÁ, K. Conformational changes in humic acids in aqueous solutions. *Chemical Papers*. 2012, issue 66, vol. 9, pp. 875-880. ISSN: 0366- 6352.

Given speeches:

KARGEROVÁ, A.; PEKAŘ, M. *Interaction of hyaluronan and CTAB studied by high resolution ultrasonic spectroscopy*. 9th International Conference on Hyaluronan. Oklahoma City, Oklahoma, 2013.

KARGEROVÁ, A.; PEKAŘ, M. *High resolution ultrasonic spectroscopy for measuring of interactions of hyaluronan with surfactants contribution. hyaluronan with surfactants contribution*. In Student conference Chemistry is life, 2012.

KARGEROVÁ, A.; PEKAŘ, M. *Ultrasonic spectroscopy of systems hyaluronan surfactant*. SIS Conference 2012. Edmonton.

Conference contributions:

KARGEROVÁ, A.; PEKAŘ, M. Interaction of hyaluronan and CTAB studied by high resolution ultrasonic spectroscopy. 9th International Conference on Hyaluronan. Oklahoma City, Oklahoma, USA: University of Oklahoma Health Sciences Center (OUHSC), 2013, pp. 113-113.

KARGEROVÁ, A.; PEKAŘ, M. High resolution ultrasonic spectroscopy for measuring of interactions of hyaluronan with surfactants contribution. hyaluronan with surfactants contribution. In Student conference Chemistry is life, Collection of abstracts. 2012. pp. 316-321. ISBN: 978-80-214-4545- 8.

KARGEROVÁ, A.; PEKAŘ, M. Ultrasonic spectroscopy of systems hyaluronan surfactant. SIS Conference 2012. Edmonton: SIS 2012, 2012. pp. 87-87.

KARGEROVÁ, A.; PEKAŘ, M.; BUCKIN, V. *Interaction between hyaluronan and CTAB.* 13th European Student Colloid Conference. Sweden, Falkenberg: *Chalmers Reproservice*, 2011. pp. 59-59.

KARGEROVÁ, A.; PEKAŘ, M. *Densitometry of hyaluronan and hyaluronan with CTAB.* Chemické listy. Brno, Czech Republic: *Chemical Letters*, 2011. pp. 896-896.

12 SUPPLEMENTARY INFORMATION

Table ST1 pH value of concentration range of solution hyaluronan with CTAB and solution of 0.15 M NaCl with CTAB measured with pH meter S220.

c_{CTAB}	pH hya n water		pH hya in 0.15M NaCl	
mmol/l	90-130 kDa	1500-2000 kDa	90-130 kDa	1500-2000 kDa
0.000	5.82	5.80	5.51	5.75
0.005	5.76	5.79	5.58	5.83
0.010	5.69	5.74	5.59	5.84
0.015	5.65	5.73	5.58	5.83
0.020	5.64	5.72	5.57	5.82
0.025	5.69	5.74	5.57	5.81
0.030	5.66	5.73	5.57	5.80
0.034	5.63	5.72	5.57	5.79
0.039	5.62	5.74	5.56	5.80
0.044	5.61	5.74	5.55	5.79
0.049	5.61	5.74	5.56	5.79
0.068	5.61	5.70	5.55	5.79
0.086	5.62	5.71	5.56	5.80
0.104	5.61	5.72	5.55	5.79

Table ST2 pH value of concentration range of solution hyaluronan with CTAB and solution of water or 0.15 M NaCl with CTAB measured with pH meter S220.

c_{CTAB}	water	M_{w} hya n water		0.15M NaCl	M_{w} hyain 0.15M NaCl	
mmol/l		kDa			kDa	
		90-130	1500-2000		90-130	1500-2000
0.0000	6.43	6.33	6.50	5.86	5.72	5.95
1.3807	5.83	6.09	6.13*	5.94	5.62	5.90
1.5748	5.83	5.96	6.09	5.94	5.74	5.86
1.7682	5.82	5.88	6.07	5.95	5.79	5.86
1.9608	5.81	5.84	6.03	5.95	5.80	5.86
2.1526	5.80	5.78	5.95	5.97	5.80	5.86
2.3438	5.79	5.68	5.90	5.96	5.81	5.86
2.5341	5.77	5.61	5.82	5.97	5.81	5.86
2.7237	5.76	5.57	5.72	5.97	5.81	5.86
2.9126	5.75	5.54*	5.68	5.97	5.81	5.86
3.0068	5.74	5.54	5.61	5.97	5.82	5.86
3.1008	5.74	5.54	5.66	5.97	5.82	5.86
3.1946	5.74	5.54	5.65	5.97	5.82	5.86
3.2882	5.74	5.54	5.64	5.97	5.82	5.86
3.3816	5.73	5.54	5.65	5.97	5.82	5.86
3.4749	5.73	5.54	5.64	5.97	5.82	5.86
3.5680	5.73	5.54	5.64	5.98	5.82	5.86
3.6609	5.73	5.53	5.64	5.98	5.83	5.86
3.7536	5.73	5.53	5.64	5.98	5.83	5.86
3.8462	5.73	5.53	5.64	5.98	5.83	5.86
3.9385	5.73	5.53	5.64	5.98	5.83	5.86
4.0307	5.73	5.53	5.64	5.98	5.84	5.86
4.1227	5.73	5.53	5.64	5.98	5.84	5.86
4.2146	5.73	5.53	5.64	5.98	5.84	5.86

4.3062	5.73	5.53	5.64	5.98	5.84	5.86
4.3977	5.73	5.53	5.64	5.98	5.84	5.86
4.4890	5.73	5.53	5.64	5.98	5.85	5.86
4.5802	5.73	5.52	5.64	5.99	5.85	5.86
4.6711	5.73	5.52	5.65	5.99	5.85	5.86
4.7619	5.73	5.52	5.65	5.99	5.86	5.86
4.8525	5.73	5.52	5.65	5.99	5.86	5.86
4.9430	5.72	5.51	5.65	5.99	5.86	5.86
5.0332	5.72	5.51	5.65	5.99	5.86	5.86
5.1233	5.72	5.51	5.64	5.99	5.86	5.86
5.2133	5.72	5.51	5.65	5.99	5.86	5.86
5.3030	5.72	5.51	5.65	5.99	5.86	5.86
7.2590	5.72	5.50	5.64	5.99	5.86	5.86
9.1468	5.72	5.50	5.61	5.99	5.85	5.86
12.1515	5.72	5.49	5.60	5.99	5.85	5.85
16.7832	5.72	5.49	5.58	5.99	5.86	5.85

Table ST3 pH value of concentration range of solution hyaluronan with TTAB and solution of water or 0.15 M NaCl with TTAB measured with pH meter S220.

c_{TTAB}	water	$M_{w\,hya\ in\ water}$		0.15M NaCl	$M_{w\,hya\ in\ 0.15M\ NaCl}$	
mmol/l		kDa			kDa	
		90-130	1500-2000		90-130	1500-2000
0.0518	6.27	6.35	6.48	6.00	5.69	5.81
0.2488	5.74	6.34	6.58	5.90	5.66	5.84
0.4950	5.74	6.27	6.50	5.89	5.64	5.85
0.9804	5.72	6.22	6.40	5.89	5.62	5.83
1.4563	5.68	6.15	6.18	5.88	5.62	5.83
1.9231	5.69	6.09	6.09	5.90	5.62	5.82
2.1531	5.67	6.03	5.02	5.91	5.62	5.82
2.3810	5.69	6.00	5.93	5.91	5.62	5.82
2.6066	5.69	5.97	5.88	5.92	5.62	5.82
2.8302	5.69	5.93	5.80	5.92	5.62	5.82
3.0516	5.68	5.89	5.74	5.93	5.62	5.82
3.2710	5.67	5.85	5.70	5.94	5.62	5.82
3.4884	5.66	5.83	*5.72	5.94	5.62	5.82
3.7037	5.65	5.82	5.70	5.95	5.62	5.82
3.9171	5.62	5.80	5.69	5.96	5.62	5.82
4.1284	5.61	5.81	5.68	5.97	5.62	5.82
4.3379	5.60	5.82	5.67	5.97	5.62	5.82
4.5455	5.59	5.83	5.66	5.98	5.62	5.82
4.7511	5.59	5.85	5.66	5.98	5.62	5.82
4.9550	5.59	5.85	5.66	5.99	5.62	5.82
5.1570	5.59	5.88	5.66	5.99	5.62	5.82
5.3571	5.59	5.91	5.66	6.00	5.62	5.82
5.5556	5.58	5.91	5.66	6.00	5.62	5.82
5.7522	5.58	5.92	5.66	6.00	5.62	5.81
5.9471	5.58	5.94	5.66	6.00	5.63	5.81
6.1404	5.58	5.98	5.66	6.00	5.63	5.81
6.5217	5.58	5.96	5.66	6.00	5.63	5.81
6.8966	5.58	5.97	5.65	6.00	5.63	5.81
7.2650	5.58	5.97	5.65	6.00	5.63	5.81
7.6271	5.57	5.96	5.65	6.00	5.63	5.81
7.9832	5.57	5.96	5.65	6.00	5.64	5.82

8.3333	5.57	5.95	5.66	6.01	5.64	5.82
8.6777	5.57	5.95	5.66	6.01	5.64	5.82
9.0164	5.57	5.94	5.66	6.01	5.65	5.82
9.3496	5.57	5.95	5.66	6.01	5.65	5.82
12.5689	5.57	5.95	5.66	6.01	5.66	5.83
15.8960	5.57	5.92	5.67	6.01	5.66	5.83
17.3689	5.57	5.93	5.67	6.01	5.66	5.83
20.3698	5.57	5.92	5.67	6.01	5.66	5.84
25.6897	5.57	5.90	5.67	6.01	5.66	5.84

Table ST4 Density measurement solution of hyaluronan of molecular weight 70-90 kDa and 1500-2000 kDa in 0.15M NaBr with addition of 2mM CTAB measured with DMA 4500.

90-130 kDa				1500-2000 kDa		
c_{CTAB}	density		σ	c_{CTAB}	density	σ
mmol/l	g/cm^3		10^{-4}	mmol/l	g/cm^3	10^{-4}
0.00000	0.99771	±	2.3	0.00000	0.99769	2.4
0.00499	0.99776	±	2.4	0.00499	0.99782	1.7
0.00995	0.99776	±	2.3	0.00995	0.99775	2.4
0.01489	0.99779	±	2.5	0.01489	0.99779	2.6
0.01980	0.99781	±	2.5	0.01980	0.99788	1.6
0.02469	0.99797	±	0.8	0.02469	0.99789	2.1
0.02956	0.99796	±	0.4	0.02956	0.99788	2.3
0.03440	0.99798	±	0.5	0.03440	0.99791	2.5
0.03922	0.99802	±	0.5	0.03922	0.99794	1.9
0.04401	0.99804	±	0.4	0.04401	0.99798	2.1
0.04878	0.99810	±	0.3	0.04878	0.99803	2.0

Table ST5 Density of hyaluronan measured with DMA 4500 in different days.

$M_{w\,hya}$	c_{hya}	density g/cm^3						
kDa	%w/w	1st day	2nd day	3rd day	7th day	14th day	21th day	30th day
70-90	0.05	0.99756	0.99758	0.99757	0.99758	0.99757	0.99752	0.99753
	0.10	0.99776	0.99772	0.99776	0.99775	0.99775	0.99798	0.99792
	0.20	0.99779	0.99780	0.99780	0.99776	0.99775	0.99776	0.99776
	0.40	0.99907	0.99906	0.99907	0.99909	0.99907	0.99908	0.99914
	0.80	1.00069	1.00065	1.00064	1.00067	1.00068	1.00070	1.00074
	1.00	1.00165	1.00146	1.00150	1.00157	1.00153	1.00153	1.00127
	1.50	1.00356	1.00374	1.00372	1.00380	1.00371	1.00371	1.00367
1500-2000	0.05	0.99761	0.99755	0.99757	0.99759	0.99757	0.99760	0.99757
	0.10	0.99774	0.99781	0.99778	0.99782	0.99778	0.99777	0.99777
	0.20	0.99850	0.99857	0.99854	0.99855	0.99850	0.99853	0.99853
	0.40	0.99890	0.99896	0.99922	0.99905	0.99905	0.99904	0.99904
	0.80	1.00066	1.00077					
	1.00	1.00130	1.00146					
	1.50	1.00423	1.00404					

Table ST6 Density of concentration line of surfactant in hyaluronan measured with DMA 4500 in different days.

$M_{w\,hya}$	c_{CTAB}	density g/cm^3						
kDa	mmol/l	1st day	2nd day	3rd day	7th day	14th day	21th day	30th day
	0.000	0.99772	0.99772	0.99776	0.99775	0.99775	0.99798	0.99792
	0.005	0.99781	0.99779	0.99781	0.99780	0.99776	0.99789	0.99805
	0.010	0.99784	0.99785	0.99785	0.99783	0.99783	0.99791	0.99809
	0.015	0.99787	0.99788	0.99797	0.99785	0.99786	0.99793	0.99812
	0.020	0.99790	0.99785	0.99792	0.99789	0.99794	0.99799	0.99809
70-90	0.025	0.99791	0.99795	0.99794	0.99790	0.99795	0.99800	0.99812
	0.030	0.99793	0.99799	0.99797	0.99793	0.99799	0.99807	0.99813
	0.034	0.99798	0.99797	0.99799	0.99798	0.99801	0.99810	0.99811
	0.039	0.99800	0.99804	0.99805	0.99800	0.99805	0.99811	0.99818
	0.044	0.99803	0.99806	0.99803	0.99802	0.99807	0.99814	0.99819
	0.049	0.99806	0.99809	0.99801	0.99804	0.99811	0.99816	0.99822
	0.000	0.99780	0.99781	0.99778	0.99782	0.99778	0.99777	0.99777
	0.005	0.99787	0.99782	0.99784	0.99781	0.99779	0.99784	
	0.010	0.99785	0.99784	0.99779	0.99786	0.99799	0.98829	0.99785
	0.015	0.99786	0.99788	0.99793	0.99787	0.99799	0.99792	0.99780
	0.020	0.99785	0.99789	0.99798	0.99790	0.99800	0.99796	0.99794
1500-2000	0.025	0.99792	0.99793	0.99797	0.99793	0.99808	0.99800	0.99795
	0.030	0.99793	0.99794	0.99799	0.99797	0.99807	0.99805	0.99701
	0.034	0.99795	0.99797	0.99801	0.99799	0.99810	0.99807	
	0.039	0.99798	0.99801	0.99803	0.99800	0.99814	0.99813	0.99801
	0.044	0.99802	0.99802	0.99804	0.99803	0.99811	0.99816	0.99802
	0.049	0.99808	0.99805	0.99805	0.99805	0.99818	0.99817	0.99807

Table ST7 Density measurement of hyaluronan aqueous solution with NaN_3 at 25 °C measured with DMA 4500.

$M_{w\,hya}$	c_{hya}	σ	density	σ	$M_{w\,hya}$	c_{hya}	σ	density	σ
kDa	%w/w	10^{-3}	g/cm^3	10^{-4}	kDa	%w/w	10^{-3}	g/cm^3	10^{-4}
	2.0034 ±	5.71	1.00556 ±	1.0		1.5687 ±	0.72	1.00406 ±	4.8
	1.8035 ±	7.42	1.00493 ±	1.7		1.4115 ±	4.30	1.00325 ±	1.5
	1.6055 ±	3.33	1.00417 ±	0.0		1.2934 ±	4.23	1.00270 ±	0.6
	1.4098 ±	6.72	1.00335 ±	0.9		1.1966 ±	13.8	1.00231 ±	1.5
	1.2060 ±	13.7	1.00244 ±	0.0		1.1005 ±	3.51	1.00191 ±	0.6
	1.0577 ±	1.31	1.00187 ±	0.5		1.0636 ±	5.04	1.00176 ±	1.4
	0.8989 ±	1.39	1.00105 ±	0.4		0.8975 ±	15.7	1.00113 ±	1.7
	0.8015 ±	4.36	1.00067 ±	0.3		0.8031 ±	4.44	1.00071 ±	1.2
10-30	0.7026 ±	2.10	1.00023 ±	0.3	110-130	0.7060 ±	4.74	1.00030 ±	1.3
	0.6007 ±	3.56	0.99980 ±	0.6		0.6060 ±	2.06	0.99985 ±	0.7
	0.5023 ±	2.41	0.99938 ±	0.3		0.5057 ±	0.13	0.99945 ±	0.7
	0.3971 ±	1.07	0.99894 ±	0.5		0.4006 ±	1.20	0.99900 ±	0.5
	0.3002 ±	0.19	0.99853 ±	0.2		0.3004 ±	0.06	0.99860 ±	0.8
	0.2006 ±	0.56	0.99811 ±	0.1		0.2017 ±	4.89	0.99819 ±	0.7
	0.1042 ±	1.46	0.99767 ±	0.3		0.1042 ±	0.64	0.99782 ±	1.3
	0.0719 ±	1.07	0.99757 ±	0.3		0.0722 ±	0.24	0.99767 ±	0.8
	0.0514 ±	0.99	0.99748 ±	0.2		0.0511 ±	0.45	0.99756 ±	0.6

	0.0307	±	0.34	0.99741	±	0.5		0.0306	±	0.22	0.99747	± 0.5
	0.0102	±	0.14	0.99733	±	0.5		0.0102	±	0.14	0.99737	± 0.2
	0.0093	±	0.01	0.99733	±	0.4		0.0093	±	0.26	0.99738	± 0.5
	0.0071	±	0.09	0.99733	±	0.4		0.0071	±	0.05	0.99737	± 0.4
	0.0051	±	0.15	0.99732	±	0.2		0.0051	±	0.05	0.99736	± 0.4
	0.0031	±	0.08	0.99729	±	0.1		0.0031	±	0.05	0.99735	± 0.4
	0.0010	±	0.02	0.99726	±	0.0		0.0010	±	0.01	0.99733	± 0.3
	0.0000			0.99726	±	0.1		0.0000			0.99731	± 0.1
	1.0583	±	2.74	1.00171	±	0.5		0.5096	±	0.61	0.99931	± 1.08
	0.9077	±	3.72	1.00119	±	1.4		0.4005	±	0.38	0.99896	± 0.49
	0.7934	±	5.86	1.00070	±	1.5		0.2973	±	4.48	0.99853	± 0.57
	0.7042	±	1.04	1.00027	±	1.0		0.2014	±	0.66	0.99816	± 0.57
	0.5903	±	5.20	0.99983	±	0.1		0.1049	±	2.44	0.99772	± 0.07
	0.5036	±	1.14	0.99944	±	0.4		0.0903	±	2.21	0.99767	± 0.07
	0.3991	±	0.27	0.99901	±	0.4		0.0801	±	1.78	0.99762	± 0.05
	0.2994	±	3.33	0.99860	±	0.3		0.0708	±	1.74	0.99758	± 0.05
	0.2014	±	0.17	0.99816	±	0.5		0.0604	±	1.53	0.99754	± 0.09
	0.1042	±	0.97	0.99777	±	0.4		0.0526	±	1.97	0.99750	± 0.16
300-500	0.0716	±	0.35	0.99764	±	0.5	1500-2000	0.0405	±	1.51	0.99745	± 0.12
	0.0514	±	0.16	0.99753	±	0.5		0.0303	±	1.06	0.99741	± 0.12
	0.0307	±	0.01	0.99741	±	0.2		0.0204	±	0.70	0.99738	± 0.14
	0.0101	±	0.14	0.99734	±	0.4		0.0102	±	0.21	0.99734	± 0.07
	0.0093	±	0.12	0.99733	±	0.4		0.0091	±	0.33	0.99734	± 0.02
	0.0082	±	0.10	0.99733	±	0.4		0.0081	±	0.32	0.99734	± 0.07
	0.0071	±	0.15	0.99731	±	0.2		0.0071	±	0.23	0.99733	± 0.02
	0.0062	±	0.01	0.99731	±	0.7		0.0061	±	0.23	0.99733	± 0.01
	0.0051	±	0.13	0.99730	±	0.3		0.0051	±	0.18	0.99733	± 0.02
	0.0031	±	0.02	0.99729	±	0.4		0.0031	±	0.06	0.99732	± 0.01
	0.0011	±	0.01	0.99728	±	0.4		0.0011	±	0.01	0.99730	± 0.05
	0.0000			0.99727	±	0.4		0.0000			0.99731	± 0.07

Table ST8 Experimental data on density and calculated apparent and partial specific volumes of hyaluronan 10-30 kDa in water.

T	c_{hya}	σ	ρ_{sample}	σ	V_{app}	$\bar{V}_{sp,hya}$
° C	% w/w	10^{-3}	g/cm^3	10^{-4}	10^{-3} cm^3/g	10^{-3} cm^3/g
	1.9977 ± 6.9		1.00560 ± 0.6		578 ± 6	594 ± 3
	1.7977 ± 8.9		1.00464 ± 1.5		583 ± 12	593 ± 3
	1.5973 ± 5.3		1.00389 ± 2.7		577 ± 20	592 ± 3
	1.4005 ± 8.4		1.00300 ± 1.9		580 ± 18	592 ± 3
	1.1995 ± 7.4		1.00220 ± 2.0		576 ± 22	591 ± 3
25	1.0638 ± 9.2		1.00160 ± 1.7		577 ± 22	591 ± 3
	0.8025 ± 9.8		1.00058 ± 1.5		565 ± 28	590 ± 3
	0.5019 ± 5.3		0.99947 ± 0.5			589 ± 3
	0.2997 ± 2.9		0.99845 ± 1.8			588 ± 3
	0.1027 ± 0.6		0.99766 ± 1.8			587 ± 3
	0.0507 ± 0.3		0.99744 ± 2.0			587 ± 3
	0.0101 ± 0.1		0.99726 ± 2.0			587 ± 3

	0.0010 ± 0.01	0.99724 ± 2.2		587 ± 3
	0.0000	0.99708 ± 0.3		
30	1.9977 ± 6.9	1.00416 ± 0.5	580 ± 6	596 ± 3
	1.7977 ± 8.9	1.00321 ± 1.5	585 ± 12	595 ± 3
	1.5973 ± 5.3	1.00246 ± 2.7	579 ± 20	595 ± 3
	1.4005 ± 8.4	1.00157 ± 1.9	583 ± 18	594 ± 3
	1.1995 ± 7.4	1.00078 ± 2.0	578 ± 22	593 ± 3
	1.0638 ± 9.2	1.00019 ± 1.6	580 ± 22	593 ± 3
	0.8025 ± 9.8	0.99917 ± 1.5	567 ± 27	592 ± 3
	0.5019 ± 5.3	0.99807 ± 0.5		591 ± 3
	0.2997 ± 2.9	0.99705 ± 1.8		590 ± 3
	0.1027 ± 0.6	0.99627 ± 1.8		590 ± 3
	0.0507 ± 0.3	0.99605 ± 1.9		590 ± 3
	0.0101 ± 0.1	0.99587 ± 2.0		589 ± 3
	0.0010 ± 0.01	0.99585 ± 2.1		589 ± 3
	0.0000	0.99569 ± 0.3		
35	1.9977 ± 6.9	1.00250 ± 0.5	582 ± 5	598 ± 3
	1.7977 ± 8.9	1.00156 ± 1.5	588 ± 12	598 ± 3
	1.5973 ± 5.3	1.00081 ± 2.6	582 ± 20	597 ± 3
	1.4005 ± 8.4	0.99993 ± 1.9	585 ± 18	596 ± 3
	1.1995 ± 7.4	0.99915 ± 2.0	580 ± 22	596 ± 3
	1.0638 ± 9.2	0.99855 ± 1.6	582 ± 22	595 ± 3
	0.8025 ± 9.8	0.99754 ± 1.5	570 ± 27	594 ± 3
	0.5019 ± 5.3	0.99644 ± 0.5		593 ± 3
	0.2997 ± 2.9	0.99543 ± 1.8		593 ± 3
	0.1027 ± 0.6	0.99465 ± 1.8		592 ± 3
	0.0507 ± 0.3	0.99443 ± 1.9		592 ± 3
	0.0101 ± 0.1	0.99425 ± 2.0		592 ± 3
	0.0010 ± 0.01	0.99423 ± 2.1		592 ± 3
	0.0000	0.99407 ± 0.3		
40	1.9977 ± 6.9	1.00065 ± 0.5	584 ± 5	600 ± 3
	1.7977 ± 8.9	0.99971 ± 1.4	590 ± 12	600 ± 3
	1.5973 ± 5.3	0.99897 ± 2.6	584 ± 19	599 ± 3
	1.4005 ± 8.4	0.99809 ± 1.9	587 ± 18	598 ± 3
	1.1995 ± 7.4	0.99731 ± 2.0	582 ± 21	598 ± 3
	1.0638 ± 9.2	0.99671 ± 1.6	584 ± 21	597 ± 3
	0.8025 ± 9.8	0.99571 ± 1.4	572 ± 27	596 ± 3
	0.5019 ± 5.3	0.99461 ± 0.5		595 ± 3
	0.2997 ± 2.9	0.99361 ± 1.7		595 ± 3
	0.1027 ± 0.6	0.99282 ± 1.8		594 ± 3
	0.0507 ± 0.3	0.99261 ± 1.9		594 ± 3
	0.0101 ± 0.1	0.99243 ± 2.0		594 ± 3
	0.0010 ± 0.01	0.99241 ± 2.1		594 ± 3

	0.0000	0.99225 ± 0.3		
45	1.9977 ± 6.9	0.99861 ± 0.5	586 ± 5	602 ± 3
	1.7977 ± 8.9	0.99768 ± 1.4	591 ± 12	601 ± 3
	1.5973 ± 5.3	0.99694 ± 2.6	585 ± 20	601 ± 3
	1.4005 ± 8.4	0.99606 ± 1.8	589 ± 17	600 ± 3
	1.1995 ± 7.4	0.99528 ± 1.9	584 ± 21	599 ± 3
	1.0638 ± 9.2	0.99469 ± 1.6	586 ± 21	599 ± 3
	0.8025 ± 9.8	0.99369 ± 1.4	573 ± 27	598 ± 3
	0.5019 ± 5.3	0.99260 ± 0.5		597 ± 3
	0.2997 ± 2.9	0.99160 ± 1.7		596 ± 3
	0.1027 ± 0.6	0.99082 ± 1.8		596 ± 3
	0.0507 ± 0.3	0.99060 ± 1.9		596 ± 3
	0.0101 ± 0.1	0.99042 ± 2.0		596 ± 3
	0.0010 ± 0.01	0.99041 ± 2.1		595 ± 3
	0.0000	0.99024 ± 0.3		
50	1.9977 ± 6.9	0.99641 ± 0.6	588 ± 5	604 ± 3
	1.7977 ± 8.9	0.99547 ± 1.4	593 ± 11	603 ± 3
	1.5973 ± 5.3	0.99474 ± 2.6	587 ± 19	603 ± 3
	1.4005 ± 8.4	0.99386 ± 1.7	591 ± 16	602 ± 3
	1.1995 ± 7.4	0.99309 ± 1.9		601 ± 3
	1.0638 ± 9.2	0.99249 ± 1.6		601 ± 3
	0.8025 ± 9.8	0.99150 ± 1.4		600 ± 3
	0.5019 ± 5.3	0.99041 ± 0.5		599 ± 3
	0.2997 ± 2.9	0.98941 ± 1.7		598 ± 3
	0.1027 ± 0.6	0.98863 ± 1.8		598 ± 3
	0.0507 ± 0.3	0.98842 ± 1.9		597 ± 3
	0.0101 ± 0.1	0.98824 ± 2.0		597 ± 3
	0.0010 ± 0.01	0.98822 ± 2.1		597 ± 3
	0.0000	0.98806 ± 0.2		

Table ST9 Experimental data on density and calculated apparent and partial specific volumes of hyaluronan 90-130 kDa in water.

T	c_{hya}	σ	ρ_{sample}	σ	V_{app}	$\bar{V}_{sp,hya}$
° C	% w/w	10^{-3}	g/cm^3	10^{-4}	10^{-3} cm^3/g	10^{-3} cm^3/g
25	1.5331 ± 1.1	1.00332 ± 2.0	601 ± 25	592 ± 3
	1.3948 ± 4.6	1.00305 ± 2.5	581 ± 32	592 ± 4
	1.3150 ± 0.6	1.00266 ± 2.5	584 ± 33	591 ± 3
	1.2005 ± 6.2	1.00214 ± 3.1	587 ± 43	591 ± 3
	1.1068 ± 14	1.00170 ± 2.9		591 ± 4
	1.0644 ± 16	1.00151 ± 2.4	593 ± 45	591 ± 3
	0.8010 ± 15	1.00070 ± 1.4	577 ± 49	590 ± 3
	0.5007 ± 8.8	0.99942 ± 0.5	585 ± 54	589 ± 3
	0.3033 ± 4.3	0.99840 ± 2.1		588 ± 3

	0.1059 ± 4.7	0.99765 ± 1.8		587 ± 4
	0.0518 ± 2.7	0.99740 ± 1.6		587 ± 3
	0.0107 ± 0.8	0.99719 ± 1.2		587 ± 3
	0.0010 ± 0.04	0.99719 ± 1.6		587 ± 3
	0.0000	0.99716 ± 1.8		
30	1.5331 ± 1.1	1.00190 ± 2.0	603 ± 28	595 ± 3
	1.3948 ± 4.6	1.00163 ± 2.6	583 ± 39	594 ± 3
	1.3150 ± 0.6	1.00124 ± 2.4	586 ± 36	594 ± 3
	1.2005 ± 6.2	1.00072 ± 3.1	590 ± 45	593 ± 3
	1.1068 ± 14	1.00025 ± 2.8		593 ± 3
	1.0644 ± 16	1.00010 ± 2.4	595 ± 44	593 ± 3
	0.8010 ± 15	0.99929 ± 1.4	579 ± 47	592 ± 3
	0.5007 ± 8.8	0.99801 ± 0.5	587 ± 52	591 ± 3
	0.3033 ± 4.3	0.99700 ± 2.1		590 ± 3
	0.1059 ± 4.7	0.99626 ± 1.8		590 ± 3
	0.0518 ± 2.7	0.99601 ± 1.6		590 ± 3
	0.0107 ± 0.8	0.99582 ± 1.4		589 ± 3
	0.0010 ± 0.04	0.99580 ± 1.6		589 ± 3
	0.0000	0.99576 ± 1.8		
35	1.5331 ± 1.1	1.00223 ± 3.8	605 ± 27	596 ± 3
	1.3948 ± 4.6	1.00156 ± 1.5	585 ± 38	596 ± 3
	1.3150 ± 0.6	1.00081 ± 2.6	589 ± 36	596 ± 3
	1.2005 ± 6.2	0.99993 ± 1.9	592 ± 45	595 ± 3
	1.1068 ± 14	0.99915 ± 2.0		595 ± 3
	1.0644 ± 16	0.99855 ± 1.6	597 ± 44	595 ± 3
	0.8010 ± 15	0.99766 ± 1.4	582 ± 47	594 ± 3
	0.5007 ± 8.8	0.99638 ± 0.5	590 ± 53	593 ± 3
	0.3033 ± 4.3	0.99543 ± 1.8		593 ± 3
	0.1059 ± 4.7	0.99465 ± 1.8		592 ± 3
	0.0518 ± 2.7	0.99439 ± 1.5		592 ± 3
	0.0107 ± 0.8	0.99423 ± 1.7		592 ± 3
	0.0010 ± 0.04	0.99418 ± 1.6		592 ± 3
	0.0000	0.99415 ± 1.8		
40	1.5331 ± 1.1	1.00038 ± 3.7	607 ± 27	598 ± 3
	1.3948 ± 4.6	0.99971 ± 1.4	585 ± 41	598 ± 3
	1.3150 ± 0.6	0.99897 ± 2.6	591 ± 35	598 ± 3
	1.2005 ± 6.2	0.99809 ± 1.9	594 ± 44	597 ± 3
	1.1068 ± 14	0.99731 ± 2.0		597 ± 3
	1.0644 ± 16	0.99671 ± 1.6	599 ± 43	597 ± 3
	0.8010 ± 15	0.99582 ± 1.4	584 ± 46	596 ± 3
	0.5007 ± 8.8	0.99456 ± 0.7	591 ± 55	595 ± 3
	0.3033 ± 4.3	0.99361 ± 1.7		595 ± 3
	0.1059 ± 4.7	0.99282 ± 1.8		594 ± 3

	0.0518	± 2.7	0.99257	± 1.5		594 ± 3
	0.0107	± 0.8	0.99241	± 1.7		594 ± 3
	0.0010	± 0.04	0.99236	± 1.5		594 ± 3
	0.0000		0.99233	± 1.8		
45	1.5331	± 1.1	0.99835	± 3.7	754 ± 26	600 ± 3
	1.3948	± 4.6	0.99768	± 1.4	745 ± 38	600 ± 3
	1.3150	± 0.6	0.99694	± 2.6	761 ± 34	600 ± 3
	1.2005	± 6.2	0.99606	± 1.8	780 ± 43	599 ± 3
	1.1068	± 14	0.99528	± 1.9		599 ± 3
	1.0644	± 16	0.99469	± 1.6	810 ± 40	599 ± 3
	0.8010	± 15	0.99380	± 1.4	863 ± 42	598 ± 3
	0.5007	± 8.8	0.99254	± 0.8	1041 ± 52	597 ± 3
	0.3033	± 4.3	0.99160	± 1.7		597 ± 3
	0.1059	± 4.7	0.99082	± 1.8		596 ± 3
	0.0518	± 2.7	0.99058	± 1.7		596 ± 3
	0.0107	± 0.8	0.99040	± 1.6		596 ± 3
	0.0010	± 0.04	0.99036	± 1.5		595 ± 3
	0.0000		0.99032	± 1.7		
50	1.5331	± 1.1	0.99614	± 3.8	611 ± 27	602 ± 3
	1.3948	± 4.6	0.99547	± 1.4	588 ± 41	602 ± 3
	1.3150	± 0.6	0.99474	± 2.6	594 ± 35	601 ± 3
	1.2005	± 6.2	0.99386	± 1.7	597 ± 44	601 ± 3
	1.1068	± 14	0.99309	± 1.9		601 ± 3
	1.0644	± 16	0.99249	± 1.6	602 ± 43	601 ± 3
	0.8010	± 15	0.99161	± 1.4	587 ± 46	600 ± 3
	0.5007	± 8.8	0.99032	± 1.2	598 ± 66	599 ± 3
	0.3033	± 4.3	0.98941	± 1.7		598 ± 3
	0.1059	± 4.7	0.98863	± 1.8		598 ± 3
	0.0518	± 2.7	0.98840	± 1.7		597 ± 3
	0.0107	± 0.8	0.98822	± 1.6		597 ± 3
	0.0010	± 0.04	0.98817	± 1.5		597 ± 3
	0.0000		0.98814	± 1.7		

Table ST10 Experimental data on density and calculated apparent and partial specific volumes of hyaluronan 300-500 kDa in water.

T	c_{hya}	σ	ρ_{sample}	σ	V_{app}	$\bar{V}_{sp,hya}$
° C	% w/w	10^{-3}	g/cm^3	10^{-4}	10^{-3} cm^3/g	10^{-3} cm^3/g
25	1.0340	± 21	1.00135	± 1.3	585 ± 24	590 ± 4
	0.9039	± 12	1.00103	± 1.1	560 ± 21	590 ± 3
	0.8020	± 6.7	1.00044	± 0.8	577 ± 17	590 ± 3
	0.7068	± 5.6	1.00019	± 2.0	555 ± 35	589 ± 3
	0.5089	± 4.5	0.99931	± 2.3	555 ± 55	589 ± 3
	0.3032	± 3.9	0.99844	± 2.3		588 ± 3

	0.1059 ± 3.7	0.99762 ± 1.7		587 ± 3
	0.0540 ± 5.4	0.99739 ± 2.3		587 ± 4
	0.0104 ± 0.4	0.99725 ± 2.0		587 ± 3
	0.0011 ± 0.04	0.99719 ± 1.7		587 ± 3
	0.0000	0.99704 ± 0.3		
	1.0340 ± 21	0.99993 ± 1.3	588 ± 23	593 ± 3
	0.9039 ± 12	0.99961 ± 1.1	563 ± 21	592 ± 3
	0.8020 ± 6.7	0.99903 ± 0.8	579 ± 17	592 ± 3
	0.7068 ± 5.6	0.99878 ± 2.0	557 ± 35	592 ± 3
	0.5089 ± 4.5	0.99790 ± 2.2	558 ± 52	591 ± 3
30	0.3032 ± 3.9	0.99704 ± 2.3		590 ± 3
	0.1059 ± 3.7	0.99622 ± 1.6		590 ± 3
	0.0540 ± 5.4	0.99598 ± 2.5		590 ± 3
	0.0104 ± 0.4	0.99585 ± 2.0		589 ± 3
	0.0011 ± 0.04	0.99577 ± 1.6		589 ± 3
	0.0000	0.99564 ± 0.3		
	1.0340 ± 21	0.99830 ± 1.2	590 ± 23	595 ± 3
	0.9039 ± 12	0.99798 ± 1.0	565 ± 20	595 ± 3
	0.8020 ± 6.7	0.99740 ± 0.8	582 ± 17	594 ± 3
	0.7068 ± 5.6	0.99715 ± 1.9	560 ± 35	594 ± 3
	0.5089 ± 4.5	0.99626 ± 1.9	564 ± 47	593 ± 3
35	0.3032 ± 3.9	0.99542 ± 2.3		593 ± 3
	0.1059 ± 3.7	0.99459 ± 1.5		592 ± 3
	0.0540 ± 5.4	0.99436 ± 2.4		592 ± 3
	0.0104 ± 0.4	0.99424 ± 1.9		592 ± 3
	0.0011 ± 0.04	0.99403 ± 3.1		592 ± 3
	0.0000	0.99403 ± 0.3		
	1.0340 ± 21	0.99646 ± 1.2	592 ± 23	597 ± 3
	0.9039 ± 12	0.99615 ± 1.0	568 ± 20	597 ± 3
	0.8020 ± 6.7	0.99557 ± 0.8	584 ± 16	596 ± 3
	0.7068 ± 5.6	0.99532 ± 1.9	562 ± 34	596 ± 3
	0.5089 ± 4.5	0.99446 ± 2.3	561 ± 54	595 ± 3
40	0.3032 ± 3.9	0.99360 ± 2.2		595 ± 3
	0.1059 ± 3.7	0.99273 ± 1.4		594 ± 3
	0.0540 ± 5.4	0.99240 ± 2.6		594 ± 3
	0.0104 ± 0.4	0.99242 ± 1.9		594 ± 3
	0.0011 ± 0.04	0.99234 ± 1.9		594 ± 3
	0.0000	0.99221 ± 0.2		
	1.0340 ± 21	0.99444 ± 1.2	594 ± 22	599 ± 3
	0.9039 ± 12	0.99413 ± 1.0	569 ± 20	598 ± 3
	0.8020 ± 6.7	0.99355 ± 0.8	586 ± 16	598 ± 3
45	0.7068 ± 5.6	0.99331 ± 1.9	564 ± 33	598 ± 3
	0.5089 ± 4.5	0.99244 ± 2.3	563 ± 53	597 ± 3
	0.3032 ± 3.9	0.99159 ± 2.2		597 ± 3

	0.1059 ± 3.7	0.99066 ± 2.0		596 ± 3
	0.0540 ± 5.4	0.99046 ± 2.3		595 ± 3
	0.0104 ± 0.4	0.99041 ± 1.9		595 ± 3
	0.0011 ± 0.04	0.99033 ± 1.9		595 ± 3
	0.0000	0.99021 ± 0.2		
	1.0340 ± 21	0.99219 ± 0.8	543 ± 18	601 ± 3
	0.9039 ± 12	0.99192 ± 1.2	506 ± 20	600 ± 3
	0.8020 ± 6.7	0.99133 ± 0.4	516 ± 9	600 ± 3
	0.7068 ± 5.6	0.99112 ± 1.9	480 ± 31	600 ± 3
	0.5089 ± 4.5	0.99026 ± 2.3	443 ± 52	599 ± 3
50	0.3032 ± 3.9	0.98941 ± 2.2		598 ± 3
	0.1059 ± 3.7	0.98828 ± 2.2		598 ± 3
	0.0540 ± 5.4	0.98823 ± 1.9		597 ± 3
	0.0104 ± 0.4	0.98815 ± 1.9		597 ± 3
	0.0011 ± 0.04	0.98743 ± 0.1		597 ± 3
	0.0000	0.98803 ± 0.2		

Table ST11 Experimental data on density and calculated apparent and partial specific volumes of hyaluronan 1500-1750 kDa in water.

T	c_{hya}	σ	ρ_{sample}	σ	V_{app}	$\overline{V}_{sp,hya}$
° C	% w/w	10^{-3}	g/cm^3	10^{-4}	10^{-3} cm^3/g	10^{-3} cm^3/g
	0.5106 ± 2.4	0.99903 ± 1.2	612 ± 25	589 ± 3
	0.3997 ± 2.3	0.99866 ± 1.4	597 ± 36	588 ± 3
	0.2978 ± 3.9	0.99836 ± 2.0	560 ± 73	588 ± 3
	0.1995 ± 1.0	0.99788 ± 1.5		588 ± 3
	0.1076 ± 2.0	0.99753 ± 2.1		587 ± 3
25	0.0924 ± 1.3	0.99748 ± 1.6		587 ± 3
	0.0723 ± 1.2	0.99732 ± 0.3		587 ± 3
	0.0535 ± 0.9	0.99732 ± 1.7		587 ± 3
	0.0103 ± 0.2	0.99716 ± 1.7		587 ± 3
	0.0010 ± 0.03	0.99713 ± 1.6		587 ± 3
	0.0000	0.99705 ± 0.01		
	0.5106 ± 2.4	0.99763 ± 1.2	615 ± 25	591 ± 3
	0.3997 ± 2.3	0.99728 ± 1.2	595 ± 34	591 ± 3
	0.2978 ± 3.9	0.99696 ± 2.0	562 ± 73	590 ± 3
	0.1995 ± 1.0	0.99649 ± 1.5		590 ± 3
	0.1076 ± 2.0	0.99616 ± 1.8		590 ± 3
30	0.0924 ± 1.3	0.99609 ± 1.6		590 ± 3
	0.0723 ± 1.2	0.99593 ± 0.3		590 ± 3
	0.0535 ± 0.9	0.99592 ± 1.7		590 ± 3
	0.0103 ± 0.2	0.99577 ± 1.7		589 ± 3
	0.0010 ± 0.03	0.99574 ± 1.6		589 ± 3
	0.0000	0.99565 ± 0.01		

	0.5106 ± 2.4	0.99600 ± 1.2	618 ± 25	593 ± 3
	0.3997 ± 2.3	0.99566 ± 1.2	596 ± 33	593 ± 3
	0.2978 ± 3.9	0.99533 ± 2.0	566 ± 74	593 ± 3
	0.1995 ± 1.0	0.99486 ± 1.5		592 ± 3
	0.1076 ± 2.0	0.99454 ± 1.8		592 ± 3
35	0.0924 ± 1.3	0.99447 ± 1.5		592 ± 3
	0.0723 ± 1.2	0.99431 ± 0.3		592 ± 3
	0.0535 ± 0.9	0.99431 ± 1.6		592 ± 3
	0.0103 ± 0.2	0.99415 ± 1.7		592 ± 3
	0.0010 ± 0.03	0.99412 ± 1.6		592 ± 3
	0.0000	0.99404 ± 0.01		
	0.5106 ± 2.4	0.99417 ± 1.2	621 ± 25	595 ± 3
	0.3997 ± 2.3	0.99384 ± 1.1	597 ± 32	595 ± 3
	0.2978 ± 3.9	0.99350 ± 2.1	571 ± 78	595 ± 3
	0.1995 ± 1.0	0.99303 ± 1.6		594 ± 3
	0.1076 ± 2.0	0.99273 ± 1.7		594 ± 3
40	0.0924 ± 1.3	0.99265 ± 1.5		594 ± 3
	0.0723 ± 1.2	0.99250 ± 0.3		594 ± 3
	0.0535 ± 0.9	0.99249 ± 1.6		594 ± 3
	0.0103 ± 0.2	0.99234 ± 1.7		594 ± 3
	0.0010 ± 0.03	0.99230 ± 1.6		594 ± 3
	0.0000	0.99222 ± 0.02		
	0.5106 ± 2.4	0.99214 ± 1.2	627 ± 26	597 ± 3
	0.3997 ± 2.3	0.99183 ± 1.1	598 ± 31	597 ± 3
	0.2978 ± 3.9	0.99148 ± 2.3	578 ± 84	597 ± 3
	0.1995 ± 1.0	0.99100 ± 1.9		596 ± 3
	0.1076 ± 2.0	0.99072 ± 1.7		596 ± 3
45	0.0924 ± 1.3	0.99065 ± 1.5		596 ± 3
	0.0723 ± 1.2	0.99049 ± 0.3		596 ± 3
	0.0535 ± 0.9	0.99048 ± 1.6		595 ± 3
	0.0103 ± 0.2	0.99033 ± 1.6		595 ± 3
	0.0010 ± 0.03	0.99030 ± 1.6		595 ± 3
	0.0000	0.99021 ± 0.02		
	0.5106 ± 2.4	0.98992 ± 1.5	652 ± 33	599 ± 3
	0.3997 ± 2.3	0.98965 ± 1.1	621 ± 31	599 ± 3
	0.2978 ± 3.9	0.98926 ± 2.7	618 ± 97	598 ± 3
	0.1995 ± 1.0	0.98878 ± 2.6		598 ± 3
	0.1076 ± 2.0	0.98853 ± 1.7		598 ± 3
50	0.0924 ± 1.3	0.98847 ± 1.5		598 ± 3
	0.0723 ± 1.2	0.98831 ± 0.3		598 ± 3
	0.0535 ± 0.9	0.98830 ± 1.6		597 ± 3
	0.0103 ± 0.2	0.98815 ± 1.6		597 ± 3
	0.0010 ± 0.03	0.98812 ± 1.6		597 ± 3
	0.0000	0.98803 ± 0.01		

Table ST12 Experimental data on density and calculated apparent and partial specific volumes of hyaluronan 10-30 kDa in 0.15 M NaCl.

T	c_{hya}	σ	ρ_{sample}	σ	V_{app}	$\bar{V}_{sp,hya}$
° C	% w/w	10^{-3}	g/cm^3	10^{-4}	10^{-3} cm^3/g	10^{-3} cm^3/g
25	2.0109	± 5.9	1.01148	± 0.7	591 ± 5	593 ± 3
	1.8010	± 1.0	1.01108	± 1.0	566 ± 6	592 ± 3
	1.6073	± 1.8	1.01004	± 0.9	577 ± 7	591 ± 3
	1.4112	± 3.9	1.00925	± 0.1	574 ± 3	591 ± 3
	1.2106	± 0.9	1.00830	± 0.7	581 ± 7	590 ± 3
	1.0591	± 2.3	1.00758	± 0.1	588 ± 3	589 ± 3
	0.7966	± 6.9	1.00664	± 0.3	570 ± 9	589 ± 3
	0.5024	± 1.7	1.00542	± 0.5	561 ± 14	588 ± 3
	0.2991	± 2.1	1.00456	± 0.4	550 ± 19	587 ± 3
	0.1038	± 1.4	1.00372	± 0.2		586 ± 3
	0.0509	± 0.5	1.00354	± 0.1		586 ± 3
	0.0102	± 0.1	1.00330	± 0.1		586 ± 3
	0.0010	± 0.1	1.00324	± 0.1		586 ± 3
	0.0000		1.00321	± 0.1		
30	2.0109	± 5.9	1.00999	± 0.6	594 ± 5	595 ± 3
	1.8010	± 1.0	1.00959	± 0.9	568 ± 6	594 ± 3
	1.6073	± 1.8	1.00858	± 0.3	578 ± 3	594 ± 3
	1.4112	± 3.9	1.00776	± 0.1	577 ± 3	593 ± 3
	1.2106	± 0.9	1.00682	± 0.7	584 ± 7	592 ± 3
	1.0591	± 2.3	1.00611	± 0.1	590 ± 2	592 ± 3
	0.7966	± 6.9	1.00517	± 0.3	573 ± 9	591 ± 3
	0.5024	± 1.7	1.00395	± 0.5	564 ± 14	590 ± 3
	0.2991	± 2.1	1.00310	± 0.4	552 ± 19	589 ± 3
	0.1038	± 1.4	1.00226	± 0.2		589 ± 3
	0.0509	± 0.5	1.00208	± 0.1		588 ± 3
	0.0102	± 0.1	1.00184	± 0.1		588 ± 3
	0.0010	± 0.1	1.00178	± 0.2		588 ± 3
	0.0000		1.00176	± 0.1		
35	2.0109	± 5.9	1.00828	± 0.7	596 ± 5	597 ± 3
	1.8010	± 1.0	1.00789	± 0.9	570 ± 6	596 ± 3
	1.6073	± 1.8	1.00688	± 0.3	580 ± 3	596 ± 3
	1.4112	± 3.9	1.00607	± 0.1	579 ± 3	595 ± 3
	1.2106	± 0.9	1.00513	± 0.7	586 ± 7	595 ± 3
	1.0591	± 2.3	1.00442	± 0.1	593 ± 2	594 ± 3
	0.7966	± 6.9	1.00349	± 0.3	575 ± 9	593 ± 3
	0.5024	± 1.7	1.00227	± 0.5	566 ± 14	592 ± 3
	0.2991	± 2.1	1.00143	± 0.4	554 ± 19	591 ± 3
	0.1038	± 1.4	1.00059	± 0.1		591 ± 3
	0.0509	± 0.5	1.00042	± 0.1		591 ± 3
	0.0102	± 0.1	1.00018	± 0.1		591 ± 3

	0.0010 ± 0.1	1.00012 ± 0.1		591 ± 3
	0.0000	1.00009 ± 0.1		
40	2.0109 ± 5.9	1.00639 ± 0.7	598 ± 5	599 ± 3
	1.8010 ± 1.0	1.00600 ± 0.9	572 ± 6	598 ± 3
	1.6073 ± 1.8	1.00500 ± 0.4	582 ± 3	598 ± 3
	1.4112 ± 3.9	1.00419 ± 0.1	581 ± 3	597 ± 3
	1.2106 ± 0.9	1.00325 ± 0.7	588 ± 7	596 ± 3
	1.0591 ± 2.3	1.00255 ± 0.1	595 ± 2	596 ± 3
	0.7966 ± 6.9	1.00162 ± 0.3	577 ± 9	595 ± 3
	0.5024 ± 1.7	1.00041 ± 0.5	568 ± 15	594 ± 3
	0.2991 ± 2.1	0.99956 ± 0.4	556 ± 19	593 ± 3
	0.1038 ± 1.4	0.99873 ± 0.2		593 ± 3
	0.0509 ± 0.5	0.99855 ± 0.1		593 ± 3
	0.0102 ± 0.1	0.99832 ± 0.1		593 ± 3
	0.0010 ± 0.1	0.99826 ± 0.1		592 ± 3
	0.0000	0.99823 ± 0.1		
45	2.0109 ± 5.9	1.00432 ± 0.7	622 ± 49	601 ± 3
	1.8010 ± 1.0	1.00393 ± 0.9	599 ± 54	600 ± 3
	1.6073 ± 1.8	1.00293 ± 0.4	612 ± 58	600 ± 3
	1.4112 ± 3.9	1.00212 ± 0.1	614 ± 65	599 ± 3
	1.2106 ± 0.9	1.00119 ± 0.7		598 ± 3
	1.0591 ± 2.3	1.00049 ± 0.1		598 ± 3
	0.7966 ± 6.9	0.99957 ± 0.3		597 ± 3
	0.5024 ± 1.7	0.99836 ± 0.5		596 ± 3
	0.2991 ± 2.1	0.99751 ± 0.4		595 ± 3
	0.1038 ± 1.4	0.99669 ± 0.1		595 ± 3
	0.0509 ± 0.5	0.99651 ± 0.1		595 ± 3
	0.0102 ± 0.1	0.99628 ± 0.1		594 ± 3
	0.0010 ± 0.1	0.99622 ± 0.1		594 ± 3
	0.0000	0.99664 ± 0.9		
50	2.0109 ± 5.9	1.00208 ± 0.7	602 ± 97	603 ± 3
	1.8010 ± 1.0	1.00170 ± 0.9	576 ± 108	602 ± 3
	1.6073 ± 1.8	1.00070 ± 0.4	585 ± 118	601 ± 3
	1.4112 ± 3.9	0.99989 ± 0.1	584 ± 134	601 ± 3
	1.2106 ± 0.9	0.99897 ± 0.7		600 ± 3
	1.0591 ± 2.3	0.99827 ± 0.1		600 ± 3
	0.7966 ± 6.9	0.99735 ± 0.3		599 ± 3
	0.5024 ± 1.7	0.99614 ± 0.5		598 ± 3
	0.2991 ± 2.1	0.99530 ± 0.4		597 ± 3
	0.1038 ± 1.4	0.99448 ± 0.1		596 ± 3
	0.0509 ± 0.5	0.99430 ± 0.1		596 ± 3
	0.0102 ± 0.1	0.99407 ± 0.1		596 ± 3
	0.0010 ± 0.1	0.99401 ± 0.1		596 ± 3
	0.0000	0.99398 ± 0.2		

Table ST13 Experimental data on density and calculated apparent and partial specific volumes of hyaluronan 90-130 kDa in 0.15 M NaCl.

T	c_{hya}	σ	ρ_{sample}	σ	V_{app}	$\bar{V}_{sp,hya}$
° C	% w/w	10^{-3}	g/cm^3	10^{-4}	10^{-3} cm^3/g	10^{-3} cm^3/g
25	1.5303	± 9.7	1.00937	± 0.1	599 ± 3	593 ± 4
	1.4035	± 9.1	1.00907	± 0.1	585 ± 4	593 ± 4
	1.3112	± 9.1	1.00886	± 0.0	571 ± 4	593 ± 4
	1.1930	± 2.8	1.00827	± 0.2	577 ± 3	592 ± 4
	1.1142	± 9.7	1.00784	± 1.1	586 ± 14	592 ± 5
	1.0662	± 8.1	1.00754	± 0.7	595 ± 12	592 ± 5
	0.8061	± 8.1	1.00667	± 0.8	571 ± 16	591 ± 5
	0.5027	± 4.9	1.00546	± 1.1	554 ± 26	590 ± 5
	0.3057	± 0.7	1.00465	± 1.1		589 ± 5
	0.1025	± 2.0	1.00368	± 0.5		589 ± 5
	0.0504	± 1.1	1.00365	± 1.4		588 ± 5
	0.0100	± 0.3	1.00346	± 2.0		588 ± 5
	0.0011	± 0.02	1.00344	± 2.2		588 ± 5
	0.0000		1.00321	± 0.01		
30	1.5303	± 9.7	1.00789	± 0.04	601 ± 3	595 ± 5
	1.4035	± 9.1	1.00758	± 0.1	587 ± 4	595 ± 5
	1.3112	± 8.1	1.00738	± 0.0	574 ± 4	595 ± 5
	1.1930	± 2.8	1.00679	± 0.2	580 ± 3	594 ± 5
	1.1142	± 9.7	1.00639	± 0.8	586 ± 11	594 ± 5
	1.0662	± 8.1	1.00606	± 0.7	597 ± 12	594 ± 5
	0.8061	± 8.1	1.00521	± 0.8	573 ± 16	593 ± 5
	0.5027	± 4.9	1.00399	± 1.1	556 ± 26	592 ± 5
	0.3057	± 0.7	1.00319	± 1.1		591 ± 5
	0.1025	± 2.0	1.00222	± 0.4		591 ± 5
	0.0504	± 1.1	1.00219	± 1.4		590 ± 5
	0.0100	± 0.3	1.00201	± 2.0		590 ± 5
	0.0011	± 0.02	1.00198	± 2.1		590 ± 5
	0.0000		1.00176	± 0.01		
35	1.5303	± 9.7	1.00620	± 0.05	603 ± 3	597 ± 4
	1.4035	± 9.1	1.00589	± 0.1	589 ± 4	597 ± 4
	1.3112	± 8.1	1.00569	± 0.0	576 ± 4	596 ± 4
	1.1930	± 2.8	1.00511	± 0.2	582 ± 3	596 ± 4
	1.1142	± 9.7	1.00470	± 0.7	588 ± 10	596 ± 4
	1.0662	± 8.1	1.00438	± 0.7	599 ± 12	596 ± 4
	0.8061	± 8.1	1.00353	± 0.9	575 ± 17	595 ± 4
	0.5027	± 4.9	1.00232	± 1.1	558 ± 26	594 ± 4
	0.3057	± 0.7	1.00152	± 1.1		593 ± 4
	0.1025	± 2.0	1.00055	± 0.4		592 ± 4
	0.0504	± 1.1	1.00052	± 1.4		592 ± 4
	0.0100	± 0.3	1.00034	± 2.0		592 ± 5

	0.0011 ± 0.02	1.00032 ± 2.1		592 ± 5
	0.0000	1.00009 ± 0.01		
40	1.5303 ± 9.7	1.00432 ± 0.05	605 ± 3	599 ± 4
	1.4035 ± 9.1	1.00401 ± 0.1	591 ± 4	599 ± 4
	1.3112 ± 8.1	1.00381 ± 0.0	577 ± 4	598 ± 4
	1.1930 ± 2.8	1.00323 ± 0.2	584 ± 3	598 ± 4
	1.1142 ± 9.7	1.00283 ± 0.7	590 ± 10	598 ± 4
	1.0662 ± 8.1	1.00251 ± 0.7	601 ± 12	597 ± 4
	0.8061 ± 8.1	1.00166 ± 0.9	577 ± 17	597 ± 4
	0.5027 ± 4.9	1.00045 ± 1.1	560 ± 26	596 ± 4
	0.3057 ± 0.7	0.99965 ± 1.1		595 ± 4
	0.1025 ± 2.0	0.99869 ± 0.4		594 ± 4
	0.0504 ± 1.1	0.99866 ± 1.4		594 ± 4
	0.0100 ± 0.3	0.99848 ± 2.0		594 ± 4
	0.0011 ± 0.02	0.99846 ± 2.1		594 ± 4
	0.0000	0.99823 ± 0.01		
45	1.5303 ± 9.7	1.00226 ± 0.04	607 ± 3	601 ± 4
	1.4035 ± 9.1	1.00195 ± 0.1	593 ± 4	600 ± 4
	1.3112 ± 8.1	1.00175 ± 0.0	579 ± 4	600 ± 4
	1.1930 ± 2.8	1.00117 ± 0.2	585 ± 3	600 ± 4
	1.1142 ± 9.7	1.00078 ± 0.7	591 ± 10	599 ± 4
	1.0662 ± 8.1	1.00045 ± 0.7	603 ± 12	599 ± 4
	0.8061 ± 8.1	0.99961 ± 0.8	578 ± 17	598 ± 4
	0.5027 ± 4.9	0.99840 ± 1.1	562 ± 26	597 ± 4
	0.3057 ± 0.7	0.99761 ± 1.1		597 ± 4
	0.1025 ± 2.0	0.99665 ± 0.4		596 ± 4
	0.0504 ± 1.1	0.99662 ± 1.4		596 ± 4
	0.0100 ± 0.3	0.99644 ± 2.0		596 ± 4
	0.0011 ± 0.02	0.99642 ± 2.1		596 ± 4
	0.0000	0.99619 ± 0.01		
50	1.5303 ± 9.7	1.00003 ± 0.04	609 ± 3	602 ± 4
	1.4035 ± 9.1	0.99973 ± 0.1	594 ± 4	602 ± 4
	1.3112 ± 8.1	0.99953 ± 0.0	581 ± 4	601 ± 4
	1.1930 ± 2.8	0.99895 ± 0.2	587 ± 3	601 ± 4
	1.1142 ± 9.7	0.99855 ± 0.7	593 ± 10	601 ± 4
	1.0662 ± 8.1	0.99823 ± 0.7	605 ± 12	601 ± 4
	0.8061 ± 8.1	0.99739 ± 0.8	580 ± 17	600 ± 4
	0.5027 ± 4.9	0.99619 ± 1.1	563 ± 26	599 ± 4
	0.3057 ± 0.7	0.99540 ± 1.1		598 ± 4
	0.1025 ± 2.0	0.99444 ± 0.4		598 ± 4
	0.0504 ± 1.1	0.99441 ± 1.4		597 ± 4
	0.0100 ± 0.3	0.99423 ± 2.0		597 ± 4
	0.0011 ± 0.02	0.99421 ± 2.1		597 ± 4
	0.0000	0.99398 ± 0.1		

Table ST14 Experimental data on density and calculated apparent and partial specific volumes of hyaluronan 300-500 kDa in 0.15 M NaCl.

T	c_{hya}	σ	ρ_{sample}	σ	V_{app}	$\bar{V}_{sp,hya}$
° C	% w/w	10^{-3}	g/cm^3	10^{-4}	10^{-3} cm^3/g	10^{-3} cm^3/g
25	1.0197	6.1	1.00775	0.2	558 ± 6	562 ± 4
	0.9039	3.7	1.00729	0.7	551 ± 11	561 ± 4
	0.8020	2.8	1.00695	0.6	536 ± 11	561 ± 4
	0.7068	9.8	1.00639	0.8	552 ± 19	560 ± 5
	0.5089	8.6	1.00568	1.3		560 ± 5
	0.3032	7.0	1.00471	1.1		559 ± 5
	0.1059	2.8	1.00374	0.1		558 ± 5
	0.0540	1.4	1.00354	0.3		558 ± 5
	0.0104	0.5	1.00331	0.2		558 ± 5
	0.0011	0.1	1.00328	0.5		558 ± 5
	0.0000		1.00322	0.1		
30	1.0197	6.1	1.00624	0.6	563 ± 10	566 ± 4
	0.9039	3.7	1.00582	0.7	553 ± 11	566 ± 4
	0.8020	2.8	1.00541	0.2	546 ± 6	566 ± 4
	0.7068	9.8	1.00492	0.7	555 ± 18	565 ± 4
	0.5089	8.6	1.00422	1.2		565 ± 4
	0.3032	7.0	1.00325	1.1		564 ± 4
	0.1059	2.8	1.00228	0.1		563 ± 4
	0.0540	1.4	1.00209	0.3		563 ± 4
	0.0104	0.5	1.00186	0.2		563 ± 4
	0.0011	0.1	1.00182	0.5		563 ± 4
	0.0000		1.00176	0.1		
35	1.0197	6.1	1.00454	0.5	566 ± 9	569 ± 4
	0.9039	3.7	1.00413	0.7	555 ± 11	568 ± 4
	0.8020	2.8	1.00374	0.1	548 ± 5	568 ± 4
	0.7068	9.8	1.00324	0.8	557 ± 18	568 ± 4
	0.5089	8.6	1.00254	1.2		567 ± 4
	0.3032	7.0	1.00158	1.1		566 ± 4
	0.1059	2.8	1.00061	0.2		566 ± 4
	0.0540	1.4	1.00042	0.3		565 ± 4
	0.0104	0.5	1.00019	0.2		565 ± 4
	0.0011	0.1	1.00016	0.5		565 ± 4
	0.0000		1.00010	0.1		
40	1.0197	6.1	1.00263	0.6	571 ± 10	573 ± 5
	0.9039	3.7	1.00226	0.7	557 ± 11	572 ± 5
	0.8020	2.8	1.00185	0.3	551 ± 7	572 ± 5
	0.7068	9.8	1.00137	0.7	559 ± 18	571 ± 5
	0.5089	8.6	1.00067	1.2		571 ± 5
	0.3032	7.0	0.99971	1.1		570 ± 5

	0.1059 ± 2.8	0.99875 ± 0.1		569 ± 5
	0.0540 ± 1.4	0.99856 ± 0.3		569 ± 5
	0.0104 ± 0.5	0.99833 ± 0.2		569 ± 5
	0.0011 ± 0.1	0.99830 ± 0.5		569 ± 5
	0.0000	0.99824 ± 0.1		
	1.0197 ± 6.1	1.00055 ± 0.7	576 ± 97	575 ± 5
	0.9039 ± 3.7	1.00020 ± 0.7	559 ± 108	575 ± 5
	0.8020 ± 2.8	0.99981 ± 0.2	552 ± 116	575 ± 5
	0.7068 ± 9.8	0.99932 ± 0.8		574 ± 5
	0.5089 ± 8.6	0.99863 ± 1.2		574 ± 5
45	0.3032 ± 7.0	0.99767 ± 1.1		573 ± 5
	0.1059 ± 2.8	0.99671 ± 0.1		572 ± 5
	0.0540 ± 1.4	0.99652 ± 0.3		572 ± 5
	0.0104 ± 0.5	0.99629 ± 0.2		572 ± 5
	0.0011 ± 0.1	0.99626 ± 0.5		572 ± 5
	0.0000	0.99620 ± 0.1		
	1.0197 ± 6.1	0.99831 ± 0.8	585 ± 194	577 ± 5
	0.9039 ± 3.7	0.99799 ± 0.7	567 ± 217	577 ± 5
	0.8020 ± 2.8	0.99760 ± 0.0	559 ± 236	576 ± 5
	0.7068 ± 9.8	0.99710 ± 0.8		576 ± 5
	0.5089 ± 8.6	0.99641 ± 1.2		575 ± 5
50	0.3032 ± 7.0	0.99545 ± 1.1		574 ± 5
	0.1059 ± 2.8	0.99450 ± 0.1		574 ± 5
	0.0540 ± 1.4	0.99431 ± 0.3		574 ± 5
	0.0104 ± 0.5	0.99408 ± 0.2		573 ± 5
	0.0011 ± 0.1	0.99405 ± 0.5		573 ± 5
	0.0000	0.99399 ± 0.2		

Table ST15 Experimental data on density and calculated apparent and partial specific volumes of hyaluronan 1500-1750 kDa in 0.15 M NaCl.

T	c_{hya}	σ	ρ_{sample}	σ	V_{app}	$\overline{V}_{sp,hya}$
° C	% w/w	10^{-3}	g/cm^3	10^{-4}	10^{-3} cm^3/g	10^{-3} cm^3/g
	0.5096 ± 2.5	1.00528 ± 1.4	593 ± 33	582 ± 11
	0.4005 ± 3.4	1.00507 ± 1.8	536 ± 51	581 ± 11
	0.3009 ± 2.3	1.00457 ± 1.1	547 ± 46	581 ± 11
	0.2009 ± 2.9	1.00419 ± 0.8	512 ± 55	581 ± 11
	0.1050 ± 0.6	1.00372 ± 0.8		580 ± 11
25	0.0900 ± 0.1	1.00368 ± 0.1		580 ± 11
	0.0708 ± 0.2	1.00359 ± 0.3		580 ± 11
	0.0506 ± 3.2	1.00346 ± 0.5		580 ± 11
	0.0098 ± 0.5	1.00335 ± 0.2		580 ± 11
	0.0010 ± 0.1	1.00327 ± 0.1		580 ± 11
	0.0000	1.00321 ± 0.2		

	0.5096 ± 2.5	1.00382 ± 1.4	595 ± 33	585 ± 11
	0.4005 ± 3.4	1.00360 ± 1.7	539 ± 51	584 ± 11
	0.3009 ± 2.3	1.00312 ± 1.0	548 ± 44	584 ± 11
	0.2009 ± 2.9	1.00273 ± 0.7	516 ± 52	583 ± 11
	0.1050 ± 0.6	1.00227 ± 0.8		583 ± 11
30	0.0900 ± 0.1	1.00228 ± 0.7		583 ± 11
	0.0708 ± 0.2	1.00214 ± 0.3		583 ± 11
	0.0506 ± 3.2	1.00200 ± 0.5		583 ± 11
	0.0098 ± 0.5	1.00190 ± 0.2		583 ± 11
	0.0010 ± 0.1	1.00182 ± 0.1		583 ± 11
	0.0000	1.00175 ± 0.2		
	0.5096 ± 2.5	1.00215 ± 1.4	596 ± 33	585 ± 11
	0.4005 ± 3.4	1.00193 ± 1.7	541 ± 51	585 ± 11
	0.3009 ± 2.3	1.00145 ± 1.0	549 ± 44	584 ± 11
	0.2009 ± 2.9	1.00106 ± 0.7	517 ± 52	584 ± 11
	0.1050 ± 0.6	1.00060 ± 0.8		584 ± 11
35	0.0900 ± 0.1	1.00056 ± 0.1		583 ± 11
	0.0708 ± 0.2	1.00047 ± 0.3		583 ± 11
	0.0506 ± 3.2	1.00033 ± 0.5		583 ± 11
	0.0098 ± 0.5	1.00023 ± 0.2		583 ± 11
	0.0010 ± 0.1	1.00015 ± 0.1		583 ± 11
	0.0000	1.00009 ± 0.2		
	0.5096 ± 2.5	1.00028 ± 1.4	598 ± 33	587 ± 11
	0.4005 ± 3.4	1.00006 ± 1.7	543 ± 51	586 ± 11
	0.3009 ± 2.3	0.99958 ± 1.0	551 ± 44	586 ± 11
	0.2009 ± 2.9	0.99919 ± 0.7	519 ± 53	586 ± 11
	0.1050 ± 0.6	0.99874 ± 0.8		585 ± 11
40	0.0900 ± 0.1	0.99870 ± 0.1		585 ± 11
	0.0708 ± 0.2	0.99861 ± 0.3		585 ± 11
	0.0506 ± 3.2	0.99847 ± 0.5		585 ± 11
	0.0098 ± 0.5	0.99837 ± 0.2		585 ± 11
	0.0010 ± 0.1	0.99829 ± 0.1		585 ± 11
	0.0000	0.99823 ± 0.2		
	0.5096 ± 2.5	0.99824 ± 1.4	599 ± 33	588 ± 11
	0.4005 ± 3.4	0.99802 ± 1.7	543 ± 51	588 ± 11
	0.3009 ± 2.3	0.99754 ± 1.0	551 ± 44	587 ± 11
	0.2009 ± 2.9	0.99715 ± 0.7	519 ± 53	587 ± 11
	0.1050 ± 0.6	0.99669 ± 0.8		587 ± 11
45	0.0900 ± 0.1	0.99666 ± 0.1		587 ± 11
	0.0708 ± 0.2	0.99657 ± 0.3		587 ± 11
	0.0506 ± 3.2	0.99643 ± 0.5		587 ± 11
	0.0098 ± 0.5	0.99633 ± 0.2		586 ± 11
	0.0010 ± 0.1	0.99625 ± 0.1		586 ± 11
	0.0000	0.99619 ± 0.2		

	0.5096 ± 2.5	0.99603 ± 1.4	600 ± 34	588 ± 11
	0.4005 ± 3.4	0.99581 ± 1.7	544 ± 52	588 ± 11
	0.3009 ± 2.3	0.99533 ± 1.0	552 ± 44	588 ± 11
	0.2009 ± 2.9	0.99495 ± 0.8	518 ± 56	587 ± 11
	0.1050 ± 0.6	0.99448 ± 0.8		587 ± 11
50	0.0900 ± 0.1	0.99440 ± 0.7		587 ± 11
	0.0708 ± 0.2	0.99436 ± 0.3		587 ± 11
	0.0506 ± 3.2	0.99422 ± 0.5		587 ± 11
	0.0098 ± 0.5	0.99412 ± 0.2		587 ± 11
	0.0010 ± 0.1	0.99404 ± 0.1		587 ± 11
	0.0000	0.99398 ± 0.2		

Table ST16 Regression characteristics of models fitting density data for hyaluronans of different molecular weights in water or in 0.15 M NaCl.

Solution	$M_{w\,\mathrm{hya}}$ / *kDa*	Model	R	R^2	R_p	MEP / 10^{-8}	AIC
water	10-30	linear	0.997592	0.995189	0.990190	8.7	-4878
		quadratic	0.999262	0.998525	0.996971	2.7	-5231
	90-130	linear	0.993972	0.987981	0.975694	18.5	-5860
		quadratic	0.996151	0.992317	0.984327	11.9	-6027
	300-500	linear	0.996330	0.992673	0.984965	8.9	-3571
		quadratic	0.998726	0.997453	0.994727	3.1	-3801
	1500-1750	linear	0.996756	0.993522	0.986531	6.8	-2675
		quadratic	0.999875	0.999750	0.999468	0.27	-3200
0.15M NaCl	10-30	linear	0.998169	0.996342	0.992360	7.0	-2554
		quadratic	0.999651	0.999302	0.998510	1.4	-2809
	90-130	linear	0.997688	0.995380	0.990377	7.3	-2565
		quadratic	0.999497	0.998995	0.997876	1.6	-2801
	300-500	linear	0.997665	0.995335	0.990158	6.3	-1990
		quadratic	0.999762	0.999524	0.998980	0.7	-2262
	1500-1750	linear	0.997002	0.994014	0.987518	6.6	-2581
		quadratic	0.999630	0.999261	0.998418	0.83	-2905
water	10-1750	linear	0.995935	0.991886	0.983736	12.5	-16845
		quadratic	0.997944	0.995893	0.991733	6.4	-17565
0.15M NaCl		linear	0.997709	0.995424	0.990762	7.1	-9661
		quadratic	0.999480	0.998961	0.997888	1.6	-10529

Table ST17 Parameters of linear models of density data for hyaluronans of different molecular weight in water or in 0.15 M NaCl.

$M_{w\,hya}$	solvent	a_0	a_w	a_t
kDa		g/cm^3	$10^{-4}\ g/cm^3$	$10^{-4}\ g/cm^3°C$
10-30	water	1.00671 ± 7.9 ×10^{-5}	4.1 ± 0.03	-3.6 ± 0.02
110-130		1.00672 ± 10 ×10^{-5}	4.0 ± 0.04	-3.7 ± 0.03
300-500		1.00657 ± 9.3 ×10^{-5}	4.1 ± 0.05	-3.6 ± 0.02
1500-1750		1.00645 ± 9.3 ×10^{-5}	3.8 ± 0.12	-3.6 ± 0.02
10-30	NaCl	1.01296 ± 9.8 ×10^{-5}	4.1 ± 0.03	-3.7 ± 0.02
110-130		1.01305 ± 10 ×10^{-5}	4.0 ± 0.04	-3.7 ± 0.02
300-500		1.01296 ± 11 ×10^{-5}	4.3 ± 0.06	-3.7 ± 0.03
1500-1750		1.01288 ± 9.4 ×10^{-5}	4.2 ± 0.12	-3.7 ± 0.02

Table ST18 Limiting partial specific volume, extrapolated apparent and partial specific volumes of four molecular weights of hyaluronan in water or in 0.15M NaCl.

a) In water

$M_{w\,hya}$	T	V^0_{app}	$\bar{v}^0_{sp,hya}$	$\bar{V}^{0\,*}_{sp,hya}$
kDa	°C	10^{-3} cm^3/g	10^{-3} cm^3/g	10^{-3} cm^3/g
10-30	25	563 ± 6	587 ± 3	587
	30	565 ± 6	589 ± 3	589
	35	568 ± 6	592 ± 3	592
	40	570 ± 6	594 ± 3	594
	45	571 ± 6	595 ± 3	596
	50	573 ± 6	597 ± 3	597
90-130	25	542 ± 23	587 ± 3	587
	30	545 ± 23	589 ± 3	589
	35	549 ± 26	592 ± 3	592
	40	559 ± 35	594 ± 3	594
	45	584 ± 72	595 ± 3	595
	50		597 ± 3	597
300-500	25	526 ± 22	587 ± 3	587
	30	529 ± 22	589 ± 3	589
	35	537 ± 22	592 ± 3	592
	40	532 ± 21	594 ± 3	594
	45	533 ± 21	596 ± 3	595
	50		597 ± 3	597
1500-1750	25	542 ± 28	587 ± 3	587
	30	544 ± 27	589 ± 3	589
	35	550 ± 28	592 ± 3	592
	40	559 ± 29	594 ± 3	594
	45	577 ± 35	596 ± 3	595
	50	600 ± 15	597 ± 3	597

* Standard deviation is less than 5×10^{-5}cm^3/g.

b) In 0.15 M NaCl

$M_{w\,hya}$ kDa	T °C	V^0_{app} 10^{-3} cm^3/g	$\bar{v}^0_{sp,hya}$ 10^{-3} cm^3/g	$\bar{V}^{0\,*}_{sp,hya}$ 10^{-3} cm^3/g
10-30	25	564 ± 10	586 ± 3	586
	30	566 ± 10	588 ± 3	588
	35	569 ± 10	591 ± 3	591
	40	571 ± 10	592 ± 3	593
	45	602 ± 45	594 ± 3	594
	50	573 ± 10	596 ± 3	596
90-130	25	543 ± 14	599 ± 5	599
	30	545 ± 14	601 ± 4	601
	35	547 ± 14	603 ± 4	603
	40	549 ± 14	604 ± 4	604
	45	550 ± 14	606 ± 4	606
	50	552 ± 14	608 ± 4	608
300-500	25	486 ± 22	558 ± 5	558
	30	488 ± 10	563 ± 4	563
	35	489 ± 10	565 ± 4	565
	40	490 ± 10	569 ± 5	569
	45	489 ± 10	572 ± 5	572
	50	502 ± 19	573 ± 5	573
1500-1750	25	467 ± 31	580 ± 11	580
	30	470 ± 29	583 ± 11	583
	35	472 ± 29	583 ± 11	583
	40	474 ± 29	585 ± 11	585
	45	473 ± 29	586 ± 11	586
	50	471 ± 29	587 ± 11	586

* Standard deviation is less than 5×10^{-5}cm^3/g.

Table ST19 Ultrasonic velocity, compressibility and hydration number of hyaluronan 10-30 kDa in water.

T	c_{hya}	σ	velocity	σ	β_{sample}	n_h
° C	%w/w	10^{-3}	m/s	10^{-2}	10^{-10} Pa^{-1}	
25	2.000079	± 5.9	1503.8	± 4	4.40	20
	1.799269	± 1.0	1503.5	± 16	4.40	20
	1.601005	± 1.8	1502.7	± 11	4.41	20
	1.400640	± 3.9	1502.1	± 15	4.42	20
	1.201529	± 0.9	1501.3	± 14	4.43	20
	1.062243	± 2.3	1500.7	± 11	4.43	20
	0.806757	± 6.9	1499.9	± 3	4.44	21
	0.500070	± 1.7	1498.8	± 3	4.45	23
	0.298891	± 2.1	1498.1	± 1	4.46	22
	0.102646	± 1.4	1497.3	± 1	4.47	

	0.049651 ± 0.5	1497.5 ± 2	4.47	
	0.010079 ± 0.1	1497.1 ± 20	4.47	
	0.001019 ± 0.1	1496.7 ± 11	4.47	
	0.000000	1496.7 4	4.48	
30	2.000079 ± 5.9	1515.8 ± 18	4.33	19
	1.799269 ± 1.0	1515.4 ± 17	4.34	19
	1.601005 ± 1.8	1514.6 ± 11	4.35	20
	1.400640 ± 3.9	1514.0 ± 14	4.36	20
	1.201529 ± 0.9	1513.3 ± 14	4.36	20
	1.062243 ± 2.3	1512.7 ± 9	4.37	20
	0.806757 ± 6.9	1512.0 ± 4	4.38	20
	0.500070 ± 1.7	1510.9 ± 2	4.39	22
	0.298891 ± 2.1	1510.2 ± 1	4.40	22
	0.102646 ± 1.4	1509.4 ± 1	4.41	
	0.049651 ± 0.5	1509.7 ± 3	4.40	
	0.010079 ± 0.1	1509.3 ± 17	4.41	
	0.001019 ± 0.1	1509.0 ± 10	4.41	
	0.000000	1509.0 9	4.41	
35	2.000079 ± 5.9	1526.2 ± 25	4.28	19
	1.799269 ± 1.0	1525.8 ± 16	4.29	19
	1.601005 ± 1.8	1525.1 ± 10	4.30	19
	1.400640 ± 3.9	1524.5 ± 14	4.30	19
	1.201529 ± 0.9	1523.8 ± 13	4.31	19
	1.062243 ± 2.3	1523.2 ± 7	4.32	19
	0.806757 ± 6.9	1522.5 ± 4	4.33	20
	0.500070 ± 1.7	1521.4 ± 2	4.34	22
	0.298891 ± 2.1	1520.8 ± 2	4.34	21
	0.102646 ± 1.4	1520.1 ± 1	4.35	24
	0.049651 ± 0.5	1520.4 ± 1	4.35	
	0.010079 ± 0.1	1520.0 ± 17	4.35	
	0.001019 ± 0.1	1519.7 ± 10	4.36	
	0.000000	1519.6 12	4.36	
40	2.000079 ± 5.9	1535.0 ± 25	4.24	19
	1.799269 ± 1.0	1534.6 ± 17	4.25	18
	1.601005 ± 1.8	1534.0 ± 10	4.25	19
	1.400640 ± 3.9	1533.4 ± 13	4.26	19
	1.201529 ± 0.9	1532.7 ± 12	4.27	19
	1.062243 ± 2.3	1532.2 ± 7	4.27	19
	0.806757 ± 6.9	1531.5 ± 4	4.28	20
	0.500070 ± 1.7	1530.5 ± 2	4.29	21
	0.298891 ± 2.1	1529.9 ± 1	4.30	21
	0.102646 ± 1.4	1529.2 ± 1	4.31	
	0.049651 ± 0.5	1529.5 ± 1	4.31	

	0.010079 ± 0.1	1529.1 ± 16	4.31	
	0.001019 ± 0.1	1528.9 ± 10	4.31	
	0.000000	1528.7 14	4.31	
45	2.000079 ± 5.9	1542.4 ± 28	4.21	18
	1.799269 ± 1.0	1542.1 ± 16	4.22	18
	1.601005 ± 1.8	1541.4 ± 10	4.22	18
	1.400640 ± 3.9	1540.9 ± 13	4.23	18
	1.201529 ± 0.9	1540.2 ± 12	4.24	19
	1.062243 ± 2.3	1539.7 ± 5	4.24	19
	0.806757 ± 6.9	1539.0 ± 4	4.25	19
	0.500070 ± 1.7	1538.0 ± 4	4.26	21
	0.298891 ± 2.1	1537.5 ± 1	4.27	
	0.102646 ± 1.4	1536.8 ± 1	4.27	
	0.049651 ± 0.5	1537.1 ± 2	4.27	
	0.010079 ± 0.1	1536.7 ± 16	4.28	
	0.001019 ± 0.1	1536.5 ± 9	4.28	
	0.000000	1536.4 15	4.28	
50	2.000079 ± 5.9	1548.5 ± 40	4.18	18
	1.799269 ± 1.0	1548.1 ± 17	4.19	18
	1.601005 ± 1.8	1547.4 ± 11	4.20	18
	1.400640 ± 3.9	1546.9 ± 13	4.20	18
	1.201529 ± 0.9	1546.3 ± 12	4.21	18
	1.062243 ± 2.3	1545.8 ± 8	4.22	18
	0.806757 ± 6.9	1545.2 ± 4	4.22	19
	0.500070 ± 1.7	1544.2 ± 4	4.23	21
	0.298891 ± 2.1	1543.7 ± 1	4.24	21
	0.102646 ± 1.4	1543.0 ± 1	4.25	
	0.049651 ± 0.5	1543.3 ± 2	4.25	
	0.010079 ± 0.1	1543.0 ± 17	4.25	
	0.001019 ± 0.1	1542.7 ± 10	4.25	
	0.000000	1542.6 15	4.25	

Table ST20 Ultrasonic velocity, compressibility and hydration number of hyaluronan 90-130 kDa in water.

T	c_{hya}	σ	velocity	σ	β_{sample}	n_h
° C	%w/w	10^{-3}	m/s	10^{-2}	10^{-10} Pa^{-1}	
25	1.533050	± 5.9	1502.5	± 48	4.41	20
	1.394846	± 1.0	1502.1	± 34	4.42	20
	1.315008	± 1.8	1501.8	± 31	4.42	20
	1.200498	± 3.9	1501.3	± 32	4.43	20
	1.106839	± 0.9	1501.0	± 10	4.43	20
	1.064364	± 2.3	1500.6	± 8	4.43	19
	0.801029	± 6.9	1500.0	± 12	4.44	21
	0.500704	± 1.7	1498.9	± 25	4.45	23
	0.303349	± 2.1	1498.2	± 24	4.46	21
	0.105866	± 1.4	1497.5	± 25	4.47	
	0.051776	± 0.5	1497.3	± 23	4.47	
	0.010672	± 0.1	1497.1	± 35	4.47	
	0.001037	± 0.1	1496.8	± 32	4.48	
	0.000000		1497.0	39	4.47	
30	1.533050	± 5.9	1514.5	± 50	4.35	19
	1.394846	± 1.0	1514.0	± 36	4.35	19
	1.315008	± 1.8	1513.7	± 32	4.36	19
	1.200498	± 3.9	1513.3	± 32	4.36	19
	1.106839	± 0.9	1513.0	± 15	4.37	19
	1.064364	± 2.3	1512.6	± 6	4.37	18
	0.801029	± 6.9	1512.1	± 13	4.38	20
	0.500704	± 1.7	1511.0	± 24	4.39	21
	0.303349	± 2.1	1510.3	± 24	4.40	18
	0.105866	± 1.4	1509.7	± 27	4.40	
	0.051776	± 0.5	1509.4	± 24	4.41	
	0.010672	± 0.1	1509.3	± 29	4.41	
	0.001037	± 0.1	1509.1	± 31	4.41	
	0.000000		1509.3	31	4.41	
35	1.533050	± 5.9	1524.9	± 50	4.30	18
	1.394846	± 1.0	1524.5	± 37	4.30	19
	1.315008	± 1.8	1524.2	± 32	4.31	18
	1.200498	± 3.9	1523.8	± 33	4.31	18
	1.106839	± 0.9	1523.6	± 17	4.31	18
	1.064364	± 2.3	1523.2	± 5	4.32	17
	0.801029	± 6.9	1522.6	± 11	4.32	19
	0.500704	± 1.7	1521.6	± 24	4.33	20
	0.303349	± 2.1	1520.9	± 23	4.34	17
	0.105866	± 1.4	1520.3	± 29	4.35	17
	0.051776	± 0.5	1520.1	± 23	4.35	
	0.010672	± 0.1	1520.0	± 41	4.35	
	0.001037	± 0.1	1519.8	± 29	4.35	

	0.000000	1520.0 31	4.35		
40	1.533050 ± 5.9	1533.9 ± 50	4.26	18	
	1.394846 ± 1.0	1533.4 ± 36	4.26	18	
	1.315008 ± 1.8	1533.1 ± 32	4.26	18	
	1.200498 ± 3.9	1532.7 ± 33	4.27	18	
	1.106839 ± 0.9	1532.5 ± 17	4.27	18	
	1.064364 ± 2.3	1532.1 ± 5	4.27	17	
	0.801029 ± 6.9	1531.6 ± 11	4.28	18	
	0.500704 ± 1.7	1530.6 ± 23	4.29	19	
	0.303349 ± 2.1	1529.9 ± 21	4.30	16	
	0.105866 ± 1.4	1529.4 ± 1	4.31		
	0.051776 ± 0.5	1529.2 ± 23	4.31		
	0.010672 ± 0.1	1529.1 ± 39	4.31		
	0.001037 ± 0.1	1528.9 ± 28	4.31		
	0.000000	1529.1 31	4.31		
45	1.533050 ± 5.9	1541.3 ± 50	4.22	17	
	1.394846 ± 1.0	1540.9 ± 36	4.23	18	
	1.315008 ± 1.8	1540.6 ± 33	4.23	17	
	1.200498 ± 3.9	1540.2 ± 32	4.24	17	
	1.106839 ± 0.9	1540.0 ± 17	4.24	18	
	1.064364 ± 2.3	1539.6 ± 4	4.24	17	
	0.801029 ± 6.9	1539.1 ± 8	4.25	18	
	0.500704 ± 1.7	1538.2 ± 21	4.26	18	
	0.303349 ± 2.1	1537.5 ± 20	4.27		
	0.105866 ± 1.4	1537.0 ± 1	4.27		
	0.051776 ± 0.5	1536.8 ± 29	4.27		
	0.010672 ± 0.1	1536.7 ± 38	4.28		
	0.001037 ± 0.1	1536.6 ± 27	4.28		
	0.000000	1536.7 30	4.27		
50	1.533050 ± 5.9	1547.3 ± 49	4.20	17	
	1.394846 ± 1.0	1546.9 ± 36	4.20	17	
	1.315008 ± 1.8	1546.7 ± 34	4.21	17	
	1.200498 ± 3.9	1546.3 ± 33	4.21	17	
	1.106839 ± 0.9	1546.1 ± 17	4.21	17	
	1.064364 ± 2.3	1545.7 ± 3	4.22	16	
	0.801029 ± 6.9	1545.3 ± 6	4.22	17	
	0.500704 ± 1.7	1544.3 ± 20	4.23	18	
	0.303349 ± 2.1	1543.7 ± 18	4.24	15	
	0.105866 ± 1.4	1543.2 ± 1	4.25		
	0.051776 ± 0.5	1543.0 ± 23	4.25		
	0.010672 ± 0.1	1542.9 ± 37	4.25		
	0.001037 ± 0.1	1542.8 ± 26	4.25		
	0.000000	1543.0 29	4.25		

Table ST21 Ultrasonic velocity, compressibility and hydration number of hyaluronan 300-500 kDa in water.

T	c_{hya}	σ	velocity	σ	β_{sample}	n_h
° C	% w/w	10^{-3}	m/s	10^{-2}	10^{-10} Pa^{-1}	
	1.052802	± 6.1	1500.9	± 23	4.43	21
	0.912913	± 3.7	1500.5	± 16	4.44	21
	0.808652	± 2.8	1500.1	± 17	4.44	21
	0.710005	± 9.8	1499.7	± 19	4.45	21
	0.509741	± 8.6	1499.0	± 7	4.46	20
25	0.302009	± 7.0	1498.2	± 2	4.46	18
	0.106337	± 2.8	1497.5	± 38	4.47	
	0.051672	± 1.4	1497.3	± 24	4.47	
	0.010312	± 0.5	1497.1	± 26	4.47	
	0.001037	± 0.1	1497.1	± 34	4.47	
	0.000000		1496.9		4.48	
	1.052802	± 6.1	1513.0	± 31	4.37	20
	0.912913	± 3.7	1512.5	± 17	4.37	21
	0.808652	± 2.8	1512.2	± 17	4.38	21
	0.710005	± 9.8	1511.7	± 17	4.38	20
	0.509741	± 8.6	1511.0	± 6	4.39	19
30	0.302009	± 7.0	1510.2	± 1	4.40	18
	0.106337	± 2.8	1509.7	± 35	4.41	
	0.051672	± 1.4	1509.4	± 25	4.41	
	0.010312	± 0.5	1509.3	± 25	4.41	
	0.001037	± 0.1	1509.3	± 33	4.41	
	0.000000		1509.2		4.41	
	1.052802	± 6.1	1523.5	± 32	4.32	20
	0.912913	± 3.7	1523.0	± 16	4.32	20
	0.808652	± 2.8	1522.7	± 18	4.32	20
	0.710005	± 9.8	1522.3	± 16	4.33	20
	0.509741	± 8.6	1521.6	± 6	4.34	19
35	0.302009	± 7.0	1520.8	± 1	4.35	17
	0.106337	± 2.8	1520.3	± 33	4.35	
	0.051672	± 1.4	1520.0	± 24	4.35	
	0.010312	± 0.5	1519.9	± 24	4.35	
	0.001037	± 0.1	1519.9	± 35	4.36	
	0.000000		1519.8		4.36	
	1.052802	± 6.1	1532.4	± 30	4.27	19
	0.912913	± 3.7	1532.0	± 16	4.28	20
	0.808652	± 2.8	1531.7	± 18	4.28	19
40	0.710005	± 9.8	1531.3	± 16	4.29	19
	0.509741	± 8.6	1530.6	± 5	4.29	18
	0.302009	± 7.0	1529.9	± 1	4.30	17

	0.106337 ± 2.8	1529.4 ± 32	4.31	
	0.051672 ± 1.4	1529.1 ± 23	4.31	
	0.010312 ± 0.5	1529.0 ± 23	4.31	
	0.001037 ± 0.1	1528.8 ± 1	4.31	
	0.000000	1528.9	4.31	
	1.052802 ± 6.1	1539.9 ± 29	4.24	19
	0.912913 ± 3.7	1539.5 ± 14	4.24	19
	0.808652 ± 2.8	1539.2 ± 17	4.25	19
	0.710005 ± 9.8	1538.8 ± 16	4.25	19
	0.509741 ± 8.6	1538.2 ± 3	4.26	18
45	0.302009 ± 7.0	1537.5 ± 1	4.27	
	0.106337 ± 2.8	1537.0 ± 30	4.27	
	0.051672 ± 1.4	1536.6 ± 3	4.28	
	0.010312 ± 0.5	1536.7 ± 21	4.28	
	0.001037 ± 0.1	1536.4 ± 1	4.28	
	0.000000	1536.6	4.28	
	1.052802 ± 6.1	1545.7 ± 4	4.22	18
	0.912913 ± 3.7	1545.5 ± 8	4.22	18
	0.808652 ± 2.8	1545.2 ± 13	4.22	18
	0.710005 ± 9.8	1545.0 ± 16	4.23	18
	0.509741 ± 8.6	1544.2 ± 11	4.24	17
50	0.302009 ± 7.0	1543.6 ± 4	4.24	
	0.106337 ± 2.8	1543.0 ± 5	4.25	
	0.051672 ± 1.4	1542.8 ± 4	4.25	
	0.010312 ± 0.5	1542.9 ± 19	4.25	
	0.001037 ± 0.1	1542.7 ± 3	4.25	
	0.000000	1542.8	4.25	

Table ST22 Ultrasonic velocity, compressibility and hydration number of hyaluronan 1500-1750 kDa in water.

T	c_{hya}	σ	velocity	σ	β_{sample}	n_h
° C	% w/w	10^{-3}	m/s	10^{-2}	10^{-10} Pa^{-1}	
	0.510564	± 6.1	1498.9	± 22	4.46	22
	0.399714	± 3.7	1498.8	± 11	4.46	25
	0.297765	± 2.8	1498.4	± 7	4.46	27
	0.199482	± 9.8	1497.8	± 27	4.47	27
	0.107570	± 8.6	1497.6	± 24	4.47	36
25	0.092412	± 7.0	1497.5	± 24	4.47	40
	0.072306	± 2.8	1497.6	± 13	4.47	
	0.053538	± 1.4	1497.5	± 18	4.47	
	0.010274	± 0.5	1497.2	± 27	4.47	
	0.001026	± 0.1	1496.7	± 4	4.48	
	0.000000		1497.0		4.48	
	0.510564	± 6.1	1511.0	± 21	4.39	20
	0.399714	± 3.7	1510.9	± 11	4.39	22
	0.297765	± 2.8	1510.5	± 7	4.40	24
	0.199482	± 9.8	1510.0	± 24	4.40	24
	0.107570	± 8.6	1509.7	± 23	4.40	29
30	0.092412	± 7.0	1509.7	± 25	4.40	32
	0.072306	± 2.8	1509.7	± 14	4.41	
	0.053538	± 1.4	1509.6	± 23	4.41	
	0.010274	± 0.5	1509.4	± 25	4.41	
	0.001026	± 0.1	1509.1	± 5	4.41	
	0.000000		1509.3		4.41	
	0.510564	± 6.1	1521.6	± 22	4.34	19
	0.399714	± 3.7	1521.5	± 13	4.34	22
	0.297765	± 2.8	1521.1	± 7	4.34	23
	0.199482	± 9.8	1520.7	± 24	4.35	23
	0.107570	± 8.6	1520.3	± 23	4.35	27
35	0.092412	± 7.0	1520.3	± 24	4.35	29
	0.072306	± 2.8	1520.3	± 15	4.35	
	0.053538	± 1.4	1520.3	± 25	4.35	
	0.010274	± 0.5	1520.0	± 25	4.35	
	0.001026	± 0.1	1519.8	± 4	4.36	
	0.000000		1520.0		4.36	
	0.510564	± 6.1	1530.6	± 21	4.26	18
	0.399714	± 3.7	1530.5	± 16	4.26	20
	0.297765	± 2.8	1530.2	± 7	4.27	22
40	0.199482	± 9.8	1529.7	± 25	4.27	21
	0.107570	± 8.6	1529.4	± 21	4.27	25
	0.092412	± 7.0	1529.4	± 24	4.27	27

	0.072306 ± 2.8	1529.4 ± 15	4.27	
	0.053538 ± 1.4	1529.4 ± 26	4.27	
	0.010274 ± 0.5	1529.1 ± 25	4.28	
	0.001026 ± 0.1	1529.0 ± 2	4.28	
	0.000000	1529.1	4.28	
	0.510564 ± 6.1	1538.2 ± 20	4.26	18
	0.399714 ± 3.7	1538.1 ± 19	4.26	20
	0.297765 ± 2.8	1537.8 ± 7	4.27	22
	0.199482 ± 9.8	1537.3 ± 25	4.27	21
	0.107570 ± 8.6	1537.0 ± 21	4.27	25
45	0.092412 ± 7.0	1537.0 ± 23	4.27	
	0.072306 ± 2.8	1537.1 ± 16	4.27	
	0.053538 ± 1.4	1537.0 ± 28	4.27	
	0.010274 ± 0.5	1536.7 ± 24	4.28	
	0.001026 ± 0.1	1536.7 ± 16	4.28	
	0.000000	1536.7	4.28	
	0.510564 ± 6.1	1544.3 ± 20	4.24	17
	0.399714 ± 3.7	1544.3 ± 18	4.24	20
	0.297765 ± 2.8	1544.0 ± 5	4.24	22
	0.199482 ± 9.8	1543.6 ± 25	4.24	20
	0.107570 ± 8.6	1543.2 ± 20	4.25	24
50	0.092412 ± 7.0	1543.2 ± 23	4.25	
	0.072306 ± 2.8	1543.3 ± 16	4.25	
	0.053538 ± 1.4	1543.2 ± 24	4.25	
	0.010274 ± 0.5	1542.9 ± 24	4.25	
	0.001026 ± 0.1	1543.1 ± 41	4.25	
	0.000000	1542.9	4.25	

Table ST23 Ultrasonic velocity, compressibility and hydration number of hyaluronan 10-30 kDa in 0.15M NaCl.

T	c_{hya}	σ	velocity	σ	β_{sample}	n_h
° C	% w/w	10^{-3}	m/s	10^{-2}	10^{-10} Pa^{-1}	
25	2.010922	± 5.9	1513.5	± 14	4.32	19
	1.801025	± 1.0	1513.2	± 16	4.32	20
	1.607347	± 1.8	1512.4	± 10	4.33	20
	1.411229	± 3.9	1511.7	± 9	4.34	20
	1.210558	± 0.9	1510.9	± 11	4.34	20
	1.059100	± 2.3	1510.2	± 4	4.35	19
	0.796556	± 6.9	1509.4	± 1	4.36	20
	0.502393	± 1.7	1508.3	± 4	4.37	21
	0.299120	± 2.1	1507.6	± 5	4.38	22
	0.103819	± 1.4	1506.6	± 2	4.39	
	0.050889	± 0.5	1506.5	± 1	4.39	
	0.010210	± 0.1	1506.3	± 15	4.39	
	0.001038	± 0.1	1506.1	± 1	4.39	
	0.000000		1506.5	8	4.39	
30	2.010922	± 5.9	1525.0	± 11	4.26	19
	1.801025	± 1.0	1524.8	± 14	4.26	20
	1.607347	± 1.8	1524.1	± 13	4.27	20
	1.411229	± 3.9	1523.3	± 1	4.28	20
	1.210558	± 0.9	1522.5	± 12	4.28	20
	1.059100	± 2.3	1521.9	± 2	4.29	19
	0.796556	± 6.9	1521.1	± 1	4.30	20
	0.502393	± 1.7	1520.1	± 8	4.31	20
	0.299120	± 2.1	1519.4	± 5	4.32	21
	0.103819	± 1.4	1518.6	± 1	4.33	
	0.050889	± 0.5	1518.4	± 1	4.33	
	0.010210	± 0.1	1518.3	± 2	4.33	
	0.001038	± 0.1	1518.2	± 1	4.33	
	0.000000		1518.3	9	4.33	
35	2.010922	± 5.9	1535.1	± 11	4.21	18
	1.801025	± 1.0	1534.9	± 13	4.21	19
	1.607347	± 1.8	1534.2	± 1	4.22	19
	1.411229	± 3.9	1533.4	± 1	4.23	19
	1.210558	± 0.9	1532.7	± 12	4.23	19
	1.059100	± 2.3	1532.1	± 2	4.24	18
	0.796556	± 6.9	1531.4	± 1	4.25	19
	0.502393	± 1.7	1530.4	± 1	4.26	20
	0.299120	± 2.1	1529.7	± 5	4.27	21
	0.103819	± 1.4	1529.0	± 1	4.27	22
	0.050889	± 0.5	1528.7	± 1	4.28	
	0.010210	± 0.1	1528.7	± 1	4.28	
	0.001038	± 0.1	1528.6	± 1	4.28	

	0.000000	1528.7 10	4.28	
40	2.010922 ± 5.9	1543.7 ± 10	4.17	18
	1.801025 ± 1.0	1543.5 ± 13	4.17	19
	1.607347 ± 1.8	1542.8 ± 1	4.18	19
	1.411229 ± 3.9	1542.1 ± 9	4.19	19
	1.210558 ± 0.9	1541.4 ± 12	4.20	19
	1.059100 ± 2.3	1540.8 ± 2	4.20	18
	0.796556 ± 6.9	1540.1 ± 8	4.21	19
	0.502393 ± 1.7	1539.2 ± 1	4.22	19
	0.299120 ± 2.1	1538.6 ± 4	4.23	20
	0.103819 ± 1.4	1537.9 ± 1	4.23	
	0.050889 ± 0.5	1537.8 ± 1	4.23	
	0.010210 ± 0.1	1537.5 ± 1	4.24	
	0.001038 ± 0.1	1537.5 ± 1	4.24	
	0.000000	1537.5 11	4.24	
45	2.010922 ± 5.9	1550.9 ± 9	4.14	17
	1.801025 ± 1.0	1550.7 ± 13	4.14	18
	1.607347 ± 1.8	1549.9 ± 2	4.15	18
	1.411229 ± 3.9	1549.3 ± 9	4.16	18
	1.210558 ± 0.9	1548.7 ± 13	4.16	18
	1.059100 ± 2.3	1548.1 ± 1	4.17	17
	0.796556 ± 6.9	1547.4 ± 8	4.18	18
	0.502393 ± 1.7	1546.5 ± 1	4.19	19
	0.299120 ± 2.1	1545.9 ± 4	4.19	
	0.103819 ± 1.4	1545.3 ± 1	4.20	
	0.050889 ± 0.5	1545.1 ± 1	4.20	
	0.010210 ± 0.1	1544.9 ± 1	4.21	
	0.001038 ± 0.1	1544.9 ± 2	4.21	
	0.000000	1544.9 12	4.21	
50	2.010922 ± 5.9	1556.7 ± 9	4.12	17
	1.801025 ± 1.0	1556.5 ± 12	4.12	18
	1.607347 ± 1.8	1555.8 ± 1	4.13	18
	1.411229 ± 3.9	1555.2 ± 8	4.14	18
	1.210558 ± 0.9	1554.6 ± 14	4.14	18
	1.059100 ± 2.3	1554.0 ± 1	4.15	17
	0.796556 ± 6.9	1553.4 ± 7	4.16	18
	0.502393 ± 1.7	1552.5 ± 1	4.17	19
	0.299120 ± 2.1	1551.9 ± 5	4.17	19
	0.103819 ± 1.4	1551.3 ± 1	4.18	
	0.050889 ± 0.5	1551.1 ± 1	4.18	
	0.010210 ± 0.1	1551.0 ± 1	4.18	
	0.001038 ± 0.1	1550.9 ± 4	4.18	
	0.000000	1551.0 13	4.18	

Table ST24 Ultrasonic velocity, compressibility and hydration number of hyaluronan 90-130 kDa in 0.15M NaCl.

T	c_{hya}	σ	velocity	σ	β_{sample}	n_h
° C	%w/w	10^{-3}	m/s	10^{-2}	10^{-10} Pa^{-1}	
25	1.530283	± 5.9	1511.7	± 2	4.34	19
	1.403506	± 1.0	1511.6	± 1	4.34	20
	1.311217	± 1.8	1511.4	± 1	4.34	21
	1.192987	± 3.9	1510.8	± 1	4.35	20
	1.114233	± 0.9	1510.6	± 1	4.35	20
	1.066185	± 2.3	1510.1	± 11	4.35	19
	0.806150	± 6.9	1509.5	± 11	4.36	21
	0.502710	± 1.7	1508.4	± 12	4.37	22
	0.305671	± 2.1	1507.8	± 13	4.38	23
	0.102510	± 1.4	1506.7	± 18	4.39	
	0.050406	± 0.5	1506.8	± 2	4.39	
	0.010038	± 0.1	1507.0	± 1	4.39	
	0.001082	± 0.1	1506.4	± 30	4.39	
	0.000000		1506.4	6	4.39	
30	1.530283	± 5.9	1523.3	± 1	4.28	18
	1.403506	± 1.0	1523.2	± 1	4.28	19
	1.311217	± 1.8	1523.1	± 2	4.28	20
	1.192987	± 3.9	1522.5	± 5	4.28	19
	1.114233	± 0.9	1522.2	± 0	4.29	19
	1.066185	± 2.3	1521.8	± 11	4.29	19
	0.806150	± 6.9	1521.2	± 11	4.30	20
	0.502710	± 1.7	1520.2	± 13	4.31	21
	0.305671	± 2.1	1519.6	± 14	4.32	23
	0.102510	± 1.4	1518.6	± 2	4.33	
	0.050406	± 0.5	1518.6	± 8	4.33	
	0.010038	± 0.1	1518.9	± 1	4.33	
	0.001082	± 0.1	1518.5	± 30	4.33	
	0.000000		1518.3	6	4.33	
35	1.530283	± 5.9	1533.5	± 1	4.23	18
	1.403506	± 1.0	1533.4	± 2	4.23	19
	1.311217	± 1.8	1533.3	± 2	4.23	20
	1.192987	± 3.9	1532.7	± 5	4.24	19
	1.114233	± 0.9	1532.4	± 1	4.24	19
	1.066185	± 2.3	1532.1	± 10	4.24	18
	0.806150	± 6.9	1531.5	± 10	4.25	20
	0.502710	± 1.7	1530.5	± 13	4.26	21
	0.305671	± 2.1	1529.9	± 14	4.27	22
	0.102510	± 1.4	1529.0	± 1	4.28	20
	0.050406	± 0.5	1529.0	± 7	4.28	
	0.010038	± 0.1	1529.2	± 1	4.27	
	0.001082	± 0.1	1528.9	± 29	4.28	

	0.000000	1528.6 6	4.28	
40	1.530283 ± 5.9	1542.1 ± 1	4.19	17
	1.403506 ± 1.0	1542.0 ± 4	4.19	18
	1.311217 ± 1.8	1541.9 ± 2	4.19	19
	1.192987 ± 3.9	1541.4 ± 5	4.20	19
	1.114233 ± 0.9	1541.1 ± 1	4.20	18
	1.066185 ± 2.3	1540.7 ± 11	4.20	18
	0.806150 ± 6.9	1540.2 ± 10	4.21	19
	0.502710 ± 1.7	1539.3 ± 13	4.22	20
	0.305671 ± 2.1	1538.7 ± 13	4.23	22
	0.102510 ± 1.4	1537.8 ± 1	4.23	
	0.050406 ± 0.5	1537.8 ± 1	4.23	
	0.010038 ± 0.1	1538.0 ± 2	4.23	
	0.001082 ± 0.1	1537.7 ± 28	4.24	
	0.000000	1537.5 6	4.24	
45	1.530283 ± 5.9	1549.3 ± 1	4.16	17
	1.403506 ± 1.0	1549.3 ± 1	4.16	18
	1.311217 ± 1.8	1549.1 ± 2	4.16	19
	1.192987 ± 3.9	1548.6 ± 5	4.16	18
	1.114233 ± 0.9	1548.4 ± 1	4.17	18
	1.066185 ± 2.3	1548.0 ± 10	4.17	17
	0.806150 ± 6.9	1547.5 ± 11	4.18	19
	0.502710 ± 1.7	1546.6 ± 13	4.19	20
	0.305671 ± 2.1	1546.0 ± 14	4.19	
	0.102510 ± 1.4	1545.2 ± 1	4.20	
	0.050406 ± 0.5	1545.2 ± 3	4.20	
	0.010038 ± 0.1	1545.4 ± 1	4.20	
	0.001082 ± 0.1	1545.1 ± 26	4.20	
	0.000000	1544.9 6	4.21	
50	1.530283 ± 5.9	1555.2 ± 1	4.13	17
	1.403506 ± 1.0	1555.1 ± 2	4.14	18
	1.311217 ± 1.8	1555.0 ± 2	4.14	18
	1.192987 ± 3.9	1554.5 ± 6	4.14	18
	1.114233 ± 0.9	1554.3 ± 1	4.15	18
	1.066185 ± 2.3	1553.9 ± 9	4.15	17
	0.806150 ± 6.9	1553.4 ± 9	4.15	18
	0.502710 ± 1.7	1552.6 ± 13	4.16	19
	0.305671 ± 2.1	1552.0 ± 13	4.17	21
	0.102510 ± 1.4	1551.2 ± 1	4.18	
	0.050406 ± 0.5	1551.2 ± 1	4.18	
	0.010038 ± 0.1	1551.4 ± 3	4.18	
	0.001082 ± 0.1	1551.2 ± 25	4.18	
	0.000000	1550.9 6	4.18	

Table ST25 Ultrasonic velocity, compressibility and hydration number of hyaluronan 300-500 kDa in 0.15M NaCl.

T	c_{hya}	σ	velocity	σ	β_{sample}	n_h
° C	%w/w	10^{-3}	m/s	10^{-2}	10^{-10} Pa^{-1}	
25	1.019705	± 6.1	1510.1	± 1	4.35	20
	0.909342	± 3.7	1510.2	± 13	4.35	22
	0.800683	± 2.8	1509.8	± 6	4.36	23
	0.712100	± 9.8	1509.3	± 10	4.36	21
	0.510570	± 8.6	1508.7	± 18	4.37	24
	0.303556	± 7.0	1507.9	± 11	4.38	25
	0.103121	± 2.8	1506.8	± 30	4.39	
	0.050825	± 1.4	1506.8	± 8	4.39	
	0.010209	± 0.5	1506.6	± 1	4.39	
	0.001037	± 0.1	1506.3	± 21	4.39	
	0.000000		1506.4		4.39	
30	1.019705	± 6.1	1521.8	± 2	4.29	20
	0.909342	± 3.7	1521.9	± 13	4.29	21
	0.800683	± 2.8	1521.5	± 5	4.30	22
	0.712100	± 9.8	1521.0	± 11	4.30	21
	0.510570	± 8.6	1520.5	± 9	4.31	23
	0.303556	± 7.0	1519.7	± 11	4.32	24
	0.103121	± 2.8	1518.7	± 16	4.33	
	0.050825	± 1.4	1518.6	± 8	4.33	
	0.010209	± 0.5	1518.4	± 1	4.33	
	0.001037	± 0.1	1518.2	± 8	4.33	
	0.000000		1518.3		4.33	
35	1.019705	± 6.1	1532.1	± 4	4.24	19
	0.909342	± 3.7	1532.1	± 12	4.24	21
	0.800683	± 2.8	1531.7	± 11	4.25	21
	0.712100	± 9.8	1531.3	± 13	4.25	20
	0.510570	± 8.6	1530.8	± 16	4.26	22
	0.303556	± 7.0	1530.0	± 11	4.27	23
	0.103121	± 2.8	1529.1	± 13	4.27	
	0.050825	± 1.4	1529.0	± 7	4.28	
	0.010209	± 0.5	1528.8	± 1	4.28	
	0.001037	± 0.1	1528.7	± 5	4.28	
	0.000000		1528.7		4.28	
40	1.019705	± 6.1	1540.8	± 3	4.20	18
	0.909342	± 3.7	1540.8	± 11	4.20	20
	0.800683	± 2.8	1540.4	± 9	4.21	20
	0.712100	± 9.8	1540.0	± 13	4.21	20
	0.510570	± 8.6	1539.5	± 14	4.22	22
	0.303556	± 7.0	1538.8	± 11	4.22	22

	0.103121 ± 2.8	1538.0 ± 11	4.23	
	0.050825 ± 1.4	1537.8 ± 8	4.23	
	0.010209 ± 0.5	1537.6 ± 1	4.24	
	0.001037 ± 0.1	1537.5 ± 4	4.24	
	0.000000	1537.5	4.24	
	1.019705 ± 6.1	1548.0 ± 3	4.17	18
	0.909342 ± 3.7	1548.0 ± 11	4.17	19
	0.800683 ± 2.8	1547.7 ± 8	4.18	20
	0.712100 ± 9.8	1547.3 ± 11	4.18	19
	0.510570 ± 8.6	1546.8 ± 13	4.19	21
45	0.303556 ± 7.0	1546.1 ± 10	4.19	
	0.103121 ± 2.8	1545.3 ± 10	4.20	
	0.050825 ± 1.4	1545.2 ± 7	4.20	
	0.010209 ± 0.5	1545.0 ± 1	4.21	
	0.001037 ± 0.1	1544.9 ± 4	4.21	
	0.000000	1544.9	4.21	
	1.019705 ± 6.1	1554.0 ± 9	4.15	18
	0.909342 ± 3.7	1554.0 ± 10	4.15	19
	0.800683 ± 2.8	1553.6 ± 8	4.15	20
	0.712100 ± 9.8	1553.3 ± 13	4.16	19
	0.510570 ± 8.6	1552.8 ± 15	4.16	21
50	0.303556 ± 7.0	1552.1 ± 9	4.17	
	0.103121 ± 2.8	1551.4 ± 9	4.18	
	0.050825 ± 1.4	1551.2 ± 7	4.18	
	0.010209 ± 0.5	1551.0 ± 1	4.18	
	0.001037 ± 0.1	1550.9 ± 2	4.18	
	0.000000	1550.9	4.18	

Table ST26 Ultrasonic velocity, compressibility and hydration number of hyaluronan 1500-1750 kDa in 0.15M NaCl.

T	c_{hya}	σ	velocity	σ	β_{sample}	n_h
° C	(% w/w)	10^{-3}	m/s	10^{-2}	10^{-10} Pa^{-1}	
25	0.509614	± 6.1	1508.3	± 12	4.37	20
	0.398740	± 3.7	1508.1	± 1	4.38	22
	0.299637	± 2.8	1507.6	± 16	4.38	22
	0.199262	± 9.8	1507.3	± 2	4.38	23
	0.104998	± 8.6	1506.9	± 3	4.39	22
	0.090015	± 7.0	1507.0	± 10	4.39	29
	0.070827	± 2.8	1506.9	± 5	4.39	
	0.049810	± 1.4	1506.6	± 8	4.39	
	0.009641	± 0.5	1506.6	± 4	4.39	
	0.000913	± 0.1	1506.2	± 6	4.39	
	0.000000		1506.4		4.39	
30	0.509614	± 6.1	1520.1	± 14	4.31	19
	0.398740	± 3.7	1519.9	± 1	4.31	21
	0.299637	± 2.8	1519.4	± 11	4.32	21
	0.199262	± 9.8	1519.2	± 6	4.32	24
	0.104998	± 8.6	1518.7	± 1	4.33	22
	0.090015	± 7.0	1518.8	± 11	4.33	29
	0.070827	± 2.8	1518.7	± 6	4.33	
	0.049810	± 1.4	1518.5	± 10	4.33	
	0.009641	± 0.5	1518.5	± 4	4.33	
	0.000913	± 0.1	1518.2	± 4	4.33	
	0.000000		1518.3		4.33	
35	0.509614	± 6.1	1530.4	± 14	4.26	19
	0.398740	± 3.7	1530.2	± 2	4.26	21
	0.299637	± 2.8	1529.8	± 10	4.27	21
	0.199262	± 9.8	1529.5	± 7	4.27	23
	0.104998	± 8.6	1529.0	± 1	4.27	21
	0.090015	± 7.0	1529.1	± 10	4.27	27
	0.070827	± 2.8	1529.1	± 6	4.28	
	0.049810	± 1.4	1528.8	± 1	4.28	
	0.009641	± 0.5	1528.8	± 2	4.28	
	0.000913	± 0.1	1528.7	± 4	4.28	
	0.000000		1528.7		4.28	
40	0.509614	± 6.1	1539.2	± 15	4.22	19
	0.398740	± 3.7	1539.0	± 2	4.22	20
	0.299637	± 2.8	1538.6	± 8	4.23	20
	0.199262	± 9.8	1538.3	± 4	4.23	23
	0.104998	± 8.6	1537.9	± 1	4.23	21
	0.090015	± 7.0	1538.0	± 10	4.23	26

	0.070827 ± 2.8	1537.9 ± 7	4.23	
	0.049810 ± 1.4	1537.7 ± 2	4.24	
	0.009641 ± 0.5	1537.7 ± 1	4.24	
	0.000913 ± 0.1	1537.5 ± 4	4.24	
	0.000000	1537.5	4.24	
	0.509614 ± 6.1	1546.5 ± 16	4.19	18
	0.398740 ± 3.7	1546.3 ± 2	4.19	20
	0.299637 ± 2.8	1545.9 ± 8	4.19	20
	0.199262 ± 9.8	1545.7 ± 8	4.20	23
	0.104998 ± 8.6	1545.2 ± 2	4.20	20
45	0.090015 ± 7.0	1545.3 ± 9	4.20	
	0.070827 ± 2.8	1545.3 ± 7	4.20	
	0.049810 ± 1.4	1545.0 ± 3	4.20	
	0.009641 ± 0.5	1545.1 ± 1	4.20	
	0.000913 ± 0.1	1544.9 ± 4	4.21	
	0.000000	1544.9	4.21	
	0.509614 ± 6.1	1552.5 ± 14	4.17	18
	0.398740 ± 3.7	1552.3 ± 1	4.17	20
	0.299637 ± 2.8	1551.9 ± 7	4.17	20
	0.199262 ± 9.8	1551.7 ± 4	4.17	22
	0.104998 ± 8.6	1551.3 ± 3	4.18	20
50	0.090015 ± 7.0	1551.3 ± 9	4.18	
	0.070827 ± 2.8	1551.3 ± 8	4.18	
	0.049810 ± 1.4	1551.1 ± 4	4.18	
	0.009641 ± 0.5	1551.1 ± 1	4.18	
	0.000913 ± 0.1	1551.0 ± 3	4.18	
	0.000000	1550.9	4.18	

Table ST27 Regression characteristics of quadratic model fitting velocity data for hyaluronan with molecular weight 10-1750 kDa.

Solution	R	R^2	R_p	MEP / 10^{-2}	AIC
water	0.999927	0.999853	0.999698	3.7	-988
0.15M NaCl	0.999904	0.999808	0.999602	4.6	-923

Table ST28 Ultrasonic velocity of hyaluronan (10-30 kDa) samples of concentration range 0-2% w/w measured with HR-US 102 at frequencies 2.5-14.7 MHz.

c_{hya} / % w/w	velocity / m/s					
	2.5 MHz	5.2 MHz	8.1 MHz	11.3 MHz	12.2 MHz	14.7 MHz
2.0163	7.084	7.068	7.042	7.009	7.067	7.046
1.8227	6.512	6.490	6.469	6.492	6.511	6.491
1.6158	5.794	5.756	5.739	5.759	5.775	5.760

1.4129	5.062	5.035	5.025	5.031	5.052	5.036
1.2096	4.339	4.309	4.300	4.313	4.321	4.312
1.0536	3.697	3.661	3.662	3.666	3.677	3.665
0.8978	3.261	3.278	3.217	3.213	3.233	3.225
0.7951	2.845	2.835	2.831	2.821	2.841	2.834
0.6948	2.481	2.477	2.474	2.463	2.481	2.478
0.5959	2.070	2.116	2.113	2.102	2.119	2.121
0.4991	1.800	1.792	1.792	1.779	1.795	1.797
0.3997	1.396	1.420	1.427	1.408	1.428	1.430
0.3007	1.051	1.078	1.081	1.065	1.079	1.084
0.2016	0.722	0.733	0.737	0.718	0.731	0.737
0.1034	0.413	0.386	0.381	0.367	0.375	0.377
0.0658	0.268	0.229	0.221	0.210	0.217	0.218
0.0469	0.168	0.080	0.166	0.150	0.154	0.160
0.0282	0.124	0.102	0.097	0.081	0.088	0.092
0.0094	0.069	0.033	0.029	0.013	0.026	0.025
0.0082	0.065	0.027	0.026	0.008	0.016	0.020
0.0065	0.058	0.022	0.021	0.003	0.011	0.015
0.0047	0.055	0.019	0.016	0.020	0.007	0.011
0.0028	0.048	0.009	0.008	0.010	0.011	0.001
0.0009	0.043	0.008	0.006	0.070	0.008	0.075
0.0000	0.013	0.004	0.010	0.001	0.001	0.002

Table ST29 Ultrasonic velocity of hyaluronan (90-130 kDa) samples of concentration range 0-2% w/w measured with HR-US 102 at frequencies 2.5-14.7 MHz.

c_{hya}	velocity					
% w/w	m/s					
	2.5 MHz	5.2 MHz	8.1 MHz	11.3 MHz	12.2 MHz	14.7 MHz
1.4948	5.446	5.510	5.372	5.379	5.425	5.399
1.3946	5.130	5.182	5.051	5.060	5.104	5.082
1.2942	4.680	4.751	4.627	4.635	4.674	4.656
1.1965	4.322	4.411	4.287	4.292	4.333	4.314
1.0983	4.041	4.105	3.979	3.984	4.021	4.005
0.9989	3.651	3.747	3.621	3.630	3.662	3.645
0.8971	3.295	3.361	3.238	3.244	3.273	3.258
0.8002	2.904	2.835	2.877	2.883	2.910	2.894
0.6832	2.547	2.599	2.489	2.496	2.514	2.502
0.5967	2.195	2.266	2.156	2.164	2.179	2.170
0.4970	1.828	1.894	1.785	1.791	1.802	1.793
0.3874	1.434	1.514	1.407	1.414	1.418	1.413
0.2990	1.184	1.197	1.093	1.097	1.101	1.096
0.1946	0.755	0.814	0.709	0.713	0.713	0.711
0.0983	0.411	0.470	0.368	0.368	0.366	0.364
0.0000	0.029	0.107	0.006	0.002	-0.003	-0.002

Table ST30 Ultrasonic velocity of hyaluronan (300-500 kDa) samples of concentration range 0-1% w/w measured with HR-US 102 at frequencies 2.5-12.2 MHz.

c_{hya} / % w/w	velocity / m/s				
	2.5 MHz	5.2 MHz	8.1 MHz	11.3 MHz	12.2 MHz
1.0778	3.973	3.933	3.911	3.930	3.932
0.9185	3.399	3.364	3.338	3.352	3.356
0.8175	3.015	3.016	2.958	2.972	2.973
0.7106	2.691	2.683	2.666	2.678	2.684
0.6036	2.255	2.229	2.216	2.219	2.224
0.5063	1.887	1.865	1.850	1.854	1.863
0.3978	1.490	3.278	1.458	1.460	1.465
0.2961	1.104	2.835	1.111	1.113	1.115
0.2039	0.763	0.758	0.754	0.749	0.757
0.1049	0.394	0.397	0.395	0.391	0.394
0.0720	0.282	0.277	0.275	0.269	0.274
0.0507	0.205	0.200	0.194	0.193	0.193
0.0307	0.130	0.130	0.122	0.121	0.125
0.0105	0.071	0.054	0.046	0.045	0.047
0.0093	0.061	0.051	0.042	0.041	0.044
0.0084	0.055	0.046	0.039	0.037	0.039
0.0075	0.055	-0.014	0.039	0.038	0.040
0.0062	0.065	0.050	0.043	0.041	0.042
0.0051	0.008	0.047	0.035	0.038	0.042
0.0031	0.035	0.038	0.041	0.037	0.029
0.0010	0.070	0.033	0.025	0.024	0.028
0.0000	0.013	0.004	-0.001	0.020	0.001

Table ST31 Ultrasonic velocity of hyaluronan (1500-1750 kDa) samples of concentration range 0-1% w/w measured with HR-US 102 at frequencies 2.5-14.7 MHz.

c_{hya} / % w/w	velocity / m/s					
	2.5 MHz	5.2 MHz	8.1 MHz	11.3 MHz	12.2 MHz	14.7 MHz
0.5135	1.881	1.892	1.892	1.912	1.922	1.902
0.4745	1.897	1.892	1.885	1.907	1.915	1.896
0.4501	1.763	1.774	1.764	1.790	1.797	1.778
0.4269	1.621	1.652	1.643	1.667	1.677	1.660
0.4042	1.559	1.559	1.549	1.574	1.583	1.567
0.3789	1.453	1.478	1.477	1.473	1.495	1.489
0.3573	1.358	1.362	1.360	1.378	1.385	1.370
0.3243	1.265	2.835	1.319	1.293	1.282	1.264
0.3002	1.189	1.224	1.264	1.236	1.225	1.208
0.2765	1.118	1.100	1.140	1.113	1.102	1.086
0.2511	1.012	1.025	1.065	1.036	1.024	1.007
0.2262	0.914	0.913	0.960	0.927	0.913	0.901
0.1987	0.854	0.844	0.887	0.856	0.844	0.832
0.0992	0.478	0.482	0.534	0.495	0.482	0.468
0.0364	0.178	0.171	0.169	0.179	0.177	0.176
0.0000	0.040	0.044	0.067	0.062	0.054	0.049

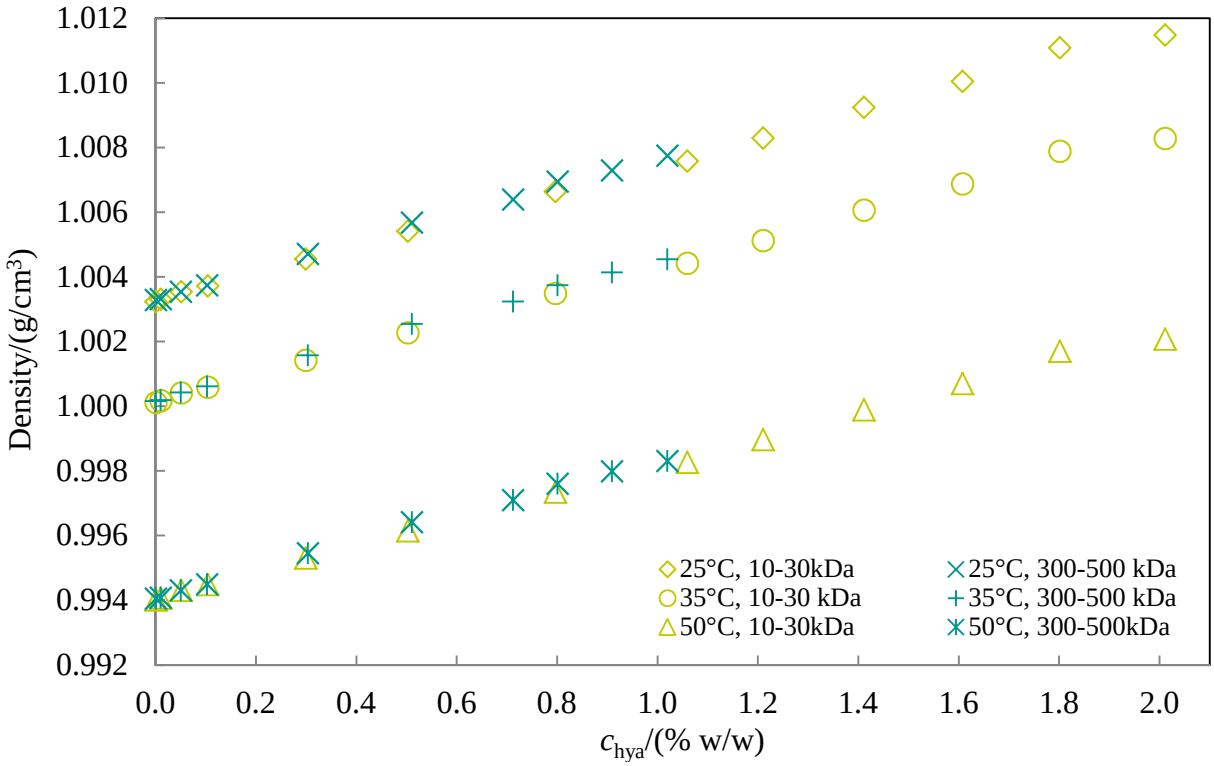

Figure SF1 The temperature and concentration dependence of density of hyaluronan solutions (10-30 kDa and 300-500 kDa) in 0.15 M NaCl.

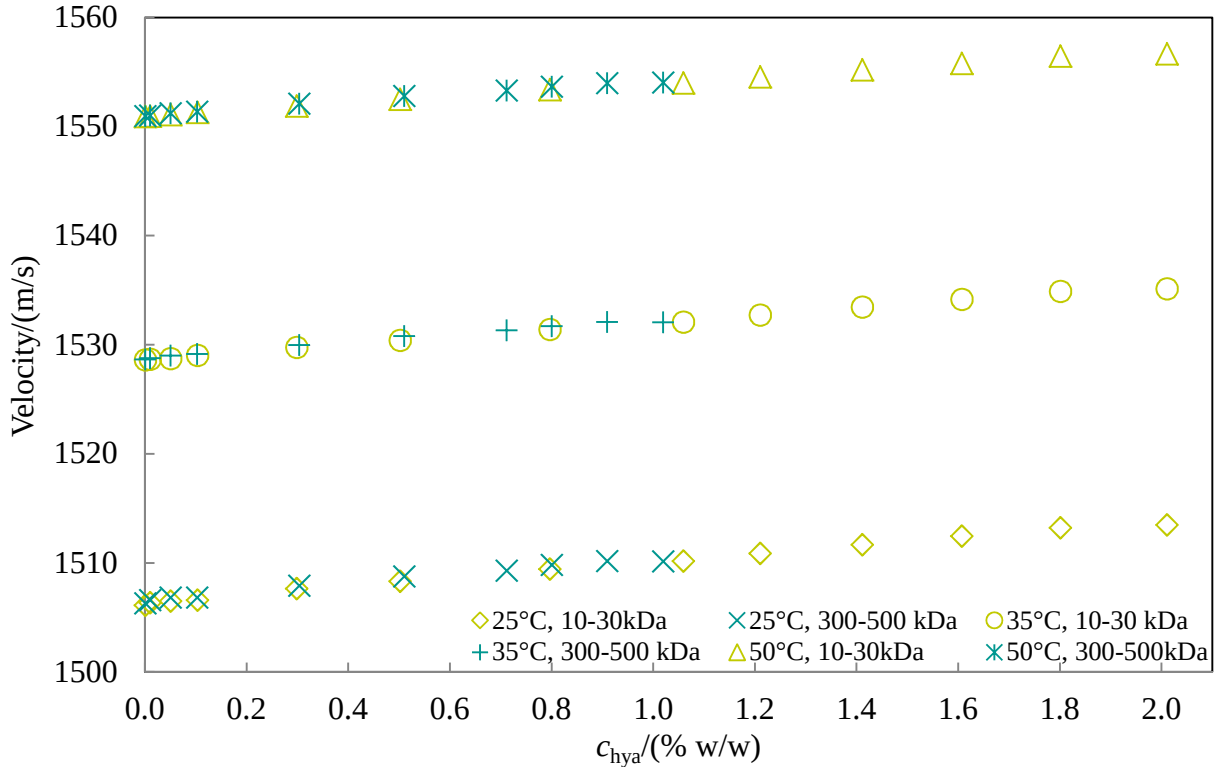

Figure SF2 The temperature and concentration dependence of velocity of hyaluronan solutions (10-30 kDa and 300-500 kDa) in 0.15 M NaCl.

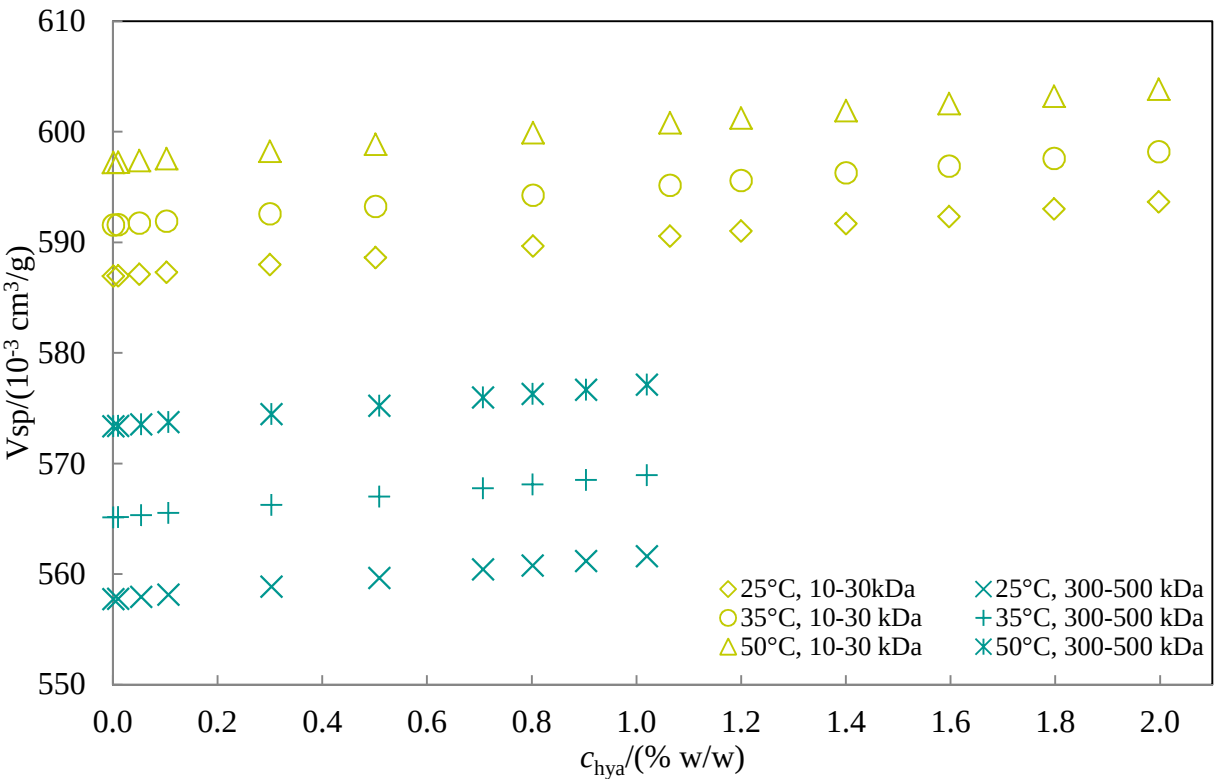

Figure SF3 The temperature and concentration of apparent specific volume of hyaluronan solutions (10-30 kDa and 300-500 kDa) in 0.15 M NaCl.

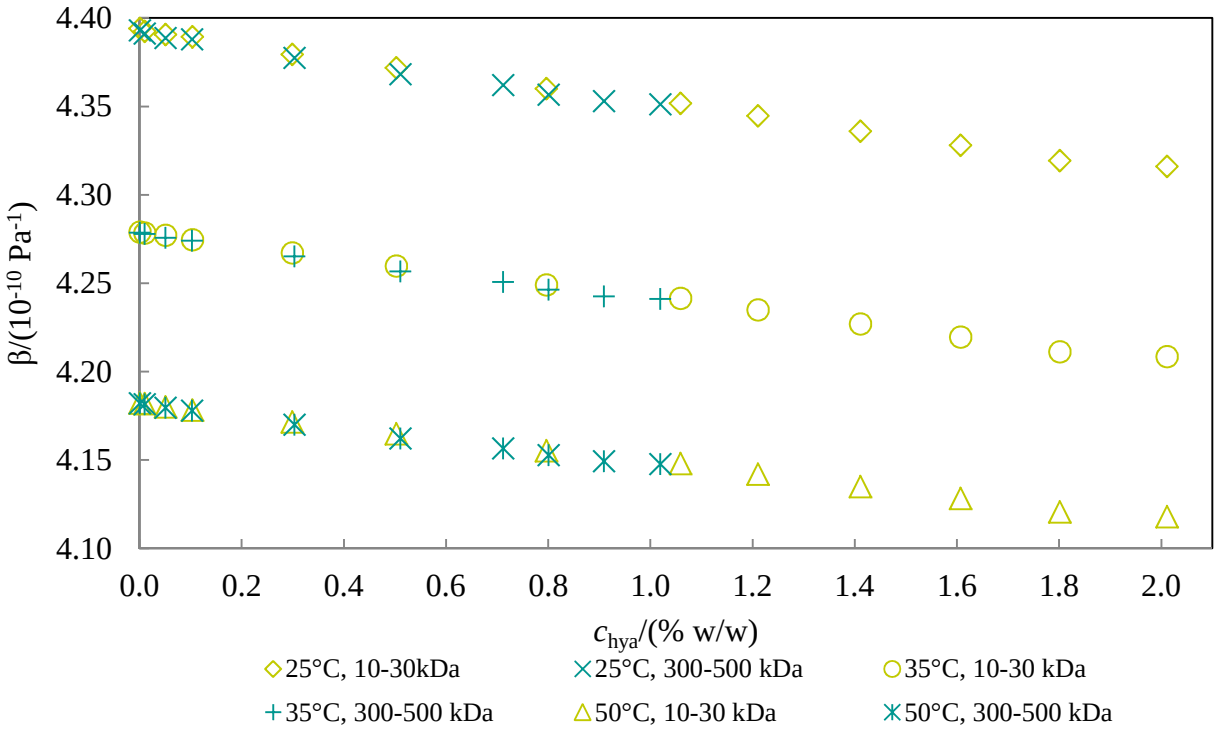

Figure SF4 The temperature and concentration dependence of compressibility of hyaluronan solutions (10-30 kDa and 300-500 kDa) in 0.15 M NaCl.

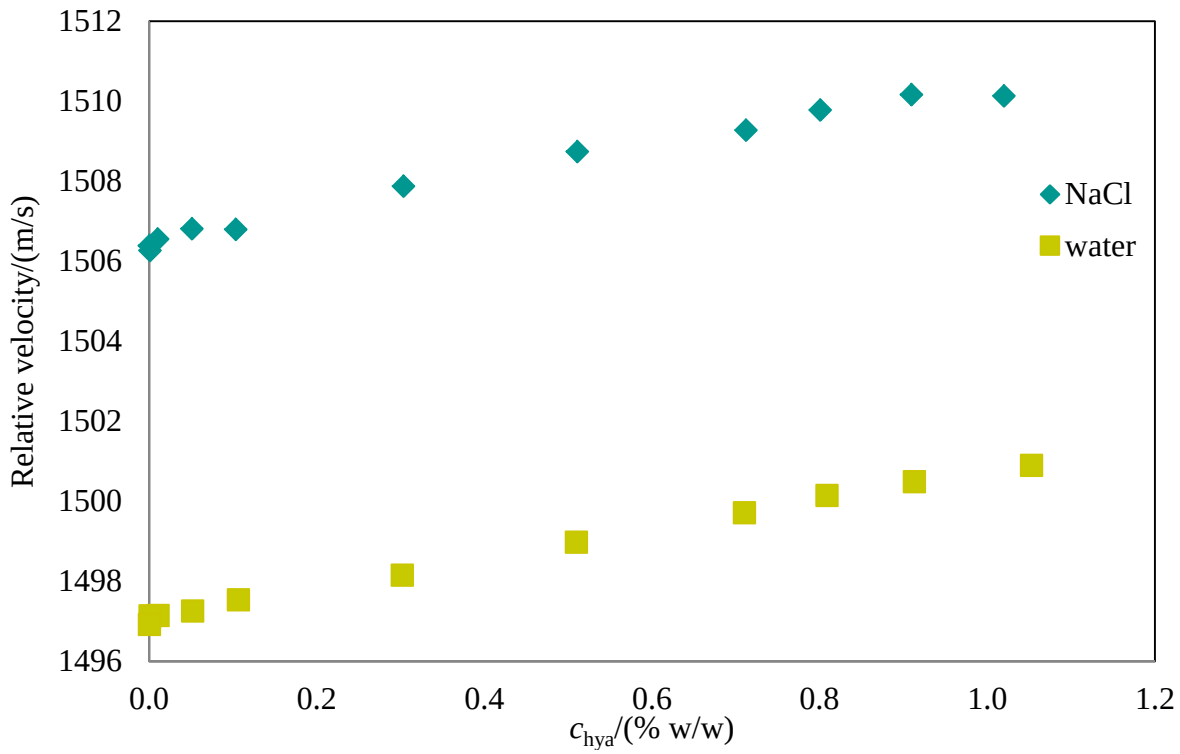

Figure SF5 Comparison of relative velocity in water and sodium chloride solution of hyaluronan with molecular weight 90-130 kDa at 25 °C measured by means of DSA 5000M.

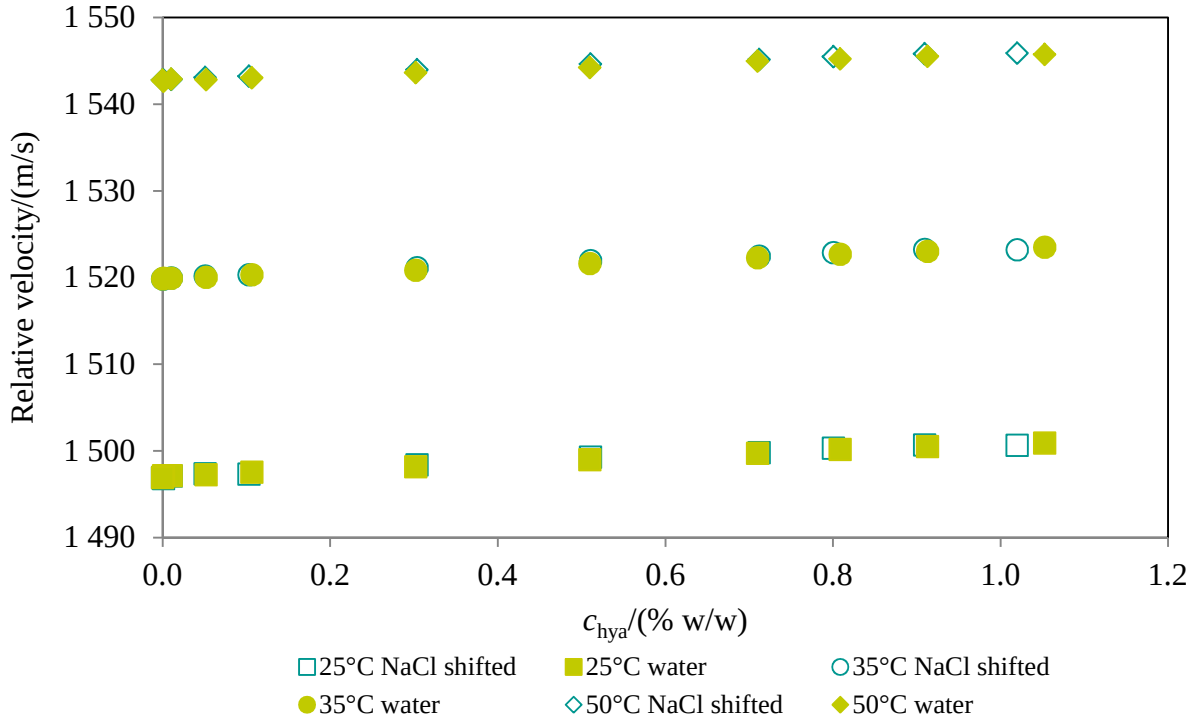

Figure SF6 The effect of NaCl (0.15 M) on ultrasonic velocity values of solutions of hyaluronan with molecular weight 300-500 kDa measured at 25 °C by DSA 5000M; the curves means used in NaCl solution point of curves measured in water. The curve of 0.15 M NaCl is shifted to the first point of water.

Table ST32 Dependence of density and ultrasonic velocity at temperature range 20-55 °C of 100mM CTAB and 50mM TTAB in water measured by means of DSA 5000M.

T	density			velocity		
° C	g/cm^3			m/s		
	water	100 mM CTAB	50 mM TTAB	water	100 mM CTAB	50 mM TTAB
20	0.998196	0.998693	0.998743	1482.58	1485.43	1484.42
21	0.997988	0.998460	0.998524	1485.50	1488.10	1487.23
22	0.997768	0.998215	0.998293	1488.42	1490.77	1490.02
23	0.997535	0.997959	0.998050	1491.27	1493.37	1492.76
24	0.997295	0.997694	0.997800	1494.04	1495.90	1495.42
25	0.997044	0.997419	0.997536	1496.75	1498.36	1498.01
26	0.996784	0.997137	0.997264	1499.38	1500.74	1500.53
27	0.996514	0.996844	0.996985	1501.93	1503.05	1502.97
28	0.996234	0.996543	0.996696	1504.41	1505.28	1505.35
29	0.995946	0.996233	0.996396	1506.83	1507.45	1507.66
30	0.995650	0.995915	0.996092	1509.17	1509.55	1509.90
31	0.995343	0.995586	0.995774	1511.45	1511.59	1512.07
32	0.995028	0.995252	0.995449	1513.66	1513.55	1514.18
33	0.994706	0.994908	0.995117	1515.80	1515.46	1516.22
34	0.994374	0.994557	0.994776	1517.88	1517.29	1518.19
35	0.994034	0.994198	0.994425	1519.90	1519.07	1520.11
36	0.993687	0.993831	0.994068	1521.85	1520.78	1521.96
37	0.993331	0.993456	0.993702	1523.74	1522.42	1523.75
38	0.992967	0.993074	0.993327	1525.56	1524.02	1525.47
39	0.992595	0.992685	0.992946	1527.33	1525.54	1527.13
40	0.992217	0.992288	0.992558	1529.03	1527.01	1528.74
41	0.991830	0.991885	0.992168	1530.67	1528.41	1530.29
42	0.991436	0.991473	0.991768	1532.25	1529.76	1531.77
43	0.991035	0.991054	0.991358	1533.77	1531.06	1533.20
44	0.990626	0.990627	0.990942	1535.24	1532.30	1534.57
45	0.990210	0.990195	0.990518	1536.65	1533.49	1535.89
46	0.989783	0.989756	0.990089	1538.00	1534.61	1537.15
47	0.989356	0.989311	0.989655	1539.30	1535.68	1538.35
48	0.988915	0.988860	0.989212	1540.55	1536.71	1539.50
49	0.988476	0.988402	0.988763	1541.72	1537.69	1540.60
50	0.988004	0.987937	0.988306	1542.86	1538.60	1541.64
51	0.987570	0.987469	0.987843	1543.93	1539.46	1542.64
52	0.986945	0.986995	0.987374	1544.96	1540.27	1543.58
53	0.986581	0.986513	0.986897	1545.95	1541.05	1544.47
54	0.985929	0.986025	0.986414	1546.87	1541.75	1545.31
55	0.985663	0.985532	0.985926	1548.03	1542.42	1546.10

Table ST33 Dependence of density and ultrasonic velocity at temperature range 20-55 °C of 100mM CTAB and 50mM TTAB in sodium chloride solution measured by means of DSA 5000M.

T	density			velocity		
° C	g/cm^3			m/s		
	0.15 M NaCl	100 mM CTAB	50 mM TTAB	0.15 M NaCl	100 mM CTAB	50 mM TTAB
20	1.004434	1.005108	1.004889	1492.58	1494.58	1493.66
21	1.004209	1.004862	1.004653	1495.39	1497.17	1496.37
22	1.003974	1.004598	1.004406	1498.17	1499.76	1499.09
23	1.003728	1.004328	1.004148	1500.91	1502.28	1501.75
24	1.003473	1.004048	1.003882	1503.59	1504.74	1504.34
25	1.003207	1.003760	1.003607	1506.21	1507.13	1506.86
26	1.002932	1.003460	1.003321	1508.76	1509.45	1509.31
27	1.002649	1.003155	1.003029	1511.23	1511.69	1511.69
28	1.002357	1.002840	1.002727	1513.64	1513.86	1513.99
29	1.002056	1.002517	1.002415	1515.99	1515.96	1516.23
30	1.001747	1.002186	1.002096	1518.26	1518.00	1518.41
31	1.001429	1.001847	1.001764	1520.48	1519.98	1520.52
32	1.001103	1.001499	1.001430	1522.63	1521.88	1522.57
33	1.000769	1.001145	1.001092	1524.71	1523.73	1524.55
34	1.000429	1.000780	1.000742	1526.74	1525.50	1526.47
35	1.000078	1.000408	1.000384	1528.69	1527.22	1528.32
36	0.999720	1.000024	1.000017	1530.59	1528.87	1530.11
37	0.999354	0.999646	0.999642	1532.42	1530.46	1531.85
38	0.998980	0.999258	0.999263	1534.19	1531.99	1533.52
39	0.998597	0.998861	0.998874	1535.90	1533.46	1535.12
40	0.998206	0.998457	0.998474	1537.55	1534.87	1536.67
41	0.997811	0.998047	0.998065	1539.14	1536.22	1538.16
42	0.997415	0.997628	0.997656	1540.67	1537.51	1539.59
43	0.997009	0.997206	0.997248	1542.14	1538.75	1540.97
44	0.996595	0.996773	0.996828	1543.57	1539.93	1542.28
45	0.996176	0.996334	0.996399	1544.93	1541.06	1543.56
46	0.995747	0.995891	0.995965	1546.24	1542.13	1544.77
47	0.995312	0.995438	0.995523	1547.50	1543.16	1545.93
48	0.994871	0.994980	0.995075	1548.71	1544.13	1547.03
49	0.994422	0.994516	0.994620	1549.86	1545.05	1548.09
50	0.993969	0.994046	0.994157	1550.95	1545.92	1549.09
51	0.993507	0.993570	0.993689	1552.00	1546.73	1550.05
52	0.993041	0.993089	0.993214	1553.00	1547.51	1550.95
53	0.992569	0.992604	0.992734	1553.95	1548.23	1551.81
54	0.992088	0.992111	0.992249	1554.85	1548.91	1552.61
55	0.991604	0.991612	0.991760	1555.70	1549.54	1553.37

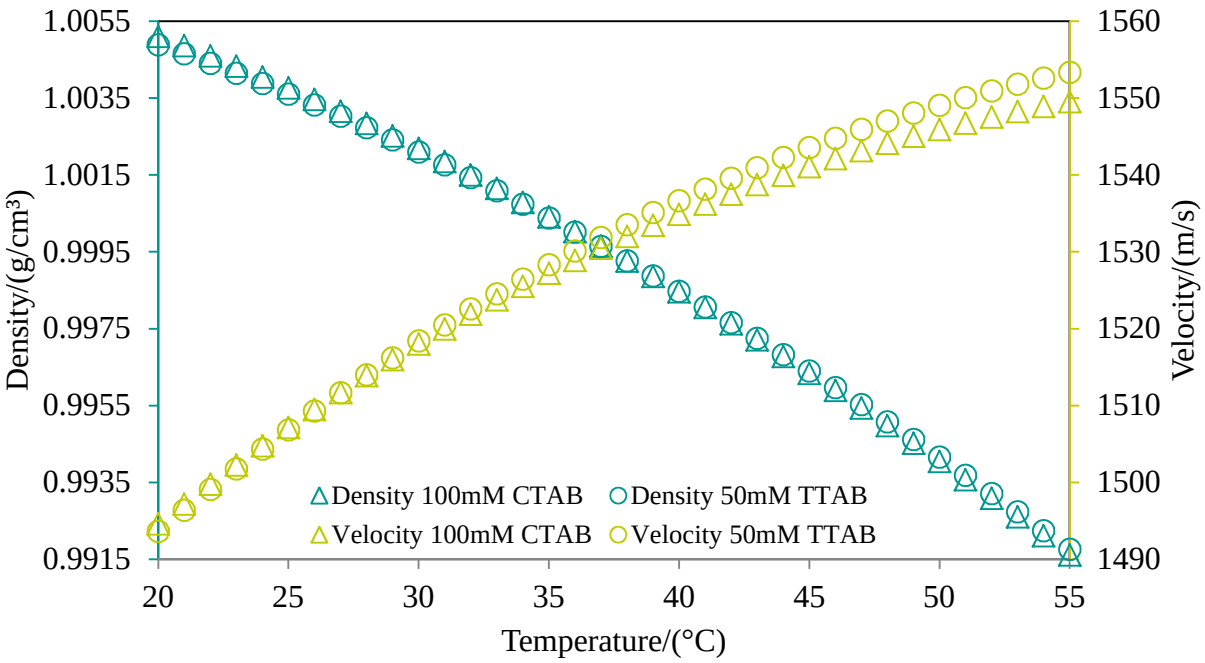

Figure SF7 Dependence of density and ultrasonic velocity at temperature range 20-55 °C of 100mM CTAB and 50mM TTAB in sodium chloride solution.

Table ST34 Density of surfactants CTAB and TTAB dissolved in water or in 0.15 M NaCl at temperature range 20-55 °C.

T / ° C	Density g/cm^3					
	water	100 mM CTAB	50 mM TTAB	0.15 M NaCl	100 mM CTAB *	50 mM TTAB*
20	0.998196	0.998693	0.998743	1.004434	1.005108	1.004889
21	0.997988	0.998460	0.998524	1.004209	1.004862	1.004653
22	0.997768	0.998215	0.998293	1.003974	1.004598	1.004406
23	0.997535	0.997959	0.998050	1.003728	1.004328	1.004148
24	0.997295	0.997694	0.997800	1.003473	1.004048	1.003882
25	0.997044	0.997419	0.997536	1.003207	1.003760	1.003607
26	0.996784	0.997137	0.997264	1.002932	1.003460	1.003321
27	0.996514	0.996844	0.996985	1.002649	1.003155	1.003029
28	0.996234	0.996543	0.996696	1.002357	1.002840	1.002727
29	0.995946	0.996233	0.996396	1.002056	1.002517	1.002415
30	0.995650	0.995915	0.996092	1.001747	1.002186	1.002096
31	0.995343	0.995586	0.995774	1.001429	1.001847	1.001764
32	0.995028	0.995252	0.995449	1.001103	1.001499	1.001430
33	0.994706	0.994908	0.995117	1.000769	1.001145	1.001092
34	0.994374	0.994557	0.994776	1.000429	1.000780	1.000742
35	0.994034	0.994198	0.994425	1.000078	1.000408	1.000384
36	0.993687	0.993831	0.994068	0.999720	1.000024	1.000017
37	0.993331	0.993456	0.993702	0.999354	0.999646	0.999642
38	0.992967	0.993074	0.993327	0.998980	0.999258	0.999263
39	0.992595	0.992685	0.992946	0.998597	0.998861	0.998874
40	0.992217	0.992288	0.992558	0.998206	0.998457	0.998474
41	0.991830	0.991885	0.992168	0.997811	0.998047	0.998065
42	0.991436	0.991473	0.991768	0.997415	0.997628	0.997656
43	0.991035	0.991054	0.991358	0.997009	0.997206	0.997248
44	0.990626	0.990627	0.990942	0.996595	0.996773	0.996828

45	0.990210	0.990195	0.990518	0.996176	0.996334	0.996399
46	0.989783	0.989756	0.990089	0.995747	0.995891	0.995965
47	0.989356	0.989311	0.989655	0.995312	0.995438	0.995523
48	0.988915	0.988860	0.989212	0.994871	0.994980	0.995075
49	0.988476	0.988402	0.988763	0.994422	0.994516	0.994620
50	0.988004	0.987937	0.988306	0.993969	0.994046	0.994157
51	0.987570	0.987469	0.987843	0.993507	0.993570	0.993689
52	0.986945	0.986995	0.987374	0.993041	0.993089	0.993214
53	0.986581	0.986513	0.986897	0.992569	0.992604	0.992734
54	0.985929	0.986025	0.986414	0.992088	0.992111	0.992249
55	0.985663	0.985532	0.985926	0.991604	0.991612	0.991760

* sodium chloride solutions

Table ST35 Velocity of different surfactants at temperature range 20-55 °C measured by means of DSA 5000M.

T	Velocity/(m/s)					
° C	water	100mM CTAB	50mM TTAB	0.15M NaCl	100mM CTAB *	50mM TTAB *
20	1482.58	1485.43	1484.42	1492.58	1494.58	1493.66
21	1485.50	1488.10	1487.23	1495.39	1497.17	1496.37
22	1488.42	1490.77	1490.02	1498.17	1499.76	1499.09
23	1491.27	1493.37	1492.76	1500.91	1502.28	1501.75
24	1494.04	1495.90	1495.42	1503.59	1504.74	1504.34
25	1496.75	1498.36	1498.01	1506.21	1507.13	1506.86
26	1499.38	1500.74	1500.53	1508.76	1509.45	1509.31
27	1501.93	1503.05	1502.97	1511.23	1511.69	1511.69
28	1504.41	1505.28	1505.35	1513.64	1513.86	1513.99
29	1506.83	1507.45	1507.66	1515.99	1515.96	1516.23
30	1509.17	1509.55	1509.90	1518.26	1518.00	1518.41
31	1511.45	1511.59	1512.07	1520.48	1519.98	1520.52
32	1513.66	1513.55	1514.18	1522.63	1521.88	1522.57
33	1515.80	1515.46	1516.22	1524.71	1523.73	1524.55
34	1517.88	1517.29	1518.19	1526.74	1525.50	1526.47
35	1519.90	1519.07	1520.11	1528.69	1527.22	1528.32
36	1521.85	1520.78	1521.96	1530.59	1528.87	1530.11
37	1523.74	1522.42	1523.75	1532.42	1530.46	1531.85
38	1525.56	1524.02	1525.47	1534.19	1531.99	1533.52
39	1527.33	1525.54	1527.13	1535.90	1533.46	1535.12
40	1529.03	1527.01	1528.74	1537.55	1534.87	1536.67
41	1530.67	1528.41	1530.29	1539.14	1536.22	1538.16
42	1532.25	1529.76	1531.77	1540.67	1537.51	1539.59
43	1533.77	1531.06	1533.20	1542.14	1538.75	1540.97
44	1535.24	1532.30	1534.57	1543.57	1539.93	1542.28
45	1536.65	1533.49	1535.89	1544.93	1541.06	1543.56
46	1538.00	1534.61	1537.15	1546.24	1542.13	1544.77
47	1539.30	1535.68	1538.35	1547.50	1543.16	1545.93
48	1540.55	1536.71	1539.50	1548.71	1544.13	1547.03
49	1541.72	1537.69	1540.60	1549.86	1545.05	1548.09
50	1542.86	1538.60	1541.64	1550.95	1545.92	1549.09
51	1543.93	1539.46	1542.64	1552.00	1546.73	1550.05
52	1544.96	1540.27	1543.58	1553.00	1547.51	1550.95
53	1545.95	1541.05	1544.47	1553.95	1548.23	1551.81
54	1546.87	1541.75	1545.31	1554.85	1548.91	1552.61
55	1548.03	1542.42	1546.10	1555.70	1549.54	1553.37

* sodium chloride solutions

Table ST36 Titration of water by surfactant (TTAB and CTAB) measured by means of HRUS 102T, at 25 °C and at frequency 15MHz.

	TTAB			CTAB	
c_{TTAB}	*U12*	*N12*	c_{CTAB}	*U12*	*N12*
mmol/l	m/s	1/m	mmol/l	m/s	1/m
0.0000	0.0316	0.2154	0.0000	0.0195	-0.1686
0.0958	0.0590	0.0988	0.1947	0.0794	0.0903
0.1913	0.0811	0.0763	0.3886	0.1266	0.0789
0.2863	0.1023	0.0878	0.5819	0.1692	0.1019
0.3811	0.1231	0.0991	0.7744	0.2071	0.0860
0.4755	0.1431	-0.0221	0.9662	0.2410	0.0930
0.5695	0.1638	0.0897	1.1573	0.2616	0.0849
0.6632	0.1836	0.1186	1.3476	0.2650	0.0814
0.7565	0.2030	0.0010	1.5373	0.2656	0.0672
0.8495	0.2244	0.0574	1.7262	0.2660	0.0950
0.9421	0.2490	-0.0318	1.9145	0.2660	0.0948
1.0344	0.2757	0.0959	2.1021	0.2660	0.0884
1.1264	0.3017	-0.0617	2.2890	0.2662	0.0993
1.2180	0.3286	0.0857	2.4752	0.2662	0.1041
1.3093	0.3541	0.0931	2.6607	0.2662	0.0980
1.4003	0.3783	0.0695	2.8455	0.2660	0.1207
1.4909	0.4015	-0.0007	3.0296	0.2661	0.1089
1.5812	0.4249	-0.0078	3.2131	0.2661	0.1043
1.6711	0.4477	0.0665	3.3959	0.2661	0.1113
1.7608	0.4698	0.0509	3.5781	0.2664	0.1354
1.8501	0.4914	0.0181	3.7596	0.2663	0.1375
1.9391	0.5130	0.1059	3.9404	0.2664	0.1298
2.0277	0.5330	-0.0120	4.1206	0.2666	0.1293
2.1161	0.5536	0.0795	4.3001	0.2669	0.1333
2.2041	0.5735	0.0664	4.4790	0.2671	0.1493
2.2918	0.5928	0.0687	4.6573	0.2675	0.1418
2.3792	0.6117	-0.0399	4.8349	0.2678	0.1519
2.4663	0.6314	0.0629	5.0118	0.2680	0.1488
2.5531	0.6509	0.0914	5.1882	0.2683	0.1589
2.6395	0.6686	-0.0687	5.3639	0.2686	0.1595
2.7257	0.6873	0.0476	5.5390	0.2690	0.1602
2.8115	0.7060	0.0679	5.7134	0.2693	0.1624
2.8971	0.7241	0.0021	5.8872	0.2699	0.1536
2.9823	0.7432	0.0615	6.0605	0.2704	0.1619
3.0673	0.7617	0.0345	6.2331	0.2710	0.1837
3.1519	0.7803	-0.0962	6.4051	0.2715	0.1864
3.2363	0.7991	-0.0284	6.5765	0.2722	0.1856
3.3203	0.8174	0.0716	6.7473	0.2730	0.1795
3.4041	0.8342	-0.0279	6.9175	0.2735	0.1913
3.4875	0.8505	-0.0129	7.0870	0.2743	0.1931

3.5707	0.8647	-0.0803	7.2560	0.2749	0.1862
3.6535	0.8776	0.0270	7.4245	0.2755	0.1814
3.7361	0.8887	0.0804	7.5923	0.2764	0.1966
3.8184	0.8974	0.0752	7.7595	0.2771	0.2038
3.9004	0.9039	0.0260	7.9262	0.2779	0.2089
4.0229	0.9122	-0.0159	8.1751	0.2791	0.2168
4.1448	0.9184	0.0490	8.4227	0.2802	0.2264
4.2660	0.9229	0.0427	8.6690	0.2818	0.2155
4.3866	0.9264	0.0582	8.9141	0.2829	0.2275
4.5066	0.9292	-0.0031	9.1579	0.2843	0.2294
4.6259	0.9309	-0.0443	9.4004	0.2856	0.2378
4.7447	0.9329	-0.0024	9.6417	0.2871	0.2371
4.8628	0.9352	0.0779	9.8818	0.2885	0.2473
4.9803	0.9360	-0.0903	10.1207	0.2899	0.2403
5.0973	0.9378	0.0884	10.3583	0.2915	0.2708
5.2136	0.9391	0.0898	10.5947	0.2932	0.2743
5.3294	0.9393	-0.0940	10.8300	0.2950	0.2670
5.4446	0.9405	0.0534	11.0640	0.2963	0.2662
5.5592	0.9415	0.0755	11.2969	0.2979	0.2633
5.6732	0.9428	0.0945	11.5286	0.2996	0.2670
5.7866	0.9435	0.0767	11.7592	0.3014	0.2798
5.8995	0.9432	-0.0647	11.9886	0.3030	0.2913
6.0118	0.9444	0.0710	12.2168	0.3046	0.2833
6.1236	0.9458	0.1018	12.4439	0.3062	0.2846
6.2348	0.9458	0.0723	12.6699	0.3080	0.2943
6.3455	0.9458	-0.0209	12.8948	0.3097	0.3134
6.4556	0.9473	0.0996	13.1186	0.3114	0.3017
6.5652	0.9476	-0.0611	13.3412	0.3133	0.2993
6.6742	0.9484	0.1036	13.5628	0.3149	0.2966
6.7827	0.9482	-0.0311	13.7833	0.3164	0.3137
6.8907	0.9493	0.0956	14.0027	0.3183	0.3297
6.9981	0.9497	0.0894	14.2211	0.3200	0.3260
7.1051	0.9503	0.0905	14.4384	0.3219	0.3313
7.2115	0.9506	0.1086	14.6546	0.3236	0.3391
7.3174	0.9505	-0.0569	14.8698	0.3251	0.3353
7.4227	0.9513	0.0853	15.0839	0.3269	0.3377
7.5276	0.9514	0.0150	15.2971	0.3285	0.3443
7.6320	0.9520	0.0988	15.5091	0.3304	0.3457
7.7359	0.9519	-0.0447	15.7202	0.3323	0.3492
7.8392	0.9531	0.1034	15.9303	0.3337	0.3468
7.9421	0.9533	0.0032	16.1394	0.3357	0.3580
8.0445	0.9533	-0.0631	16.3475	0.3374	0.3632
8.1464	0.9535	-0.0602	16.5545	0.3391	0.3565
8.2479	0.9545	0.0421	16.7607	0.3407	0.3675
8.3488	0.9545	-0.0559	16.9658	0.3426	0.3526
8.4493	0.9545	-0.0095	17.1700	0.3445	0.3726

Table ST37 Titration of sodium chloride solution (0.15 M NaCl) by surfactant (TTAB and CTAB) measured by means of HRUS 102T, at 25 °C and at frequency 15MHz.

	TTAB			CTAB	
c_{TTAB}	*U12*	*N12*	c_{CTAB}	*U12*	*N12*
mmol/l	m/s	1/m	mmol/l	m/s	1/m
0.0000	9.5587	1.2773	0.0000	9.5081	0.9910
0.0222	9.5699	0.7043	0.0235	9.5159	0.7383
0.0443	9.5837	0.6954	0.0470	9.5212	0.7994
0.0664	9.5984	0.7176	0.0705	9.5238	0.7377
0.0885	9.6122	0.6775	0.0939	9.5245	0.7404
0.1105	9.6271	0.7714	0.1172	9.5250	0.7295
0.1324	9.6408	0.6935	0.1406	9.5253	0.7286
0.1544	9.6548	0.7127	0.1638	9.5263	0.7327
0.1762	9.6692	0.7311	0.1871	9.5262	0.7077
0.1981	9.6832	0.6748	0.2103	9.5267	0.7363
0.2199	9.6974	0.6602	0.2334	9.5264	0.6922
0.2417	9.7119	0.6998	0.2565	9.5276	0.7324
0.2634	9.7267	0.7414	0.2796	9.5279	0.7446
0.2851	9.7408	0.7552	0.3026	9.5286	0.6991
0.3067	9.7549	0.7205	0.3256	9.5286	0.8181
0.3283	9.7689	0.7774	0.3485	9.5286	0.7467
0.3499	9.7831	0.7369	0.3714	9.5289	0.7453
0.3714	9.7976	0.7295	0.3942	9.5295	0.7576
0.3929	9.8117	0.6555	0.4170	9.5295	0.6967
0.4143	9.8260	0.6699	0.4398	9.5297	0.7429
0.4357	9.8406	0.7300	0.4625	9.5301	0.6986
0.4571	9.8549	0.7436	0.4852	9.5311	0.8056
0.4784	9.8690	0.7729	0.5078	9.5310	0.7434
0.4997	9.8819	0.6912	0.5304	9.5317	0.7804
0.5210	9.8959	0.8233	0.5530	9.5328	0.7750
0.5422	9.9065	0.8479	0.5755	9.5318	0.7007
0.5633	9.9193	0.7426	0.5980	9.5322	0.7790
0.5845	9.9311	0.7427	0.6204	9.5321	0.7378
0.6056	9.9421	0.7353	0.6428	9.5329	0.7062
0.6266	9.9532	0.7649	0.6651	9.5335	0.7798
0.6476	9.9627	0.7199	0.6874	9.5331	0.7373
0.6686	9.9735	0.7546	0.7097	9.5344	0.8276
0.6895	9.9835	0.7406	0.7319	9.5342	0.7336
0.7104	9.9935	0.7758	0.7541	9.5344	0.7269
0.7313	10.0030	0.7621	0.7762	9.5348	0.7054
0.7521	10.0126	0.8323	0.7983	9.5349	0.7041
0.7729	10.0220	0.7168	0.8204	9.5354	0.7256
0.7937	10.0321	0.7617	0.8424	9.5358	0.6422
0.8144	10.0406	0.7560	0.8644	9.5363	0.7566
0.8351	10.0497	0.6971	0.8864	9.5368	0.7402

0.8557	10.0600	0.7792	0.9083	9.5373	0.7342
0.8763	10.0692	0.7908	0.9301	9.5374	0.7231
0.8968	10.0781	0.7592	0.9519	9.5376	0.7168
0.9379	10.0965	0.8095	0.9737	9.5374	0.6564
0.9583	10.1062	0.8287	0.9955	9.5389	0.7186
0.9787	10.1143	0.7689	1.0172	9.5392	0.7494
0.9991	10.1238	0.7671	1.0389	9.5396	0.7460
1.0194	10.1332	0.8587	1.0605	9.5401	0.7452
1.0397	10.1415	0.7823	1.0821	9.5404	0.7258
1.0600	10.1519	0.8376	1.1036	9.5410	0.6886
1.0802	10.1600	0.7380	1.1251	9.5413	0.7478
1.1004	10.1687	0.7892	1.1466	9.5419	0.7807
1.1206	10.1787	0.7945	1.1680	9.5422	0.7356
1.1407	10.1870	0.8605	1.1894	9.5426	0.7319
1.1608	10.1949	0.7057	1.2108	9.5428	0.6571
1.1809	10.2054	0.8592	1.2321	9.5436	0.7082
1.2009	10.2132	0.7938	1.2534	9.5440	0.7101
1.2208	10.2226	0.8160	1.2746	9.5449	0.7269
1.2408	10.2309	0.8075	1.2958	9.5450	0.7250
1.2607	10.2395	0.7915	1.3170	9.5452	0.7048
1.2806	10.2490	0.8142	1.3381	9.5459	0.7240
1.3004	10.2569	0.7790	1.3592	9.5466	0.7316
1.3202	10.2657	0.7836	1.3803	9.5470	0.7675
1.3400	10.2747	0.8927	1.4013	9.5476	0.7953
1.3597	10.2834	0.7444	1.4223	9.5479	0.7404
1.3794	10.2919	0.8837	1.4432	9.5482	0.6891
1.3991	10.2999	0.8077	1.4641	9.5486	0.7818
1.4187	10.3087	0.8048	1.4850	9.5494	0.7674
1.4383	10.3171	0.8213	1.5058	9.5494	0.7398
1.4578	10.3250	0.6983	1.5266	9.5503	0.7855
1.4774	10.3344	0.8351	1.5474	9.5506	0.7366
1.4969	10.3423	0.7535	1.5681	9.5510	0.7286
1.5163	10.3514	0.7686	1.5888	9.5516	0.7348
1.5357	10.3598	0.8797	1.6095	9.5525	0.8285
1.5551	10.3680	0.8175	1.6301	9.5527	0.7799
1.5745	10.3763	0.7880	1.6507	9.5526	0.7302
1.5938	10.3849	0.8077	1.6712	9.5531	0.7366
1.6131	10.3937	0.8783	1.6917	9.5537	0.7531
1.6323	10.4012	0.8325	1.7122	9.5538	0.7366
1.6515	10.4098	0.8198	1.7326	9.5548	0.7459
1.6707	10.4183	0.8421	1.7530	9.5551	0.7963
1.6899	10.4265	0.8662	1.7734	9.5555	0.8054
1.7090	10.4353	0.8588	1.7937	9.5554	0.7228
1.7281	10.4430	0.8420	1.8140	9.5558	0.7228
1.7471	10.4518	0.8980	1.8342	9.5567	0.8321
1.7661	10.4594	0.8013	1.8545	9.5570	0.8101

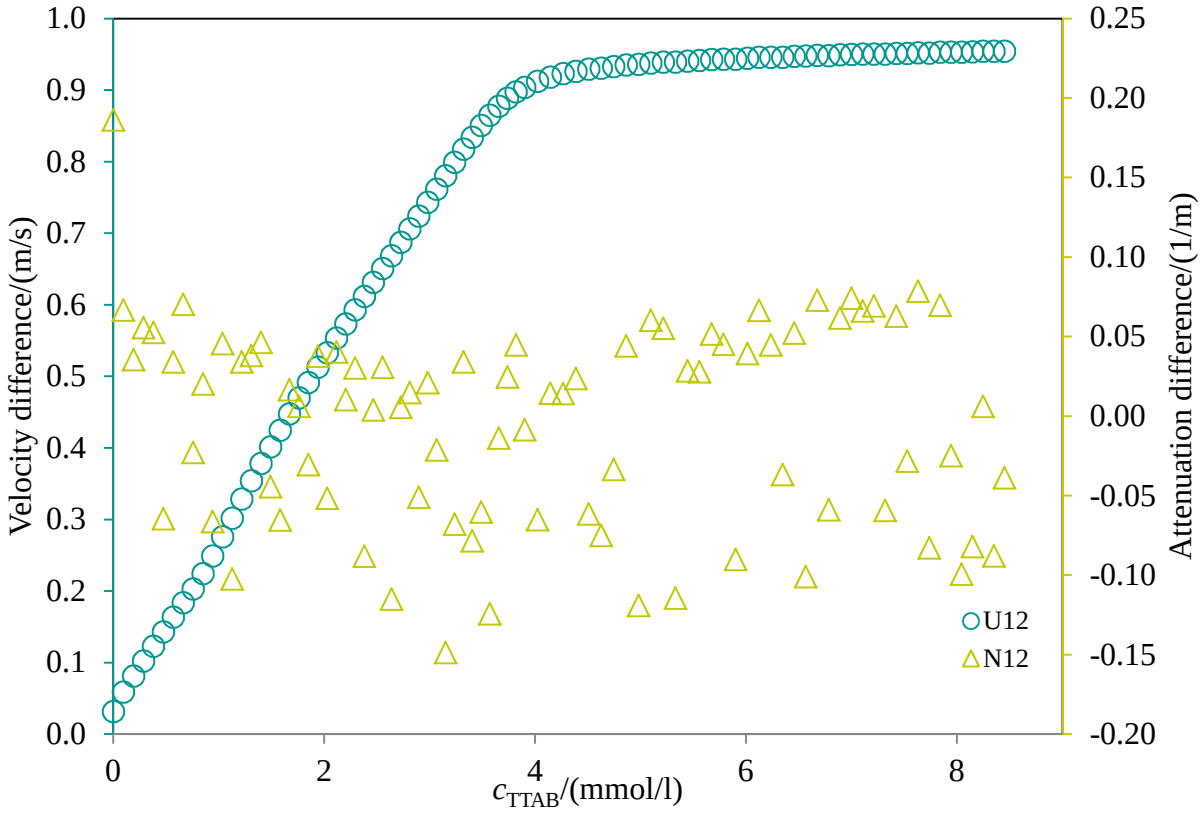

Figure SF8 The titration curve of water with TTAB at 25 °C, at frequency 15 MHz.

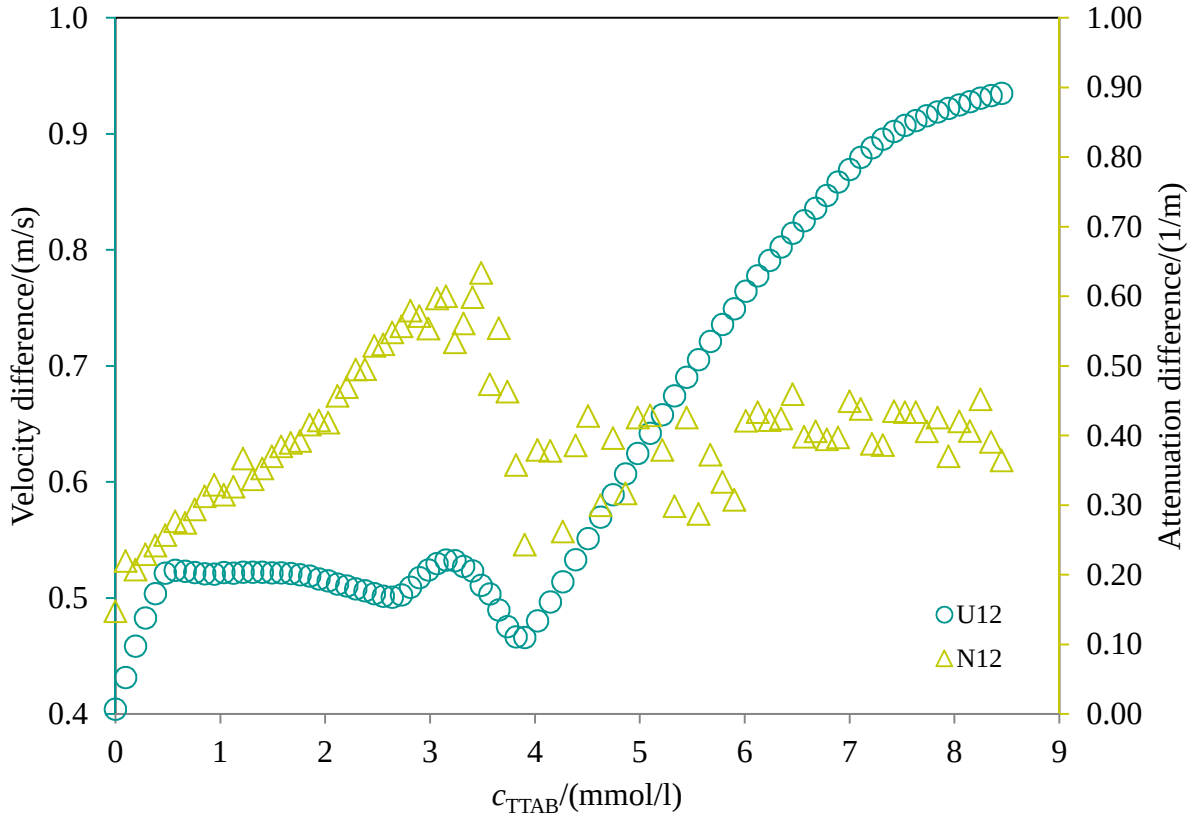

Figure SF9 The titration curve of the surfactant binding with hyaluronan of concentration 1000 mg/l and molecular weight of 300-500kDa, in water at 25 °C, at frequency 15 MHz.

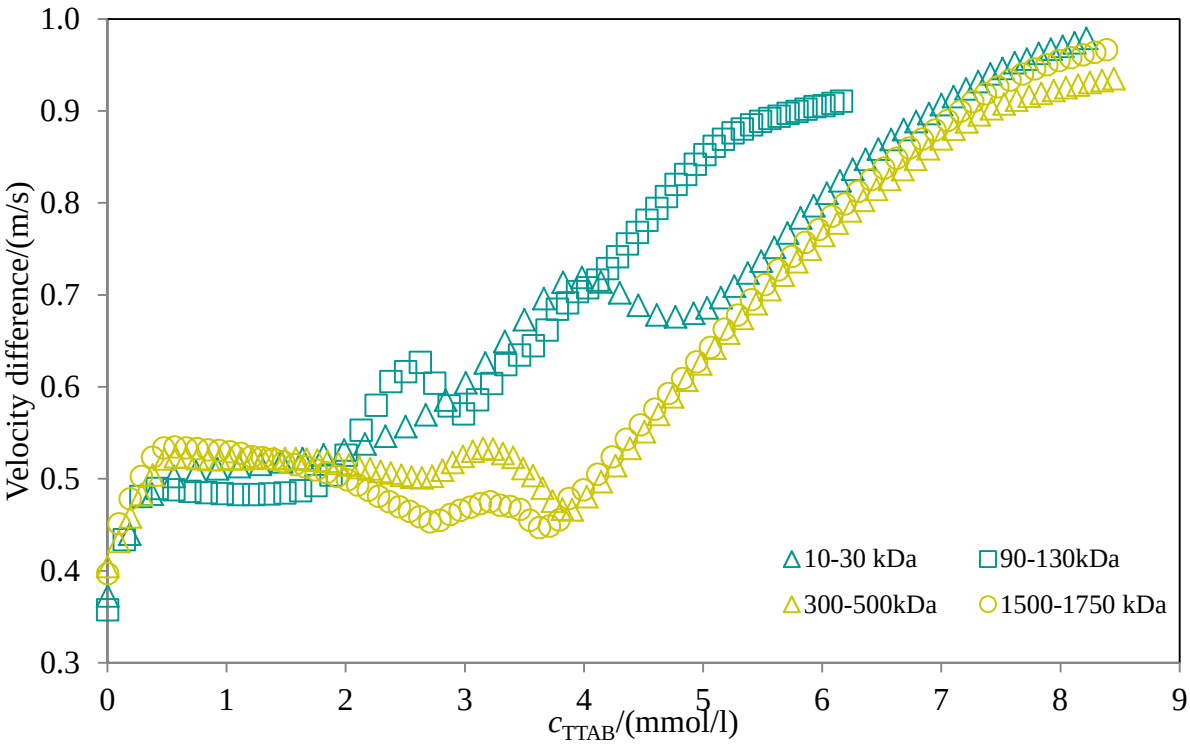

Figure SF10 The effect of molecular weight on ultrasonic velocity profile of hyaluronan-TTAB system in water, at 25 °C, at frequencies 15 MHz. Hyaluronan 1000mg/l.

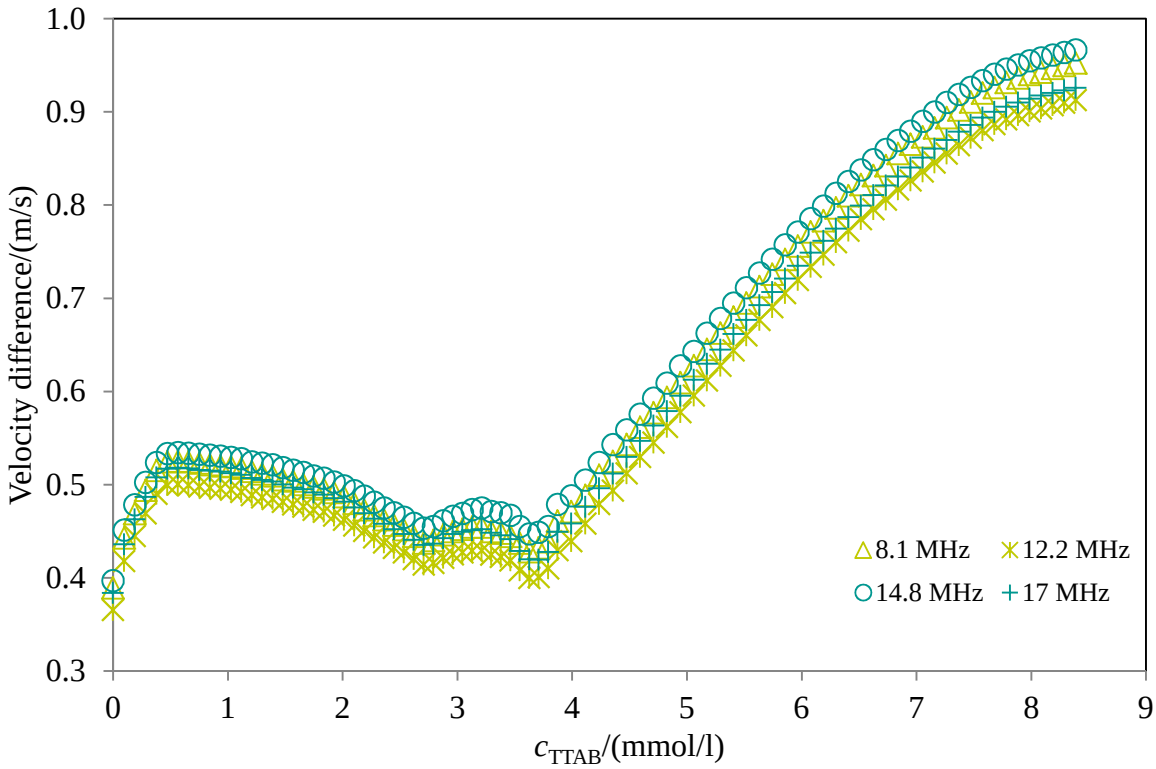

Figure SF11 The effect of frequency on ultrasonic velocity profile of hyaluronan-TTAB system in water, at 25 °C, at frequencies 2.8-17.5 MHz. Hyaluronan 1000mg/l 300-500 kDa.

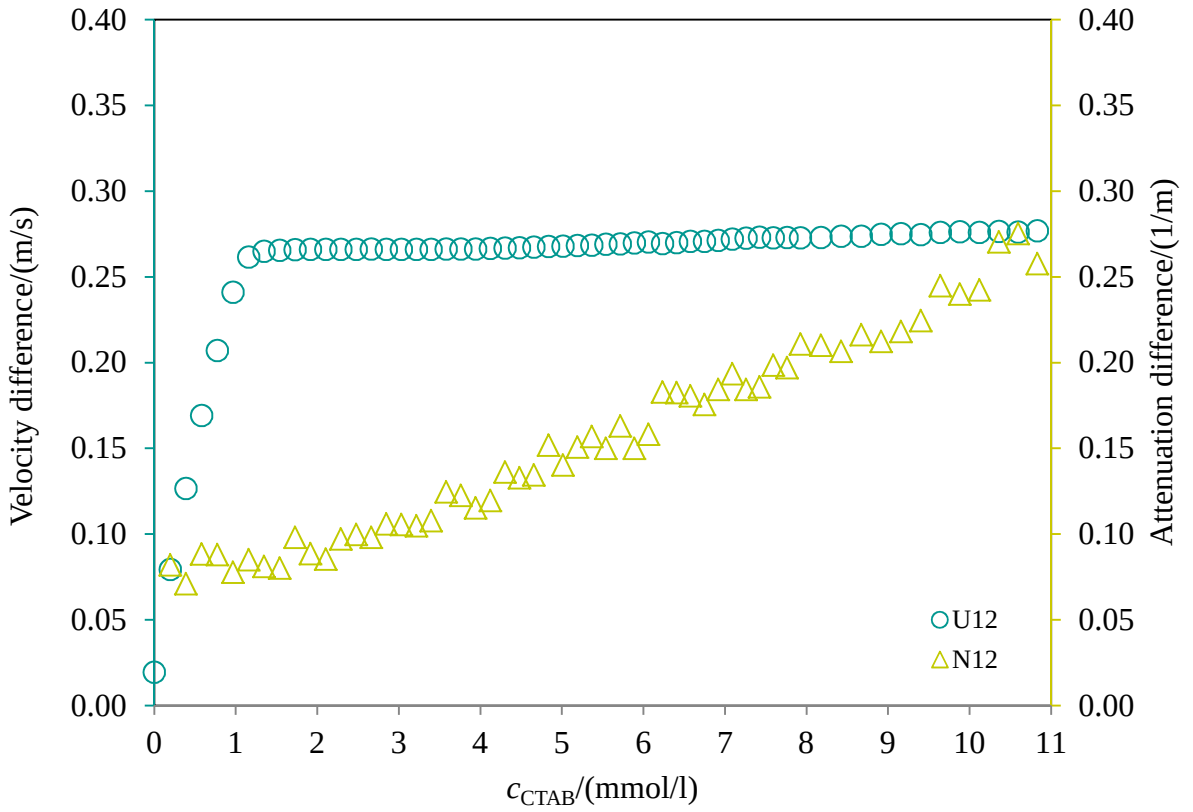

Figure SF12 The titration curve of water by CTAB at 25 °C, at frequency 15 MHz.

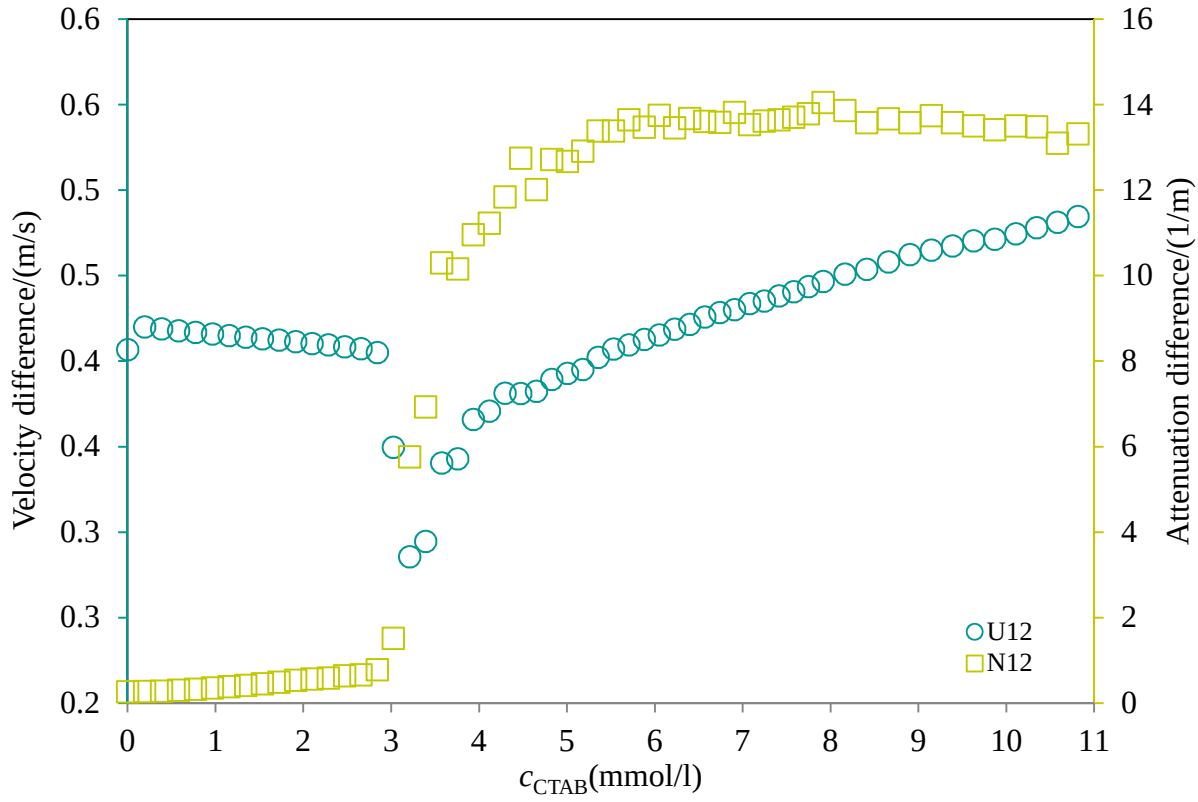

Figure SF13 The titration curve of the surfactant (CTAB) binding with hyaluronan of concentration 1000 mg/l and molecular weight of 300-500kDa, in water at 25 °C, at frequency 15 MHz.

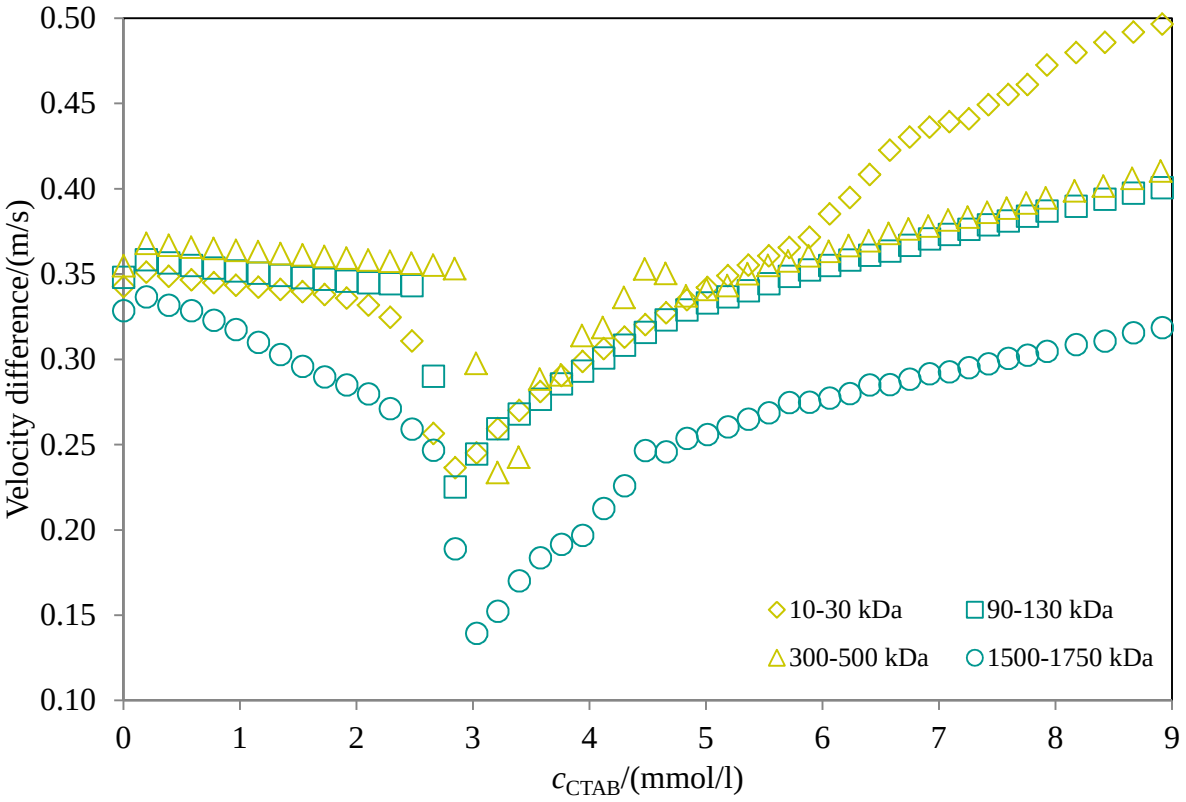

Figure SF14 The effect of molecular weigh of hyaluronan on ultrasonic velocity profile of system hyaluronan-CTAB in water, at 25 °C, at frequencies 15 MHz. Hyaluronan 1000 mg/l.

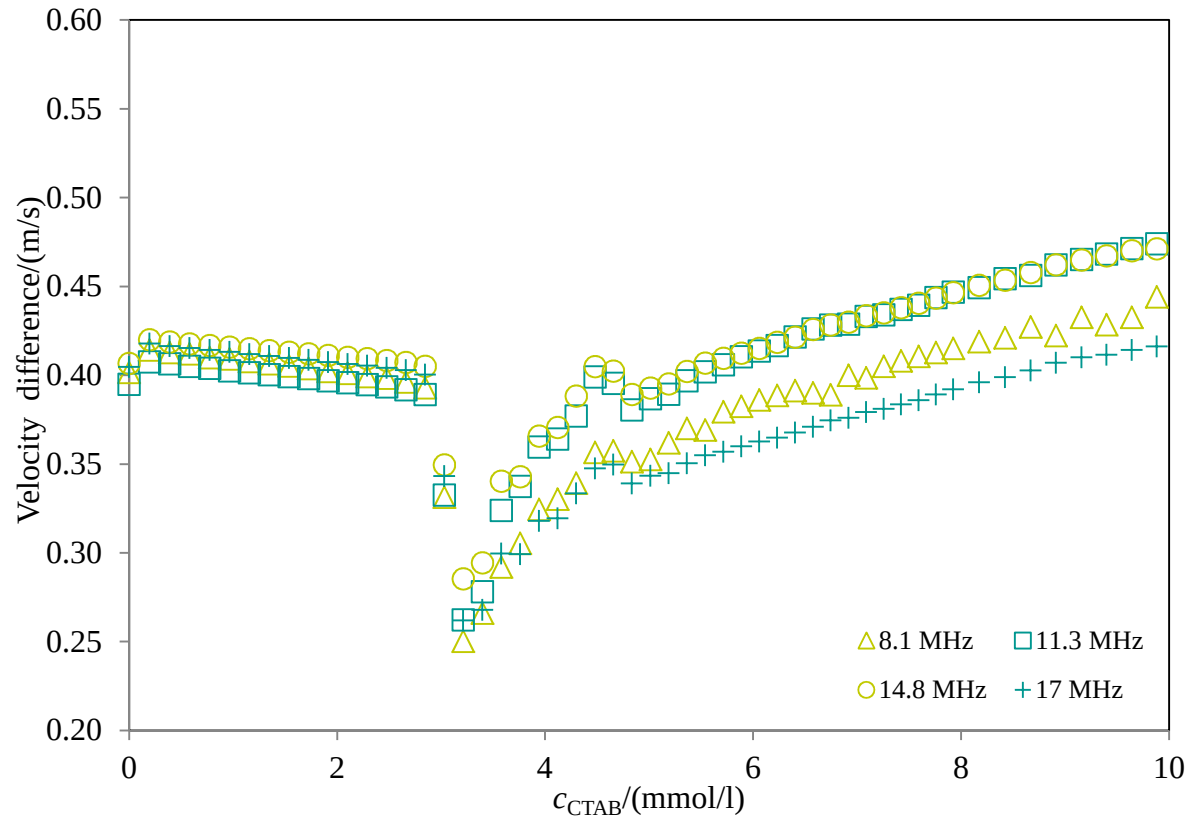

Figure SF15 The effect of frequency on ultrasonic velocity profile of hyaluronan-CTAB system in water, at 25 °C, at frequencies 2.8-17.5 MHz. Hyaluronan 1000 mg/l 300-500 kDa.

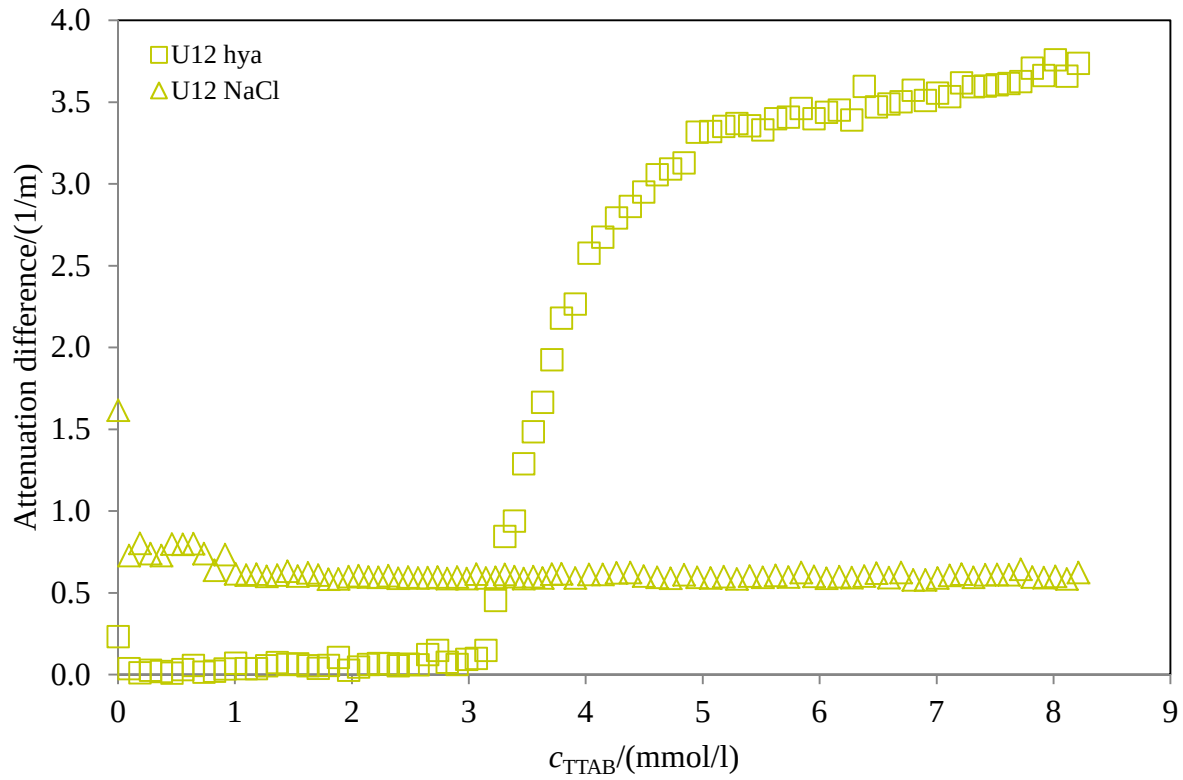

Figure SF16 The titration curve of hyaluronan of concentration 1000 mg/l and molecular weight of 300-500kDa and titration curve of water with TTAB, at frequency 15 MHz.

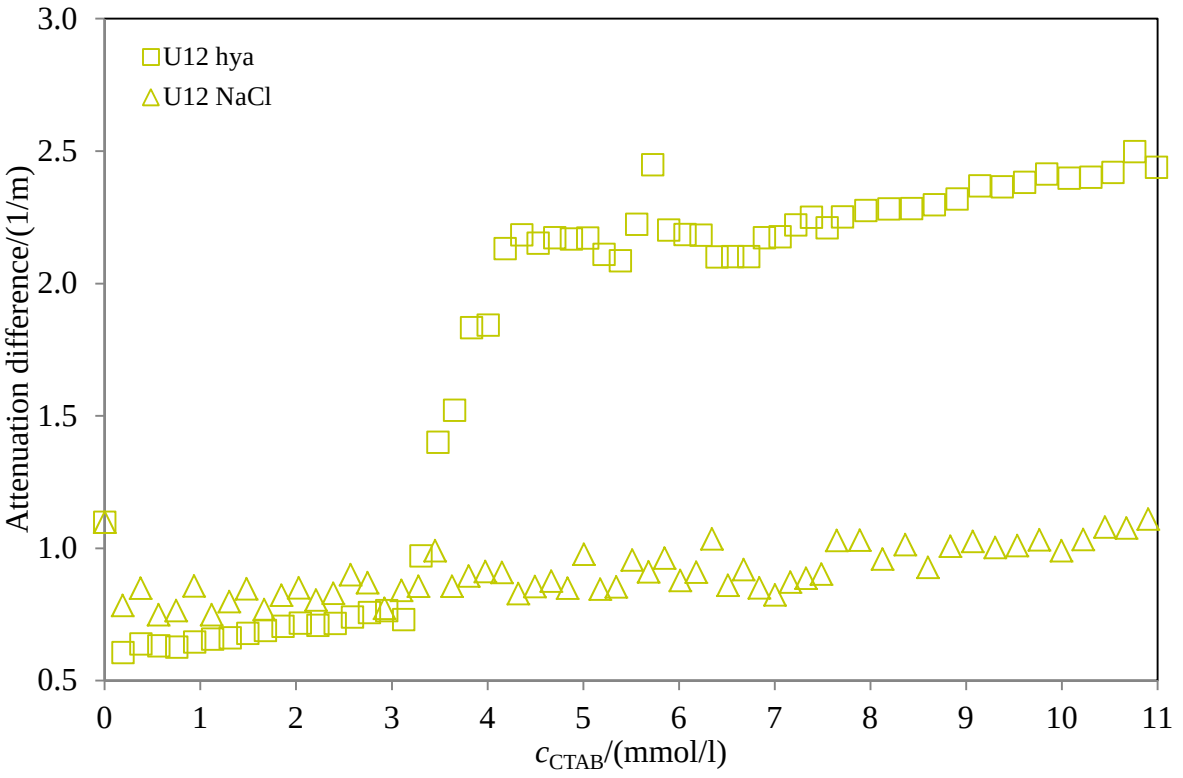

Figure SF17 The attenuation titration profile of hyaluronan of concentration 1000 mg/l and molecular weight of 300-500kDa and the titration profile of water with CTAB, at frequency 15 MHz. The titration curve of 0.15 M NaCl is shifted to first point of hyaluronan curve.

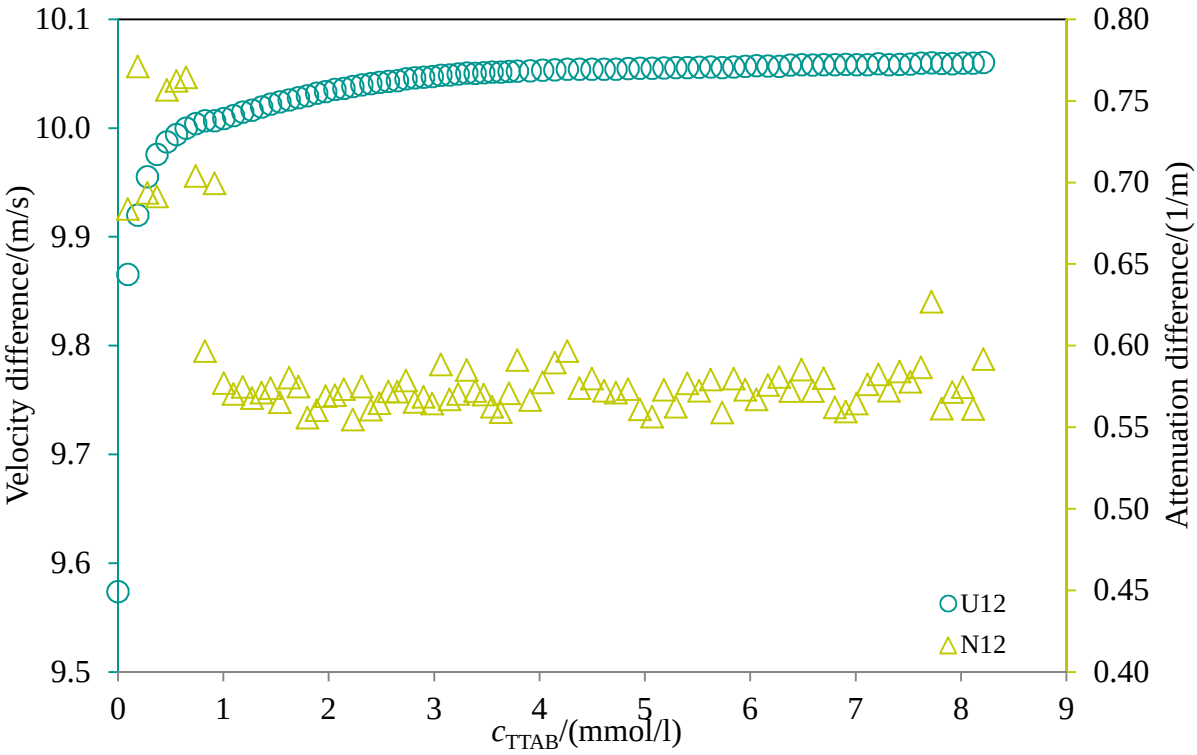

Figure SF18 The titration curve of sodium chloride solution (0.15 M NaCl) with TTAB at 25 °C, at frequency 15 MHz.

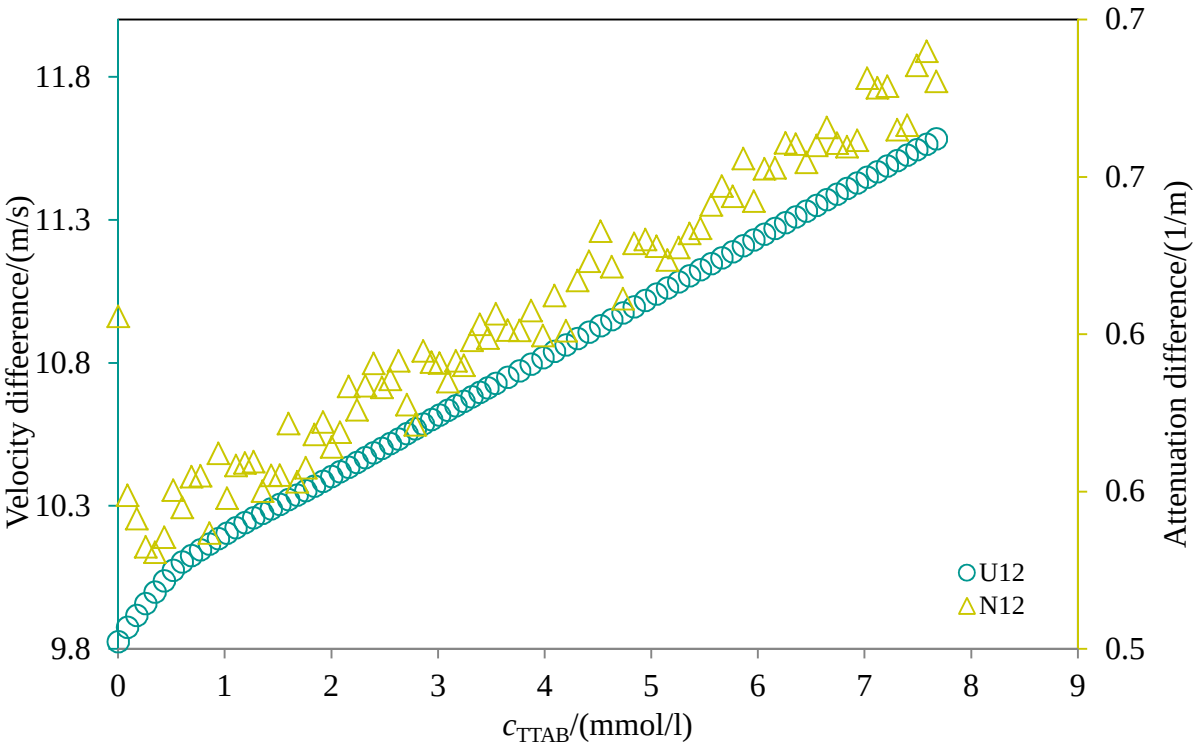

Figure SF19 Ultrasonic titration profile of hyaluronan (1000 mg/l, 10-30kDa) with surfactant TTAB in 0.15 M NaCl. Change in ultrasonic velocity in solution caused by addition of the surfactant is plotted as function of concentration of surfactant. The curve for 25 °C corresponds to the binding of surfactant micelles to hyaluronan chain, at frequency 15 MHz.

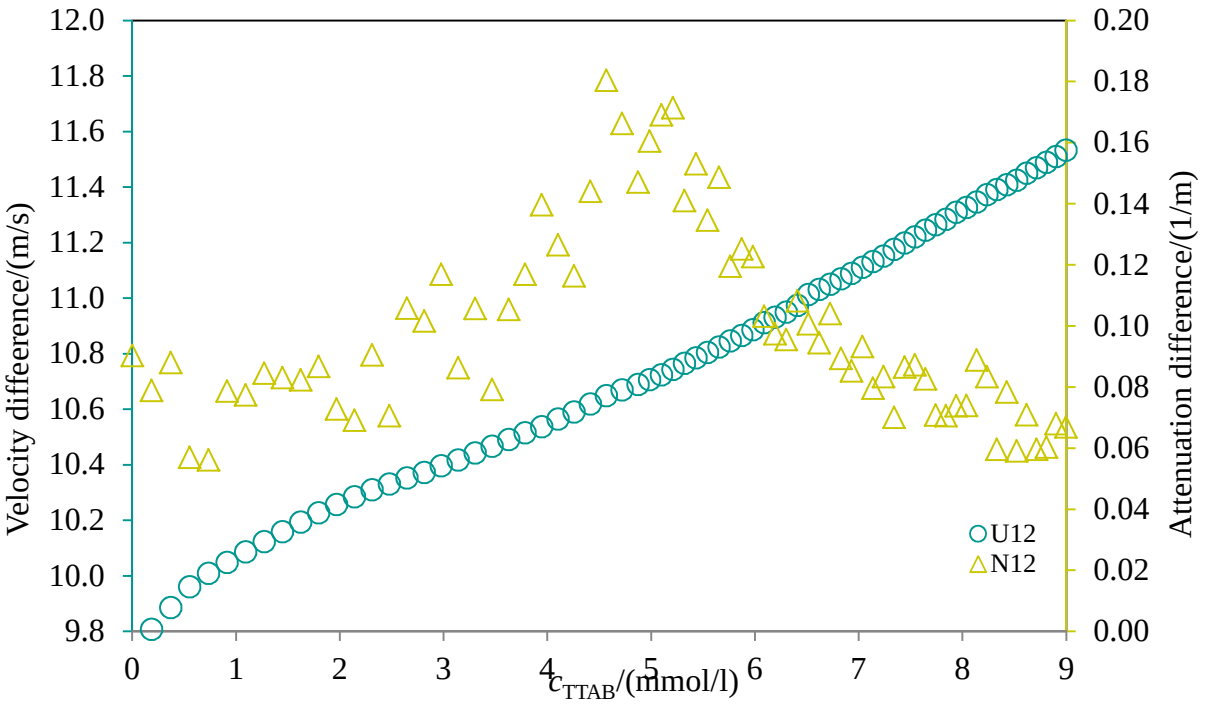

Figure SF20 Ultrasonic titration profile of hyaluronan (1000 mg/l, 90-130kDa) with surfactant TTAB in 0.15 M NaCl. Change in ultrasonic velocity in solution caused by addition of the surfactant is plotted as function of concentration of surfactant. The curve for 25 °C corresponds to the binding of surfactant micelles to hyaluronan chain, at frequency 15 MHz.

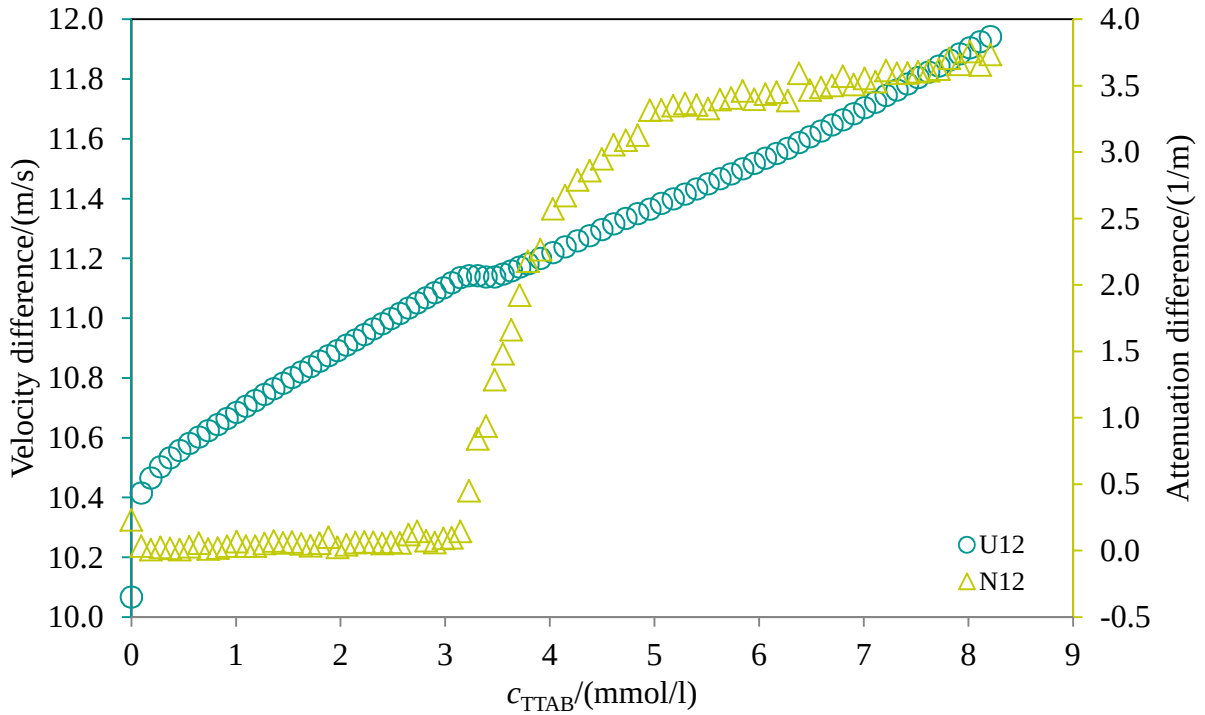

Figure SF21 Ultrasonic titration profile of hyaluronan (1000 mg/l, 300-500kDa) with surfactant TTAB in 0.15 M NaCl. Change in ultrasonic velocity in solution caused by addition of the surfactant is plotted as function of concentration of surfactant. The curve for 25 °C corresponds to the binding of surfactant micelles to hyaluronan chain, at frequency 15 MHz.

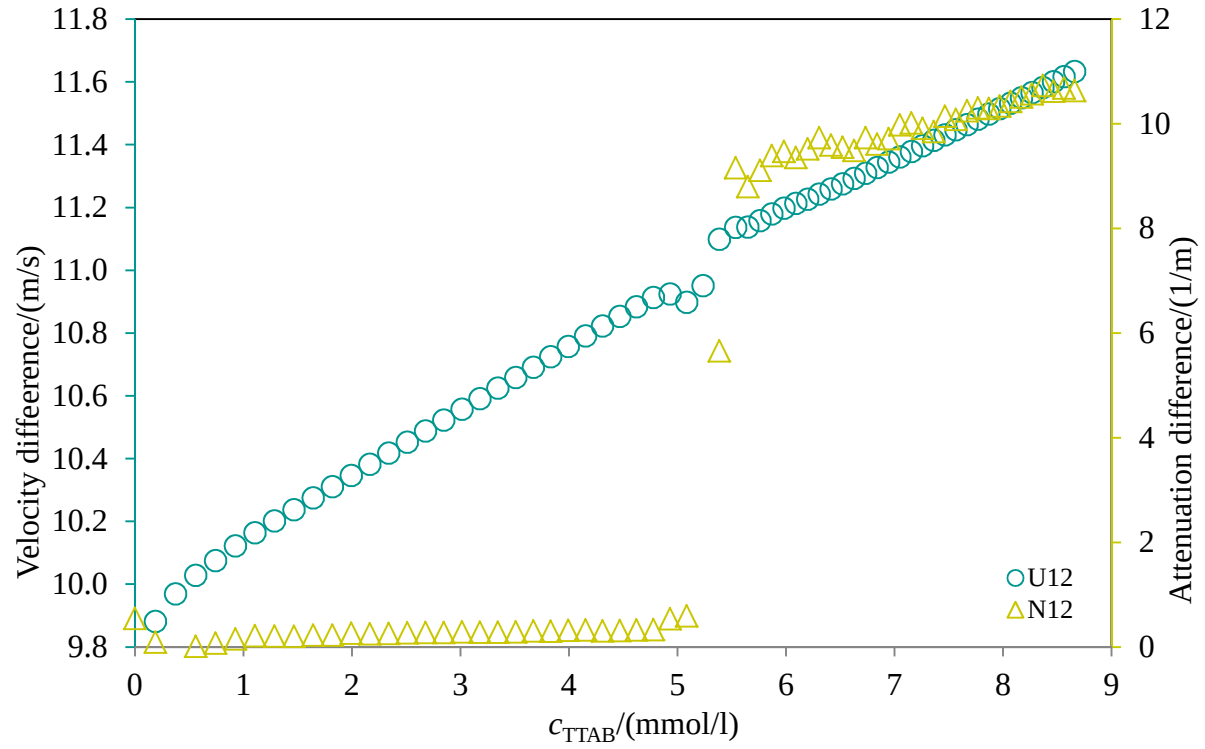

Figure SF22 Ultrasonic titration profile of hyaluronan (1000 mg/l, 1500-1750kDa) with surfactant TTAB in 0.15 M NaCl. Change in ultrasonic velocity in solution caused by addition of the surfactant is plotted as function of concentration of surfactant. The curve for 25 °C corresponds to the binding of surfactant micelles to hyaluronan chain, atfrequency 15 MHz.

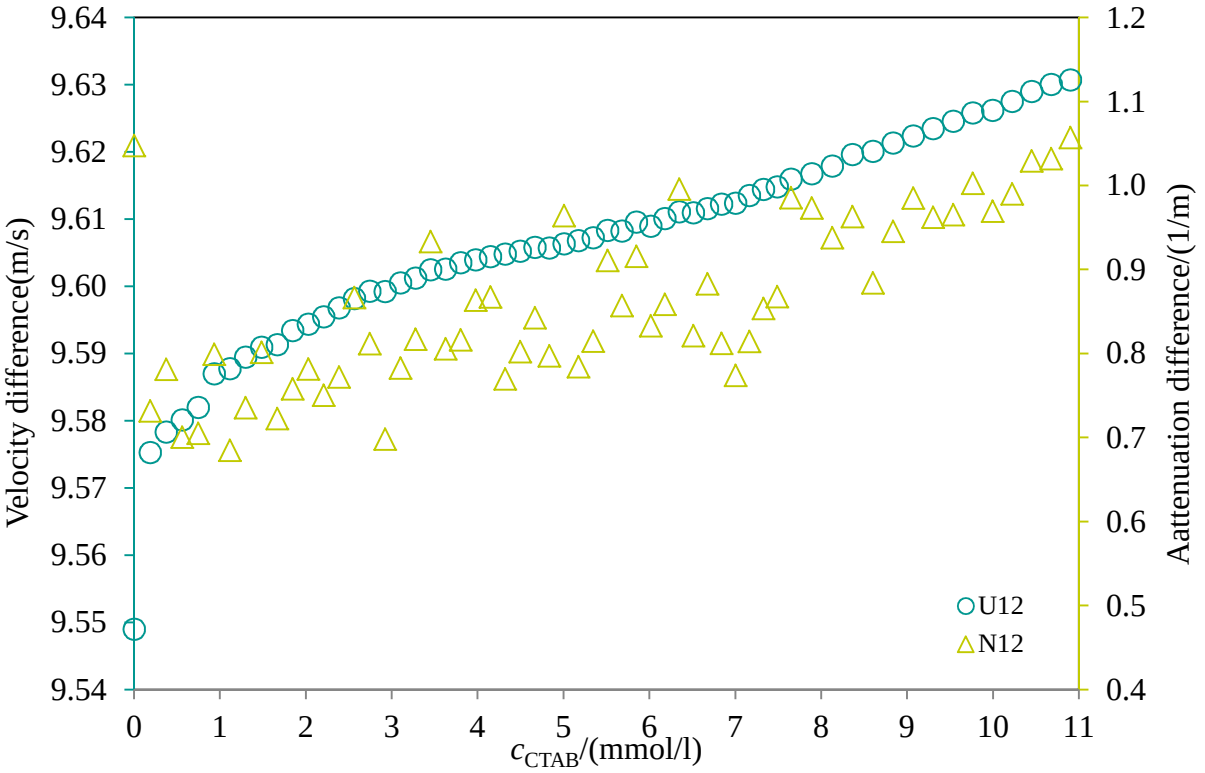

Figure SF23 The titration curve of sodium chloride solution (0.15 M NaCl) with CTAB at 25 °C, at frequency 15 MHz.

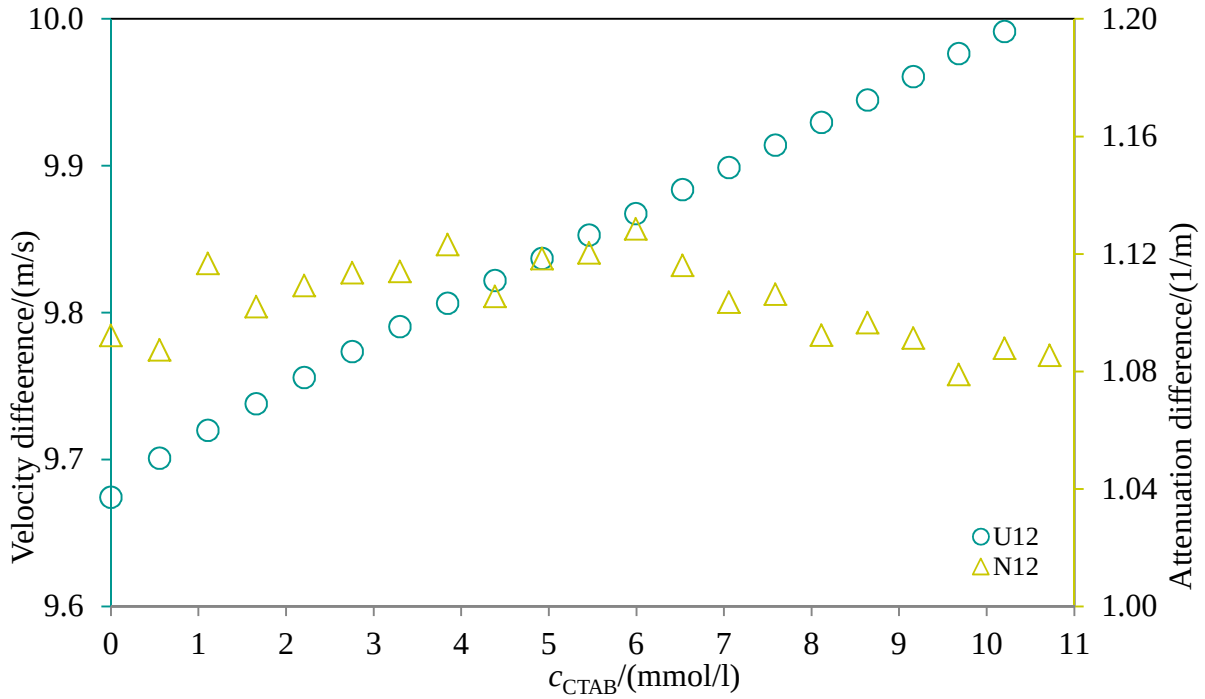

Figure SF24 Ultrasonic titration profile of hyaluronan (1000 mg/l, 10-30kDa) with surfactant CTAB in 0.15 M NaCl. Change in ultrasonic velocity in solution caused by addition of the surfactant is plotted as function of concentration of surfactant. The curve for 25 °C corresponds to the binding of surfactant micelles to hyaluronan chain, at 15 MHz.

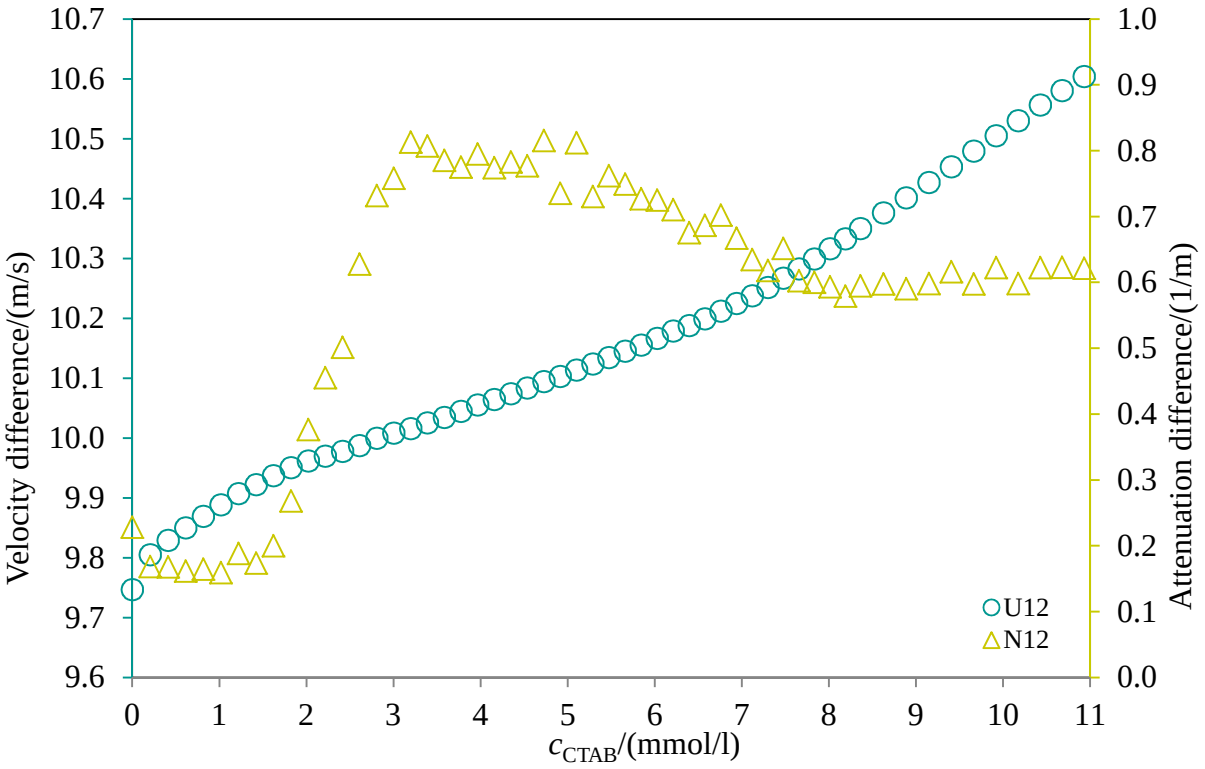

Figure SF25 Ultrasonic titration profile of hyaluronan (1000 mg/l, 90-130kDa) with surfactant CTAB in 0.15 M NaCl. Change in ultrasonic velocity in solution caused by addition of the surfactant is plotted as function of concentration of surfactant. The curve for 25 °C corresponds to the binding of surfactant micelles to hyaluronan chain, at frequency 15 MHz.

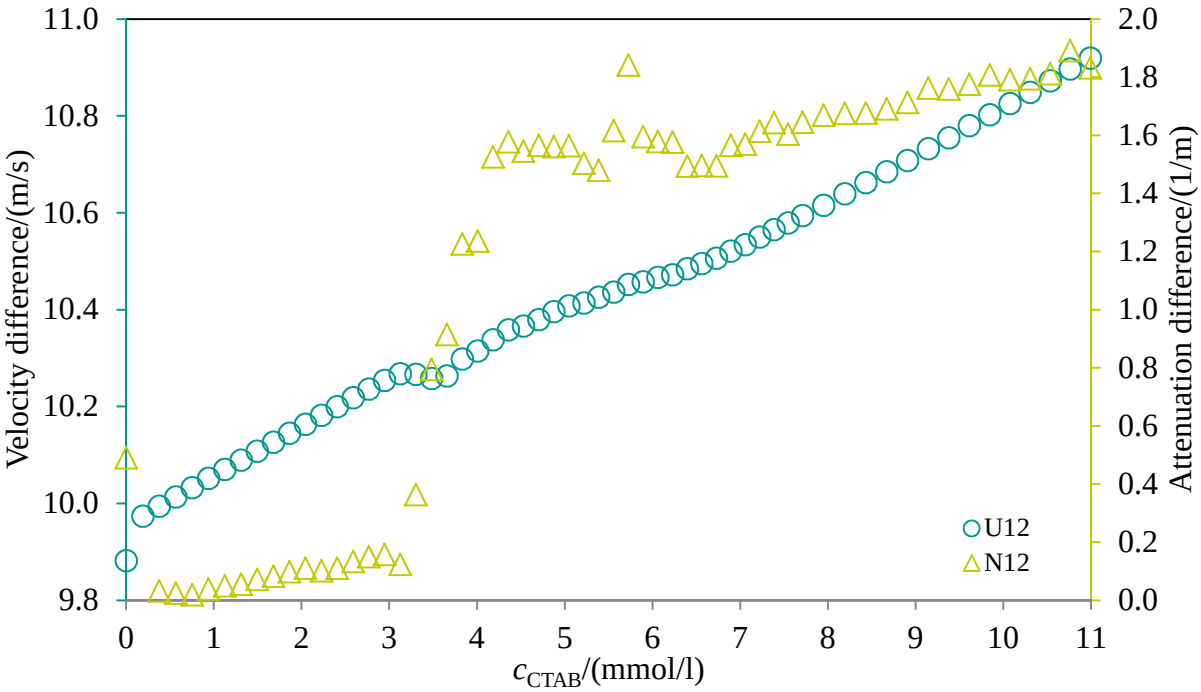

Figure SF26 Ultrasonic titration profile of hyaluronan (1000 mg/l, 300-500kDa) with surfactant CTAB in 0.15 M NaCl. Change in ultrasonic velocity in solution caused by addition of the surfactant is plotted as function of concentration of surfactant. The curve for 25 °C corresponds to the binding of surfactant micelles to hyaluronan chain, at frequency 15 MHz.

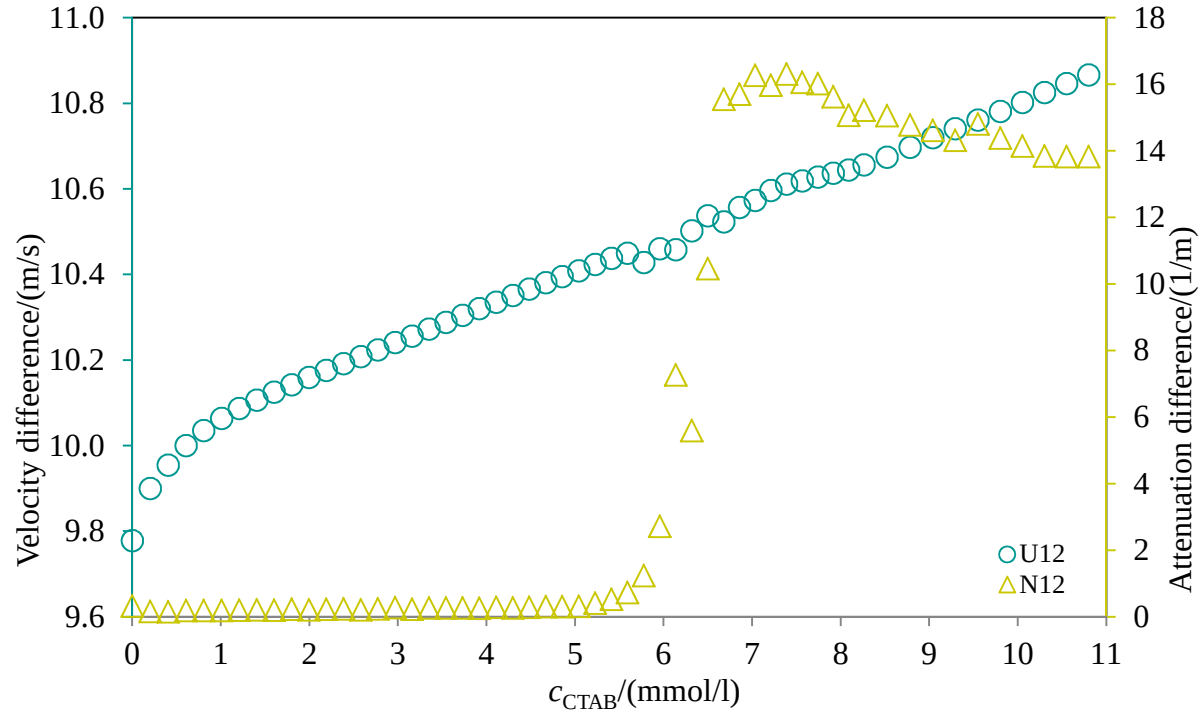

Figure SF27 Ultrasonic titration profile of hyaluronan (1000 mg/l, 1500-1750kDa) with surfactant CTAB in 0.15 M NaCl. Change in ultrasonic velocity in solution caused by addition of the surfactant is plotted as function of concentration of surfactant. The curve for 25 °C corresponds to the binding of surfactant micelles to hyaluronan chain, at frequency 15 MHz.

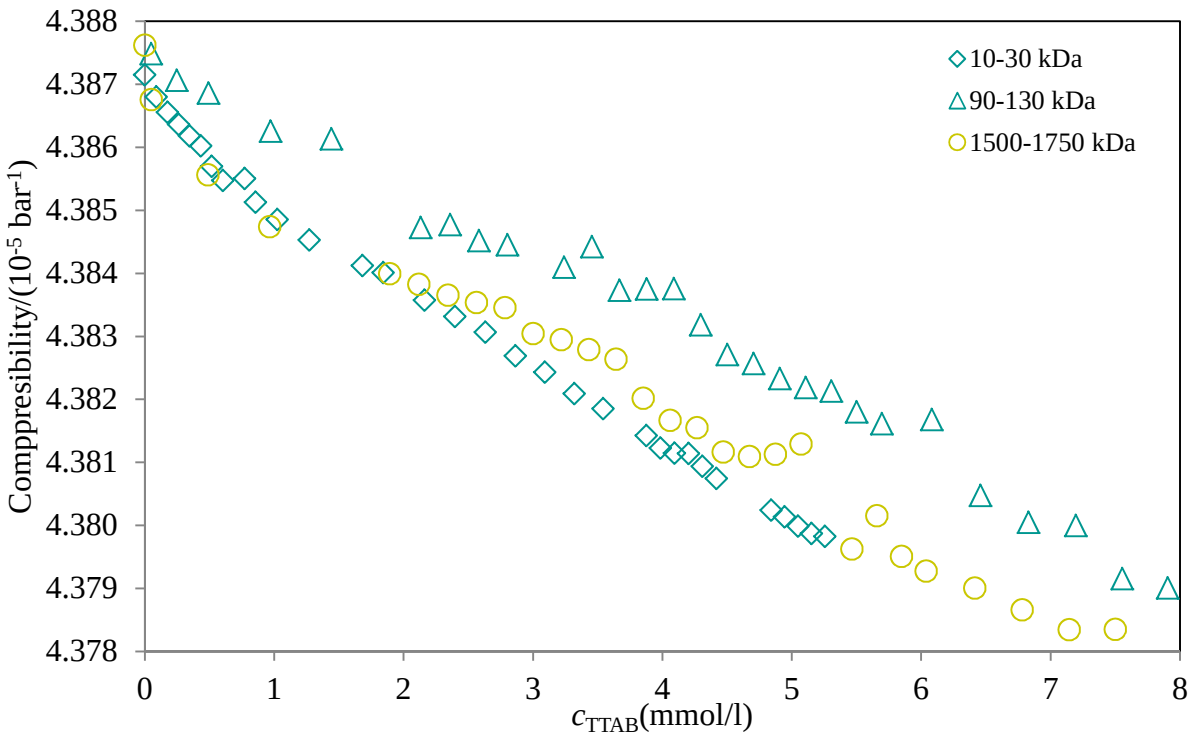

Figure SF28 Adiabatic comppresibility of hyaluronan-TTAB system in 0.15 NaCl.

13 REPRINTS OF PUBLICATIONS

KARGEROVÁ, Andrea, Miloslav PEKAŘ. Densitometry and ultrasound velocimetry of hyaluronan solutions in water and in sodium chloride solution. *Carbohydrate Polymers*. 2014.

Type of publication: research article

Carbohydrate Polymers xxx (2014) xxx–xxx

Contents lists available at ScienceDirect

Carbohydrate Polymers

journal homepage: www.elsevier.com/locate/carbpol

Densitometry and ultrasound velocimetry of hyaluronan solutions in water and in sodium chloride solution

A. Kargerová, M. Pekař*

Brno University of Technology, Faculty of Chemistry, Materials Research Centre, Purkyňova 118, Brno CZ-61200, Czech Republic

ARTICLE INFO

Article history:
Received 17 October 2013
Received in revised form 6 January 2014
Accepted 7 January 2014

Keywords:
Compressibility
Density
Hyaluronan
Hydration
Ultrasound velocity

ABSTRACT

The densities of hyaluronan solutions in water and 0.15 M NaCl were measured in the temperature range from 25 to 50 °C for the hyaluronan molecular weights from 10 to 1750 kDa. The density increased linearly with concentration and decreased with temperature. The data were fitted by the equation describing the density as a linear function of concentration and a quadratic function of temperature. The effect of molecular weight was negligible and thus single equation was sufficient to describe all data. The apparent and partial specific volumes were calculated from the density data including their extrapolated values to infinite dilutions. The measurement of ultrasound speed in the same solutions under the same conditions enabled to calculate the compressibility and its dependence on concentration and temperature. The compressibility decreased with both the concentration and the temperature but the effect of the concentration was only slight mild. The compressibility was used to estimate the hydration numbers which slightly decreased with increasing temperature and concentration. The addition of NaCl changed only the numerical values of density and ultrasound velocity while not changing the character of their dependence on temperature and concentration. Measured and calculated data indicate that hyaluronan does not disturb the specific water structure in the studied concentration range and support the idea of the existence of water clusters or nanodroplets hydrating the hyaluronan chains in solution.

1. Introduction

Hyaluronan is a linear polysaccharide built from regularly alternating monosaccharides, glucuronic acid and N-acetylglucosamine, which form a basic disaccharide unit (Lapčík, Lapčík, Smedt, Demeester, & Chabreček, 1998). It is an abundant biopolymer with a wide range of naturally occurring molecular masses from several hundreds to 10^7 g/mol. The highest concentrations of hyaluronan occur in synovial fluid, vitreous body, skin and in certain specialized tissues such as umbilical cord and rooster comb. The largest amounts are found in the intercellular matrix of skin and in musculoskeletal tissues (Kogan, Šoltés, Stern, & Gemeiner, 2006). Due to its biocompatibility and non-immunogenicity hyaluronan is an attractive material for various cosmetic and medical applications (Kuo, 2006) and is produced industrially mostly by biotechnological processes. The solution properties of hyaluronan are well documented, particularly with respect to the chain structure and size, rheology, and electrolyte-related properties. Rinaudo (2009) states that there is nothing very remarkable in the behaviour of hyaluronan in solution. It is a typical semi-flexible polyelectrolyte with the properties dependent on concentration and molecular weight. Even at low concentrations the zero shear viscosity is high and the complex viscosity remains non-Newtonian which contribute to much higher apparent molecular weight of entangled hyaluronan chains. The review (Cowman & Matsuoka, 2005) summarizes the studies of hydrodynamic properties of hyaluronan in neutral aqueous solutions in the presence of physiological NaCl concentration as the expected behaviour of a high molecular weight linear semi-flexible polymer. The dependence of the intrinsic viscosity on hyaluronan molecular weight follows two straight lines – higher slope is found in the low molecular weight region. This is in accord with the predicted change from short chains in somewhat extended shape to longer chains which are coiled into hydrodynamic spheres as the molecular weight increases. The persistence length which is a measure of the intrinsic stiffness of the chains (which is the same for both short and long chains) is used to explain the change in the slope and is reported to be between 4 and 10 nm. The unusual high viscosity of hyaluronan solutions arises from the huge hydrodynamic volume and also from transient interchain interactions. The significant nonideality found for hyaluronan solutions could be predicted by simple models for hydrodynamic interactions between polymer chains.

The studies on the density of hyaluronan solutions are scarce. Gómez-Alejandre, Blanca, Usera, Rey-Stolle, and

* Corresponding author. Tel.: +420 541149330; fax: +420 541149398.
E-mail address: pekar@fch.vutbr.cz (M. Pekař).

0144-8617/$ – see front matter © 2014 Elsevier Ltd. All rights reserved.
http://dx.doi.org/10.1016/j.carbpol.2014.01.020

Hernández-Fuentes (2000) measured the density of high molecular weight hyaluronan (1.5 MDa) either in water at different pH or in the presence of several inorganic salts. In water and in $CaCl_2$ solution they also determined the effect of temperature. Their main interest was the determination of the partial specific volume at infinite dilution and the density data were not analysed and discussed. Some density data are reported in the paper by García-Abuín, Gómez-Díaz, Navaza, Regueiro, and Vidal-Tato (2011) but its main aim was the study of viscosimetric behaviour of hyaluronan in aqueous and water-alcohol solutions. Only single hyaluronan sample of high molecular weight (1.43 MDa) was used in this work and the density was reported for five concentration points at 20 and 50 °C. No analysis of density data was given.

Our interest in density data of hyaluronan solutions comes from the studies of hyaluronan and its interactions measured by means of high resolution ultrasound spectroscopy (Sarvazyan, 1982, 1983; Buckin, Kankiya, Sarvazyan, & Uedaira, 1989). The ultrasound measurements are usually accompanied by the measurements of density in order to enable the calculations of compressibility from ultrasound velocity and density. The densitometer used in this study allowed also the measurement of the ultrasound velocity although of lower resolution and precision. Besides the density we thus report also the data on ultrasound velocity. There are several studies on ultrasound propagation in hyaluronan solutions. The speed of sound is reported in García-Abuín et al. (2011) for the same sample and conditions as described above for the density and is not further analysed. Suzuki and Uedaira (1970) and Davies, Gormally, Wyn-Jones, Wedlock, and Phillips (1982, 1983) used the compressibilities for the study of hyaluronan hydration.

In this study we used a wide range of hyaluronan molecular weights and as broad range of its concentration as possible to measure the density of solutions and the ultrasound velocity in solutions in details which have not been explored. From the measured data the additional parameters like the partial specific volume, the compressibility or the hydration number were calculated. The solutions were prepared either in water or in aqueous solution of NaCl at the physiological concentration (0.15 M).

2. Materials and methods

Hyaluronan of several molecular weights was obtained from Contipro Biotech (Czech Republic). It is produced biotechnologically and extracted from the cell walls of the bacteria *Streptococcus zooepidemicus*. This producer offers a broad range of molecular weights in predefined range of molecular weights. The following products were used in this study: 10–30 kDa, 110–130 kDa, 300–500 kDa and 1500–1750 kDa; particular molecular weights (determined by the producer using SEC-MALS) of particular samples from each range used in this study are given in Table ST0 in Supplementary information. Sodium chloride of p.a. purity was obtained from Lachner (Czech Republic).

The hyaluronan solutions were prepared at the concentration ranges reported in Tables ST1a-d and ST2a-d in Supplementary information by dissolving the original hyaluronan powder slowly in water or in 0.15 M NaCl in a closed vessel. The selected concentration range was dependent on the molecular weight and was selected in order to enable the sample injection into the densitometer without problems (not too high viscosity and no entrapment of bubbles). The solutions were prepared by weighing their components. The solutions were stirred for 24 h at the room temperature to ensure the complete dissolution; the preliminary density measurements made after up to 14 days of dissolution confirmed that 24 h are sufficient to obtain stable and reproducible results. Ultrapure deionized water from PURELAB water purification system (Option R7/15; ELGA, Great Britain) was used for the preparation of all samples.

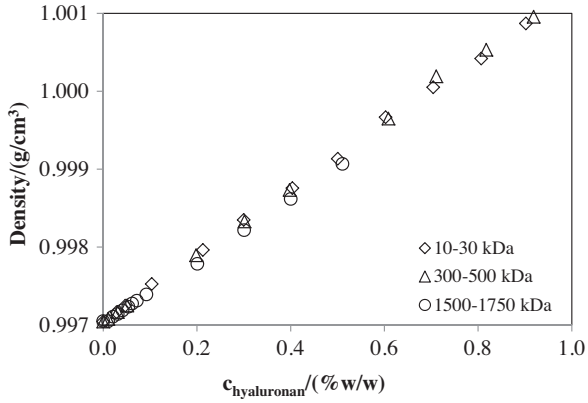

Fig. 1. The dependence of density on hyaluronan concentration at 25 °C. Solutions of hyaluronan of different molecular weights in water.

The density and ultrasound velocity were measured for all molecular weights in the temperature range from 25 to 50 °C using the densitometer DSA 5000 M (Anton Paar, Austria) with the accuracy of density measurement of 0.000005 g/cm^3. DSA 5000 M is equipped with a density cell and a sound velocity cell with the temperature controlled by a built-in Peltier thermostat. Both the density and the velocity were measured simultaneously. The temperature was controlled with integrated Pt 1000 temperature sensor with the accuracy of 0.001 °C. The calibration of densitometer was performed at 20 °C using air and water. The samples were degassed using the syringe and then they were injected into U-shaped borosilicate glass tube that was excited electronically to vibrate at its characteristics frequency. It had to be ensured that the U-tube was properly filled and that no gas bubbles were present.

The density and velocity measurements of each molecular weight range, at each concentration and for each temperature were made at least in triplicates. The data fitting and the statistical analyses were made with QC.Expert 3.3 software (TriloByte, Czech Republic).

3. Results and discussion

All the measured data on density and ultrasound velocity are collected in Tables ST1a-d, ST2a-d, ST6a-d and ST7a-d in Supplementary information. First, the result obtained for the solutions in water is discussed.

3.1. Density

The density increased with increasing concentration and decreased with increasing temperature. The data for all molecular weights are collected in Table ST1a-d in Supplementary information. The effect of molecular weight on the density was negligible. The example of the concentration dependence on the density at 25 °C in water is given in Fig. 1, where also the independence on the molecular weight is seen. The linear concentration dependence was typical for all temperatures. The example of the temperature dependence is shown in Fig. 2. The temperature dependencies were slightly curved the reason of what was the temperature effect on the density of pure solvents (see Figure SF1 in Supplementary information).

The density-concentration-temperature data were fitted for each molecular weight by two models – linear and quadratic in temperature – to compare the effect of including the slight curvature

Please cite this article in press as: Kargerová, A., & Pekař, M. Densitometry and ultrasound velocimetry of hyaluronan solutions in water and in sodium chloride solution. *Carbohydrate Polymers* (2014), http://dx.doi.org/10.1016/j.carbpol.2014.01.020

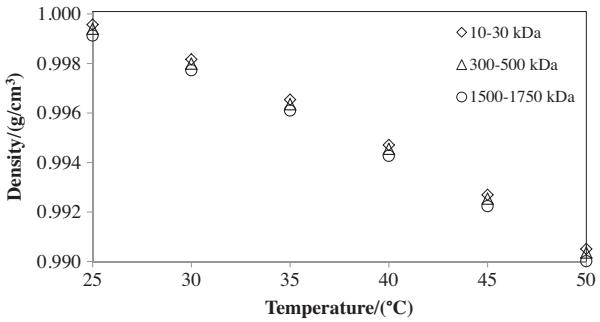

Fig. 2. The temperature dependence of density of hyaluronan solutions at the concentration of 0.5% (w/w). Solutions of hyaluronan of different molecular weights in water.

into the fitting equation. The latter model is called the quadratic model henceforth. The model equations are as follows:

$$\text{linear}: \quad \rho = a_0 + a_w c_w + a_t t$$

$$\text{quadratic}: \quad \rho = a_0 + a_w c_w + a_t t + a_{tt} t^2$$

where ρ is the density of hyaluronan solution in g/cm^3, c_w is the concentration of hyaluronan in grams per kilogram of solution, t is the temperature in °C and a_i denotes the (fitted) parameters. The results of regression fits were evaluated on the basis of following characteristics: multiple correlation coefficient (R), coefficient of determination (R^2), predicted coefficient of determination (R_p), mean quadratic error of prediction (MEP), and Akaike information criterion (AIC). These characteristics are collected in Table ST3 in Supplementary information and show that the quadratic model fits better the data. The parameters of quadratic models are given in Table 1 and the parameters of linear models in Table ST4 in Supplementary information for the sake of completeness.

Because the molecular weight did not show appreciable effect on the density the whole set of data over all molecular weights was fitted by one common equation. In this way a single equation was obtained which can serve for a reasonable estimate of density of hyaluronan solution at desired concentration and temperature which fall within their ranges used in this work and with hyaluronan molecular weights within the range from 10 up to 1750 kDa. The statistical characteristics of this overall fit are given in Table ST3 in Supplementary information and corresponding model parameters in the last row of Table 1.

Taking into account the smooth and (almost) linear dependence of the density on hyaluronan concentration and temperature it is concluded that no evident changes, e.g. in hyaluronan conformation, inter- or intrachain interactions, were detected by densitometry within used concentration and temperature ranges.

3.2. Volume characteristics

The measurements of density are usually used to calculate the volume characteristics of the solution and solvent. Perhaps the most frequently reported characteristic is the apparent specific volume defined as the difference between the solution and solvent volumes per unit solute mass; in our case:

$$V_{app} = \frac{V - V_0}{m_{hya}} \tag{1}$$

V is the solution, V_0 is the solvent volume, and m_{hya} is the hyaluronan mass in the solution. Expressing volumes in terms of densities the following relationships can be derived to calculate the apparent specific volume from measured densities:

$$V_{app} = \frac{m_0(\rho_0 - \rho)}{\rho\rho_0 m_{hya}} + \frac{1}{\rho} \tag{2}$$

$$V_{app} = \frac{m_0}{m_{hya}}\left(\frac{1}{\rho} - \frac{1}{\rho_0}\right) + \frac{1}{\rho} \tag{3}$$

where m_0 is the solvent mass in the solution, ρ_0 is the solvent and ρ the solution density. Both expressions gave identical values of V_{app} within the measurement precision of our data, as expected.

In thermodynamics, the effects of mixture components on mixture properties are rigorously described by partial quantities. They are defined as partial derivatives of a mixture property expressed as a function of relevant variables. In our case, the mixture property is the volume and the variable is the hyaluronan (solute) mass keeping the other variables (temperature, pressure) constant. The partial specific volume is then defined as follows:

$$\tilde{V}_{sp,hya} = \frac{\partial V}{\partial m_{hya}}; \quad T, p = \text{const.} \tag{4}$$

This definition can be expressed in terms of measured density using the solute mass fraction (w_{hya}):

$$\tilde{V}_{sp,hya} = \frac{1}{\rho} + (m_0 + m_{hya})\frac{\partial(1/\rho)}{\partial w_{hya}}\frac{\partial w_{hya}}{\partial m_{hya}} \tag{5}$$

Evaluating the second of the two partial derivatives, the final expression for calculating the partial specific volume from experimental data is obtained:

$$\tilde{V}^0_{sp,hya} = \frac{1}{\rho}\left[1 - \frac{1 - w_{hya}}{\rho}\frac{\partial\rho}{\partial w_{hya}}\right] \tag{6}$$

Note that this calculation requires the slope of the dependence of the solution density on hyaluronan mass fraction.

Table 1
Parameters of quadratic model and their standard deviations for hyaluronan solutions of different molecular weights.

M_w (kDa)	Solvent	a_0 (g/cm^3)	a_w (10^{-4} kg/cm^3)	a_t (10^{-5} g/cm^3 °C)	a_{tt} (10^{-6} g/cm^3(°C)^2)
10–30	Water	$1.00152 \pm 8 \times 10^{-5}$	4.1 ± 0.03	-7.2 ± 1.1	-3.9 ± 0.15
110–130		$1.00124 \pm 39 \times 10^{-5}$	4.0 ± 0.03	-5.8 ± 2.1	-4.1 ± 0.28
300–500		$1.00149 \pm 26 \times 10^{-5}$	4.1 ± 0.03	-7.6 ± 1.4	-3.8 ± 0.19
1500–1750		$1.00110 \pm 9 \times 10^{-5}$	3.8 ± 0.02	-6.1 ± 0.5	-4.0 ± 0.06
10–30	NaCl[a]	$1.00795 \pm 20 \times 10^{-5}$	4.1 ± 0.01	-9.2 ± 1.1	-3.7 ± 0.15
110–130		$1.00806 \pm 22 \times 10^{-5}$	4.0 ± 0.02	-9.1 ± 1.2	-3.7 ± 0.16
300–500		$1.00800 \pm 16 \times 10^{-5}$	4.3 ± 0.02	-9.3 ± 0.9	-3.7 ± 0.12
1500–1750		$1.00786 \pm 16 \times 10^{-5}$	4.2 ± 0.04	-8.8 ± 0.9	-3.8 ± 0.11
10–1750	Water	$1.00131 \pm 17 \times 10^{-5}$	4.1 ± 0.013	-6.6 ± 0.9	-4.0 ± 0.12
10–1750	NaCl[a]	$1.00797 \pm 17 \times 10^{-5}$	4.1 ± 0.009	-9.1 ± 0.6	-3.7 ± 0.08

[a] 0.15 M in water.

Please cite this article in press as: Kargerová, A., & Pekař, M. Densitometry and ultrasound velocimetry of hyaluronan solutions in water and in sodium chloride solution. *Carbohydrate Polymers* (2014), http://dx.doi.org/10.1016/j.carbpol.2014.01.020

Gómez-Alejandre et al. (2000) calculated hyaluronan partial specific volumes according to the following equation:

$$\bar{v}^0_{sp,hya} = \frac{1}{\rho_0}\left[1 - \frac{1}{\rho_0}\left(\frac{\partial\rho}{\partial w_{hya}}\right)^0\right] \quad (7)$$

where $\bar{v}^0_{sp,hya}$ is the hyaluronan partial specific volume at infinite dilution (we will call it the limiting partial specific volume here) and the derivative indexed by 0 is the limiting slope of the indicated dependence. This equation was called the rigorous relation but its justification is given neither in (Gómez-Alejandre et al., 2000) nor in Fabre, Tagle, Gargallo, Radic, and Hernandez-Fuentes (1989) to which the former refers. However, this equation can be arrived at as the zero-concentration limit of the partial specific volume, Eq. (6), when $\rho \to \rho_0$, $w_{hya} \to 0$, and the slope goes to its limiting value calculated at the point of zero mass fraction.

The values of the apparent and partial specific volumes are summarized in Tables ST1a-d and ST2a-d in Supplementary information. The apparent specific volume was calculated using the averages of the measured solvent and solution densities and of the corresponding hyaluronan masses. Its value and standard deviation were sensitive to measurements errors, particularly at low concentrations (and higher temperatures) where the solution density was very close to the solvent density. This is quite common situation (Kaulgud & Dhondge, 1988; Lo Surdo, Shin, & Millero, 1978) sometimes attributed also to the effect of dissolved gases in low concentrated samples (Kaulgud & Dhondge, 1988). Therefore only the values of V_{app} with the relative standard deviation not exceeding ca 20% are reported. The partial specific volume was calculated according to Eq. (6) using the averaged densities, averaged hyaluronan mass fractions and the slope of the straight line determined by fitting all experimental points. The values of the partial specific volume were determined much more reliably with the relatively standard deviation below 2% and at more consistent trends with concentration or temperature. Nevertheless, the numerical values of the averages of the two specific volumes were comparable and not too much different.

The partial specific volume slightly increases with increasing hyaluronan concentration which can be expected due to the increasing role and number of interactions with the solvent and inter-chain contacts. Analogical conclusions can be made also for the apparent specific volume. A moderate increase is observed also with the temperature growth; here the data for the partial specific volume are more conclusive. This could be expected and explained by the expansion of hyaluronan coils due to the increased mobility at elevated temperature. The effect of hyaluronan molecular weight on the specific volume was not detected. Thus the hyaluronan partial specific volume in water typically ranges, depending on concentration, between 0.587 and 0.594 cm^3/g at 25 °C and between 0.597 and 0.604 cm^3/g at 50 °C.

Partial or apparent (specific, molar, molal) quantities are typically extrapolated to zero concentration to obtain a value which is supposed to be free of the effects of solute-solute interactions. The extrapolated value should thus reflect only the solute-solvent interactions (Junquera et al., 2002). The extrapolation of the apparent specific volume is usually problematic due to the high uncertainty and nonlinearity of data at very low concentrations and only the linear part of data at reasonably higher concentrations is used to be extrapolated, see e.g. Kaulgud and Dhondge (1988) or Lo Surdo et al. (1978); the same procedure was used in this work. The dependence of the partial specific volume on the hyaluronan concentration was linear and the extrapolation thus was without problems. Eq. (7) is, in fact, also a kind of the extrapolation to the infinite dilution. Due to the linearity of partial specific volume versus hyaluronan concentration the limiting partial specific volume $\bar{v}^0_{sp,hya}$ calculated from this equation is numerically equal to the extrapolated value of the partial specific volume $\bar{V}^0_{sp,hya}$; the latter has much lower standard deviation (owing to the fitting procedure). All the zero concentration volumes are shown in Tables 2 and ST5 in Supplementary information together with their dependence on the temperature. The values slightly increase with temperature and the extrapolated apparent specific volume is somewhat lower than its partial counterparts. Durchschlag and Zipper (1994) as well as Davies et al. (1982) reported the value 0.556 cm^3/g for the extrapolated partial specific volume of sodium hyaluronate at 25 °C with no other experimental details. Gómez-Alejandre et al. (2000) determined the limiting partial specific volume of sodium hyaluronate of a molecular weight of 1500 kDa and it changed from 0.512 cm^3/g at 25 °C to 0.561 cm^3/g at 40 °C. Our values are somewhat higher; due to the lack of original data in the referenced works it is difficult to discuss these differences, we can only point to a narrower concentration range used in ref. by Gómez-Alejandre et al. (2000) and to Haxaire, Maréchal, Milas, and Rinaudo (2003a, 2003b) who reported the density of (solid) hyaluronan to be 1.61 g/cm^3 which gives the specific volume of 0.621 cm^3/g. Further, Perkins, Miller, Hardingham, and Muir (1981) determined the value of the hyaluronan partial specific volume, 0.58 cm^3/g, which is in excellent agreement with our results.

Table 2
Extrapolated partial specific volume of hyaluronan of different molecular weights dissolved in water.

t (°C)	$\bar{V}^0_{sp,hya}$ [a] (10^{-3} cm^3/g)			
	10–30 kDa	90–130 kDa	300–500 kDa	1500–1750 kDa
25	587	587	587	587
30	589	589	589	589
35	592	592	592	592
40	594	594	594	594
45	596	595	595	595
50	597	597	597	597

[a] Standard deviation was less than 5×10^{-5} cm^3/g.

3.3. Ultrasound velocity

The velocity increases (see Table ST6a-d in Supplementary information) with hyaluronan concentration linearly as for many other solutions of low concentration (Povey, 1997); see the example in Fig. 3. The dependence on temperature at given concentration is also increasing but is slightly curved what corresponds to the temperature dependence of ultrasound velocity in water. There is practically no effect of hyaluronan molecular weight (cf. Fig. 3).

The increased velocity with increased concentration is caused by dissolved rigid polymeric chains and by the hydration shell formed

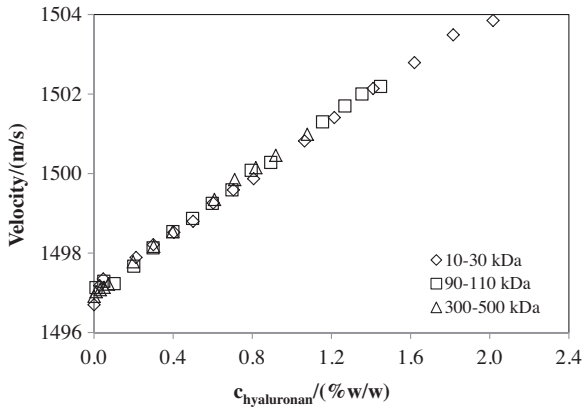

Fig. 3. The dependence of ultrasound velocity on concentration of hyaluronan at 25 °C. Solutions of hyaluronan of different molecular weights in water.

Please cite this article in press as: Kargerová, A., & Pekař, M. Densitometry and ultrasound velocimetry of hyaluronan solutions in water and in sodium chloride solution. *Carbohydrate Polymers* (2014), http://dx.doi.org/10.1016/j.carbpol.2014.01.020

around them. The higher the rigidity of medium, the higher the speed of ultrasound propagation in it (Povey, 1997). The hydration water is known to have lower compressibility than bulk water (Buckin et al., 1989) therefore the ultrasound velocity in systems containing hydrated molecules increases. As already noted by García-Abuín et al. (2011) the effect of temperature is more significant than the effect of concentration. This is probably caused by water as a solution medium namely by the response of its specific compressibility to temperature described below. Dissolving hyaluronan does not interfere with the specific properties of water regardless its supposed massive hydration shell. The negligible effect of hyaluronan molecular weight is indicative of the principal role of hyaluronan basic disaccharidic unit in determining the properties of hyaluronan solutions (the properties measured in this work, at least) – its molar amount at a given hyaluronan mass concentration is independent on the molecular weight.

3.4. Compressibility and hydration numbers

The compressibility (β) as calculated from measured density (ρ) and ultrasound velocity (u) using the well-known equation, usually called Laplace equation: $u = 1/(\sqrt{\beta\rho})$ and is given in Table ST6a-d in Supplementary information. Because both the density and the velocity increase with hyaluronan concentration the compressibility of hyaluronan solutions is a decreasing function of concentration at all temperatures; however the decrease is only mild. More concentrated solutions are thus slightly tougher, more rigid what can be explained by increased amount of hydrated structures, increasing excluded volume effects and perhaps also by interchain interactions.

The compressibility decreases also with growing temperature at given hyaluronan concentration and, once again, the effect of temperature is more significant than the effect of concentration. In a typical liquid the compressibility increases with temperature as the structure becomes more open. The decrease of the compressibility with elevated temperature is among the peculiar properties of liquid water (see the overview by Chaplin, in Web references). In fact, the adiabatic compressibility of water decreases up to 64 °C where it has a minimum. This behaviour is explained by the equilibrium between the clusters formed by water molecules through their hydrogen bonding. Basically, two cluster structures are in equilibrium – the more open or expanded structure and the more ordered or collapsed structure. Both structures are formed from twenty 14-molecule tetrahedral units. The expanded structure creates icosahedral water clusters and can collapse into the puckered central dodecahedron forming the collapsed structure. In liquid water, the cluster equilibrium shifts towards more closed structure (the collapsed cluster). As the temperature increases, the water structure is less open at these higher temperatures and the capacity for it to be compressed decreases (Kell, 1975).

Hyaluronan does not disturb this peculiar property of liquid water. This is rather surprising, taking into account the accepted view on hyaluronan high hydration and thick hydration shell. The huge hydrodynamic volume is considered to be among the causes of the high viscosity of hyaluronan solutions (Cowman & Matsuoka, 2005). It could be supposed that at ambient temperatures a rigid, less compressible hydrated structure is formed which is weakened at elevated temperature as the decrease of viscosity indicates. A simple and straightforward explanation of the compressibility-temperature behaviour could be that the cluster structure of water is not essentially disturbed by the interactions with hyaluronan and the formation of its hydration shell. Another explanation can be the establishing of equilibrium between water in hydration shell and water clusters (perhaps less sized) remaining in the bulk and still responsible for the compressibility decrease. This equilibrium should be shifted to the (closed) clusters at elevated temperature. This explanation could be modified by imaging direct interactions, mediated by hydrogen bonding, between hydration layer and surrounding water clusters which are weakened by increased temperature. Still another explanation can be the relatively week bonding of water molecules in the hydration shell – even moderate increase in the temperature releases sufficient amount of water molecules from the hydration shell to re-establish the expanded-closed structure equilibrium in the aqueous environment. The hydration of hyaluronan was studied in details in refs. Haxaire et al. (2003a, 2003b) and Maréchal, Milas, and Rinaudo (2003) using advanced infrared spectroscopy. Although they did not study the hyaluronan solutions but the hydration of the solid hyaluronan films placed in the atmosphere of controlled moisture our results seem to confirm their conclusions on the hydration mechanism. They found out that at high moisture contents the hydration takes place by the arrival of nanodroplets of water molecules (containing at least 50 molecules) extending along the hyaluronan chain.

The effect of hyaluronan molecular weight is negligible, again, which further confirms the principal role of the basic disaccharidic unit in controlling the measured and calculated properties.

The compressibility can be used to estimate the hydration numbers, i.e. the number of water molecules in hydration shell. An overview of acoustic methods for the determination of hydration numbers was published recently (Burakowski & Glinski, 2011). Here the simple and general Pasynski method was applied which gives the following equation to calculate the hydration numbers, n_h: $\eta_h = (\eta_{H_2O}/\eta_{dimer})(1 - (\beta_{sample}/\beta_{H_2O}))$, where η_{H_2O} and η_{dimer} are the molar amounts of water and the dimer of hyaluronan, respectively, β_{H_2O} and β_{sample} is the compressibility of water and sample, respectively. The value of 401.299 g/mol was used for the molecular weight of disaccharidic unit of hyaluronan (sodium form) in calculations.

The Pasynski method assumes zero compressibility of water molecules in hydration shells and simple additivity of compressibility with respect to number of (compressible) molecules. The resulting hydration numbers should better be considered as estimates than as exact true values; all acoustic methods involve similar assumptions (Burakowski and Glinski, 2011) and should be used preferably for the comparison purposes within a series of similar samples. The hydration numbers in water are given in Table ST6a-d in Supplementary information and are very weakly dependent on temperature and hyaluronan concentration. Mostly they decrease with increasing temperature and concentration which is typical for the hydration numbers calculated by this method. No effect of the hyaluronan molecular weight could be observed. The hydration numbers in water are around 20. Haxaire et al. (2003a, 2003b) determined the hydration numbers up to about 30 depending on the moisture content in the atmosphere hydrating hyaluronan films. The hydration numbers of about 20 were observed at the very high moisture content, in relative units at almost 95% moisture. At the same time this corresponds to the onset of the hydration mechanism D (for details see Haxaire et al., 2003a, 2003b) which should reflect the arrival of water nanodroplets mentioned above. Our hydration numbers which should include the water molecules in close hydration shell with zero or very low compressibility (i.e. probably the shell formed at the onset of the mechanism D) thus seem to be in reasonable agreement with infrared study regardless the inherent assumptions of the Pasynski method. The weak dependence of estimated hydration numbers on the temperature does not support the explanation of compressibility-temperature curves which would be based on thinning the hydration shell with increasing temperature.

Suzuki and Uedaira (1970) used in their ultrasound measurement different and rather complex methods arriving at the hydration numbers of about 9 or 18 (for potassium hyaluronate)

Please cite this article in press as: Kargerová, A., & Pekař, M. Densitometry and ultrasound velocimetry of hyaluronan solutions in water and in sodium chloride solution. *Carbohydrate Polymers* (2014), http://dx.doi.org/10.1016/j.carbpol.2014.01.020

depending on the level of complexity of the method and its presumptions. The value 9 is reported as an averaged value also by Davies et al. (1983) who used yet another calculation method which should determine the number of water molecules directly interacting with hydrated substrate.

3.5. Effect of NaCl

The addition of NaCl resulted in different numerical values of measured densities or ultrasound velocities (cf. Tables ST2a-d and ST7a-d in Supplementary information) but did not change their dependency on concentration or temperature. The numerical difference is rooted in the difference of pure solvents – in the density of water and NaCl solution and in the speed of ultrasound in these two media, see Figures SF1 and SF2 in Supplementary information. If this difference is accounted for by proper shifting of concentration or temperature dependencies, common curves are obtained for both solvents as illustrated in Figure SF3 in Supplementary information. The partial volumes determined in the NaCl solution for hyaluronan of the two lower molecular weights are comparable with corresponding values in water. Increasing hyaluronan molecular weight causes some differences in partial volumes – those determined in the NaCl solution are lower than corresponding values in water. This can be explained by shielding the repulsive electrostatic interactions between dissociated functional groups on hyaluronan by added low molecular electrolyte. The hyaluronan chains then adopt more compact shapes in electrolyte solutions (Cowman & Matsuoka, 2005) and if the chains are sufficiently long this is reflected in lower partial volumes. The formation of compact structures is confirmed by lower compressibilities in NaCl solution although the effect of electrolyte ions cannot be neglected. The hydration numbers are comparable in both solvents. The reference (Gómez-Alejandre et al., 2000) reported increased limiting partial volume of hyaluronan in NaCl solution and rationalized this finding by the formation of more open structures in the presence of added small ions. Again, due to the lack of original data in that reference it is difficult to discuss this difference but our compressibility measurements do not support the idea of more open structures.

4. Conclusions

The density of hyaluronan solutions in water or in 0.15 M NaCl was linearly dependent on the concentration at any used temperature and increased with the concentration. Increasing temperature decreased the density of a solution of given concentration; the temperature dependence was slightly curved and slightly deviated from linearity. The molecular weight of hyaluronan had negligible effect. Therefore all the data through all molecular weights, concentrations and temperatures used could be satisfactorily fitted with a single equation (one for each solvent); linear for concentration and quadratic for temperature. The equation can be used for reliable estimate of the density of hyaluronan solutions in the concentration range 0–2% (w/w), the molecular weight range 10–1750 kDa and the temperature range 25–50 °C. The densities were used to calculate several specific volume characteristics. The hyaluronan partial specific volume in water typically ranges, depending on concentration, between 0.587 and 0.594 cm^3/g at 25 °C and between 0.597 and 0.604 cm^3/g at 50 °C; in NaCl solution the values are slightly lower. The ultrasound velocity was primarily used to calculate the compressibility. The compressibility decreased with both the hyaluronan concentration and the temperature, the influence of the latter was stronger. The compressibility data indicated that hyaluronan – regardless of its supposed huge hydration – does not disturb the specific structure of water which is responsible for peculiar properties of water. Taking into account also the smooth and linear dependences of density and ultrasound velocity on the hyaluronan concentration it seems that the hyaluronan hydration, at least in diluted solutions, includes some type of bonding of relatively large water clusters (nanodroplets) to hyaluronan chains. The hydration in solution should thus follow especially the last step of hydration mechanism proposed for solid hyaluronan films (Haxaire et al., 2003a, 2003b; Maréchal et al., 2003). The hydration numbers determined from the compressibility data were typically about 20 and only slightly dependent on concentration. The addition of NaCl caused the changes in numerical values of measured or calculated quantities but did not change the character of their concentration or temperature behaviour. The salt thus did not cause the detectable changes in hyaluronan conformation or structure, except for the formation of rather more compacted coils at higher molecular weights. A negligible effect of molecular weight on all measured or calculated properties pointed to the principal role of the basic disaccharide unit of hyaluronan in determining these solution properties.

To conclude with a single phrase we can re-confirm the statement by Rinaudo: there is nothing too much remarkable in the behaviour of hyaluronan in solution (Rinaudo, 2009). Perhaps except that despite of its proclaimed massive hydration shell hyaluronan seems not to disturb the specific structure of water. Maybe that large water clusters bound to or entrapped within the hyaluronan chains form the structure responsible for the high viscosity of even diluted hyaluronan solutions.

Acknowledgements

This work was supported by the COST action CM1101, project No. LD12068 (Ministry of Education, Czech Republic). Materials Research Centre at Faculty of Chemistry, BUT is supported by project No. CZ.1.05/2.1.00/01.0012 from ERDF.

Appendix A. Supplementary data

Supplementary data associated with this article can be found, in the online version, at http://dx.doi.org/10.1016/j.carbpol.2014.01.020.

References

Buckin, V., Kankiya, B., Sarvazyan, A., & Uedaira, H. (1989). Acoustical investigation of poly(dA).poly(dT), poly[d(A–T)].poly[d(A–T)], poly(A).poly(U) and DNA hydration in dilute aqueous solutions. *Nucleic Acids Research*, *17*, 4189–4201.

Burakowski, A., & Glinski, J. (2011). Hydration numbers of nonelectrolytes from acoustic methods. *Chemical Reviews*, *112*, 2059–2081.

Cowman, M., & Matsuoka, S. (2005). Experimental approaches to hyaluronan structure. *Carbohydrate Research*, *340*, 791–809.

Davies, A., Gormally, J., Wyn-Jones, E., Wedlock, D., & Phillips, G. (1982). A study of hydration of sodium hyaluronate from compressibility and high precision densitometric measurements. *International Journal of Biological Macromolecules*, *4*, 436–438.

Davies, A., Gormally, J., Wyn-Jones, E., Wedlock, D., & Phillips, G. (1983). A study of factors influencing hydration of sodium hyaluronate from compressibility and high-precision densimetric measurements. *Biochemical Journal*, *213*, 363–369.

Durchschlag, H., & Zipper, P. (1994). Calculation of the partial volume of organic compounds and polymers. *Progress in Colloid & Polymer Science*, *94*, 20–39.

Fabre, M., Tagle, L., Gargallo, L., Radic, D., & Hernandez-Fuentes, I. (1989). Partial specific volume and specific refractive index increment of some poly(carbonate)s and poly(thiocarbonate)s. *European Polymer Journal*, *25*, 1315–1317.

García-Abuín, A., Gómez-Díaz, D., Navaza, J., Regueiro, L., & Vidal-Tato, I. (2011). Viscosimetric behaviour of hyaluronic acid in different aqueous solutions. *Carbohydrate Polymers*, *85*, 500–505.

Gómez-Alejandre, S., Blanca, E., Usera, C., Rey-Stolle, M., & Hernández-Fuentes, I. (2000). Partial specific volume of hyaluronic acid in different media and conditions. *International Journal of Biological Macromolecules*, *27*, 287–290.

Haxaire, K., Maréchal, Y., Milas, M., & Rinaudo, M. (2003a). Hydration of polysaccharide hyaluronan observed by IR spectrometry. I. Preliminary experiments and band assignments. *Biopolymers*, *72*, 10–20.

Please cite this article in press as: Kargerová, A., & Pekař, M. Densitometry and ultrasound velocimetry of hyaluronan solutions in water and in sodium chloride solution. *Carbohydrate Polymers* (2014), http://dx.doi.org/10.1016/j.carbpol.2014.01.020

Haxaire, K., Maréchal, Y., Milas, M., & Rinaudo, M. (2003b). Hydration of hyaluronan polysaccharide observed by IR spectrometry. II. Definition and quantitative analysis of elementary hydration spectra and water uptake. *Biopolymers*, *72*, 149–161.
Junquera, E., Olmos, D., & Aicart, E. (2002). Carbohydrate–water interactions of p-nitrophenylglycosides in aqueous solution. Ultrasonic and densitometric studies. *Physical Chemistry Chemical Physics*, *4*, 352–357.
Kaulgud, M. V., & Dhondge, S. S. (1988). Apparent molal volumes and apparent molal compressibilities of some carbohydrates in dilute aqueous solutions at different temperatures. *Indian Journal of Chemistry*, *27A*, 9–11.
Kell, G. S. (1975). Density, thermal expansivity, and compressibility of liquid water from 0° to 150 °C: Correlations and tables for atmospheric pressure and saturation reviewed and expressed on 1968 temperature scale. *Journal of Chemical and Engineering Data*, *20*, 97–105.
Kogan, G., Šoltés, L., Stern, R., & Gemeiner, P. (2006). Hyaluronic acid: A natural biopolymer with a broad range of biomedical and industrial applications. *Biotechnology Letters*, *29*, 17–25.
Kuo, J. W. (2006). *Practical aspects of hyaluronan based medical products*. Boca Raton: CRC Press.
Lapčík, L., Lapčík, L., Smedt, S., Demeester, J., & Chabreček, P. (1998). Hyaluronan: Preparation, structure, properties, and applications. *Chemical Reviews*, *98*, 2663–2684.
Lo Surdo, A., Shin, C., & Millero, F. J. (1978). The apparent molal volume and adiabatic compressibility of some organic solutes in water at 25 °C. *Journal of Chemical and Engineering Data*, *23*, 197–201.
Maréchal, Y., Milas, M., & Rinaudo, M. (2003). Hydration of hyaluronan polysaccharide observed by IR spectrometry. III. Structure and mechanism of hydration. *Biopolymers*, *72*, 162–173.
Perkins, S., Miller, A., Hardingham, T., & Muir, H. (1981). Physical properties of the hyaluronate binding region of proteoglycan from pig laryngeal cartilage. *Journal of Molecular Biology*, *150*, 69–95.
Povey, M. J. W. (1997). *Ultrasonic techniques for fluids characterization*. San Diego: Academic Press.
Rinaudo, M. (2009). Polyelectrolyte properties of a plant and animal polysaccharide. *Structural Chemistry*, *20*, 277–289.
Sarvazyan, A. P. (1982). Development of methods of precise ultrasonic measurements in small volumes of liquids. *Ultrasonics*, *20*, 151–154.
Sarvazyan, A. P. (1983). Ultrasonic velocimetry of biological compounds. *Molecular Biology*, *17*, 739–749.
Suzuki, Y., & Uedaira, H. (1970). Hydration of potassium hyaluronate. *Bulletin of the Chemical Society of Japan*, *43*, 1892–1894.

Further reading

Chaplin, M. *Water structure and science*. http://www.lsbu.ac.uk/water/index2.html Accessed 07.09.13.

Please cite this article in press as: Kargerová, A., & Pekař, M. Densitometry and ultrasound velocimetry of hyaluronan solutions in water and in sodium chloride solution. *Carbohydrate Polymers* (2014), http://dx.doi.org/10.1016/j.carbpol.2014.01.020

KARGEROVÁ, Andrea, Miloslav PEKAŘ. *Langmuir*. 2014.

Type of publication: manuscript of research article

High-resolution ultrasonic spectroscopy study of interactions between hyaluronan and cationic surfactants

Andrea Kargerová
Miloslav Pekař

Brno Univerzity of Technology
Faculty of chemistry, Institute of Physical and Applied Chemistry
xckargerova@fch.vutbr.cz

Abstract

The interaction in the system surfactant-hyaluronan in aqueous and sodium chloride solutions at temperature 25°C has been investigated by method, named high-resolution ultrasonic spectroscopy. Two main quantities, the ultrasonic velocity and the attenuation have measured in titration regime by this method. The critical micelle concentration (CMC) of alkyltrimetlyammonium bromides having tetradecyl and hexadecyl chains has been measured in two different solutions and the values of the CMC were in agreement with literature. The significant breakpoint in the ultrasonic velocity showed changes in the system surfactant-hyaluronan.

Keywords: hyaluronan, surfactants, CTAB, TTAB, high-resolution ultrasonic spectroscopy

Introduction

Hyaluronan is a linear polysaccharide built from regularly alternating monosaccharaides, glucuronic acid and N-acetylglucosamine, which form a basic disaccharide[0]. It is an abundant biopolymer with a wide range of naturally occurring molecular masses from several hundreds to 10^7 g/mol. The highest concentrations of hyaluronan occur in synovial fluid, vitreous body, skin and certain specialized tissues such as umbilical cord and rooster comb. The largest amounts are found in the intercellular matrix of skin and musculoskeletal tissues. Hyaluronan is a biodegradable, biocompatible, non-toxic, non-immunogenic and non-inflammatory polymer, which has been used for various medical applications including arthritis treatment, wound healing, ocular surgery, and tissue augmentation[(2)]. Pharmacological scientists are interested in hyaluronan as an ideal component of drug delivery systems [(3)].

Hyaluronan is a very hydrophilic polymer surrounded by a massive hydration shell. Due to the presence of dissociable (carboxyl) group on its basic unit, hyaluronan has a character of a polyelectrolyte. At physiological pH, the carboxyl groups are predominantly ionized; the hyaluronan behaves like a polyanion and can interact with or associate cationic counterions to maintain charge neutrality. Hyaluronan interactions with positively charged surfactants were thus studied as a specific case of polyelectrolyte-surfactant interactions[(4)]. Hyaluronan-surfactant complexes containing hydrophobic domains formed by surfactant molecules and bound to hyaluronan chain can also be a potential carrier system for water-insoluble pharmaceutics agents. A series of papers by Swedish research groups provided a detailed study on phase behaviour of systems containing water, hyaluronan, alkyl trimethylammonium bromides (tetradecyl derivative was the most studied type) and salt (mostly NaBr) [(5)-(11)]. Binding of surfactant to hyaluronan was detected for surfactants with alkyl chain consisting from at least ten carbon atoms. The binding was found to be considerably weaker than for most other carboxyl-containing polyelectrolytes, due to the low linear charge density of hyaluronan. Phase separation was observed as formation

of precipitate or gel-like phase upon increasing surfactant concentration. A large excess of surfactant redissolved the precipitates. Increasing concentration of added salt reduced the two-phase area unless the salt concentration was very high when phase separation occurred again. The longer the surfactant alkyl chain the larger two-phase region was observed. It was found that there is a certain cationic surfactant concentration below which only general electrostatic interactions take place and only above it marked formation of hyaluronan-surfactant complexes can be observed. The results indicated strong cooperatively of surfactant binding on hyaluronan macromolecule resulting in binding in the form of micelle-like clusters in which both hyaluronan carboxylates and background electrolyte anions participate as counterions. Increasing electrolyte (salt) concentration disfavored formation of hyaluronan-bound micelles in comparison to free micelles. The phase diagrams constructed for the studied systems essentially contain an area of homogeneous single phase surrounding the two-phase region located around the water-rich corner of the phase triangle. The longer the hydrocarbon chain of the surfactant, the larger was the two-phase region. In contrast, hyaluronan molecular weight has only a slight effect – it only slightly changed position of the two-phase region while its size was almost unaffected. Reference[11] – From an electrostatic viewpoint, a free surfactant ion, TTA^+, behaves exactly as Na^+ and a negatively charged polyelectrolyte would not show any preference for either of the two counterions. Nevertheless, the hydrophobicity (and size) of TTA^+ leads to such a preference since its contact with water (excluded volume) is reduced in the vicinity of the polyelectrolyte. The consequent higher local concentration of TTA^+ near the polyelectrolyte, as compared to the bulk, may exceed the critical micelle concentration. We propose multiple-site condensation micelles (rather than single-site condensation leading to the formation of a “pearl necklace”) onto separate NaHya chains and .a formation of multichain NaHya-TTAB complexes. The complexes formed. May is viewed as precursors to the precipitated phase appearing at lower NaCl concentrations.

In order to be able to analyse the composition of separated phases the experiments on phase diagrams were realized by mixing hyaluronan solution (at the concentration usually around 1% wt) with surfactant solutions of varying concentration and leaving the system to phase separate and then equilibrate for several days or weeks. This “static” experimental protocol is necessary when the individual equilibrated phases are to be characterized. Another approach is more focused on study of interacting molecules or macromolecules shortly after coming to a sufficiently close contact and gives a more dynamic picture of the system. Such experiments can be realized for example by conductometric[5] turbidimetric[12] or calorimetric[14), (15] titrations. In this work, the high resolution ultrasound spectrometry in the titration regime is used.The high resolution ultrasound spectrometry is a powerful technique for analysis of colloids based on precision measurements of parameters of high-frequency (ultrasound) sound waves propagating through analysed samples[16)-(19]. This technique has major advantages over many other conventional methods. It is non-destructive, robust, rapid, very precise and can be applied to concentrated and/or optically opaque samples, requires small sample volumes (1 ml). It allows direct probing of microstructural organisation and intermolecular forces in a variety of colloidal systems. Ultrasonic wave is a wave of oscillating pressure and associated longitudinal deformation travelling through sample. Molecules in the sample respond to oscillating deformations through inter-molecular repulsive (compression) and attractive (decompression) forces reflecting the measured elasticity of the sample. Elasticity is the major contributor to the first characteristic measured in this technique, ultrasonic velocity. Propagating through the medium, the ultrasonic wave loses its energy and is subjected to a scattering process, which causes ultrasonic attenuation. Attenuation (or attenuation coefficient), the second measured parameter, is determined by the reduction in amplitude of an ultrasonic wave which has travelled a known distance

through a medium per unit travelled distance. The major contributors to attenuation are fast chemical relaxation and microstructure of non-homogeneous samples. The high resolution refers primarily to the measurement of velocity and is achieved by parallel measurements of ultrasound propagation in sample and reference cells. The reference cell is filled with pure solvent (water or NaCl solution in our case).

Buckin et al.[20] used the high resolution ultrasound spectrometry for the study of interactions of DNA with cationic surfactants. Combining ultrasound data with measurements of density they found a high value of the effect of surfactant binding to DNA on compressibility. This could not be explained by hydration changes only and was considered as an indicator of the formation of micelle-like aggregates of surfactants on the DNA surface with a highly compressible core. Hickey et al.[21] published an analysis of the phase diagram and microstructural transitions in a microemulsion system containing phospholipid in which titration arrangement with the detection of ultrasound parameters was used. They demonstrated that break points (points of abrupt changes in slope) on dependences of ultrasound velocity on the concentration of titrant are located on phase boundaries and can be used to construct phase diagram. Knowledge of other physical parameters of the microemulsion system enabled to make also a quantitative characterization of various detected microphases or the state of water. Similar study on compositionally different microemulsion system was published by the same group later[22]. Singh et al.[23] investigated interactions between poly(N-vinyl-2-pyrrolidone) and sodium dodecyl sulphate using a less sensitive ultrasound equipment operating at single frequency[24]. Ultrasound velocity as a function of the surfactant concentration exhibited several breaks which were attributed to different molecular organization in the system – for instance, the formation of premicellar associates or their binding to the polymer chain. The authors also noted that ultrasound titration did not substantiated previous claims based on conductivity or viscosity data.

Materials

Hyaluronan samples were obtained from Contipro Biotech , Czech Republic, where are produced by extraction from the cell walls of the bacteria *Streptococcus zooepidemicus*. The product types are named according to the range of average molecular weight within which fall the molecular of particular product. Four product types of different ranges were used in this work and are listed in Table ST1 in Supplementary information together with the true molecular weight of all used samples – several samples of the same product type were used due to limited resources and stability. The surfactants hexadecyltrimethylammonium bromide (CTAB) of p.a. 99% purity and tetradecyltrimethylammonium bromide TTAB of p.a. 98 purity were purchased from Sigma Aldrich (Czech Republic) and sodium chloride of p.a. 99.5% purity from Lachner (Czech Republic).

Hyaluronan solutions were prepared by weighing at the concentration of 1 g/kg (0.1% w/w) by dissolving hyaluronan powder in deionized water or in 0.15M NaCl in a closed vessel. The solution was stirred for 48 hours at room temperature to ensure the complete dissolution. Ultrapure deionized water from PURELAB (Option R7/15; ELGA, Great Britain) water purification system was used for the preparation of all samples.

Methods

Ultrasonic velocity and attenuation were measured at seven selected frequencies in the range from 2.5 to 17.5 MHz using HR-US 102T ultrasonic spectrometer (Ultrasonic Scientific, Ireland) in titration regime. This device is equipped with two cells enabling the single-cell or differential measurements. The differential regime used in this work allows

the resolution of 0.2 $mm \cdot s^{-1}$ for ultrasonic velocity and 0.2% for ultrasonic attenuation. The temperature was controlled with a Haake PC300 heating bath, which provided a temperature stability of 0.01°C. The temperature was recorded by the sensor imbedded in the body of the differential ultrasonic cell as provided by the manufacturer.

The sample ultrasonic cell was closed with a stopper, which incorporated a line for injection of titrant. The measuring cell was filled with hyaluronan solution using a calibrated 1 ml Hamilton syringe. The exact amount of the solution in the cell was determined by weighing the syringe before and after filling. The titration accessory of HR-US 102T was equipped with 50µl Hamilton syringe which was used for the dosage of the titrant.

A 1 1.1 ml of deeply degassed sample was pipetted into the sample cell equilibrated at selected temperature and 1 ml deionized water had previously been pipetted into the reference cell. Ultrasonic measurements at seven preselected frequencies (2.5-17.5 MHz) were started after the sample was loaded and temperature-equilibrated. Solution of TTAB and CTAB in water or in 0.15 M NaCl was used as a titrant. The titrant solution was injected to the sample automatically in 2-µl steps by the computer-controlled titration accessory of ultrasound spectrometer. After each injection, the sample was stirred using double stirring system that provided effective mixing within seconds. Ultrasonic velocity and attenuation in the suspension were monitored over the course of the titration (time) at 25 °C.

Before every measurement baseline correction was done. The same measurements in titration regime were performed for sample cell loaded at time zero with deionised water or with 0.15M NaCl. Ultrasonic velocity and attenuation profiles measured in water or in 0.15M NaCl were subtracted from corresponding profiles in hyaluronan sample, in order to remove the effect of temperature fluctuations and fine differences in the resonance of the cells on measured values of ultrasonic parameters.

The measured data were processed using Titration Analysis software (Ultrasonic Scientific, Ireland) which also includes a correction for dilution. Each measurement was done in triplicate at least and the values were averaged.

Visual observation of titrated systems was realized outside of the machine, in a test-tube with upper and bottom stirrer with the same steps of titration program as is performed in the machine. The observation was used for systems hyaluronan (10-1750 kDa) with CTAB or TTAB in water and sodium chloride solution.

The charge ratio surfactant/hyaluronan corresponds to the ratio of concentration of charges on the surfactant molecule and hyaluronan. The ratio of charges gives the information about the possible free or occupied hyaluronan charged groups. Hyaluronan has one negative charge per one disaccharide unit; and surfactants TTAB and CTAB have one positive charge in their structure. The concentration of charges on hyaluronan chain was calculated according the following relation:

$$\frac{\text{concentration of hyaluronan in the solution (g/l)}}{\text{weight of one disaccharide unit (g/mol)}} = \text{concentration of disaccharide units (mol/l)},$$

where the weight of one disaccharide unit is 401.299 g/mol.

Results and discussion

High resolution ultrasound spectrometer gives as output the difference in velocity or attenuation measured between the sample and reference cells, i.e. the difference between the value in the sample and in water or NaCl solution in our case. Data are therefore reported in terms of velocity difference (attenuation difference).

The critical micelle concentration in water and 0.15 M NaCl

First, titrations with pure surfactants in water or NaCl solutions were performed for the purpose of verification and comparison. Critical micellar concentrations and compressibilities could be obtained and compared with literature. Further, the titration profiles in the absence of hyaluronan provided the base for investigation of its effect caused by the interactions with surfactants. The measured velocity profiles are shown in Figure SF1 and SF2 in Supplementary information. The velocity increases with increasing surfactant concentration due to the increasing number of relatively rigid surfactant molecules and especially due to their hydration shells composed of less compressible water molecules[25] The increase is linear and the point of abrupt change of the slope determines the critical micellar concentration. In water, the slope behind the critical micellar concentration is close to zero while in the NaCl solution it is still positive but smaller than below this concentration. The decreased slope is a combined result of the formation of micelles with compressible core, the release of hydration water from surfactant monomers, and the formation of new hydration shells around micelles. In the salt solution also the chloride ions are incorporated into micellization forming more rigid micellar structures and their increasing number causes the continuous velocity increase observed behind the critical micellar concentration. The critical micellar concentrations were determined from the intersection of two straight-line segments fitting the ultrasonic velocity versus concentration plots and are close to the values given in the references[26]-[28] (Table ST2 in Supplementary information, Table 1 and Table 2)

In water and below the critical micellar concentration (of CTAB) the velocity profiles of both surfactants are very close. In the micellar state the velocity in the TTAB system is several times higher than in CTAB. The TTAB micelles are thus less compressible than the CTAB micelles which corresponds to previous determinations of the apparent adiabatic compressibility of alkyltrimethylammonium bromides[29] and was attributed to the structure of the internal core of micelles which was found to be close to that in pure hydrocarbon liquids. Similar situation was observed comparing the two velocity profiles in NaCl solution. As expected, salt did not penetrated into the micelle core and affected only the micelle surface composed of polar groups and their hydration which resulted in increasing velocity within the post-micellar concentration region of both surfactants.

Binding of the surfactant with hyaluronan in water and 0.15 M NaCl

Titration of hyaluronan solution by surfactant TTAB in water

Figure 1 compares ultrasound velocity titration curves obtained during the TTAB titration into water or hyaluronan solution (300-500 kDa, initial concentration of 1 g/kg). The curve for the titration in water clearly shows the two parts corresponding to pre-micellar and post-micellar states. On the other hand, up to six parts can be found for the titration profile measured in hyaluronan solution; surfactant concentrations for their boundaries are given in Table 1. The first part is practically identical to the corresponding pre-micellar part of the titration profile obtained in water. Visually this part corresponds to clear solution; the charge ratio is well below one (see Table 1). In this part no effect of added hyaluronan is thus observed which should be a result of the prevailing presence of free surfactant molecules; some single surfactant molecules could be loosely bound to hyaluronan without changing their compressibility.

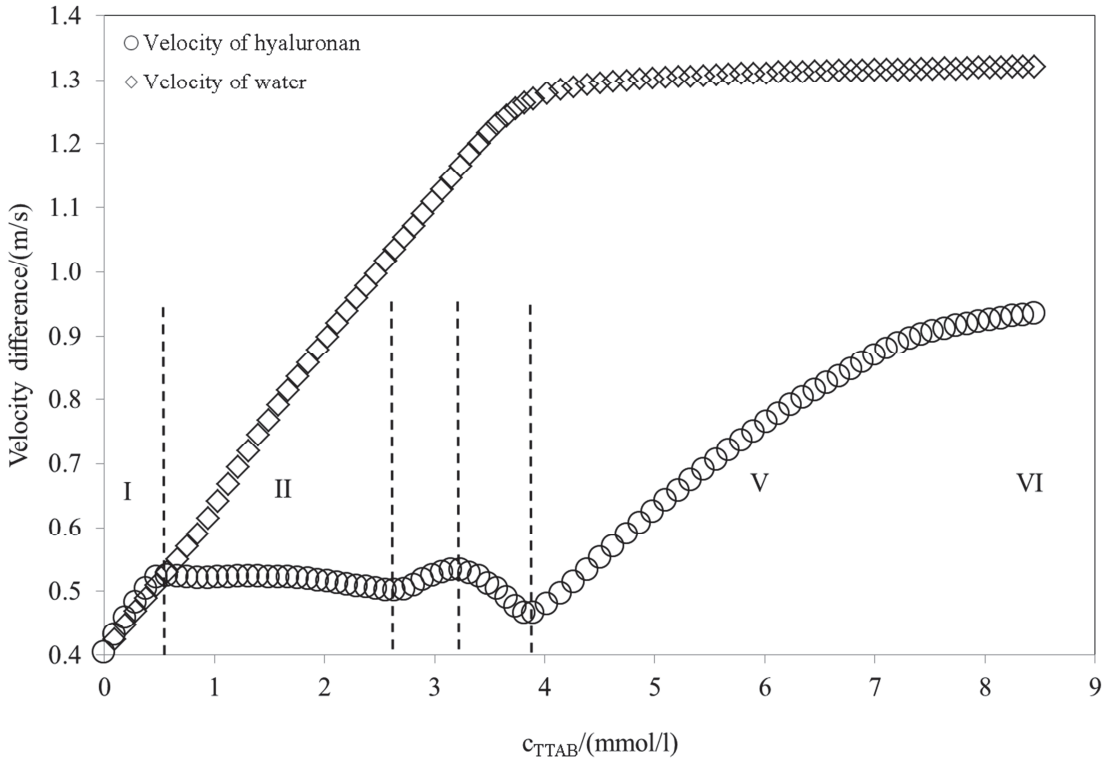

Figure 1. The velocity titration profile of hyaluronan of concentration 1000 mg/l and molecular weight of 300-500kDa and the velocity titration profile of water with TTAB, at frequency 15 MHz.

Table 1. TTAB concentrations at the boundaries of the different parts identified in the velocity titration profile and corresponding charge ratio TTAB/hyaluronan.

		Water		0.15 M NaCl	
M_w / kDa	Part	c_{TTAB} / mmol/l	Charge ratio TTAB/HYA	c_{TTAB} / mmol/l	Charge ratio TTAB/HYA
10	I	0.37	0.15	0.60	0.2
	II	3.01	1.28		
	III	3.98	1.74		
	IV	4.61	2.04		
	V	6.26	2.87		
90-130	I	0.35	0.14	0.91	0.4
	II	2.00	0.85		
	III	2.63	1.13		
	IV	2.99	1.30		
	V	7.20	3.48		
300-500	I	0.48	0.19	3.15	1.3
	II	2.73	1.16		
	III	3.15	1.35		
	IV	3.90	1.70		
	V	8.35	4.01		
1500-1750	I	0.38	0.15	4.93	2.2
	II	2.71	1.15		

III	3.04	1.30	
IV	3.99	1.73	
V	8.39	4.04	

In the second part the increase of ultrasound velocity with the surfactant concentration stops at the presence of hyaluronan. On contrary, a very slight velocity decrease is observed. This part resembles the post-micellar part of the titration profile in water. Progressive opalescence up to milky clouding was observed visually. The charge ratio approaches one closely to the end of part II. Ultrasound practically does not "see" the addition of surfactant molecules into the system. In this part binding of surfactant on hyaluronan in the form of micelles should prevail. Because the surfactant concentration is still below its normal critical micellar concentration the micellization process is induced by the presence of hyaluronan, mainly by electrostatic interactions between oppositely charged groups on hyaluronan and surfactant. Two opposite effects contribute to the almost constant ultrasound velocity in the second part. The formation of compressible micelles together with the release of the less compressible molecules of hydration water from the interaction sites decrease the velocity. Formation of new and rigid hydration shell on emerged micelles increases the velocity. The former effect thus more than compensates the latter.

The third part is characterized by re-increase of ultrasound velocity upon the addition of surfactant. This part is somewhat similar to the pre-micellar part of the titration profile in water (with smaller slope). At the end of this part (around the local maximum of ultrasound velocity) formation of macroscopic phase separated particles was observed visually. The charge ratio is slightly above one (around 1.2-1.3) (Table 1). In this part the binding of surfactant in the form of micelles is finished, free (unbound) surfactant molecules probably appear in the solution, electrostatic repulsion is removed and phase separation progresses to macroscopic level. Both the free surfactant molecules and rigid phase separated particles contribute to the velocity increase.

In part IV the velocity decreases this time more steeply than in the part II. The system progressively clarifies with increasing concentration of surfactant. In the same time the number of macroscopic separates decreases and at the end of part IV only a few particles can be observed. The decrease of velocity is thus attributable to the decreased size and number of phase separated particles which are more rigid than the liquid medium. Part IV ends when the surfactant concentration corresponds to its normal critical micellar concentration.

The velocity increases again during part V with a slope approximate to the slope of pre-micellar part of the titration profile in water. The increase goes on in part VI but with much lower slope similar to that of the post-micellar part of the titration profile in water. Visual inspection reveals no special changes or behaviour in both parts just slightly opalescent appearance. Due to the surfactant concentration formation of standard micelles should be expected in both parts. In part V the formed micelles probably interact with the previously formed hyaluronan-TTAB complexes, dissolve the macroscopically separated particles and form rather rigid structures apparently of microgel type which increase the ultrasound velocity. When the interactions are completed part VI begins where mainly new free micelles are formed.

The measurement of ultrasound attenuation is much less sensitive. From the transition between part I and II the attenuation is continuously increasing up to the transition between part III and IV (Figure SF3 in Supplementary information). Then it steeply decreases in part IV and finally stays practically constant. Increasing attenuation indicates increasing heterogeneity of the system and formation of bigger particles scattering the ultrasound wave. The step decrease corresponds to the dissolution of such particles and clarification

of the system. Constant attenuation is found where no substantial heterogeneity evolves, i.e. when only really microscopic phase separation or structures are found. In contrast to velocity, attenuation values were dependent on the frequency of ultrasound which is typical for systems containing micro-heterogeneities capable of relaxation upon ultrasound propagation[21],[30]. Depending on the mechanism of relaxation ultrasound waves of different frequency may be scattered to different amount. However, the curved shapes of attenuation profiles and their locations on the concentration axis were not affected by the frequency as is illustrated on typical example in Supplementary information (Figure SF4).

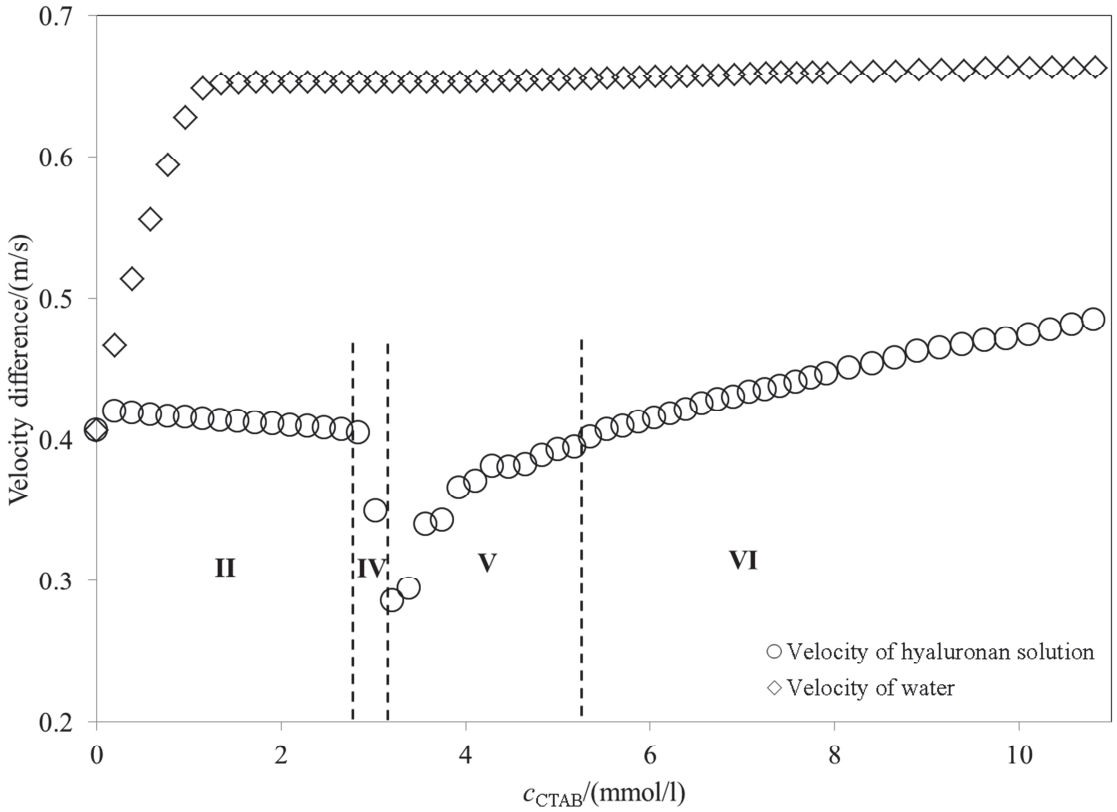

Figure 2. The titration profile of hyaluronan of concentration 1000 mg/l and molecular weight of 300-500kDa and the titration profile of water with TTAB, at frequency 15 MHz. The titration curve of water is shifted to first point of hyaluronan curve.

Figure 2 shows the titration curve of hyaluronan of concentration 1000 mg/l and molecular weight of 300-500kDa and titration curve of water with CTAB, at frequency 15 MHz. Titration profiles measured with CTAB are obviously different from those with TTAB. Some parts are missing in the velocity profile (Figure 1) and from this point of view the CTAB profile is simpler. On the basis of changes of the profile slope including its sign it is reasonable to assume that parts I and III are missing, and part V extends through much shorter concentration interval. The titration curve in the hyaluronan solution is from the first point different from that obtained in pure water. In comparison to TTAB, CTAB interacts with hyaluronan at much lower surfactant concentration, consequently, part I was not observed. Part II is characterized also by the evolution of turbidity and extends to concentrations well above the normal critical micellar concentration but it terminates also around the equivalent charge ratio (Table ST3 in Supplementary information). Visible macroscopic phase separation occurs here only in part IV and the steep velocity decrease in this part is mainly a result of particle setting out of the detection volume. The missing part III is probably a result of stronger cooperatively of CTAB binding on hyaluronan; perhaps no free surfactant molecules can be present in this case.

The precipitated particles were progressively dissolved during part V changing from precipitates through clotty structures or swelled flocks to almost clear system in part VI where also the formation of free standard micelles can be expected.

It is also interesting that the velocity difference measured in the TTAB-hyaluronan system approaches the values measured for TTAB micellar system and the values are very close for both systems starting at TTAB concentration of about 8 mmol/l. On contrary the velocity difference in the CTAB-hyaluronan system is always higher than in corresponding hyaluronan-free solutions. CTAB thus forms complexes with hyaluronan which are more rigid, less compressible than CTAB micelles whereas the opposite is found for TTAB.

The titration profile of ultrasound attenuation measured for CTAB is also different from that for TTAB (Figure SF5 in Supplementary information). It continuously and slightly increases up to the boundary between parts II and IV (remember the missing part III). Then it sharply increases (in contrast to the system with TTAB) up to the boundary between parts V and VI. In the part VI it continues to increase at first, but with lower slope, and then is essentially constant. The sharp increase reflects the increased heterogeneity due to the phase separation. The relatively high final value of attenuation, comparing to TTAB system, shows more heterogeneous structure capable of more intensive scattering of ultrasound wave formed probably by rather rigid and translucent micro- or nano-gel particles.

The effect of ultrasound frequency on both velocity and attenuation titration profiles is very similar to the effect described above for TTAB.

Effect of hyaluronan molecular weight on the shape of all measured velocity titration profiles was very small. The shapes were retained, some differences were found in the values of the surfactant concentration corresponding to the boundaries between neighboring parts. and in the velocity values within the same part of the profile. By visually observation was found that the size of precipitates increased with increasing molecular weight of hyaluronan.

The differences are seen particularly in parts III-VI and should be ascribed to the effects of differences in conformations of hyaluronan chains of different molecular weight [(31)]. On average, the two preparations of lower molecular weight differed from the two preparations of higher molecular weight which gave very similar profiles. The effect on the values of attenuation was stronger – the higher the molecular weight the higher the value of attenuation difference. This should be a result of more intensive ultrasound scattering on more complex coiled structures formed from chains of higher molecular weight. The differences in the shapes of attenuation profiles were small. Visually, the smaller the hyaluronan molecular weight the less perceptible opacity was observed.

The measurement of one experimental point during titration took 10 minutes. This is much shorter time than used in previous measurements of phase diagrams[(5)] or fluorescence studies of hyaluronan-surfactant systems[(32)]. Previous studies were based on mixing all components at a time and letting the system stand for 24 hours at least. To test potential time development of our systems several control stopped-titrations were realized. Titration was stopped at three preselected points of titration profile and ultrasound parameters were measured during following 13 hours. When the titration stopped in part II or IV no further change in the parameters was observed. After stopping the titration in part V a slight decrease of the velocity was detected (around 6% during 13 hours) which is attributable to slow sedimentation of microgel particles. Stopped titrations (Figure SF6 in Supplementary information) confirmed that dynamics and kinetics of hyaluronan-surfactant interactions were adequately recorded during ultrasound titrations and potential progressive changes in ultrasound parameters would be caused by progressive separation (sedimentation) of aggregates formed during titration.

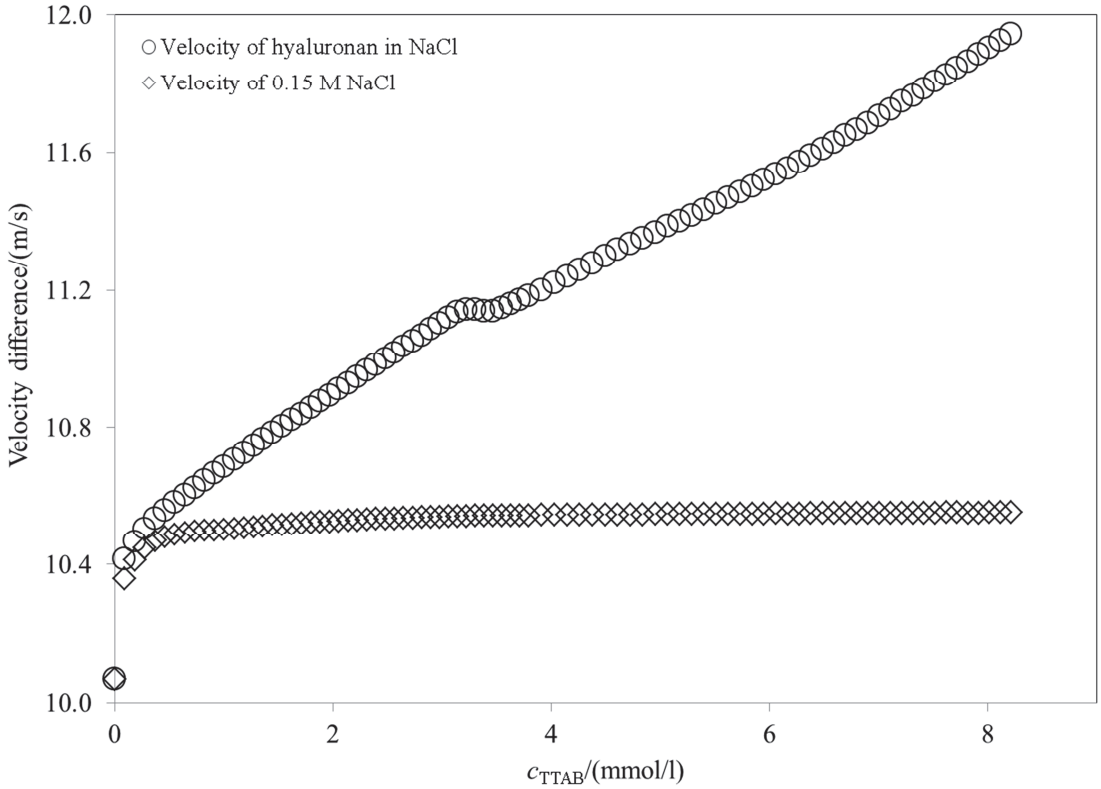

Figure 3. The velocity titration profile of hyaluronan in NaCl of concentration 1000 mg/l and molecular weight of 300-500kDa and the velocity titration profile of 0.15 M NaCl with TTAB in 0.15M NaCl, at frequency 15 MHz.

The titration profiles were significantly changed by the presence of NaCl at the concentration of 0.15 M (the physiological concentration). Ultrasound titrations of both surfactants into NaCl solution (without hyaluronan) confirmed the well-known decrease of critical micellar concentration in about one order of magnitude (Figure 3 and Figure SF7 in Supplementary information). In the case of TTAB the titration profiles at the absence and presence of hyaluronan practically coincide at low surfactant concentrations (and show a linear dependence of the ultrasound velocity on the surfactant concentration) which is the same observation as for the titrations in water. However, in the NaCl solution this coincidence survives up to the critical micellar concentration and even then the velocity increases at the presence of hyaluronan though with apparently somewhat smaller slope. Thiscontinuous increase is interrupted by a short interval of almost constant velocity which corresponds to the steep increase in the ultrasound attenuation and to the visual observation of several macroscopically phase-separated particles dispersed in a milky system. The charge ratio at the start point of this increase is about 1.3 (Table 1). It is interesting that this short interval occurs at surfactant concentrations close to critical micellar concentration in water. The system is clear before and cloudy or milky after this interval.

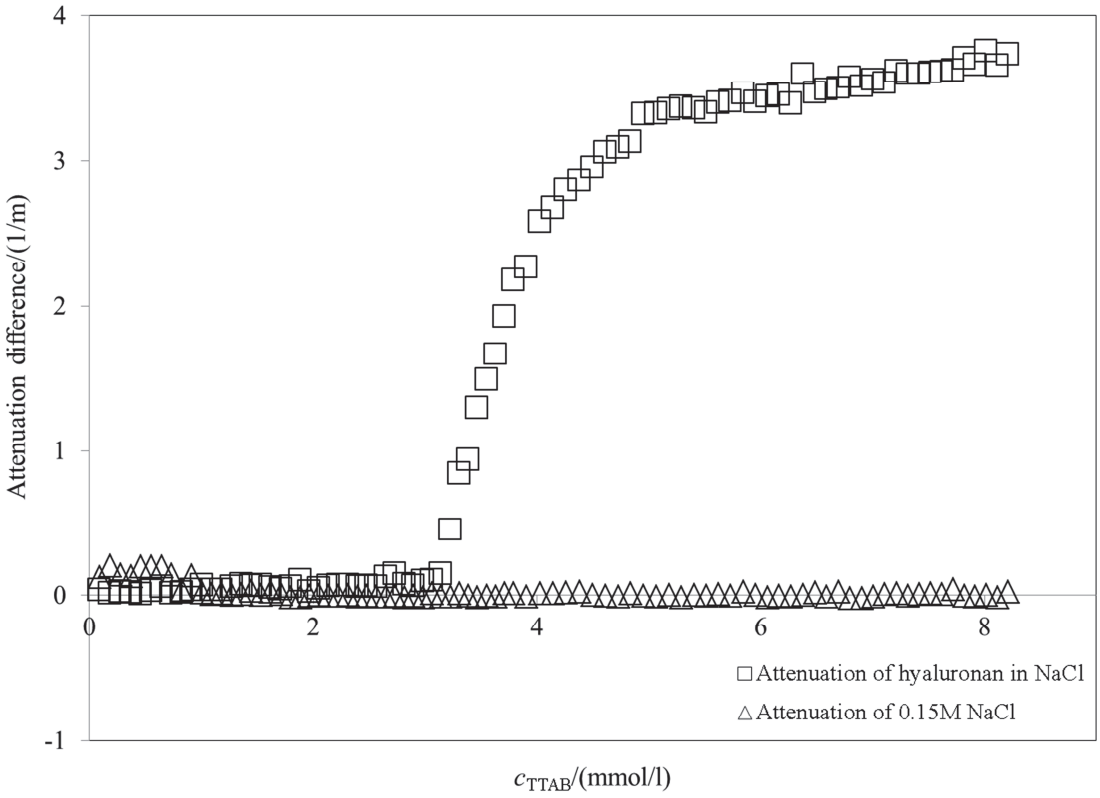

Figure 4. The attenuation titration profile of hyaluronan in NaCl of concentration 1000 mg/l and molecular weight of 300-500kDa and the attenuation titration profile of 0.15 M NaCl with TTAB in 0.15M NaCl, at frequency 15 MHz. The titration curve of 0.15 M NaCl is shifted to first point of hyaluronan curve.

The ultrasound attenuation of TTAB-hyaluronan-NaCl system does not almost change up to the start of the short region of constant velocity where it sharply increases (Figure 4). The sharp increase continues behind the region of constant velocity and then the attenuation progressively levels off and finally increases only moderately but continuously. In fact, the start of only moderate increase of attenuation corresponds to a weak bend on the velocity titration profile. The increased attenuation reflects the formation of heterogeneities – microaggregates of hyaluronan-surfactant complexes. The effect of ultrasound frequency is similar as described above – the velocity values are unaffected in contrast to the values of attenuation.

The shapes of titration profiles for CTAB in hyaluronan-NaCl system are much closer to those for TTAB than it was observed in water. The velocity increases before the critical micellar concentration (Figure SF7 in Supplementary information) but is higher than in the absence of hyaluronan, the slope of this increase is smaller behind this concentration and a narrow interval of almost constant velocity appears at much higher surfactant concentration than is the critical micellar. CTAB concentration corresponding to this constant interval is very similar as for TTAB as well as the charge ratio which is here around 1.3 (Table ST3 in Supplementary information). Thus electrostatic interactions control this behaviour. The re-increase of the velocity behind this interval is clearly (in contrast to TTAB) composed from at least two more or less linear branches intersecting around the CTAB concentration of 6 mmol/l. The initial increasing part corresponds visually to a clear system, during the constant interval some flakes or flocks and evolution of turbidity can be observed. After this interval the system is cloudy.

The attenuation reflects the changes in velocity (Figure SF8 in Supplementary information). Before the short region of constant velocity the attenuation increases moderately

then sharply within this region and even behind it. Then it remains essentially constant up to the bend mentioned in the preceding paragraph which appears around the CTAB concentration of 6 mmol/l and above this concentration it increases again. The effect of ultrasound frequency is still the same as given above.

Due to the higher velocity and increasing attenuation at low CTAB concentrations in the presence of hyaluronan it cannot be excluded that the surfactant interacts with CTAB in NaCl solution even in its normal pre-micellar region forming some more rigid structures. It cannot be concluded that micellar structures bound to hyaluronan are formed at this stage but taking into account the smaller slope of velocity increase during the normal post-micellar region (at the CTAB concentration between ca 1 and 3 mmol/l) single surfactant or "minimicelle" binding should be prefered. The steep increase of attenuation reflects increasing heterogeneity in the system which results in separation of macroscopic particles (the flakes). The interval of almost constant attenuation corresponds to re-dissolving of big particles by the excess of surfactant and is followed by progressive formation of rigid (increasing velocity) microheterogeneous (increasing attenuation in cloudy system) structures probably of microgel type as can supposed due to the increased slope of the velocity profile (from the CTAB concentration of 6-7 mmol/l).

In contrast with the titrations in water the effect of hyaluronan molecular weight was much more obvious in the presence of NaCl for both surfactants. The velocity profile for the lowest molecular weight (10-30 kDa) is practically linear, the attenuation is constant and the sample clear throughout the whole range of applied surfactant concentration. Because the velocity is systematically increasing in the presence of hyaluronan this should not directly indicate that no interactions between hyaluronan and surfactant are detected. Further, only below the critical micellar concentration (0.584 mmol/l TTAB, 0.071 mmol/l CTAB) the profiles measured at the presence and at the absence of hyaluronan coincide. Progressive formation of rigid, very small structures which do not scatter ultrasound waves should be expected. The velocity profile measured for the molecular weight of 110-130 kDa shows instead of the short interval of almost constant velocity a broader interval of "ïnflexing" behaviour during which also the attenuation markedly increases and opacity is developed. For the highest molecular weight (1500-1750 kDa) the constant velocity interval and corresponding sharp increase of attenuation are shifted to higher surfactant concentrations (4-6 mmol/l). Again, frequency affects the values of attenuation (not the shape of profiles).

As reviewed by Cowman and Matsuoka (2005) (31) in the presence of 0.15 M NaCl hyaluronan in the low molecular weight region adopts the free-draining conformation whereas in the high molecular weight region the non-free-draining ball-like conformation emerges. Short hyaluronan chains also favor intermolecular interactions whereas longer chains do not show this effect. There is very little information on the effect of hyaluronan molecular weight on its interactions with cationic surfactants. Thalberg et al. (5) determined the critical NaBr concentration needed in order to prevent phase separation in systems containing TTAB or dodecyl- or decyltrimethylammonium bromide with hyaluronan of two molecular weights (60 kDa and 3100 kDa). The higher molecular preparation had a larger two-phase region, i.e. it required a higher salt concentration to prevent the separation at the same surfactant concentration. In water, a reduced molecular weight of the polysaccharide resulted only in aslight changed position of the two-phase region. Our results suggest that in the case of very low molecular weight hyaluronan in the presence of salt, the surfactant cation may replace the polysaccharide counterion forming very small and phase non-separating structures of separate surfactant molecules bound to the biopolymer chain. An increased molecular weight of the hyaluronan leads to the formation of larger and coiled ball-like biopolymer structures with surfactant molecules bound preferably on their surface. The higher

the structure, the larger its surface and the higher surfactant amount is needed to induce (micro)phase separation.

The results clearly show differences in interactions of TTAB and CTAB with hyaluronan in water. Taking into account the molecular structure of these surfactants the differences should be caused by little bit longer alkyl chain of CTAB. In other words, besides the electrostatic contribution also the hydrophobic interactions play an important role especially in the case of CTAB which has longer hydrophobic tail. For example, hydrophobic component supports interactions at very low surfactant concentration. Ultrasound titration profiles revealed that the behavior of hyaluronan-surfactant system is more complex than simple one-phase or two-phase behaviour with a sharp boundary as could be inferred from phase diagrams. In the phase separation region several transitions were observed on the ultrasound velocity profiles which reflect formation of colloidal structures of different rigidity. The number of detected transitions was richer for TTAB therefore increasing importance of the hydrophobic interaction contribution simplifies the details of phase separation behaviour.

In water there is no significant effect of hyaluronan molecular weight similarly as in the previous studies on phase diagrams[5]. Thus the basic disaccharide unit and its interaction abilities are relevant for hyaluronan interactions with oppositely charged surfactants whereas specific conformations or coil shapes of the biopolymer chain of various lengths are not so important. In the presence of sodium chloride at the concentration of 0.15 M the effect of molecular weight is appreciable. Salts should suppress the electrostatic interactions and this was reflected in much simpler titration profiles and less rich behaviour in two-phase region. On the other side, suppressing the electrostatic part of interactions could be supposed to accentuate the differences in hydrophobic interactions observed for the two used surfactants in water. However, the titration profiles measured in the NaCl solution were much closer for both surfactants than in water. Probably, the more collapsed conformations supposed to exist in the presence of electrolyte as compared to conformations in water prevented the access of surfactant molecules to the polyelectrolyte interaction sites and consequently restricted (cooperative) interactions between surfactant alkyl chains. In other words, the effect of salt on hydrophobic interactions was mediated by sterical reasons.

Conclusion

High-resolution ultrasonic spectroscopy in titration regime enabled to reveal details of interactions between hyaluronan and oppositely charged surfactants. Due to its high sensitivity much more in-depth picture on interactions could be obtained when compared to other methods. Up to six different regions could be identified in a narrow interval of surfactant concentration corresponding to different states of hyaluronan-surfactant complexes formed by the interactions. These regions differed primarily in the shape of the dependence of ultrasound velocity on surfactant concentration values of which are determined by the compressibility of structures formed in the system. The richness of titration profiles was depressed in salt solution where essentially only two principal regions were observed. On the other side, the effect of hyaluronan molecular weight on the position of boundary between regions was more significant in the presence of salt. Very important effect on titration profiles in water had the length of the surfactant hydrophobic tail. Besides electrostatic also hydrophobic interactions are relevant for determining the behaviour of hyaluronan-surfactant systems and properties of formed complexes (aggregates).

Acknowledgements
This work was supported by the COST action CM1101, and projects No. LD12068 and LO1211 from the Czech Ministry of Education.

References

(1) Lapčík, L.; Lapčík, L.; Smedt, S. D.; Demeester, J.; Chabreček, P. *Chemical Reviews* **1998**, *98*, 2663–2684.
(2) Kogan, G.; Šoltés, L.; Stern, R.; Gemeiner, P.. *Biotechnology Letters* **2007**, *29*, 17–25.
(3) Jin, Y. -J.; Ubonvan, T.; Kim, D. -D. *Journal of Pharmaceutical Investigation* **2010**, *40*, 33-43.
(4) Holmberg, K.; Jönsson, B.; Kronberg, B.; Lindman, B. *Chichester: Wiley* **2007**.
(5) Thalberg, K.; Lindman, B. *The Journal of Physical Chemistry* **1989***, 93*, 1478-1483.
(6) Thalberg, K.; Lindman, B.; Karlstroem, G. *The Journal of Physical Chemistry* **1990***, 94*, 4289-4295.
(7) Thalberg, K.; Lindman, B.; Karlstroem, G. *The Journal of Physical Chemistry* **1991**a*, 95*, 3370-3376.
(8) Thalberg, K.; Lindman, B.; Karlstroem, G. *The Journal of Physical Chemistry* **1991**b*, 95*, 6004-6011.
(9) Thalberg, K.; Lindman, B. *Langmuir* **1991***, 7*, 277-283.
(10) Hersloef, A.; Sundeloef, L. O.; Edsman, K. *The Journal of Physical Chemistry* **1992***, 96*, 2345-2348.
(11) Bjoerling, M.; Hersloef-Bjoerling, A.; Stilbs, P. *Macromolecules* **1995***, 28*, 6970-6975.
(12) Kayitmazer, A. B.; Seyrek, E.; Dubin, P. L.; Staggemeier, B. A. *The Journal of Physical Chemistry B 2003, 107*, 8158-8165.
(13) Cooper, C. L.; Goulding, A.; Kayitmazer, A. B.; Ulrich, S.; Stoll, S.; Turksen, S.; Yusa, S. -ichi; Kumar, A.; Dubin, P. L. *Biomacromolecules* **2006***, 7*, 1025-1035.
(14) Lapitsky, Y.; Parikh, M.; Kaler, E. W. *The Journal of Physical Chemistry B 2007, 111*, 8379-8387.
(15) Bao, H.; Li, L.; Gan, L. H.; Zhang, H. Macromolecules **2008**, *41*, 9406-9412.
(16) Sarvazyan, A. P. *Ultrasonics* **1982***, 20*, 151-154.
(17) Sarvazyan, A. *Annual Review of Biophysics and Biomolecular Structure* **1991***, 20*, 321-342.
(18) Buckin, V. *Biophysical Chemistry* **1988**, *29*, 283-292.
(19) Buckin, V. A.; Kankiya, B. I.; Sarvazyan, A. P.; Uedaira, H. *Nucleic Acids Research 1989, 17*, 4189-4203.
(20) Buckin, V.; Kudryashow, E.; Morrisey, S.; Dawson, K.; Kapustina, T. *Trends in Colloid and Interface Science XII. Steinkopff* **1998**, 214-219.
(21) Hickey, S.; Lawrence, M. J.; Hagan, S. A.; Buckin, V. *Langmuir* **2006**, *22*, 5575-5583.
(22) Hickey, S.; Hagan, S.A.; Kudryashov, E.; Buckin V. *International J. of Pharmaceutics* **2010**, *388*, 213-222.
(23) Singh, P.P.; Anand, K.; Yadav O.P. *Indian J. of Chemistry* **1990**, *29*, 445-449.
(24) Anand, K.; Yadav O. P.; Singh P. P. *Colloid* 1992, 270, 1201-1207.
(25) Buckin, V. A.; Kankiya, B. I.; Sarvazyan, A. P.; Uedaira, H. Nucleic Acids Research **1989**, *17*, 4189-4203.
(26) Andreatta, G.; Bostrom, N.; Mullins, O. C. *Langmuir* **2005***, 21*, 2728-2736.
(27) Beyer, K.; Leine, D.; Blume, A. *Colloids and Surfaces B: Biointerfaces* **2006**, *49*, 31-39.
(28) Ray, G. B.; Chakraborty, I.; Ghosh, S.; Moulik, S. P.; Palepu, R. *Langmuir* **2005**, *21*, 10958-10967.

(29) Kudryashov, E.; Kapustina, T.; Morrissey, S.; Buckin, V.; Dawson, K.; Hirsch, E.; Candau, S. J.; Zana, R. *Journal of Colloid and Interface Science* **1998**, *203*, 325-332.
(30) Pavlovskaya, G.; McClements, D. J.; Povey, M. J. W. *Food Hydrocolloids* **1992**, *6*, 253-262.
(31) Cowman, M. K.; Matsuoka, S.; Itano, N.; Haxaire, K.; Buhler, E.; Milas, M.; Perez, S.; Rinaudo, M.; Mikelsaar, R. -H.; Toole, B.; CANFIELD, R. O. B. E. R. T. E.; ANFINSEN, C. H. R. I. S. T. I. A. N. B. *Carbohydrate Research* **2005**, *340*, 311-378.
(32) Halasová, T.; Krouská, J.; Mravec, F.; Pekař, M. *Colloids and Surfaces A: Physicochemical and Engineering Aspects* **2011**, *391*, 25-31.

Supplementary information

Table ST1. Molecular weights of hyaluronan used in the experimental part II.

Product name	M_w*	Batch number
kDa	kDa	
10-30	17	211-589
	16	211-263
	15	212-2069
90-130	116	210-493
	137	211-234
	101	212-1214
	116	212-2859
	117	213-3842
300-500	421	208-125
	430	212-2082
	458	213-3809
1500-1750	1730	210-636
	1800	211-180
	1697	212-1271
	1644	212-2298

* weight-average molecular weight provided by the supplier and obtained by SEC-MALS analysis.

Table ST2. The critical micelle concentration, CMC, of the surfactants TTAB and CTAB in aqueous and sodium chloride solutions at 25 °C measured by means of HR-US 102T, comparing with the CMC from literature

Surfactant/environment	CMC mmol/l (this work)	CMC mmol/l (references)
TTAB/water	3.7	3.7[1], 3.7[2], 3.5[3], 3.8 [4], 3.7[5], 3.7[6]
CTAB/water	1.0	0.9[2,3,4,5,7,9], 1.0[1]
TAB/0.15M NaCl	0.58	0.52[9]
CTAB/0.15M NaCl	0.07	0.06[9]

(1) Zieliński, R.; Ikeda, S.; Nomura, H.; Kato, S. *Journal of Colloid and Interface Science* **1989**, *129*, 175-184.
(2) Kudryashov, E.; Kapustina, T.; Morrissey, S.; Buckin, V.; Dawson, K.; Hirsch, E.; Candau, S. J.; Zana, R. *Journal of Colloid and Interface Science* **1998**, *203*, 325-332.
(3) Mosquera, V. *Journal of Colloid and Interface Science* **1998**, *206*, 66-76.
(4) González-Gaitano, G.; Crespo, A.; Tardajos, G. *The Journal of Physical Chemistry B* **2000**, *104*, 1869-1879.
(5) Buckin, V.; Kudryashow, E.; Morrisey, S.; Dawson, K.; Kapustina, T. *Trends in Colloid and Interface Science XII. Steinkopff* **1998**, 214-219.
(6) Zieliński, R.; Ikeda, S.; Nomura, H.; Kato, S. *Journal of Colloid and Interface Science* 1987, 119, 398-408.
(7) Buckin, V. *IOP Conference Series: Materials Science and Engineering* **2012**, 42.
(8) Beyer, K.; Leine, D.; Blume, A. *Colloids and Surfaces B: Biointerfaces* **2006**, *49*, 31-39.
(9) Halasová, T.; Krouská, J.; Mravec, F.; Pekař, M. *Colloids and Surfaces A: Physicochemical and Engineering Aspects* **2011**, *391*, 25-31.

Table ST3. CTAB concentrations at the boundaries of the different parts identified in the velocity titration profile and corresponding charge ratio CTAB/hyaluronan.

		Water		0.15 M NaCl	
M_w / kDa	Part	c_{CTAB} / mmol/l	Charge ratio CTAB/HYA	c_{CTAB} / mmol/l	Charge ratio CTAB/HYA
10-30	I				
	II	2.29	0.9	3.08	1.3
	III				
	IV	2.85	1.2		
	V	5.88	2.5		
90-130	I				
	II	2.48	1.0	1.13	0.5
	III				
	IV	2.85	1.2		
	V	4.84	2.0		
300-500	I				
	II	2.84	1.2	3.13	1.3
	III				
	IV	3.21	1.3		
	V	4.11	1.7		
1500-1750	I				
	II	2.66	1.1	5.16	2.2
	III				
	IV	3.03	1.3		
	V	5.36	2.3		

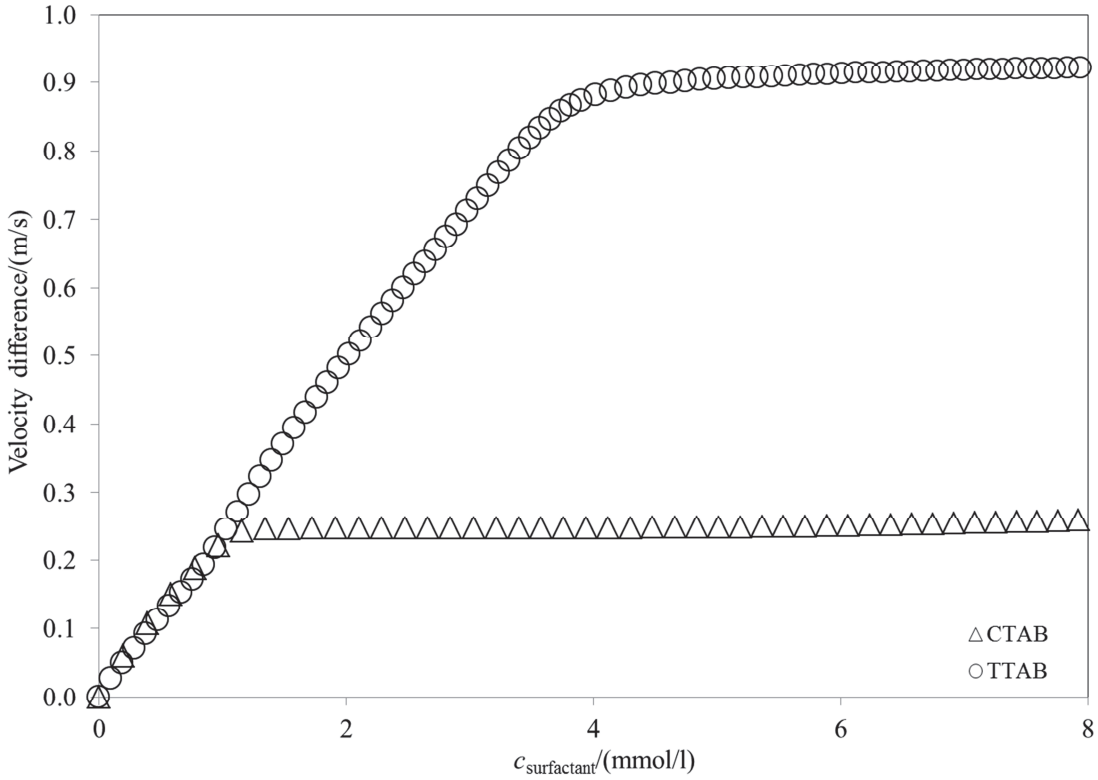

Figure SF1. The deterimnation of criticelle micelle concentration of surfactants TTAB and CTAB in water.

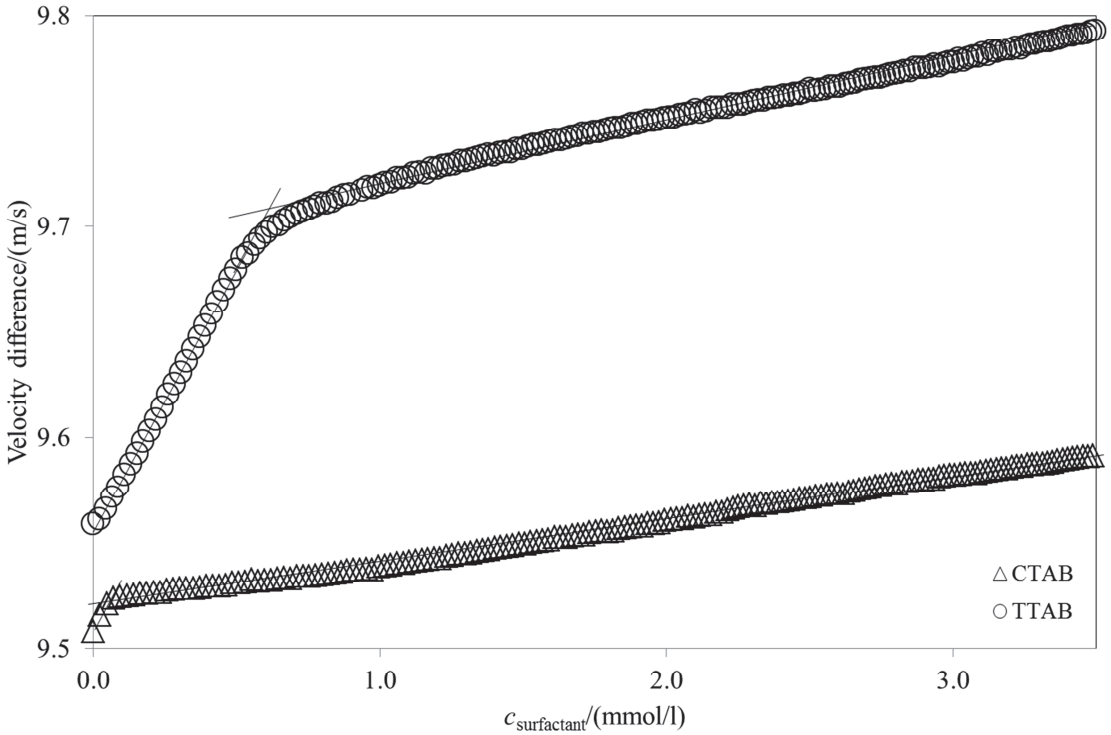

Figure SF2. The deterimnation of criticelle micelle concentration of surfactants TTAB and CTAB in 0.15 M NaCl.

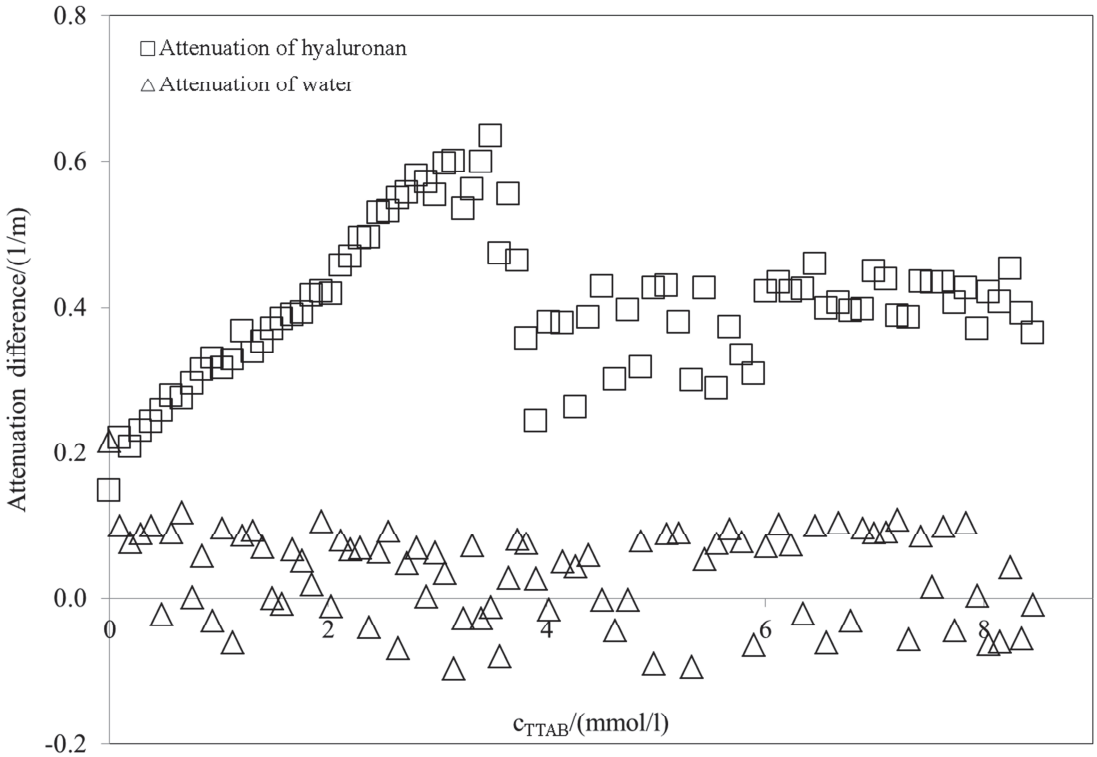

Figure SF3. The attenuation titration curve of hyaluronan of concentration 1000 mg/l and molecular weight of 300-500kDa and the attenuation titration curve of water with TTAB, at frequency 15 MHz.

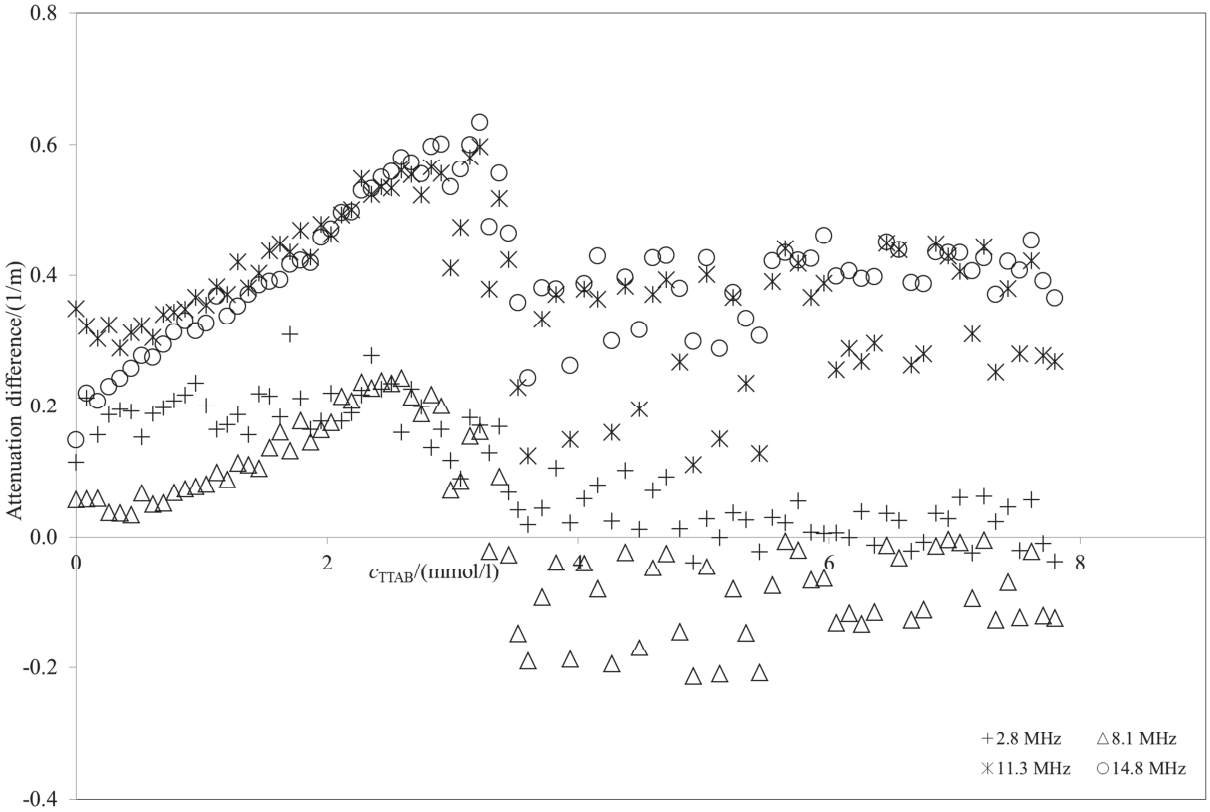

Figure SF4. The effect of frequency on ultrasonic attenuation profile of hyaluronan-TTAB system in water, at 25 °C, at frequencies 2.8-14.8 MHz. Hyaluronan 1000mg/l 300-500 kDa.

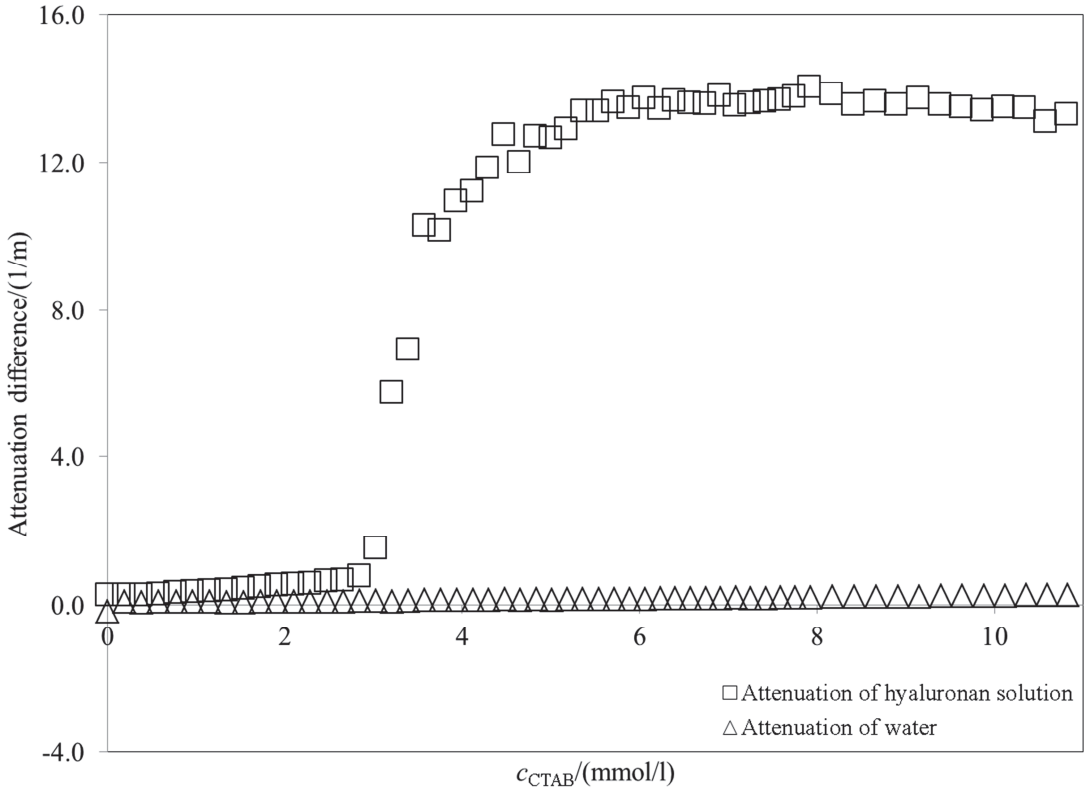

Figure SF5. The attenuation titration curve of hyaluronan of concentration 1000 mg/l and molecular weight of 300-500kDa and the attenuation titration curve of water with CTAB, at frequency 15 MHz. The titration curve of water is shifted to first point of hyaluronan curve.

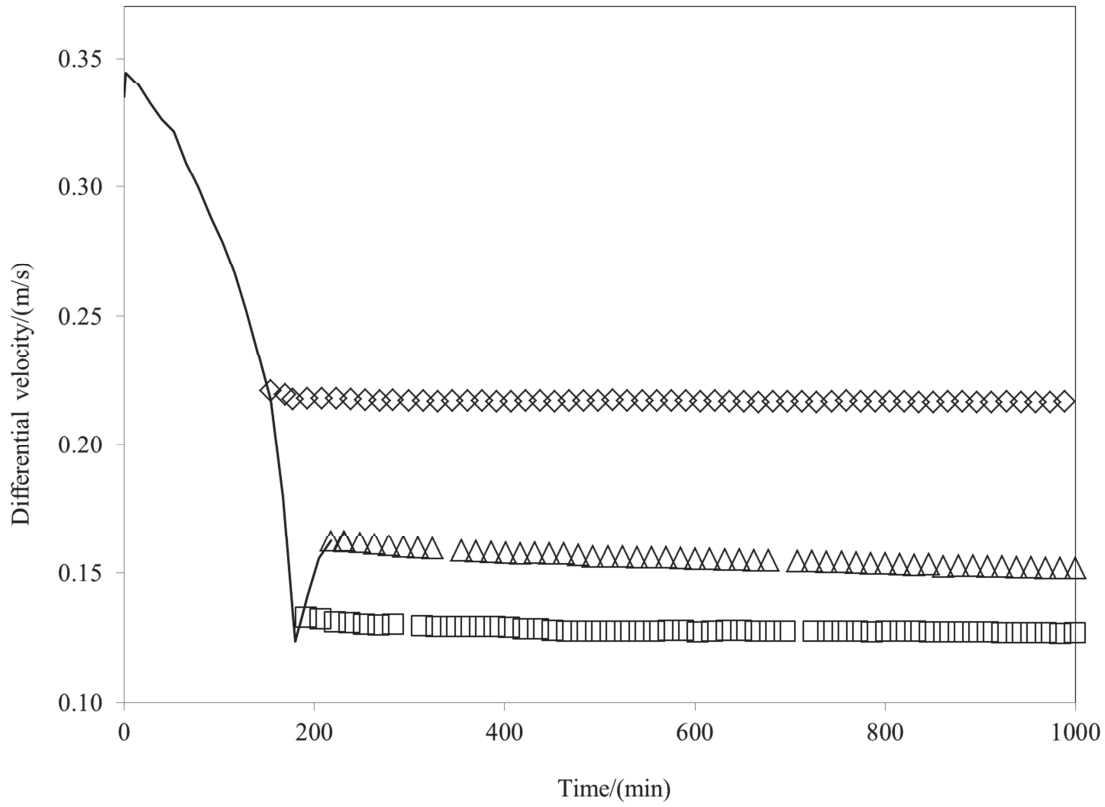

Figure SF6. Titration profiles of stop-titrations of hyaluronan (300-500 kDa). Solid line illustrates the original titration and dots correspond titration stop in the phase II-IV.

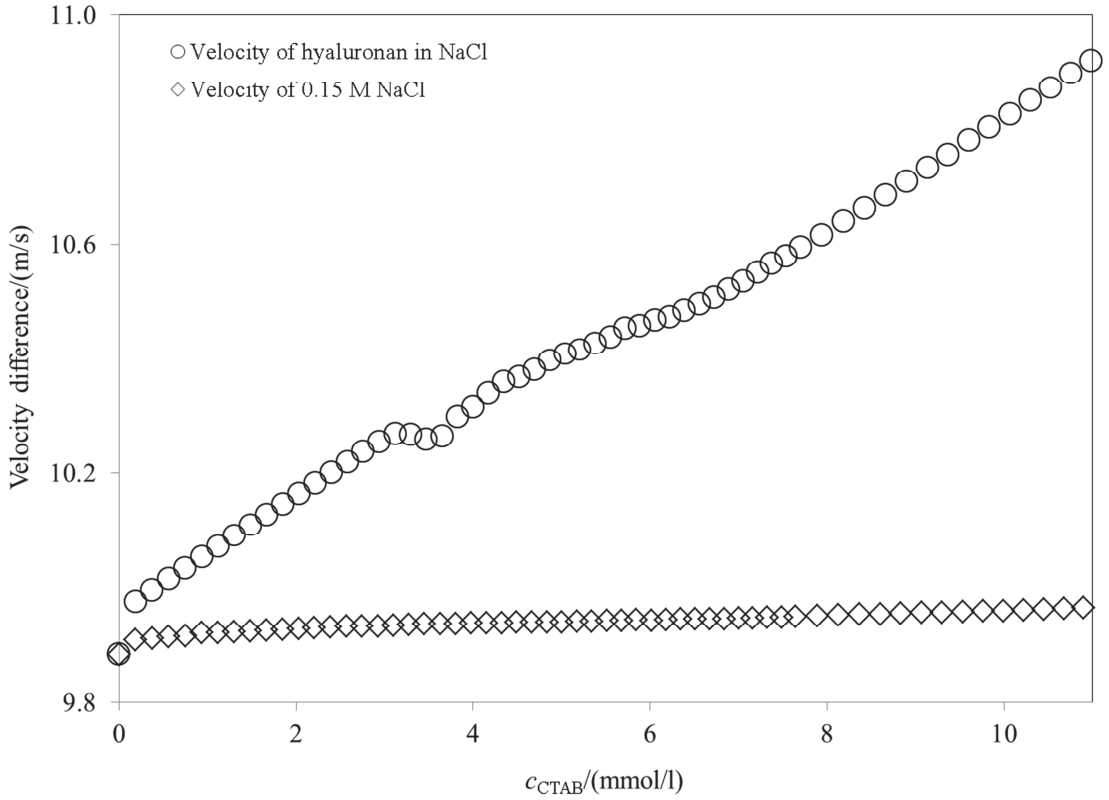

Figure SF7. The velocity titration curve of hyaluronan of concentration 1000 mg/l and molecular weight of 300-500kDa and the velocity titration curve of 0.15 M NaCl with CTAB, at frequency 15 MHz. The titration curve of 0.15 M NaCl is shifted to first point of hyaluronan curve.

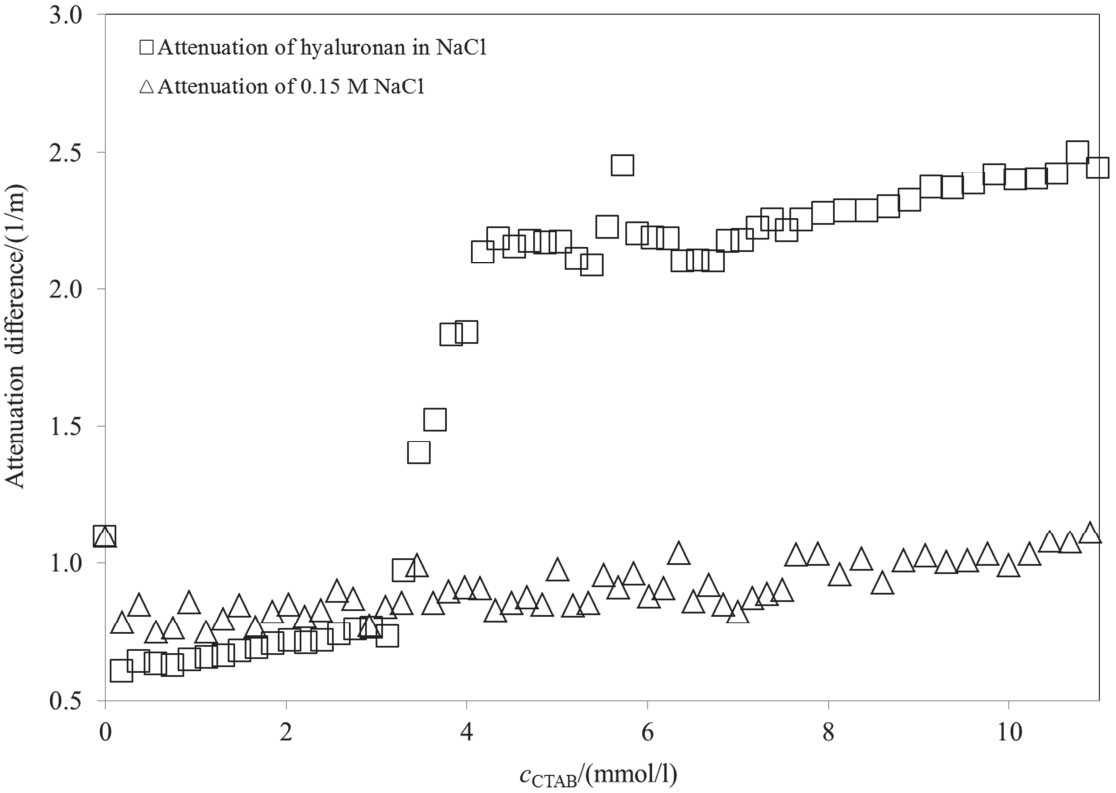

Figure SF8. The attenuation titration curve of hyaluronan in NaCl of concentration 1000 mg/l and molecular weight of 300-500kDa and the attenuation titration curve of 0.15 M NaCl with CTAB, at frequency 15 MHz. The titration curve of 0.15 M NaCl is shifted to first point of hyaluronan curve.